Atmospheric circulation of hot giant planets

Vivien Parmentier
AOPP Oxford University
moving to Observatoire de la côte d'Azur, Nice

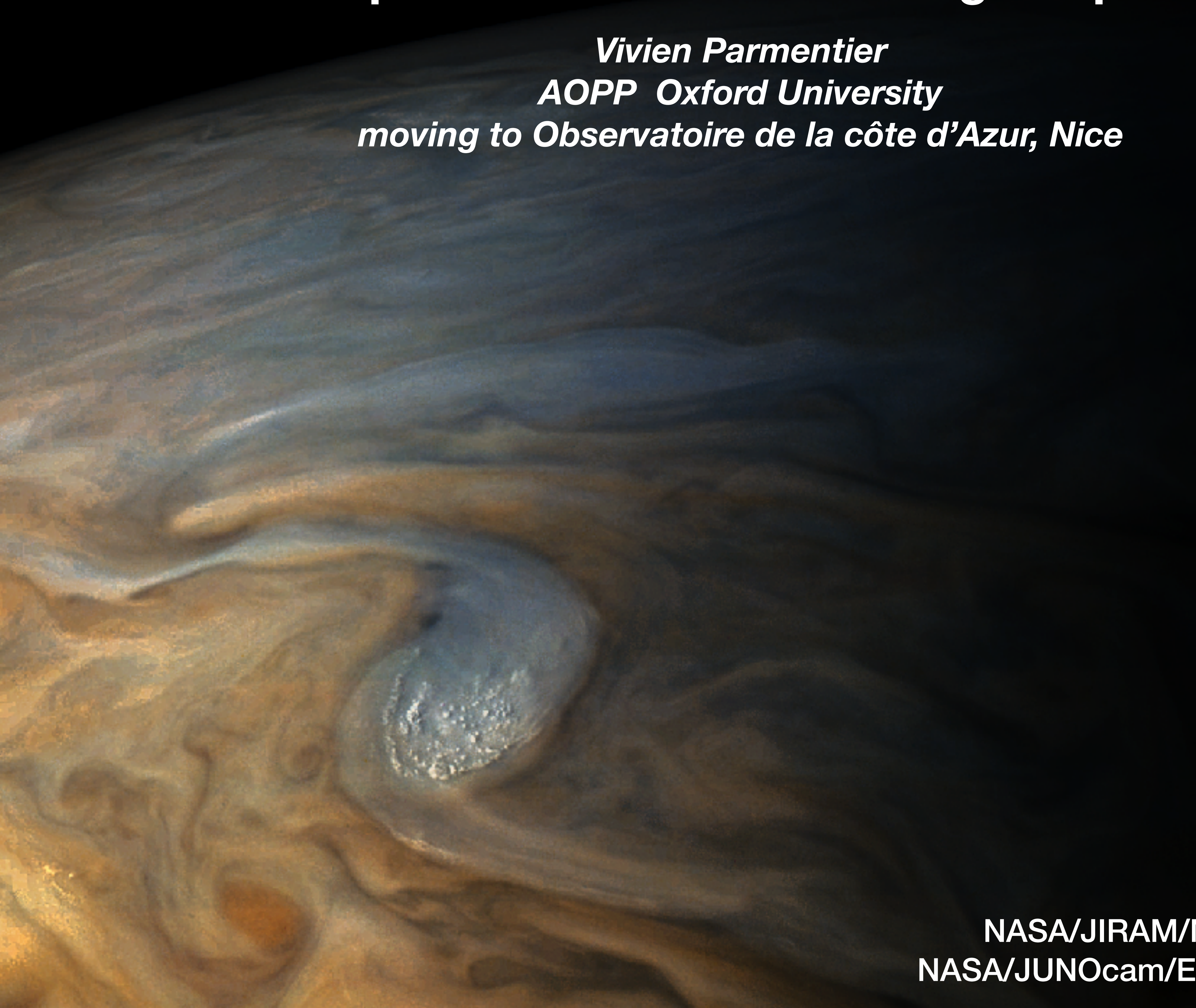

NASA/JIRAM/Matt Brealey
NASA/JUNOcam/Eichstädt & Doran

Adam Showman, 1968-2020

ATMOSPHERIC DYNAMICS OF HOT GIANT PLANETS AND BROWN DWARFS

Adam P. Showman[1,†], Xianyu Tan[2,*] and Vivien Parmentier[2,*]
[1]Lunar and Planetary Laboratory, University of Arizona, 1629 University Boulevard, Tucson, AZ 85721, USA
showman@lpl.arizona.edu
[2]Atmospheric Oceanic and Planetary Physics, Department of Physics, University of Oxford, OX1 3PU, UK

Space Science Reviews special issue on "Understanding the Diversity of Planetary Atmospheres"

https://arxiv.org/abs/2007.15363

Adam Showman, 1968-2020

https://www.youtube.com/watch?v=vkeyUFaZ3t8

Detected exo-atmospheres : Now

19 chemical species in 35 different atmospheres

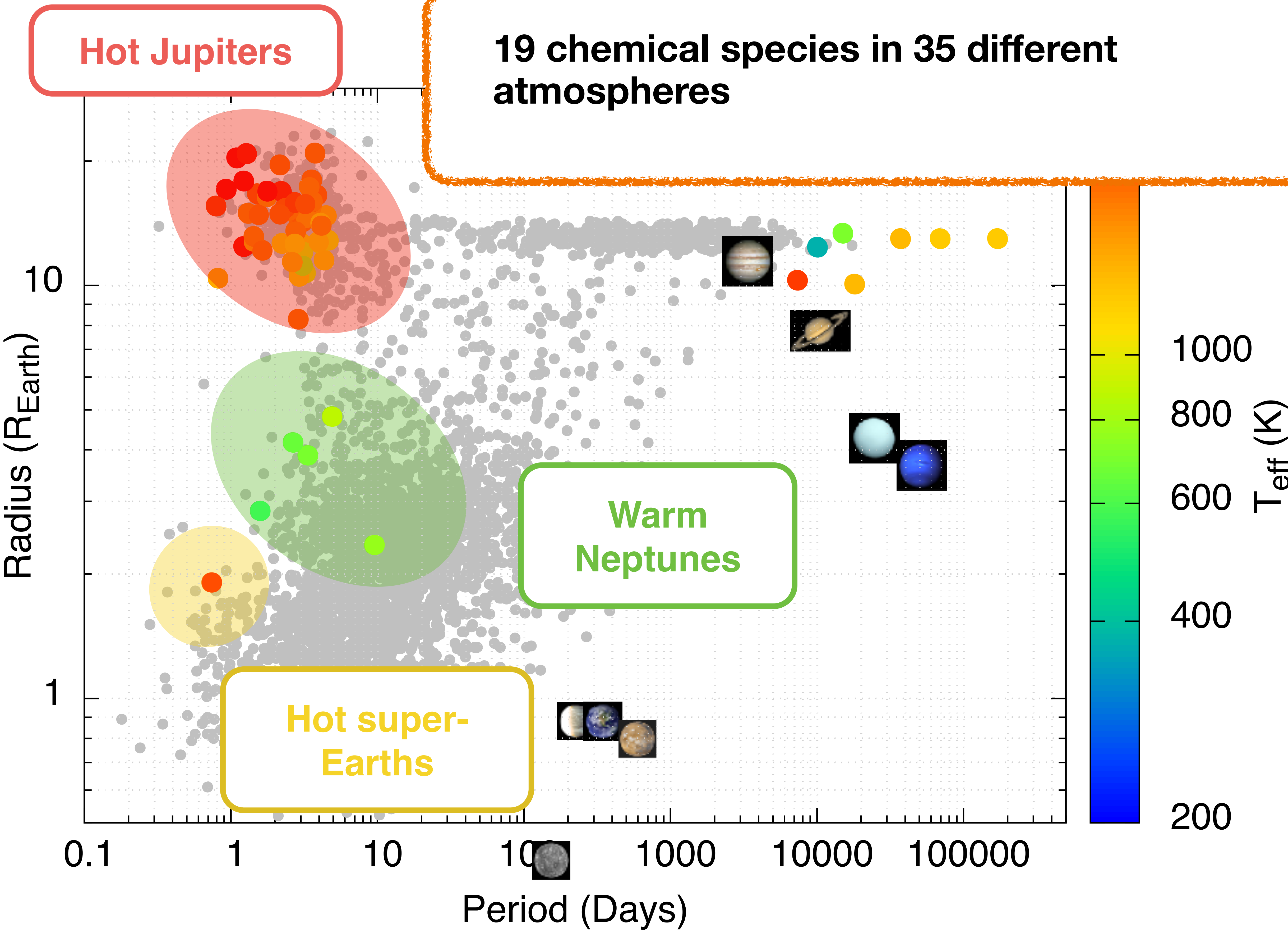

Detected exo-atmospheres : in 10 years

63 planets in JWST cycle 1
As many planets with planned high resolution obs.
More planets this year than has ever been observed by Hubble and Spitzer !

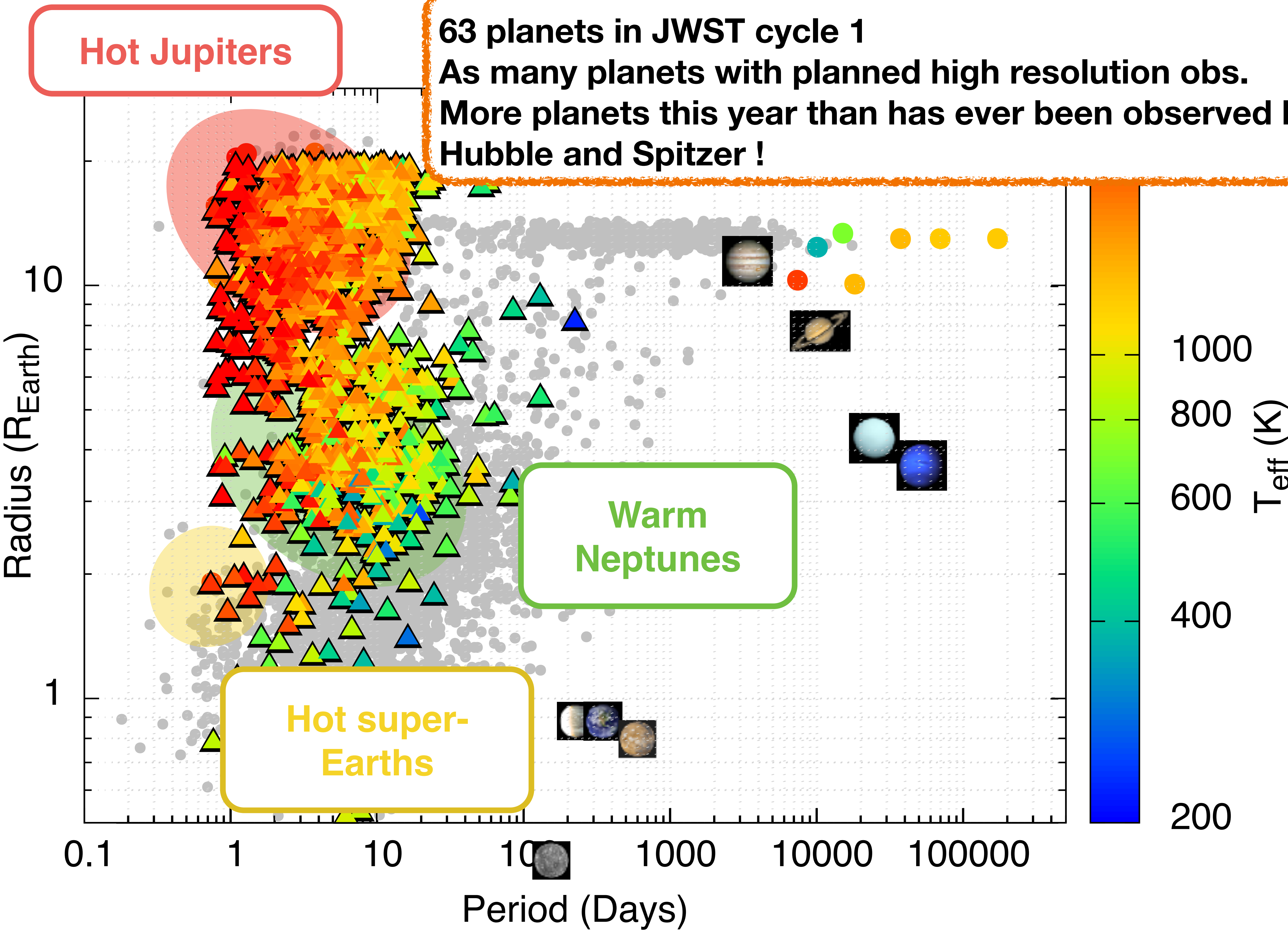

Detected exo-atmospheres : in 10 years

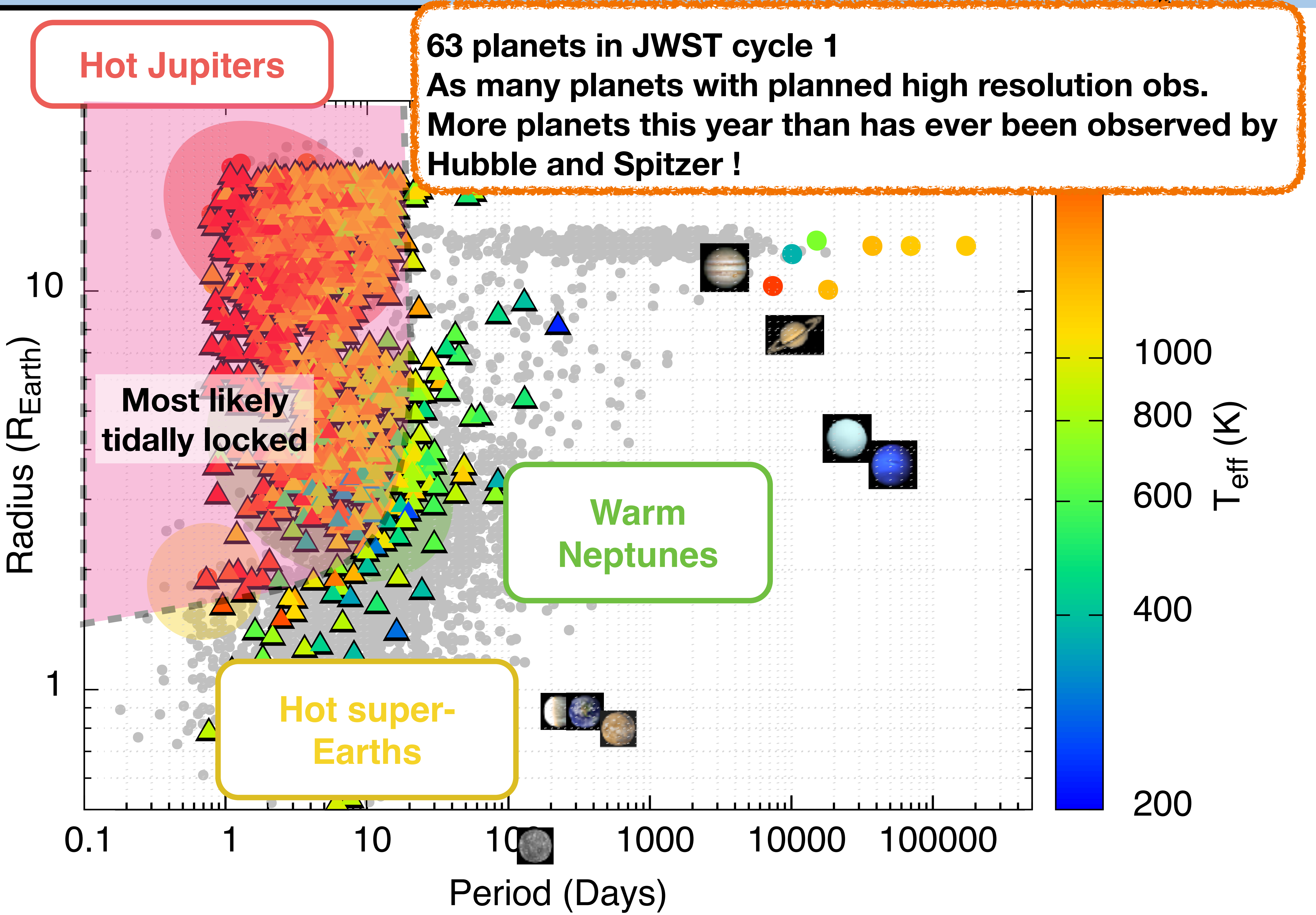

What a hot Jupiter really look like.

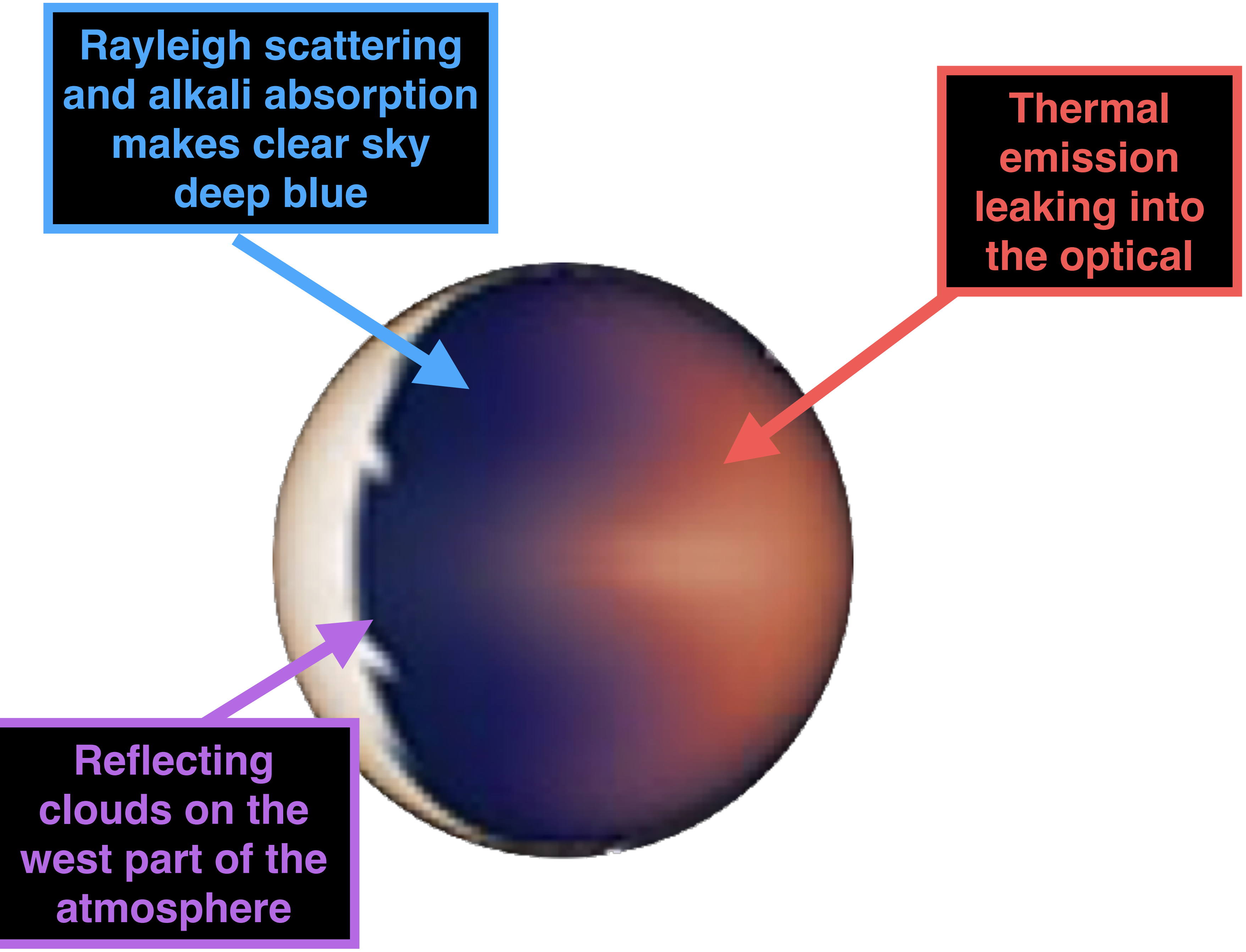

What a hot Jupiter really look like.

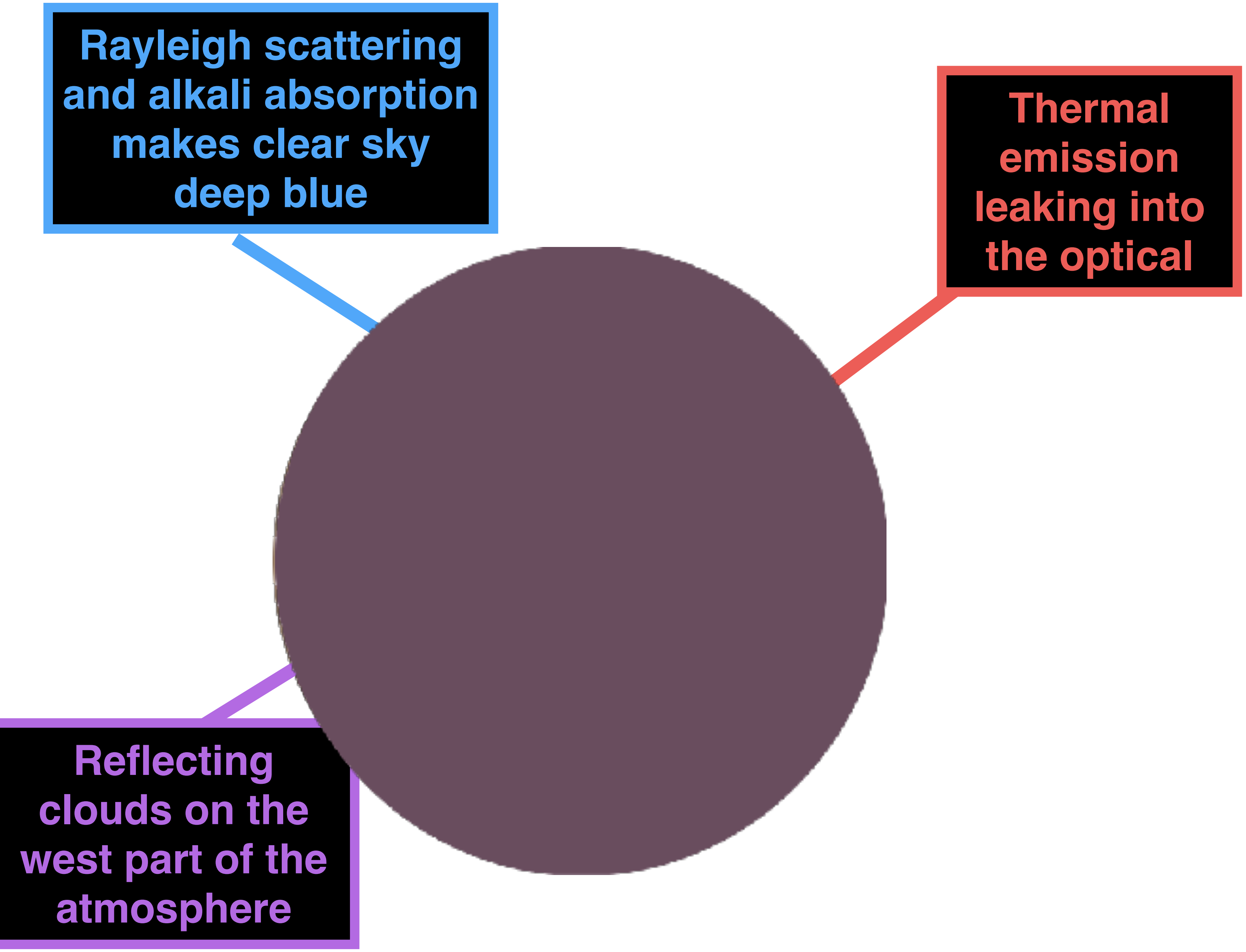

During eclipse and transit we see a mix of varied:
- **cloudiness**
- **temperature**
- **chemistry**

RGB (105,77,94)
best match : eggplant purple

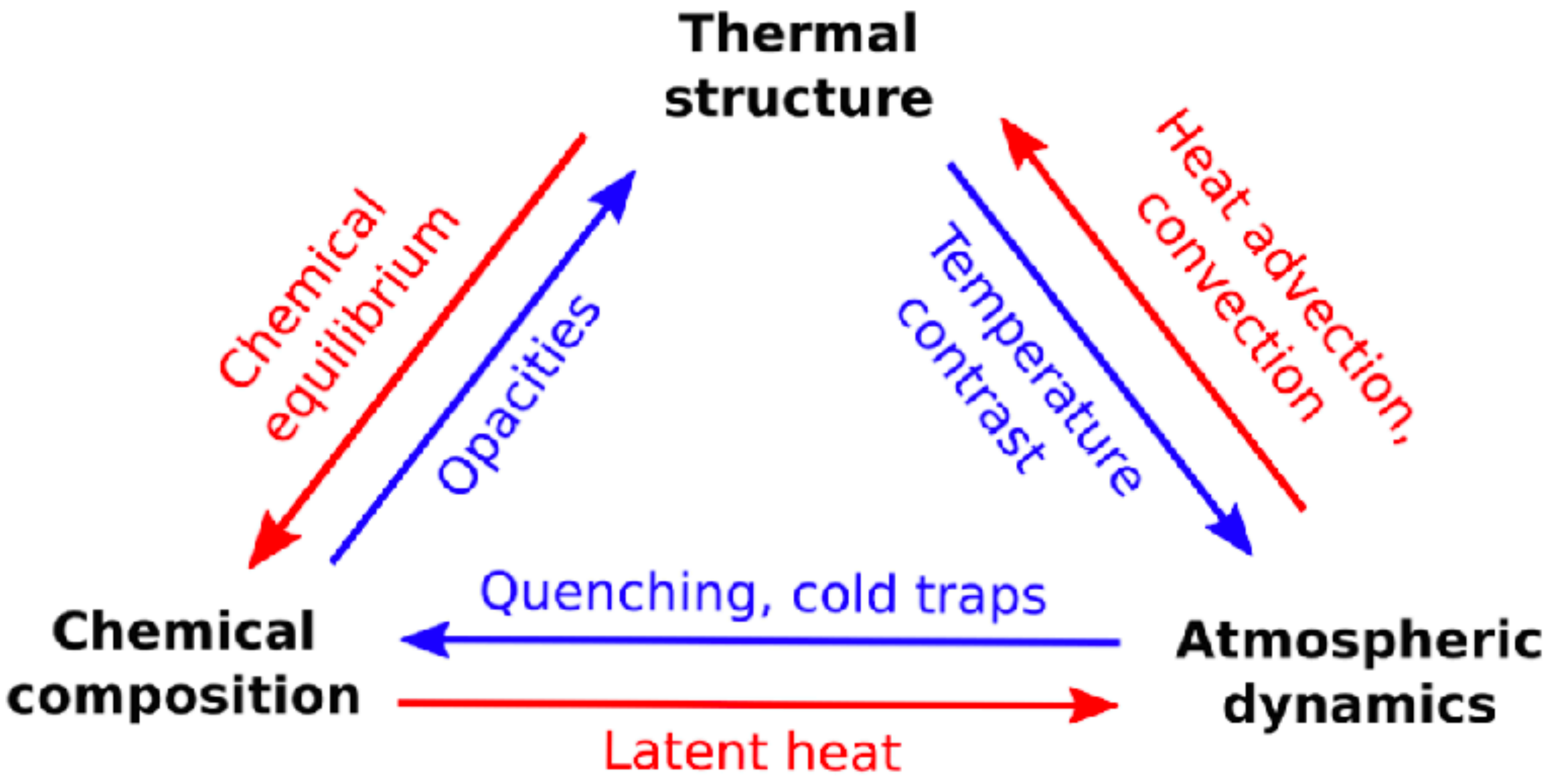

Thermal structure
Chemical equilibrium
Opacities
Temperature contrast
Heat advection, convection
Quenching, cold traps
Chemical composition
Atmospheric dynamics
Latent heat

Dynamics equations

- Newton's second law or conservation of momentum (one equation for each of the three velocity components);

$$\frac{\mathrm{D}\vec{v}}{\mathrm{D}t} = -\frac{1}{\rho}\vec{\nabla}p - \vec{g} - 2\vec{\Omega} \times \vec{v} + \vec{D}\,.$$

- the continuity equation or conservation of mass;

$$\frac{\mathrm{D}\rho}{\mathrm{D}t} = -\rho\vec{\nabla} \cdot \vec{v}$$

- the equation of state of the gas, usually taken as the ideal gas law;

$$P = \frac{\kappa_{\mathrm{B}}}{\mu}\rho T\,;$$

- the conservation of energy;

$$\frac{\mathrm{D}T}{\mathrm{D}t} = \frac{q}{c_{\mathrm{p}}} + \frac{1}{\rho c_{\mathrm{p}}}\frac{\mathrm{D}P}{\mathrm{D}t}$$

Non dimensional numbers

Rossby Number

$$Ro \equiv \frac{U}{fL},$$

Compares advection and Coriolis term

$$f = 2\Omega \sin\phi$$

Large Rossby
—> Geostrophic balance

Small Rossby
—> Coriolis small

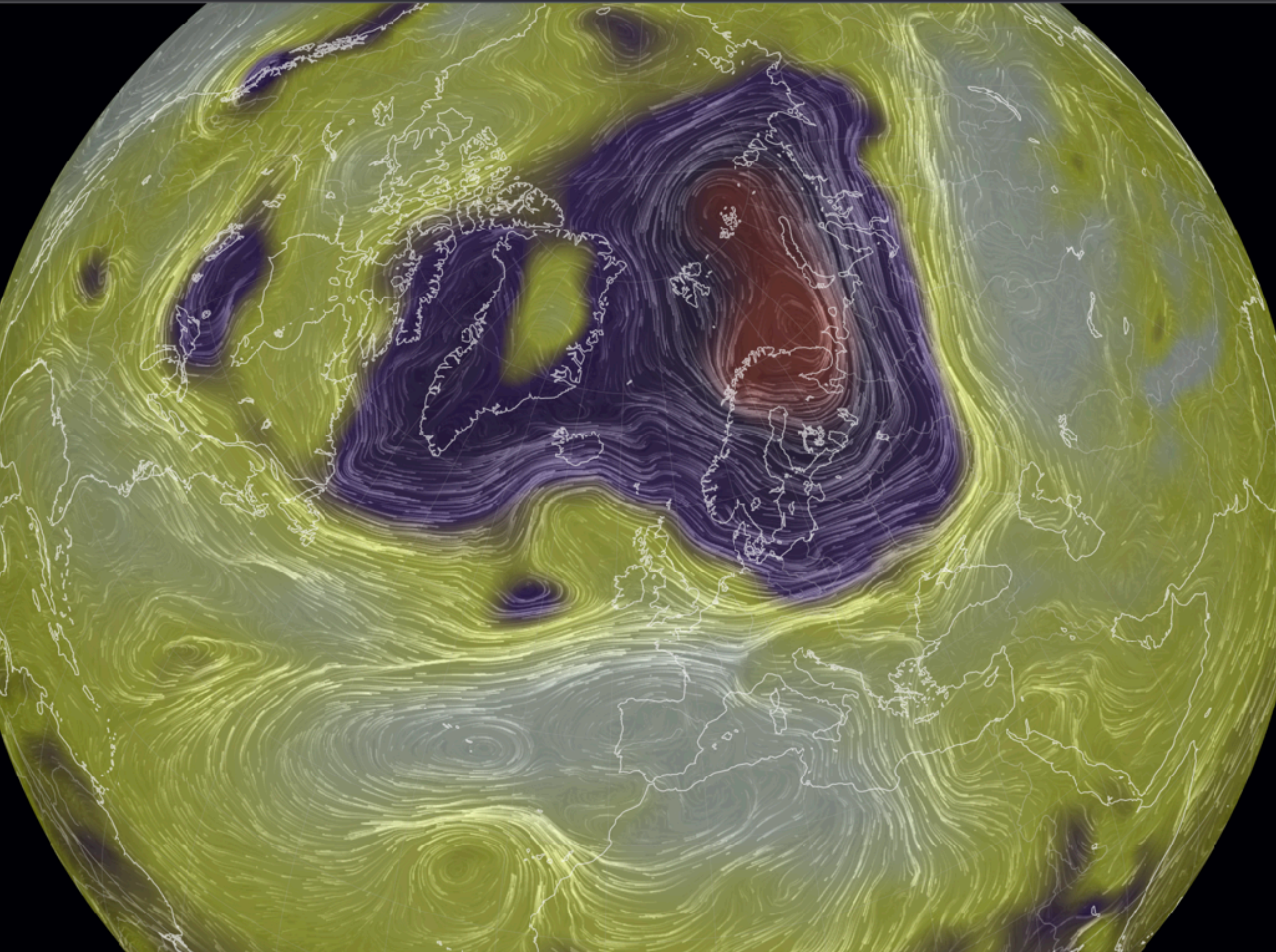

Non dimensional numbers

Rossby Number

$$Ro \equiv \frac{U}{fL},$$

Compares advection and Coriolis term

$$f = 2\Omega \sin \phi$$

Large Rossby —> Geostrophic balance

Small Rossby —> Coriolis small

Deformation radius

$$L_D = \frac{ND}{f}$$

How far gravity waves propagate before being deflected by Coriolis ?

$$N = \sqrt{c_p} k_B \sqrt{g/H}$$

Size of storms !

Non dimensional numbers

Rossby Number

$$Ro \equiv \frac{U}{fL},$$

Compares advection and Coriolis term

$$f = 2\Omega \sin\phi$$

Large Rossby —> Geostrophic balance

Small Rossby —> Coriolis small

Deformation radius

$$L_D = \frac{ND}{f}$$

How far gravity waves propagate before being deflected by Coriolis ?

$$N = \sqrt{c_{\mathrm{p}}} k_{\mathrm{B}} \sqrt{g/H}$$

Size of storms !

Rhines scale

$$L_{\mathrm{Rh}} = \pi \sqrt{\frac{U}{\beta}}$$

How big turbulent eddies become before being affected by Coriolis

$$\beta = \frac{2\Omega \cos\phi}{R_{\mathrm{p}}}$$

Size of jets !

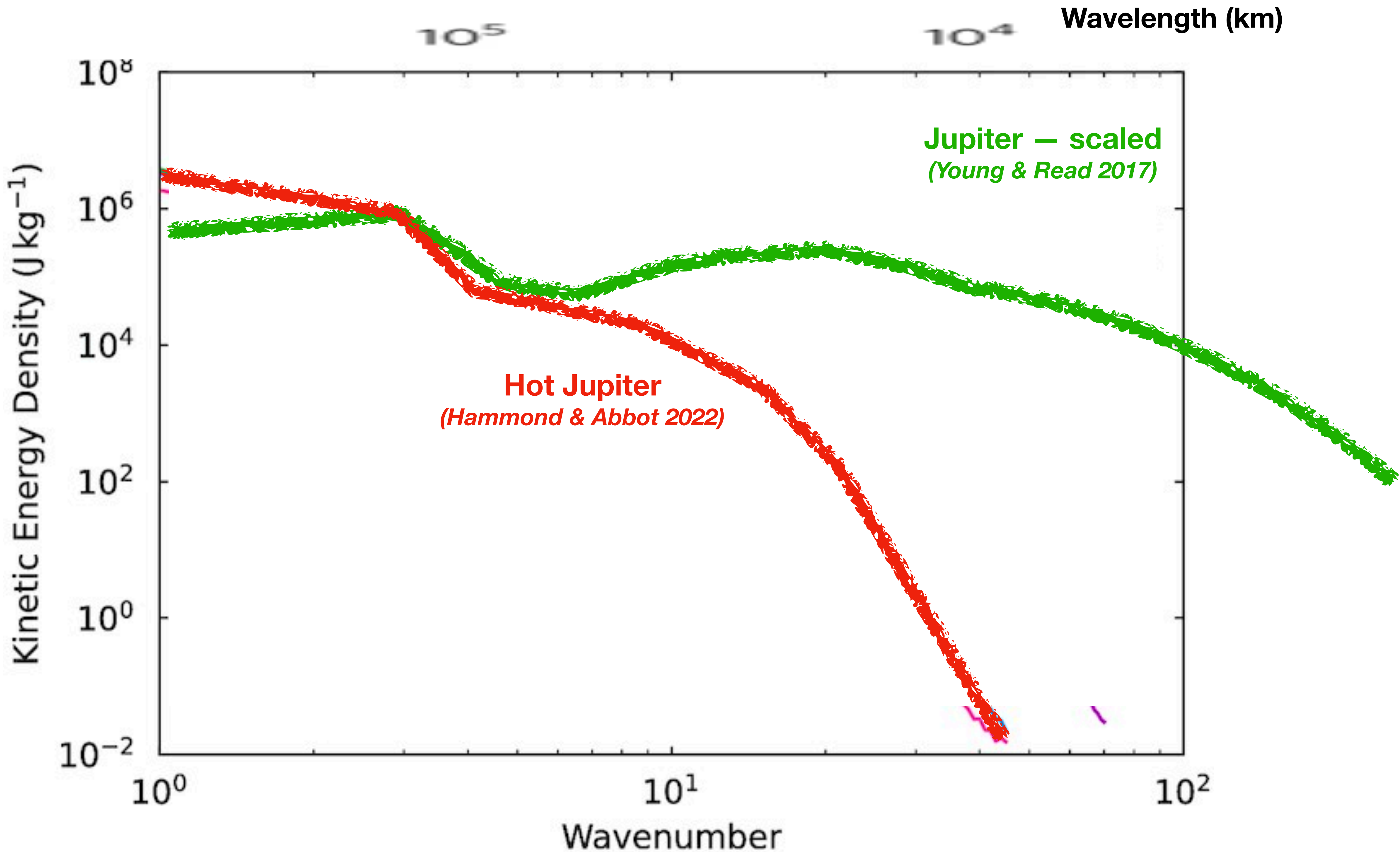

Wavelength (km)
10^5
10^4
Jupiter — scaled
(Young & Read 2017)
Hot Jupiter
(Hammond & Abbot 2022)
Kinetic Energy Density (J kg^-1)
10^8
10^6
10^4
10^2
10^0
10^-2
10^0
10^1
10^2
Wavenumber

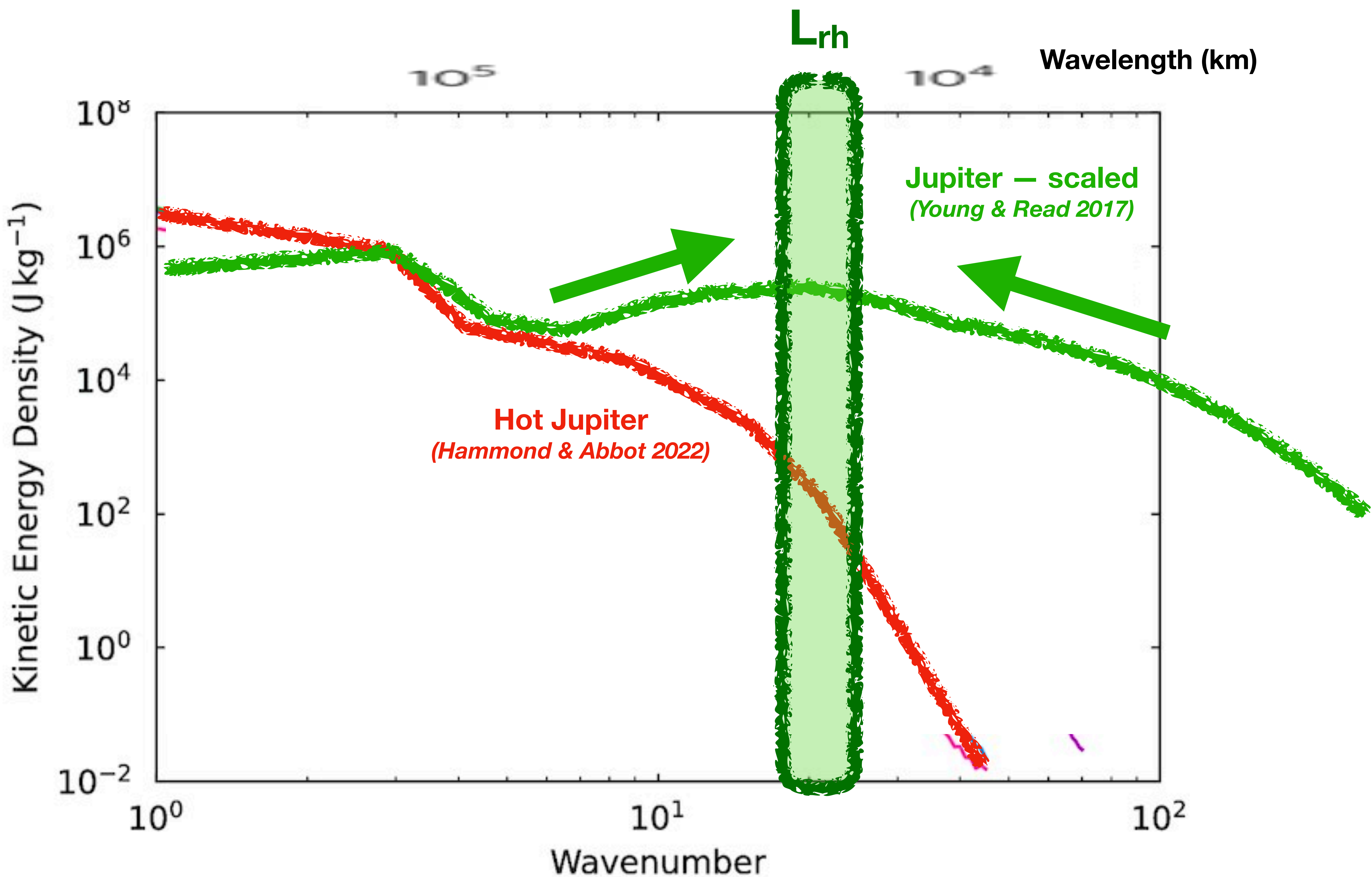

L$_{rh}$
Wavelength (km)
10⁵
10⁴
Jupiter — scaled
(Young & Read 2017)
Hot Jupiter
(Hammond & Abbot 2022)
Kinetic Energy Density (J kg⁻¹)
Wavenumber

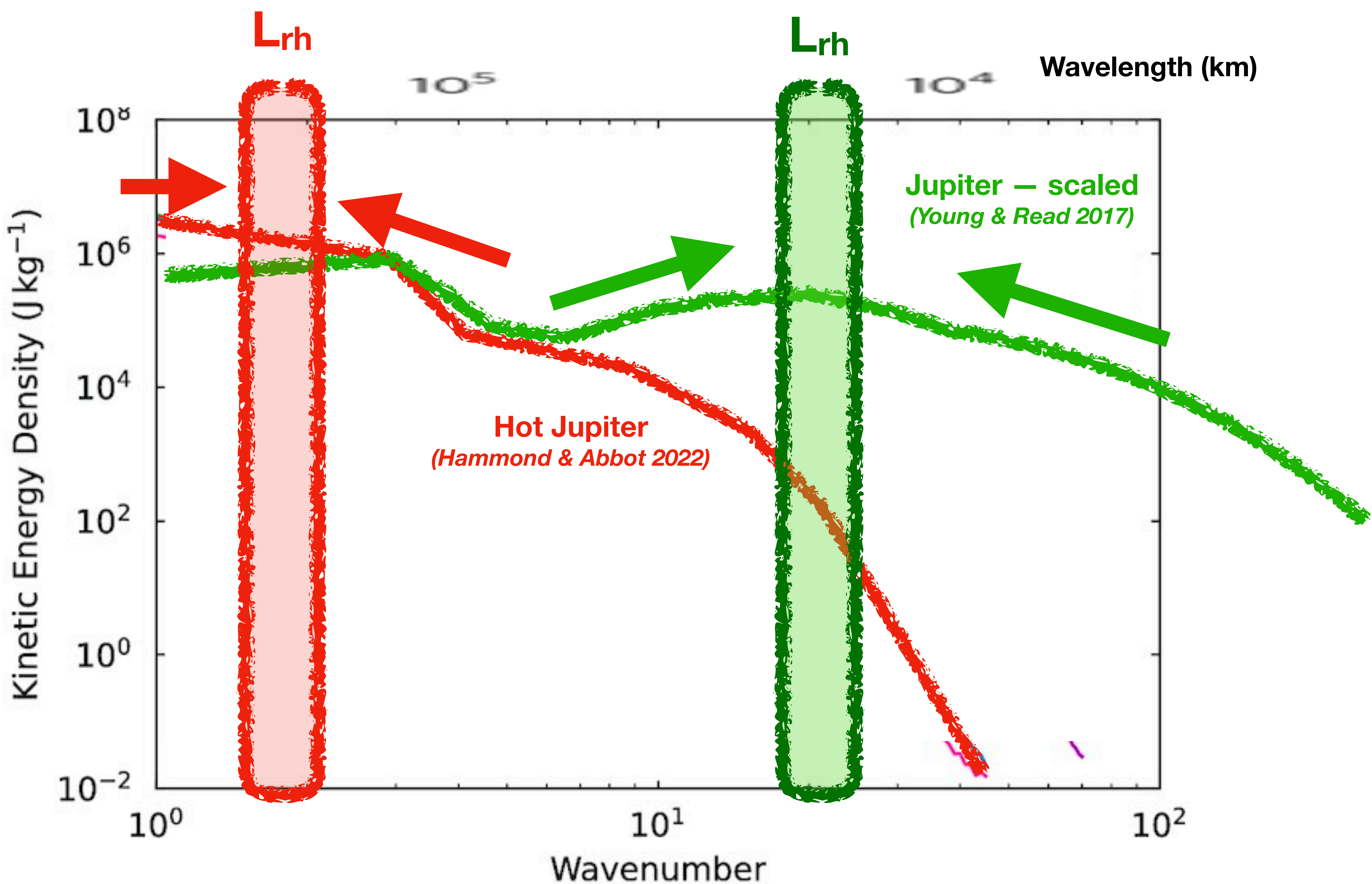

Lrh
Lrh
Wavelength (km)
10^5
10^4
Jupiter — scaled
(Young & Read 2017)
Hot Jupiter
(Hammond & Abbot 2022)
Kinetic Energy Density (J kg^−1)
10^8
10^6
10^4
10^2
10^0
10^−2
10^0
10^1
10^2
Wavenumber

3.2.3 Primitive equations

The most commonly used set of equations to study the dynamics of an entire planet are the Primitive equations. They can be derived from the full set of equations with four assumptions (see also Table 3.1) :

1. *Constant gravity.* The gravity is supposed constant through the whole atmosphere. This is valid if the vertical extent of the atmosphere is small compared to the radius of the planet.

2. *The shallow-fluid approximation.* We write the position of the gas parcel $r = R_p + z$ where R_p is the fixed radius of the planet and z is the altitude above this radius. We then re-write the *vector invariant* form of the momentum equation (3.4) assuming that $R_p >> z$

3. *The traditional approximation.* Whenever the *shallow-fluid approximation* is applied at the spherical coordinates equation and not to the vector invariant equations, the resulting equations lack of self-consistency and, in particular, they do not conserve the angular momentum anymore (Phillips 1966). In that case, the terms proportional to $1/r$ (metric terms) and the Coriolis terms proportional to f' are neglected in the momentum equations. To be valid, this approximation needs $N^2 >> \Omega^2$ (Phillips 1968), however White & Bromley (1995) show that it might break whenever large diabatic processes are at stake, a limitation further confirmed by (Mayne et al. 2014).

4. *The hydrostatic approximation.* In the vertical momentum equation, the gravitational term is assumed to be balanced by the pressure gradient term. This is valid as long as the vertical extent of the atmosphere is small compared to its vertical extent (i.e. $(H/L)^2 << 1$).

Name	Approximation	Formal Condition	HD 209458b
constant gravity	$g(r) = g_\mathrm{p} = \frac{GM_\mathrm{p}}{R_\mathrm{p}^2}$	$z \ll R_\mathrm{p}$	$\left\{ \sim 10^7 < 10^8 \right.$
shallow–fluid	$r \rightarrow R_\mathrm{p}$ & $\frac{\partial}{\partial r} \rightarrow \frac{\partial}{\partial z}$	$z \ll R_\mathrm{p}$	
traditional	$\frac{uw}{r}, \frac{vw}{r}, \frac{u^2+v^2}{r}, 2\Omega(u,w)\cos\theta \rightarrow 0$	$N^2 \gg \Omega^2$	$\sim 10^{-5} \gg 10^{-10}$
hydrostasy	$\frac{\partial p}{\partial r} = -\rho g$	$H \ll L$	$\sim 10^7 < 10^8$

Usually valid but ….. because exoplanets can be crazy, they are sometimes borderline !
Mainly planets for which the atmosphere is a significant part of their radius.

See Mayne et al papers

The Limits of the Primitive Equations of Dynamics for Warm, Slowly Rotating Small Neptunes and Super Earths.

N. J. Mayne,[1] B. Drummond,[1] F. Debras,[2] E. Jaupart,[2] J. Manners,[3] I. A. Boutle,[3] I. Baraffe,[2,1] and K. Kohary[1]

General agreement of the *broad* features

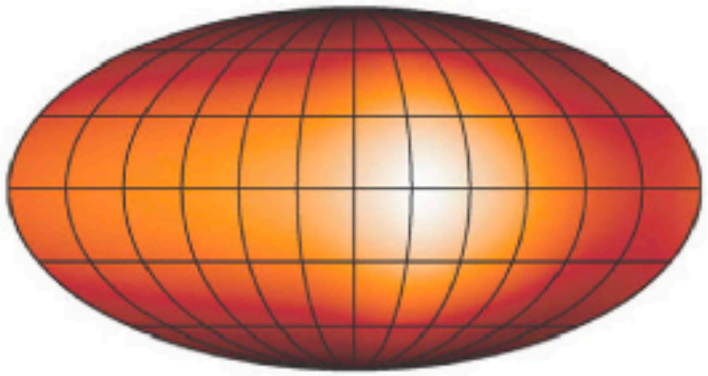

Knutson et al. (2007) (Observation)

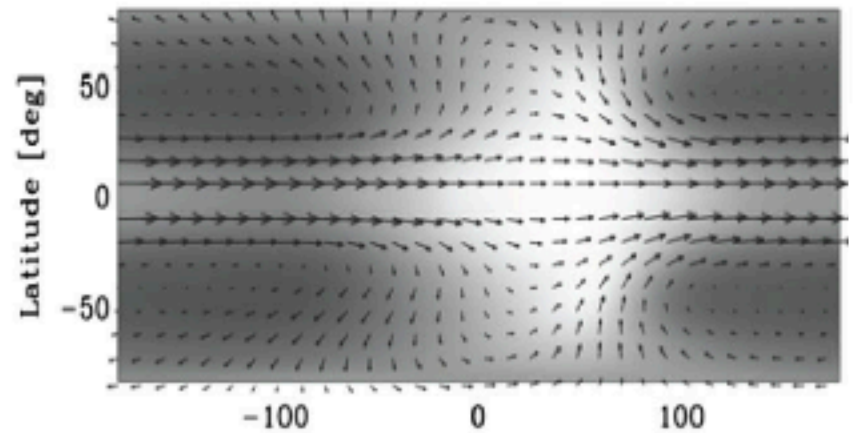

Showman & Guillot (2002)

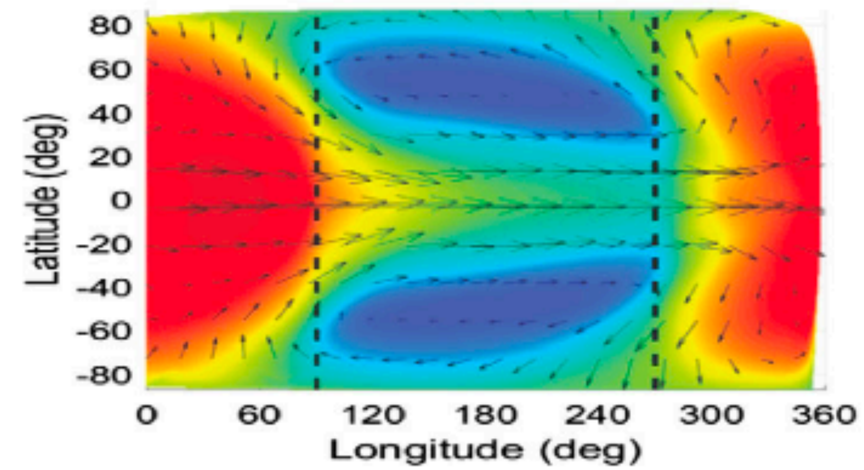

Mendonca et al. (2018)

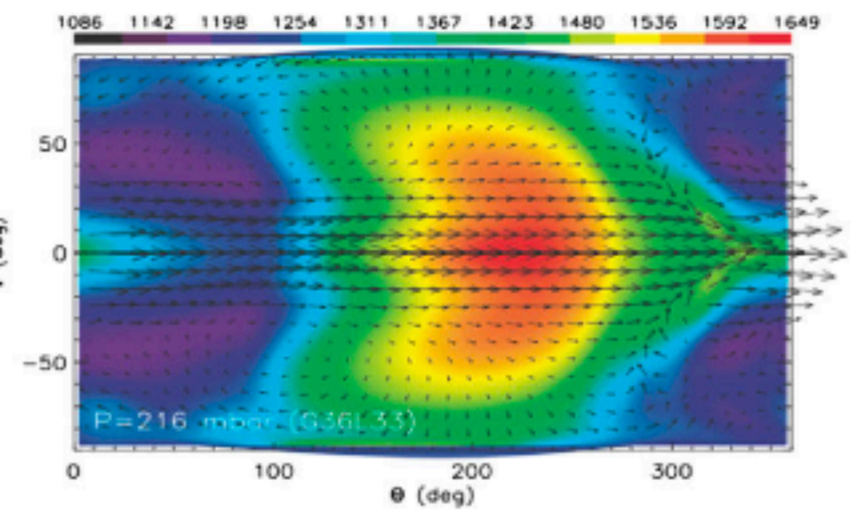

Heng et al. (2011)

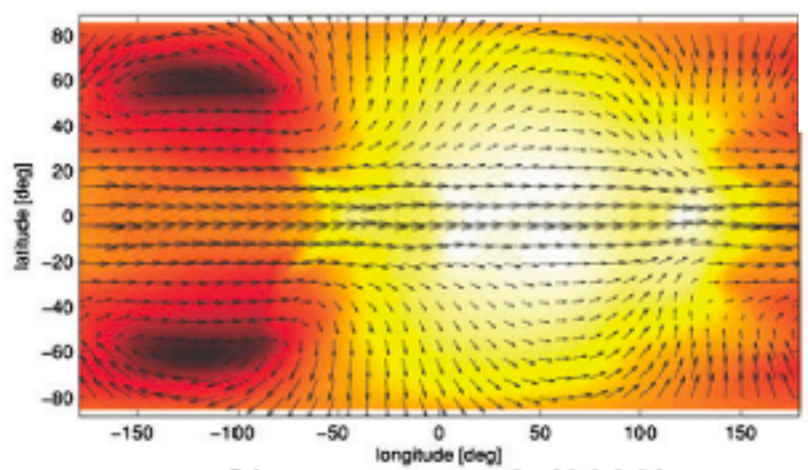

Showman et al. (2009)

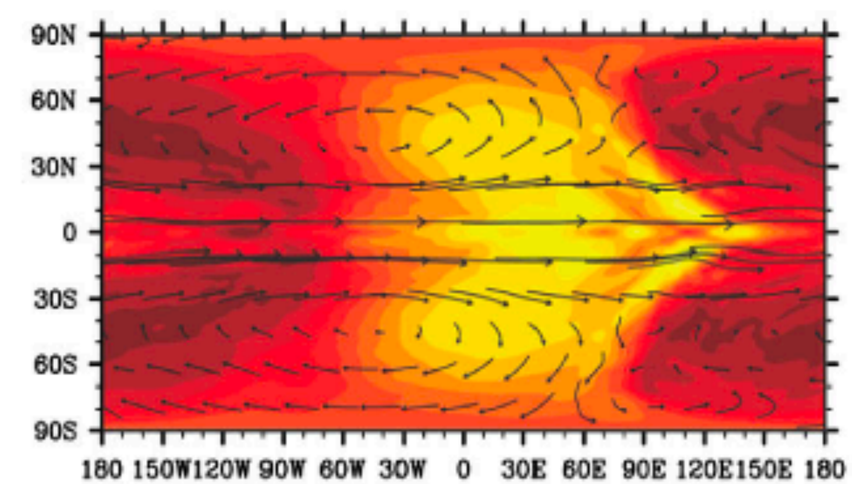

Cho et al. (2015)

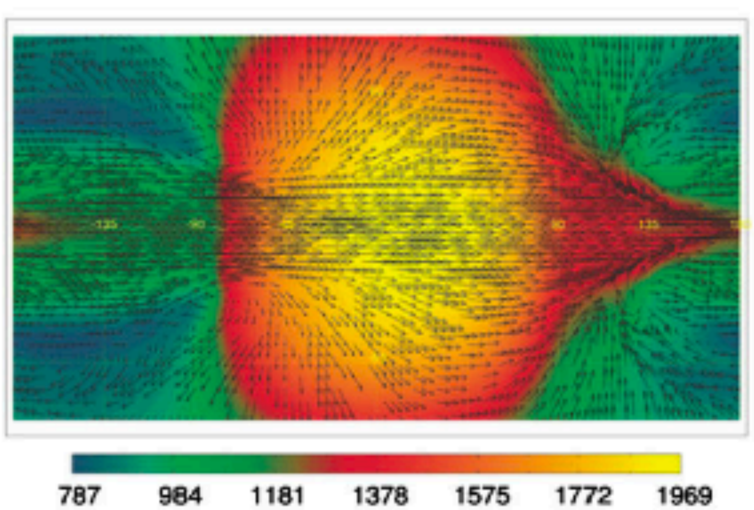

Rauscher & Menou (2012)

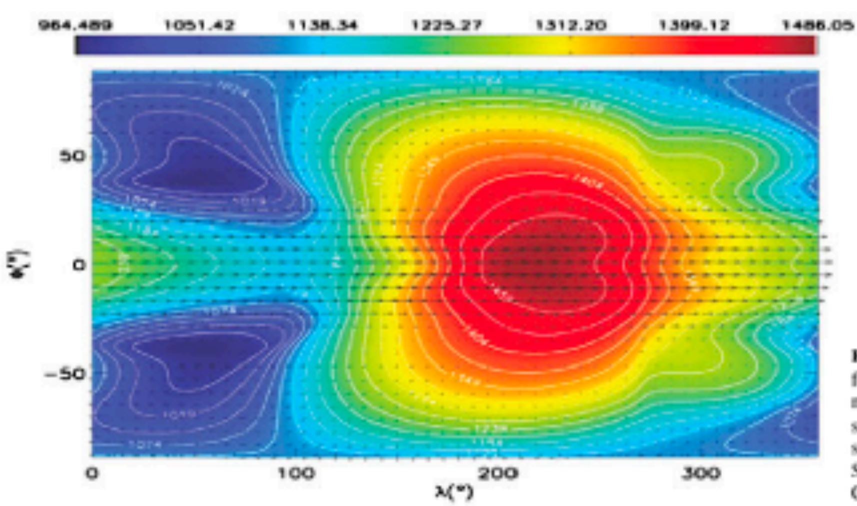

Amundsen et al. (2016)

Fig. 4 Example GCM simulations of hot Jupiters from a variety of groups in the field. Despite differences in forcing setup, numerics, and other factors, all the models exhibit similar circulation regimes, comprising significant day-night temperature differences, a fast eastward equatorial jet, and an eastward shifted dayside hot spot. All models assume synchronously rotation and conditions appropriate for typical hot Jupiters. Top left shows observations of HD 189733b from Knutson et al. (2007). Simulations of HD 209458b are shown from Showman and Guillot (2002), Heng et al. (2011b), Rauscher and Menou (2012b), Amundsen et al. (2016), Cho et al. (2015). Simulations of HD 189733b from Showman et al. (2009). Simulations of WASP-43b from Mendonça et al. (2016). These seven simulations were performed with totally distinct numerical codes, involving varying approximation of radiative forcing, and using seven independent dynamical cores. For each image, the substellar point is in the center of the panel, except for Mendonça et al. (2018), where the antistellar point is in the center

Equatorial superrotation in Hot Jupiters

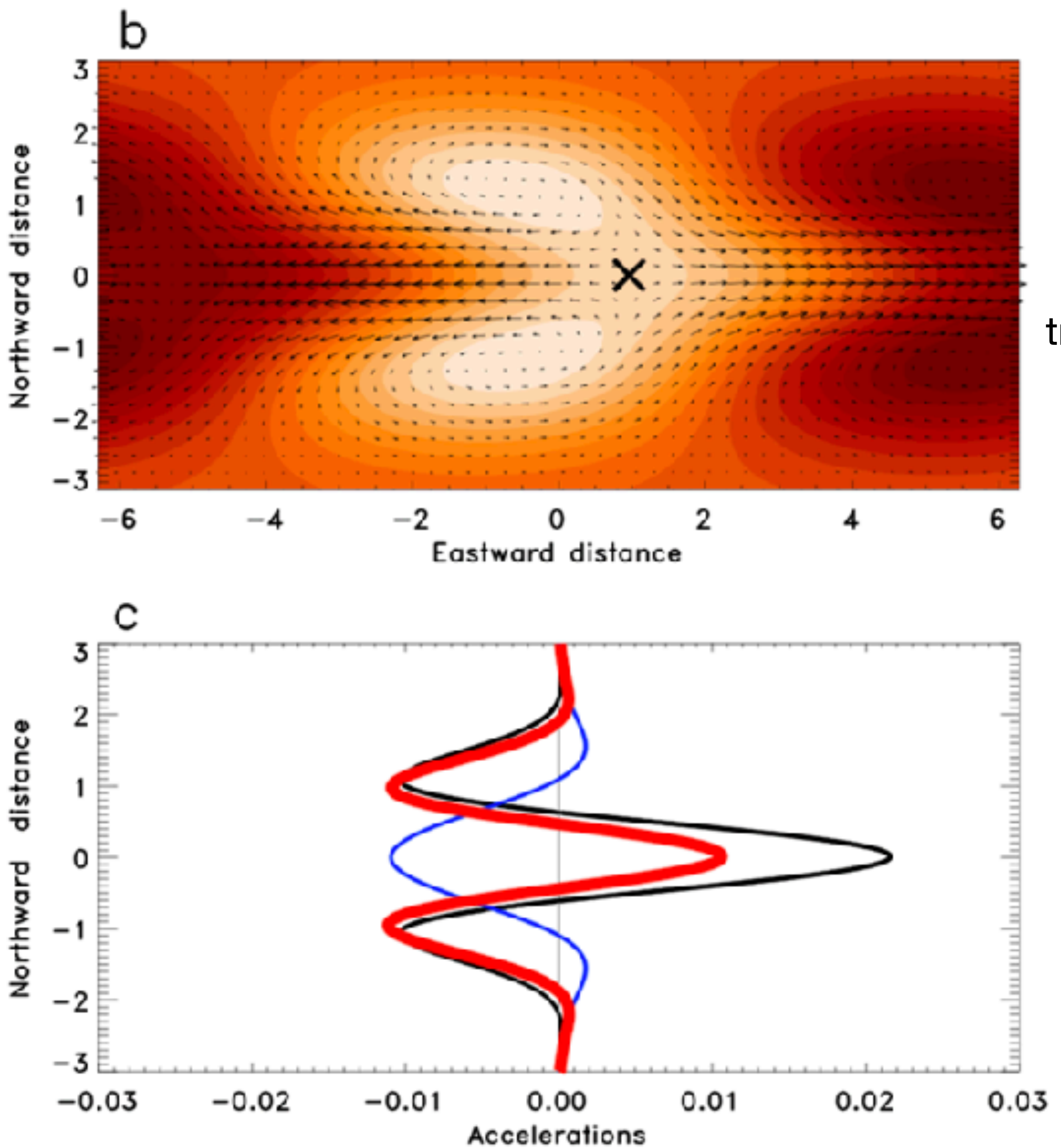

Rossby wave
at high latitude

Kelvin wave
trapped at +/-Ld latitude

Rossby wave
at high latitude

Equatorial superrotation in Hot Jupiters

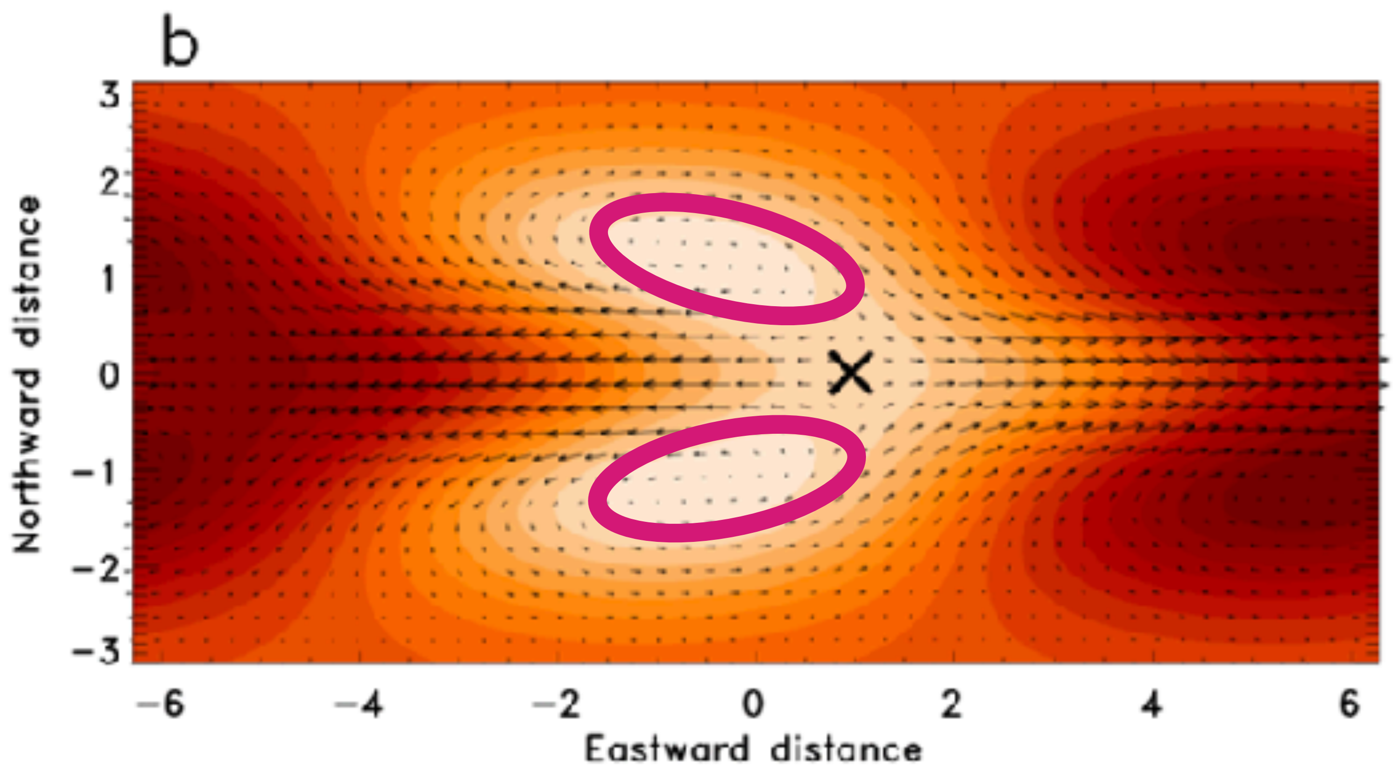

Rossby wave
at high latitude

Kelvin wave
trapped at +/-Ld latitude

Rossby wave
at high latitude

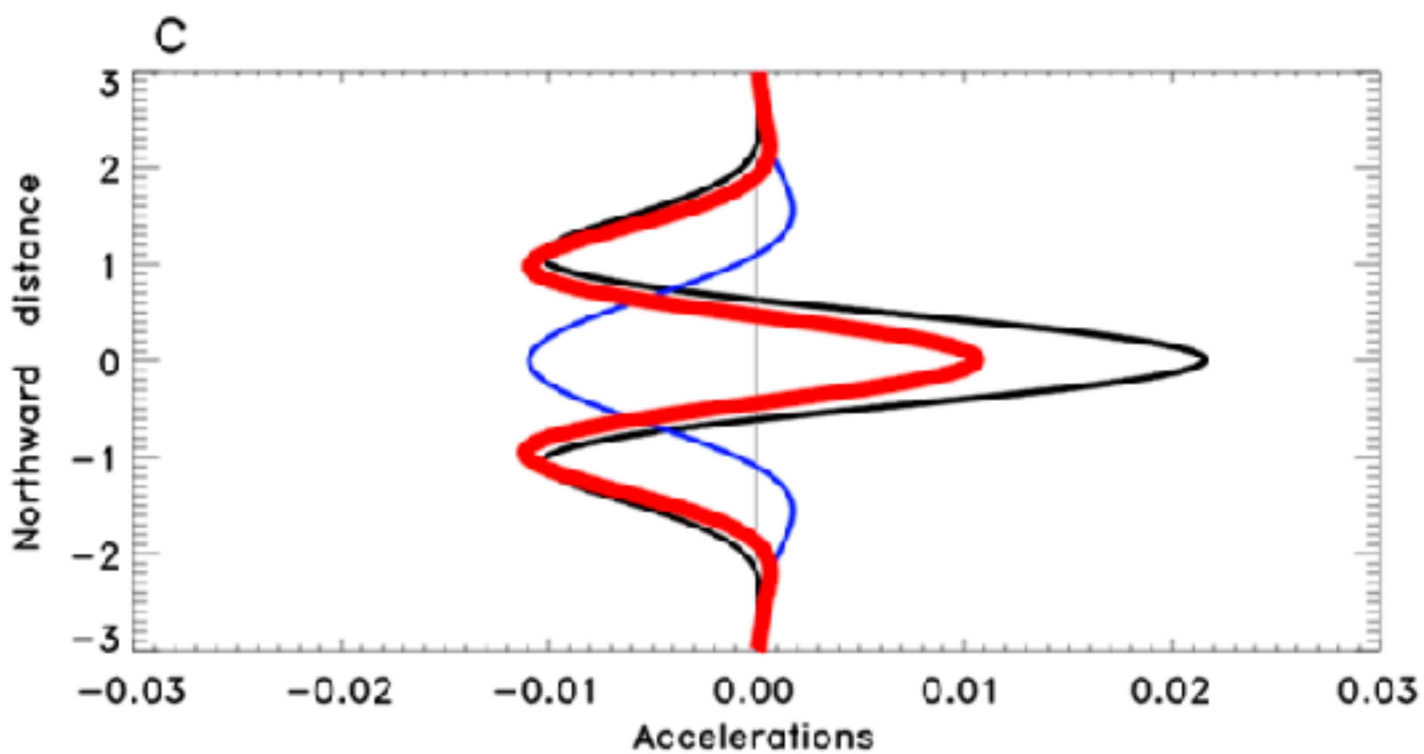

Flux of longitudinal momentum :

$$F = mu \times v$$

$$< F > = m < uv >$$

$$< F > = m < u'v' >$$

$$< F > = m < u > < v' > + m < u'v' > + m < u > < v > + m < u' > < v >$$

General agreement of the *broad* features

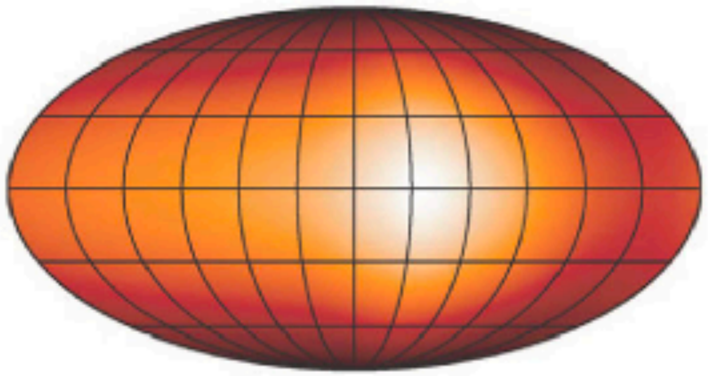

Knutson et al. (2007) (Observation)

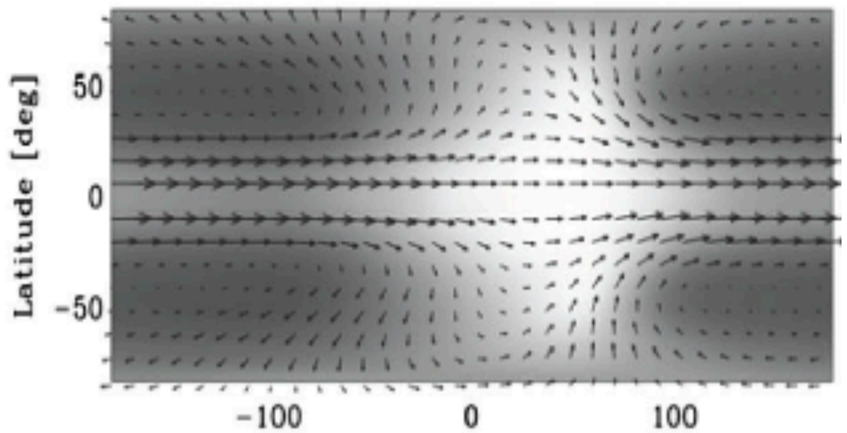

Showman & Guillot (2002)

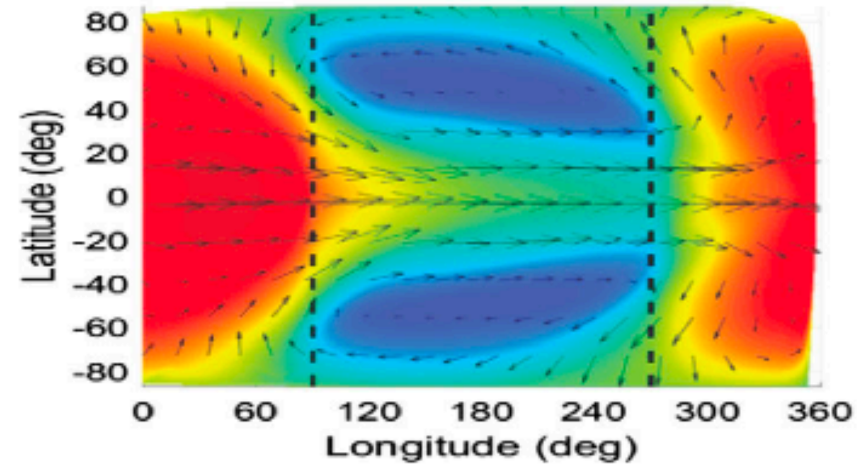

Mendonca et al. (2018)

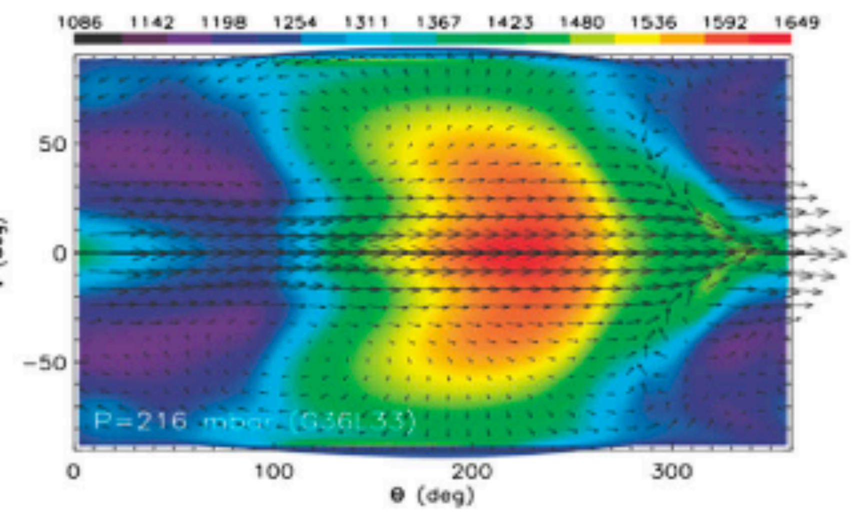

Heng et al. (2011)

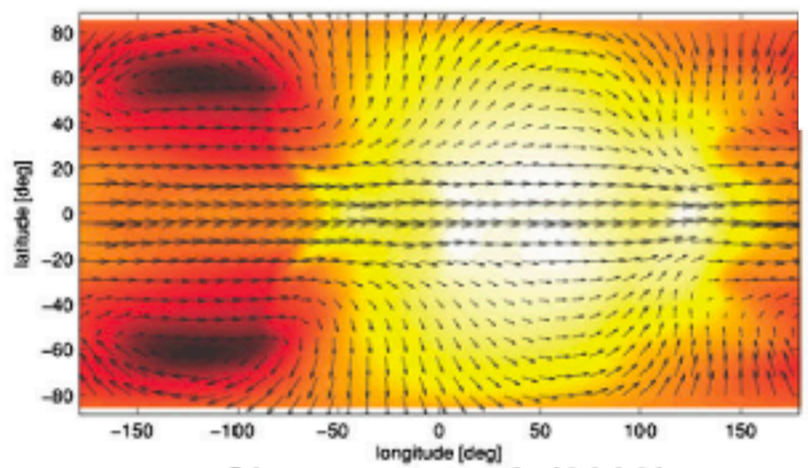

Showman et al. (2009)

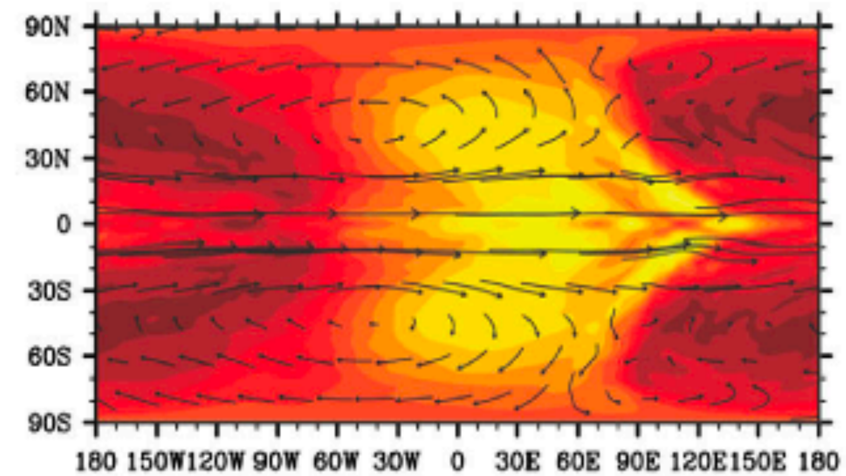

Cho et al. (2015)

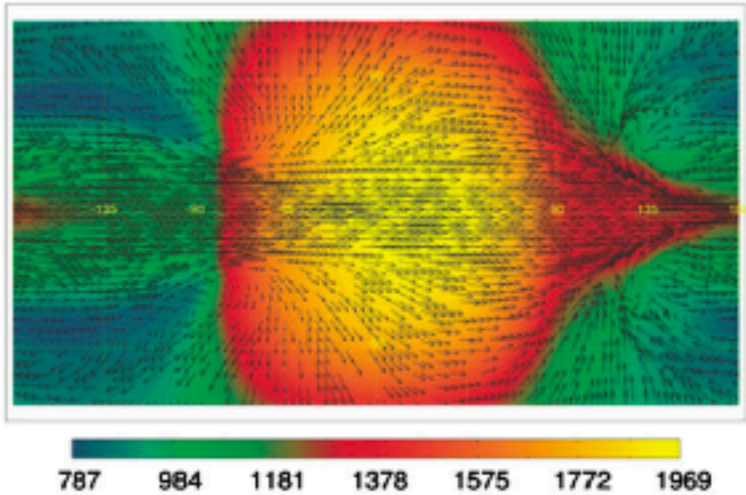

Rauscher & Menou (2012)

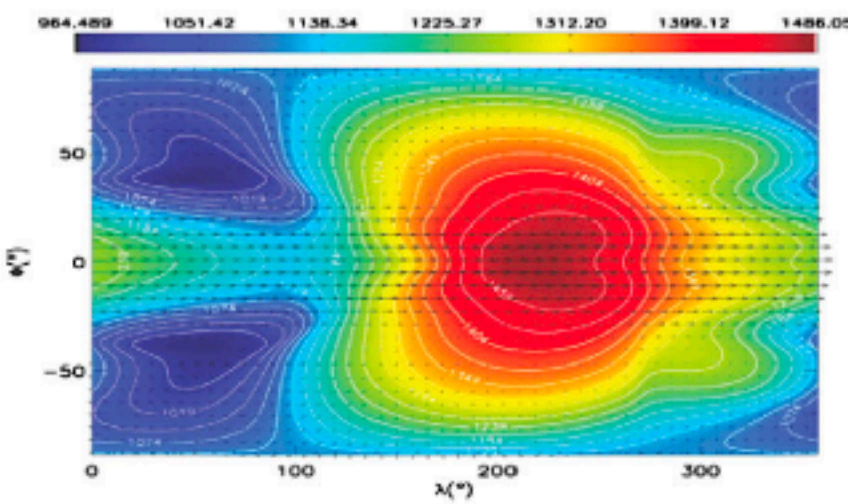

Amundsen et al. (2016)

Fig. 4 Example GCM simulations of hot Jupiters from a variety of groups in the field. Despite differences in forcing setup, numerics, and other factors, all the models exhibit similar circulation regimes, comprising significant day-night temperature differences, a fast eastward equatorial jet, and an eastward shifted dayside hot spot. All models assume synchronously rotation and conditions appropriate for typical hot Jupiters. Top left shows observations of HD 189733b from Knutson et al. (2007). Simulations of HD 209458b are shown from Showman and Guillot (2002), Heng et al. (2011b), Rauscher and Menou (2012b), Amundsen et al. (2016), Cho et al. (2015). Simulations of HD 189733b from Showman et al. (2009). Simulations of WASP-43b from Mendonça et al. (2016). These seven simulations were performed with totally distinct numerical codes, involving varying approximation of radiative forcing, and using seven independent dynamical cores. For each image, the substellar point is in the center of the panel, except for Mendonça et al. (2018), where the antistellar point is in the center

Hot Spot shift

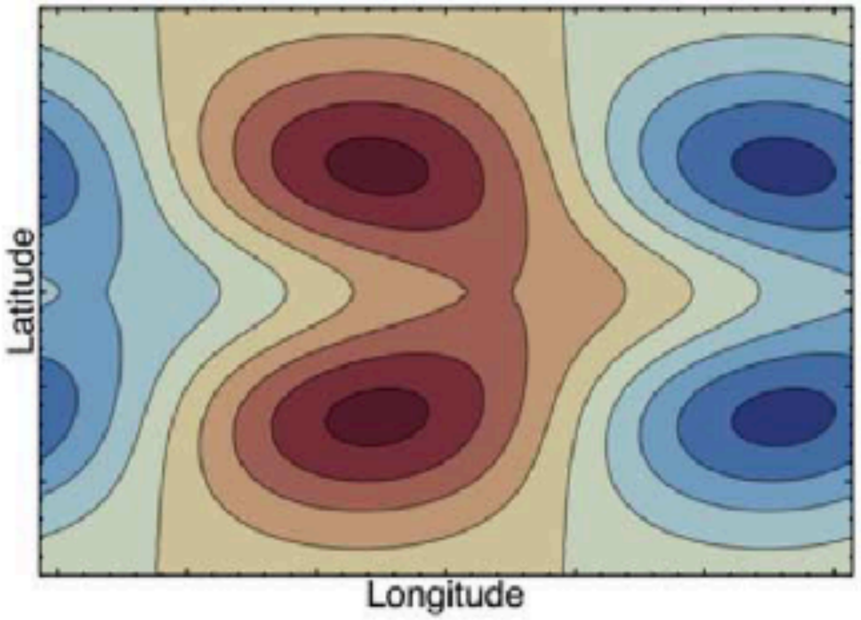

(a) **Height field of the** exact forced solution (Matsuno 1966).

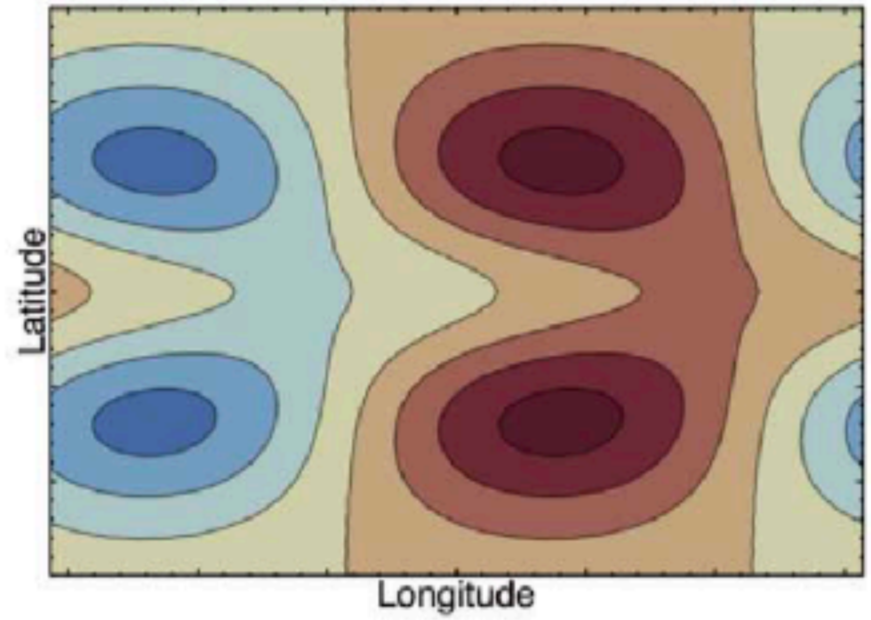

(b) Solution Doppler-shifted eastwards by jet.

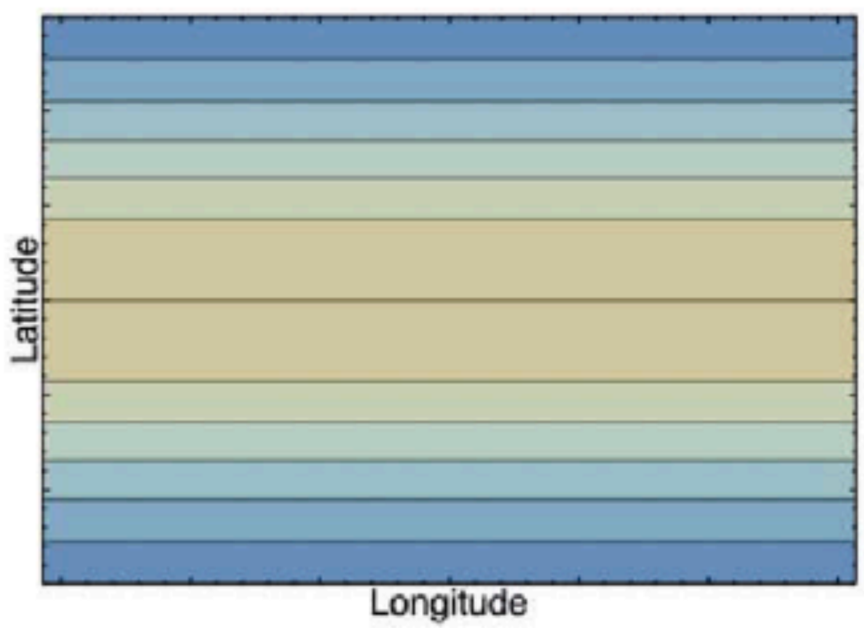

(c) Height perturbation from jet.

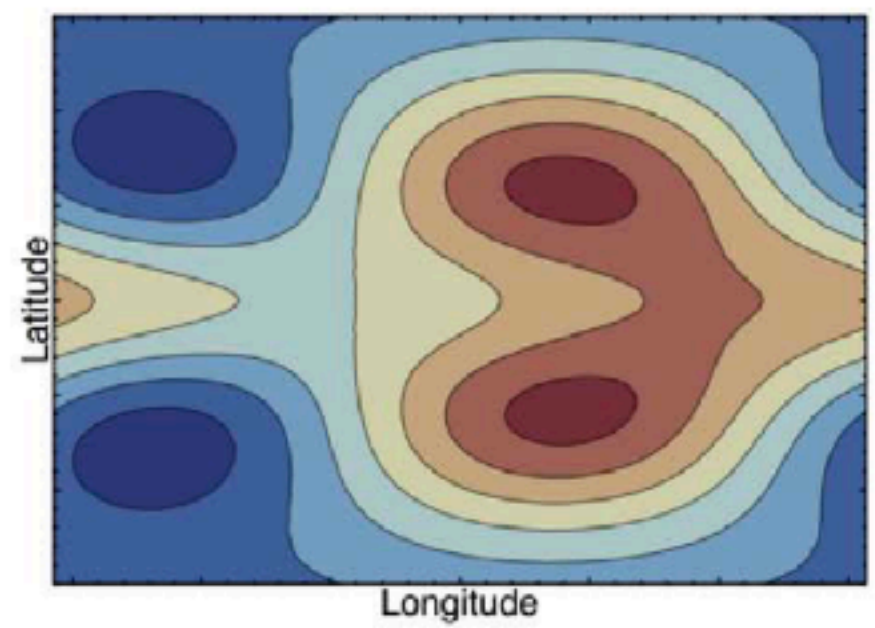

(d) Sum of (b) and (c), giving the same form as the full

Matsuno-Gill pattern

↓

Eastward jet formation

↓

Shifted Matsuno-Gill pattern

↓

Hot spot shift

Hammond & Pierrehumbert 2018

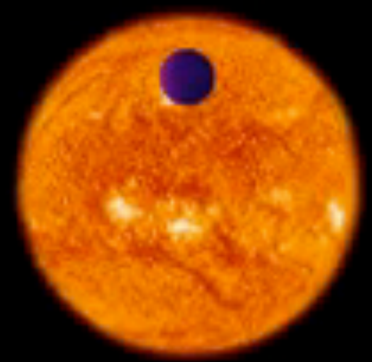

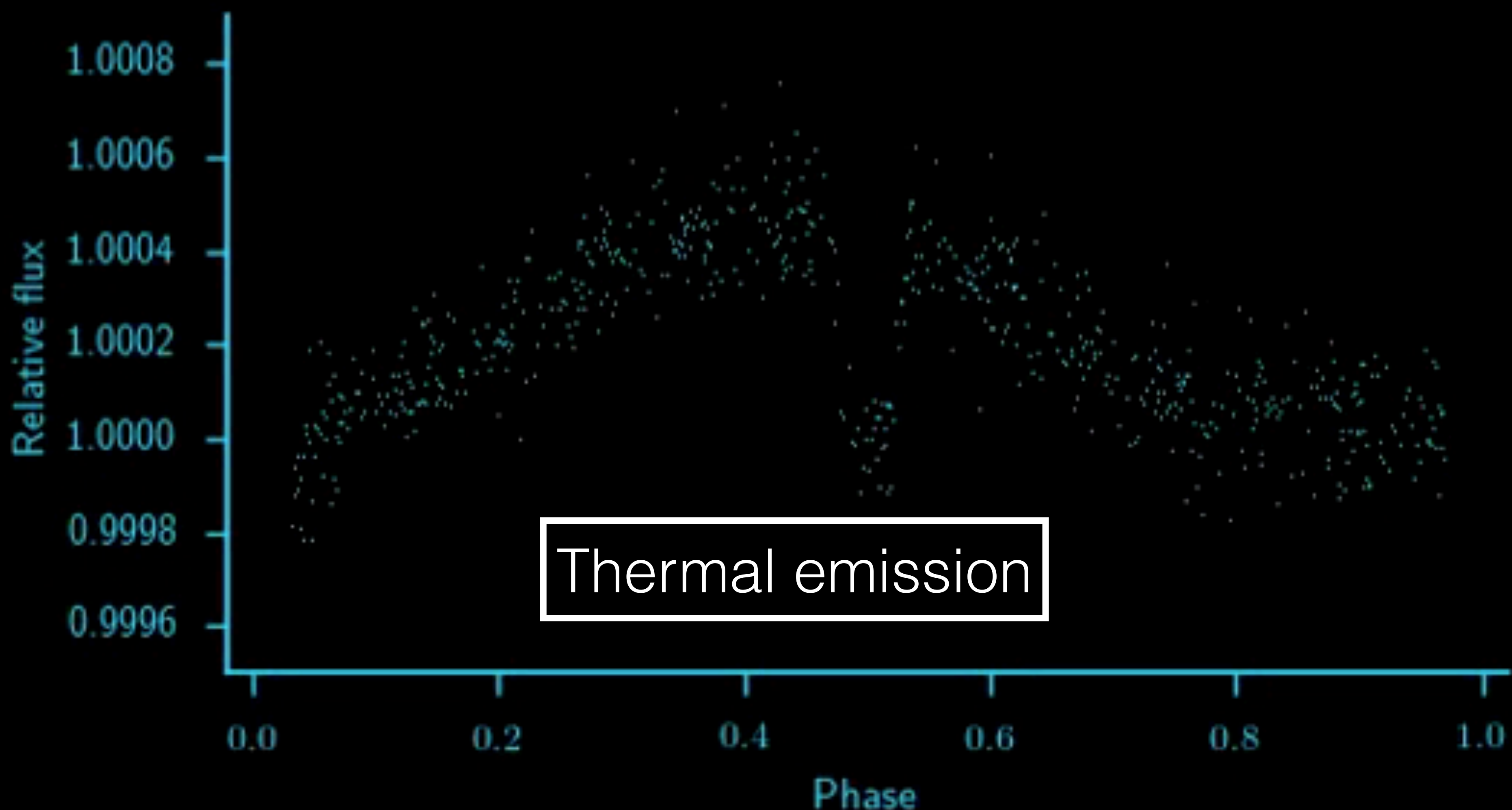

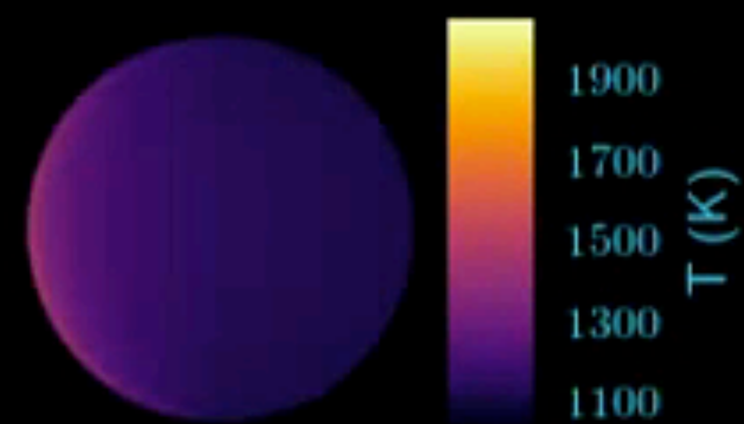

Courtesy Tom Louden

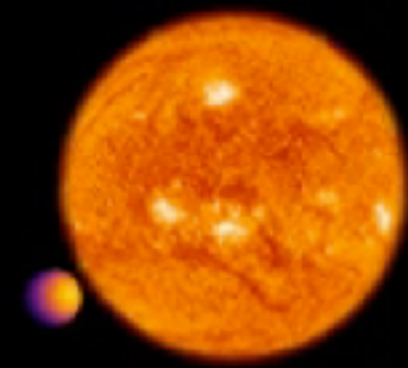

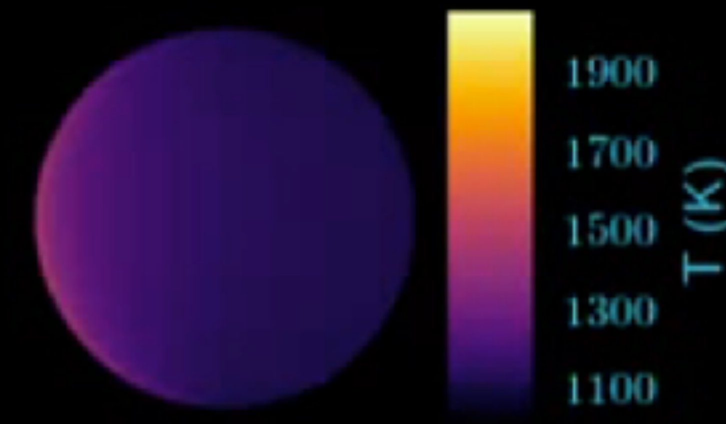

Dayside is ~ 900°C (1620°F) hotter than nightside

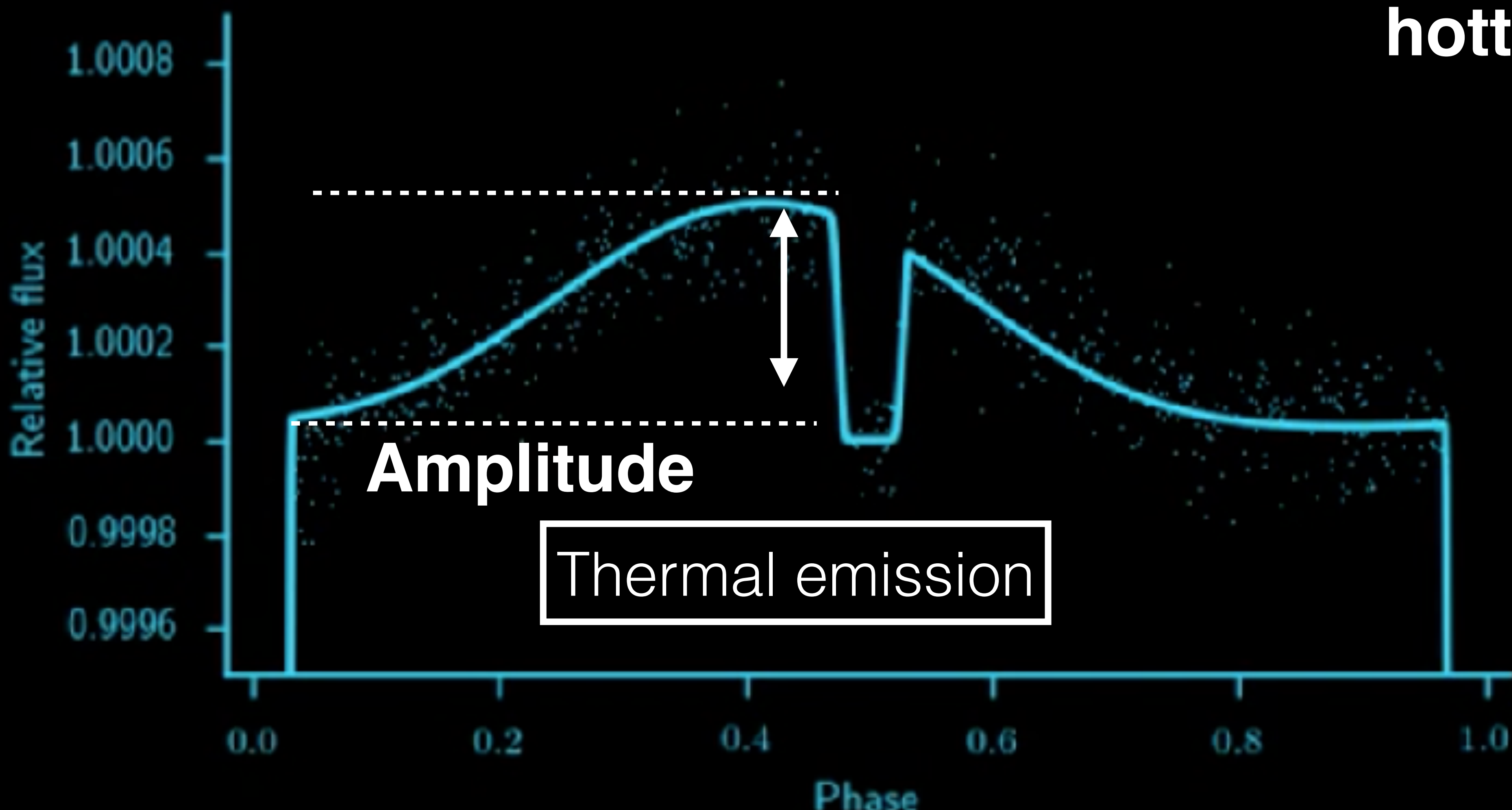

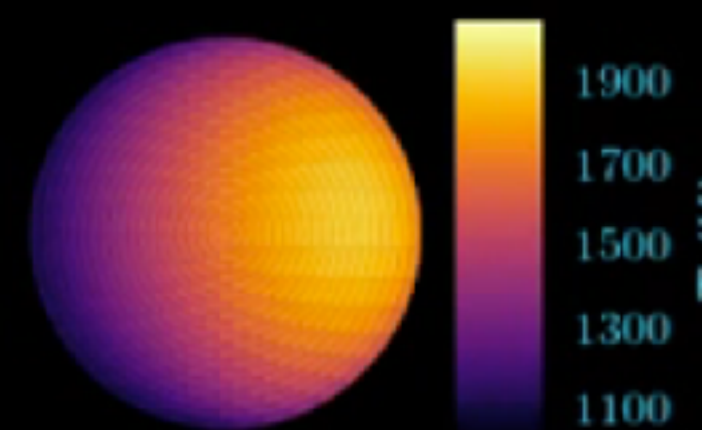

Courtesy Tom Louden

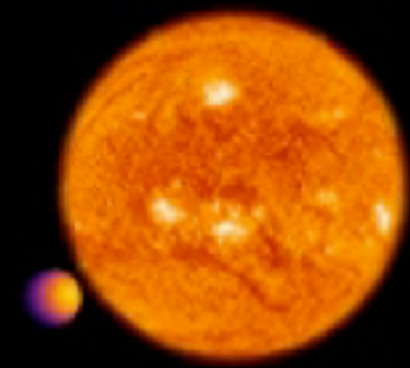

Offset of the maximum

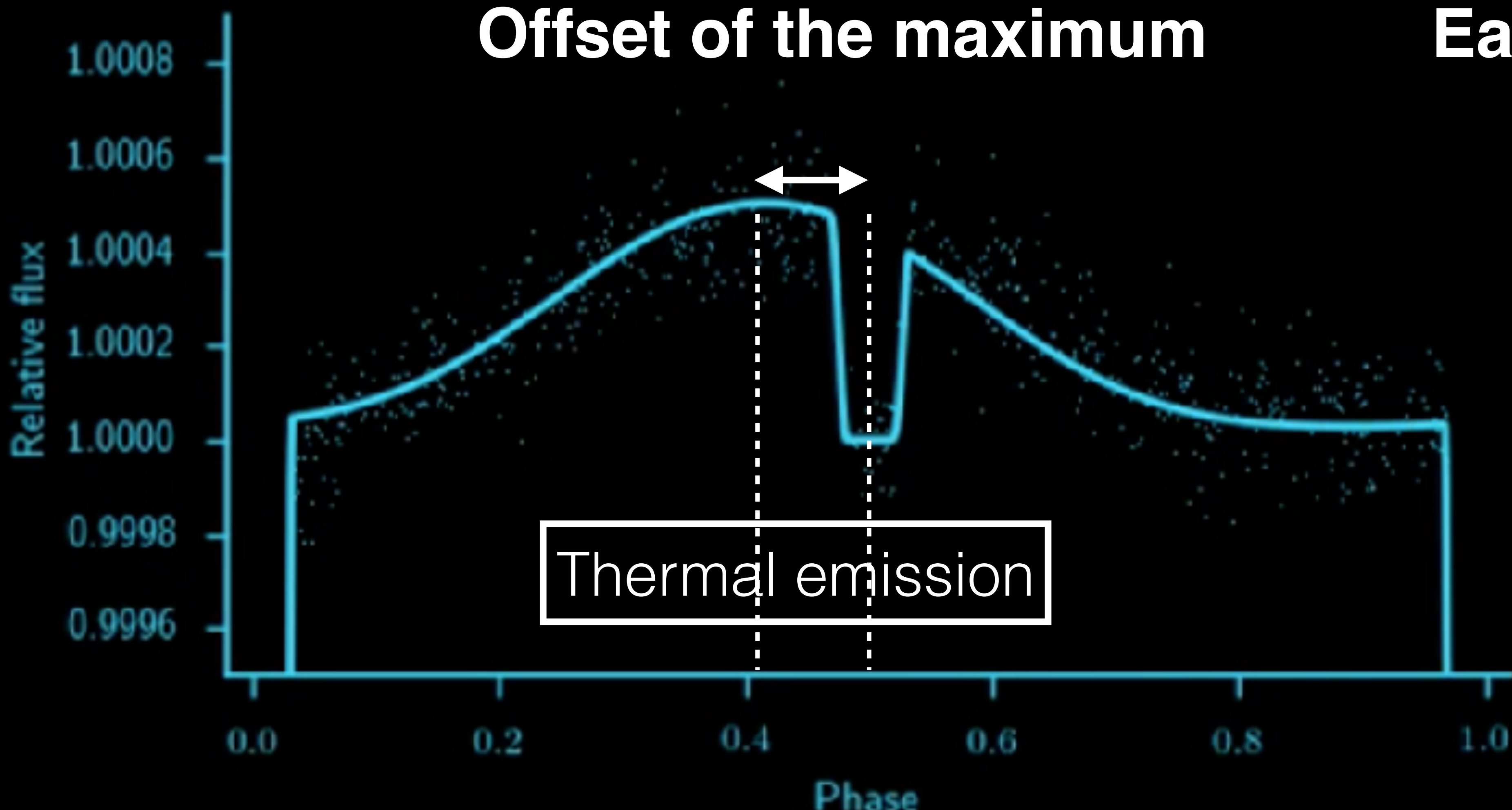

East hotter than west

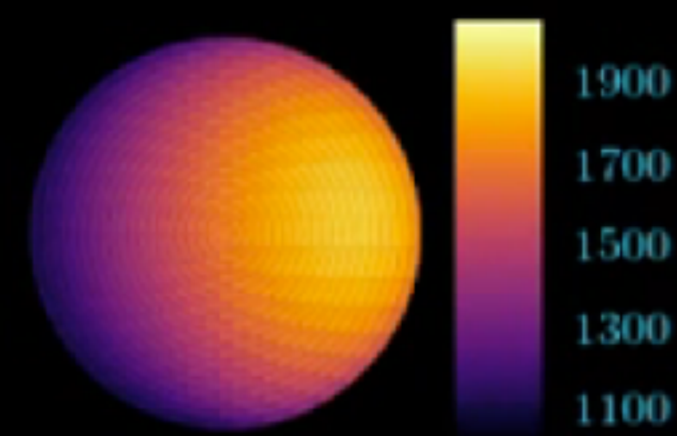

Courtesy Tom Louden

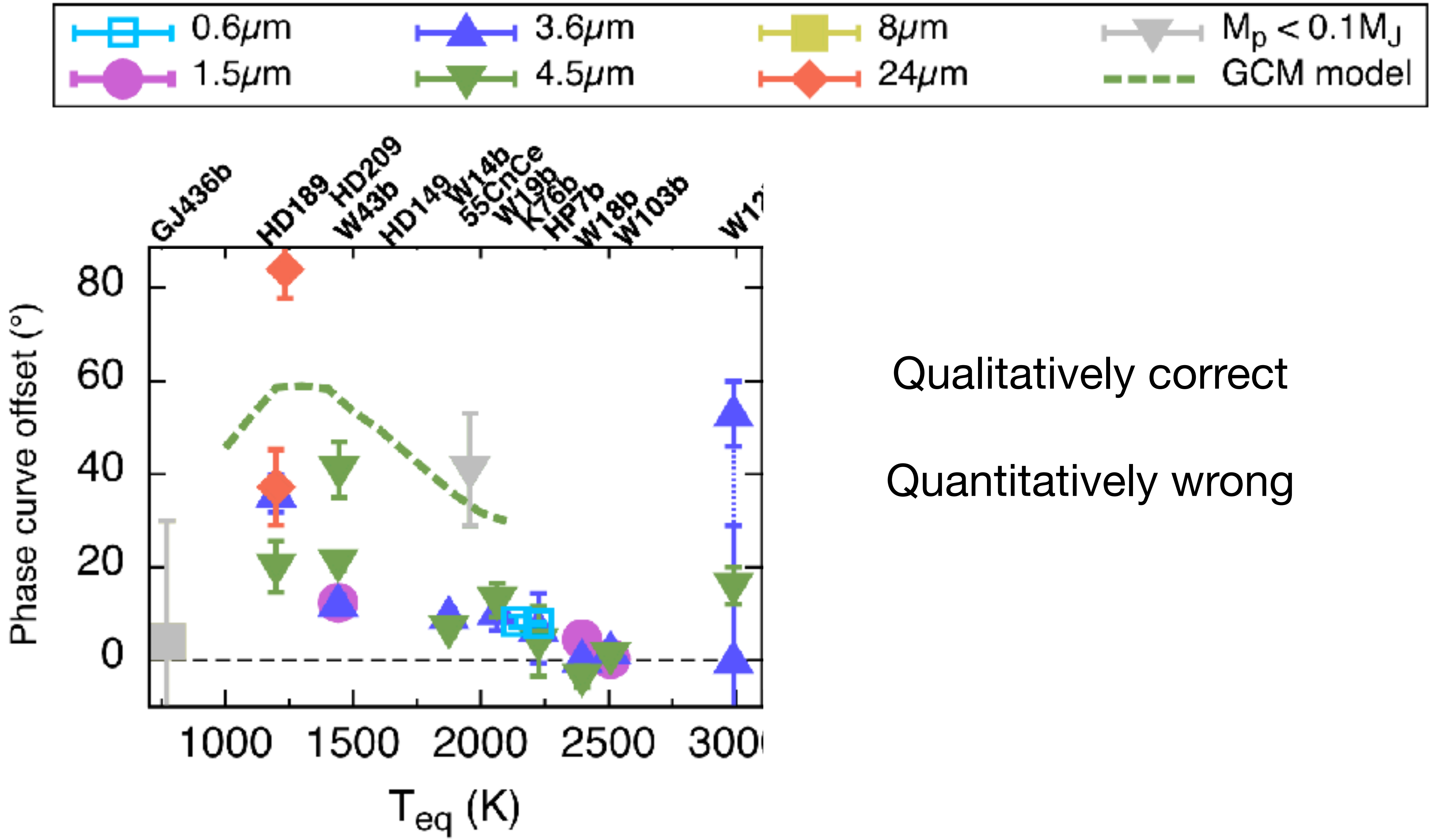

Qualitatively correct

Quantitatively wrong

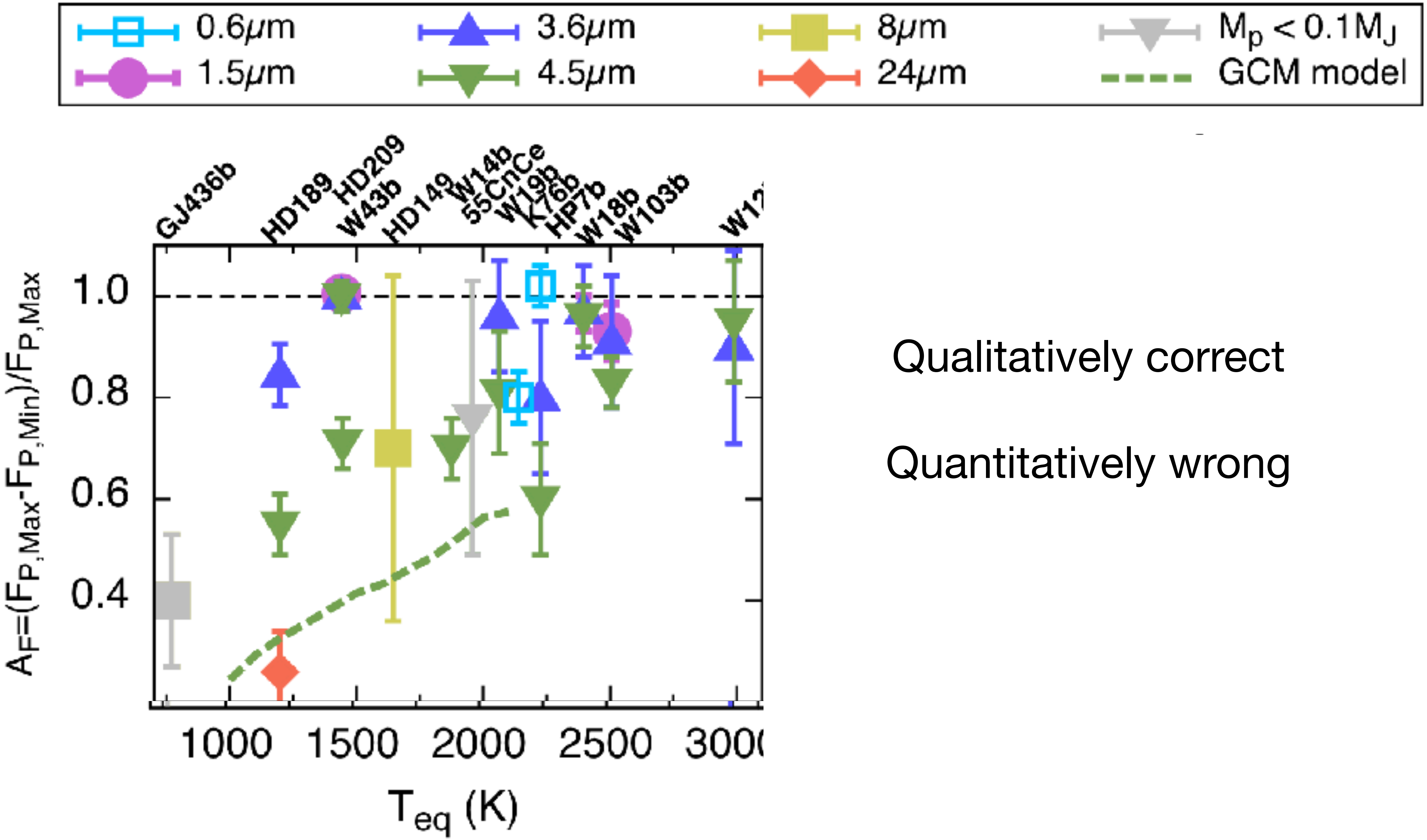

Qualitatively correct

Quantitatively wrong

Qualitative behaviour ?

Radiative timescale

$$F = 4\sigma T^3 dT$$

$$E = mc_p dT = \frac{P}{g} c_p dT$$

$$\longrightarrow \quad \frac{E}{F} = \tau_{\rm rad} \sim \frac{P}{g} \frac{c_p}{4\sigma T^3}$$

Radiative timescale

$$F = 4\sigma T^3 dT \qquad E = mc_p dT = \frac{P}{g} c_p dT$$

$$\longrightarrow \quad \frac{E}{F} = \tau_{\rm rad} \sim \frac{P}{g} \frac{c_p}{4\sigma T^3}$$

This is valid at the photosphere only !

$$\Delta T_{\text{eq}} = 1000\text{K}$$

$\tau_{\text{rad,top}}(\text{sec})$

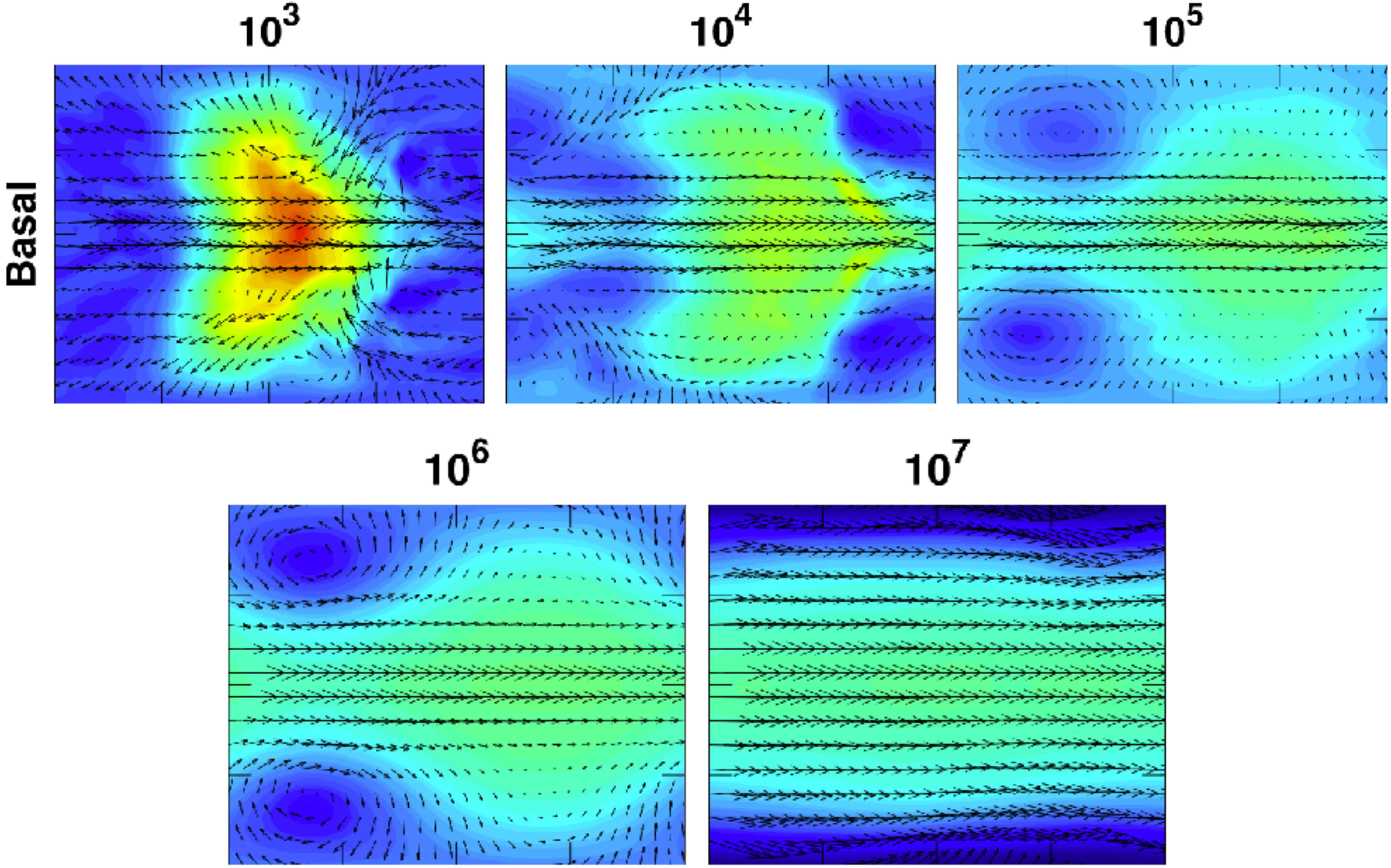

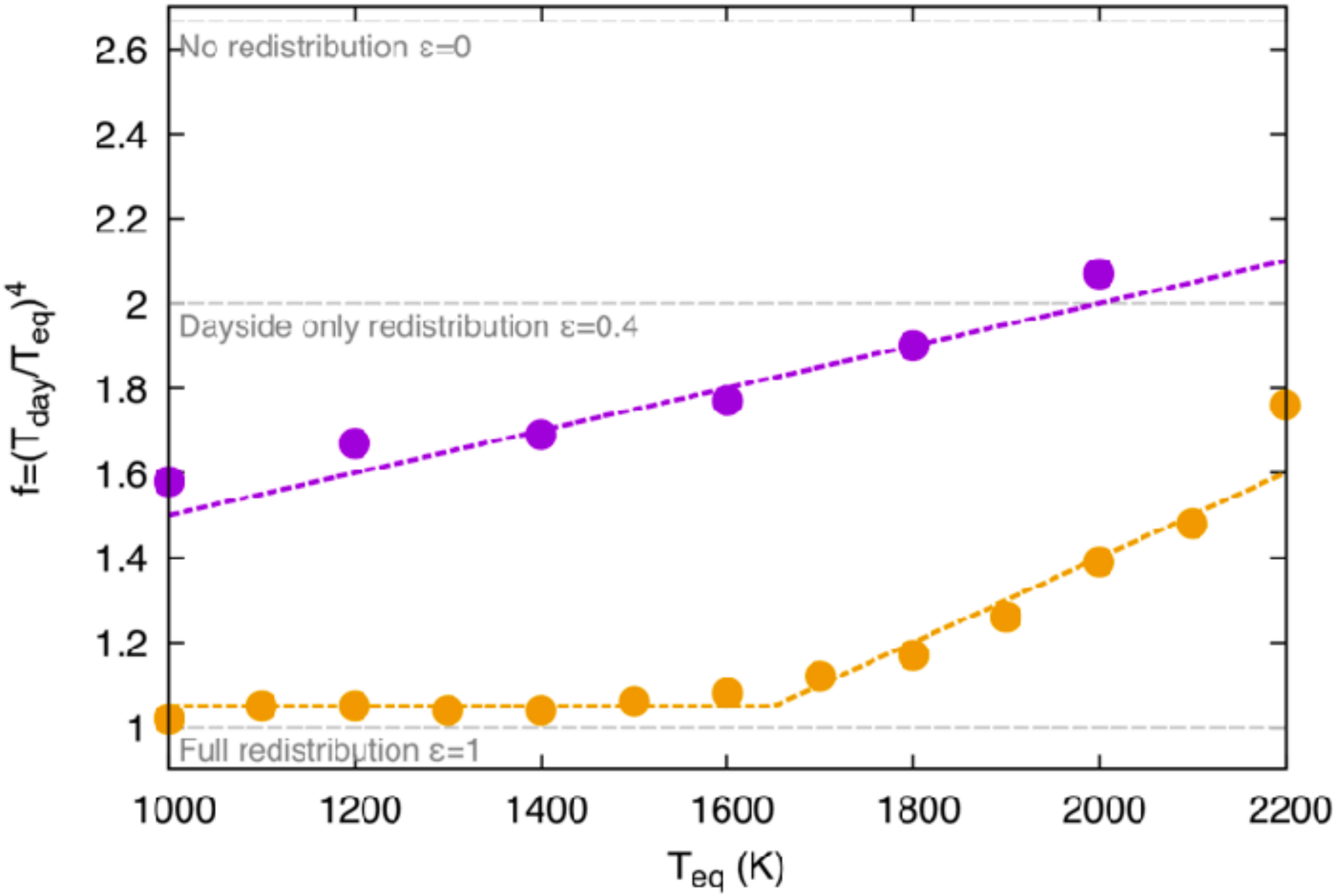

Figure 3. Heat redistribution parameter $f = (T_{\rm day}/T_{\rm eq})^4$ for models with (purple) and without (orange) nightside clouds. We additionally show the fits provided in section. 3.2. When nightside clouds are present the heat transport is much less efficient.

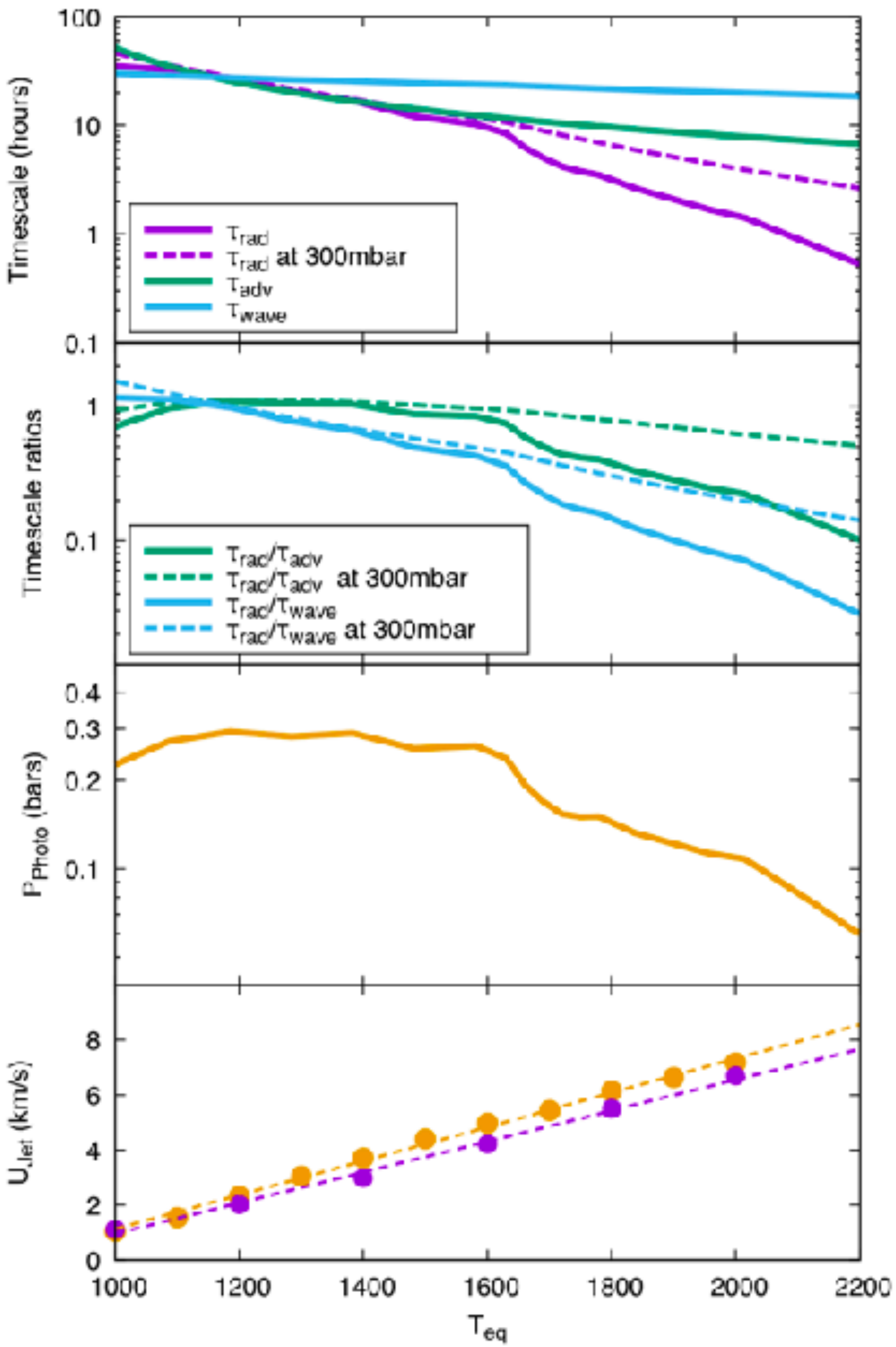

$$\tau_{\rm rad} \approx \frac{P_{\rm photo}}{g}\frac{c_{\rm p}}{4\sigma T_{\rm photo}^3} \propto \frac{P_{\rm photo}}{T_{\rm photo}^3};$$

$$\tau_{\rm wave} \approx \frac{\pi R_p}{\sqrt{k_{\rm B} T_{\rm photo}/\mu}} \propto \frac{1}{\sqrt{T_{\rm photo}}}.$$

$$\tau_{\rm adv} \approx \frac{\pi R_{\rm p}}{U_{\rm jet}} \propto \frac{1}{T_{\rm eq}}.$$

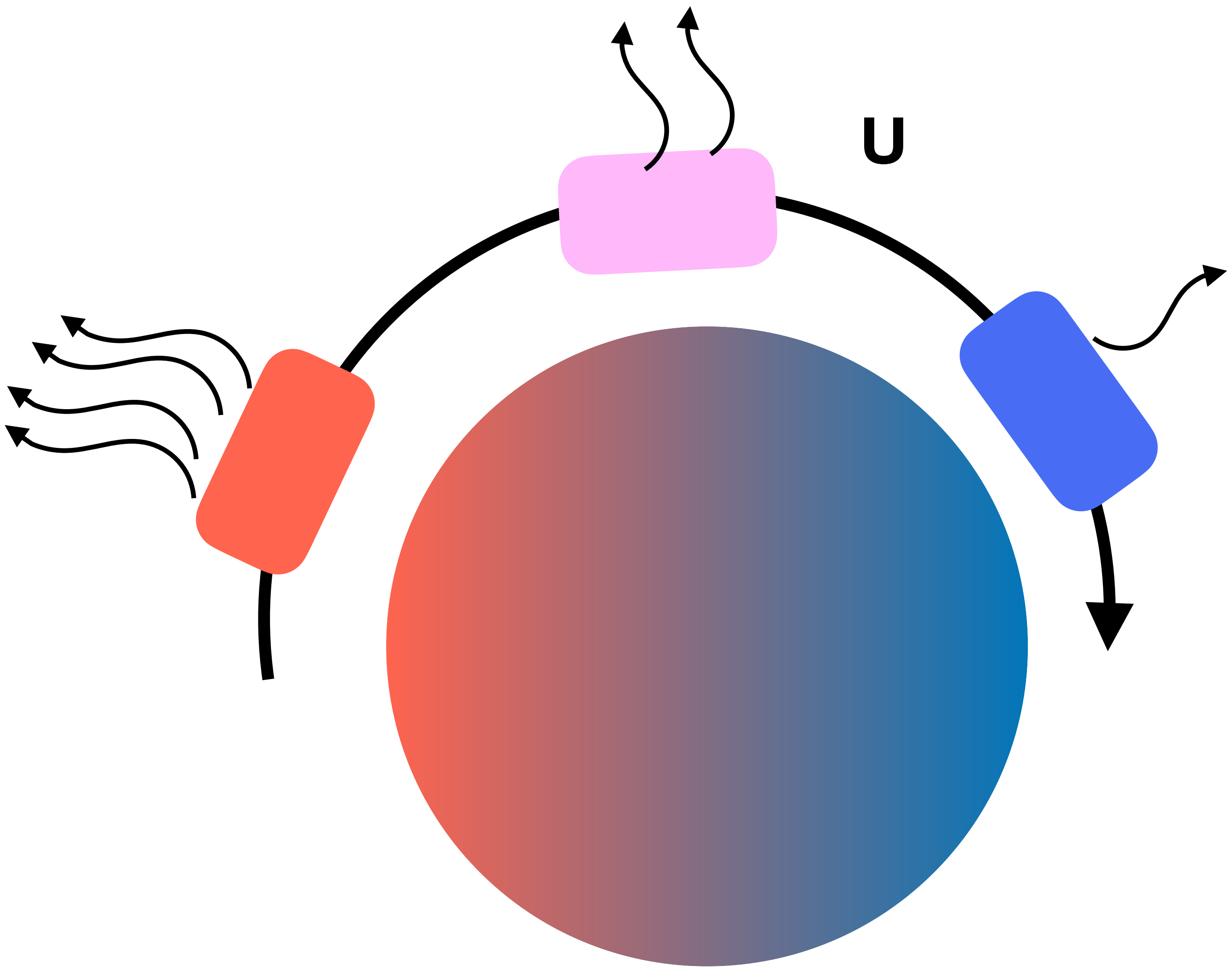

$$\tau_{\rm rad}\left(T_{\rm night}\right) \approx \tau_{\rm adv}$$

$$T_{\rm night} \approx \left(\frac{P_{\rm photo}}{g}\frac{c_{\rm p}}{4\sigma}\frac{U_{\rm jet}}{\pi R_{\rm p}}\right)^{1/3}$$

$$T_{\rm night} \propto \left(T_{\rm eq}\right)^{1/3}$$

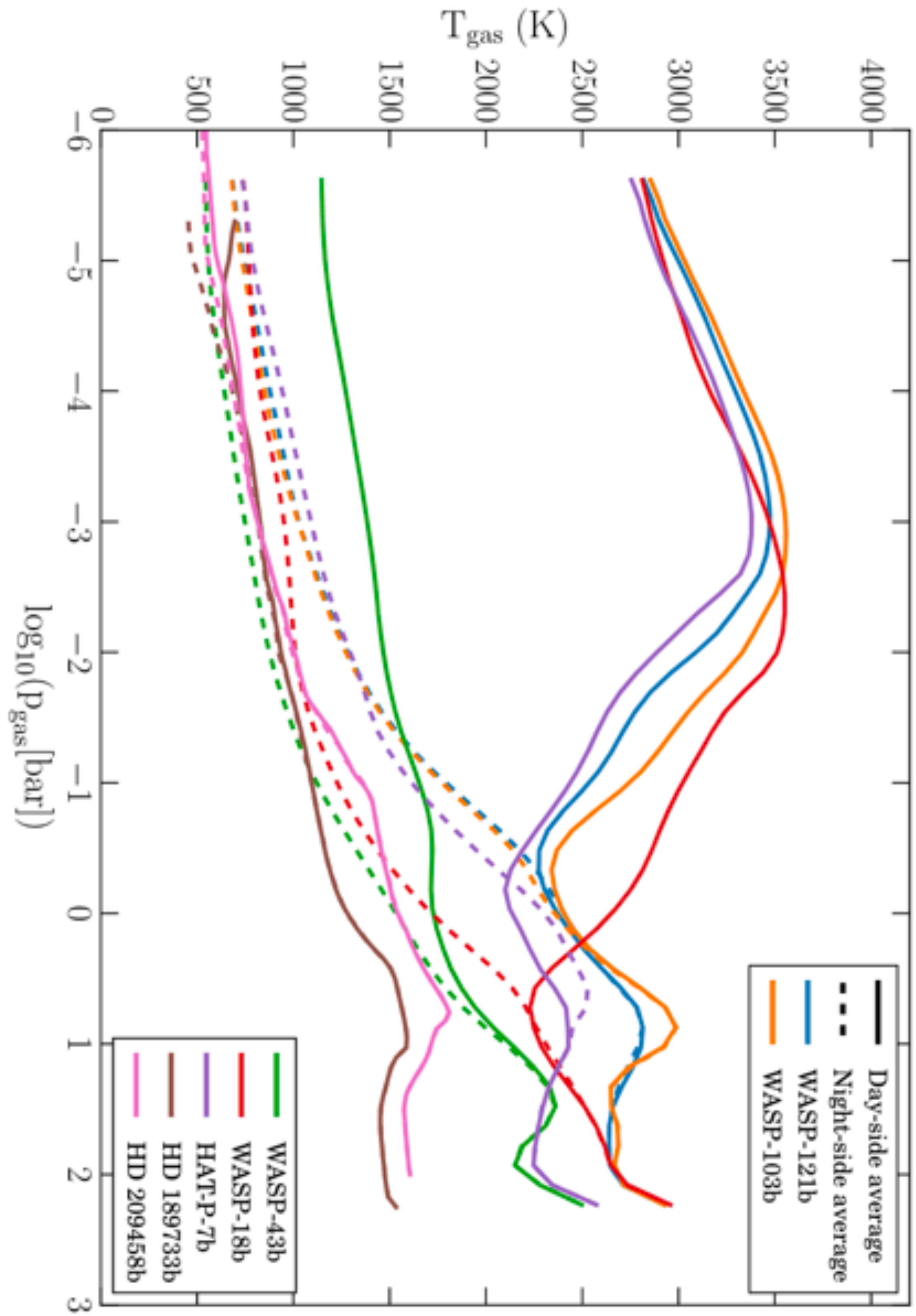

$$\tau_{\rm rad}\left(T_{\rm night}\right) \approx \tau_{\rm adv}$$

$$T_{\rm night} \approx \left(\frac{P_{\rm photo}}{g}\,\frac{c_{\rm p}}{4\sigma}\,\frac{U_{\rm jet}}{\pi R_{\rm p}}\right)^{1/3}$$

$$T_{\rm night} \propto \left(T_{\rm eq}\right)^{1/3}$$

Helling et al. 2020

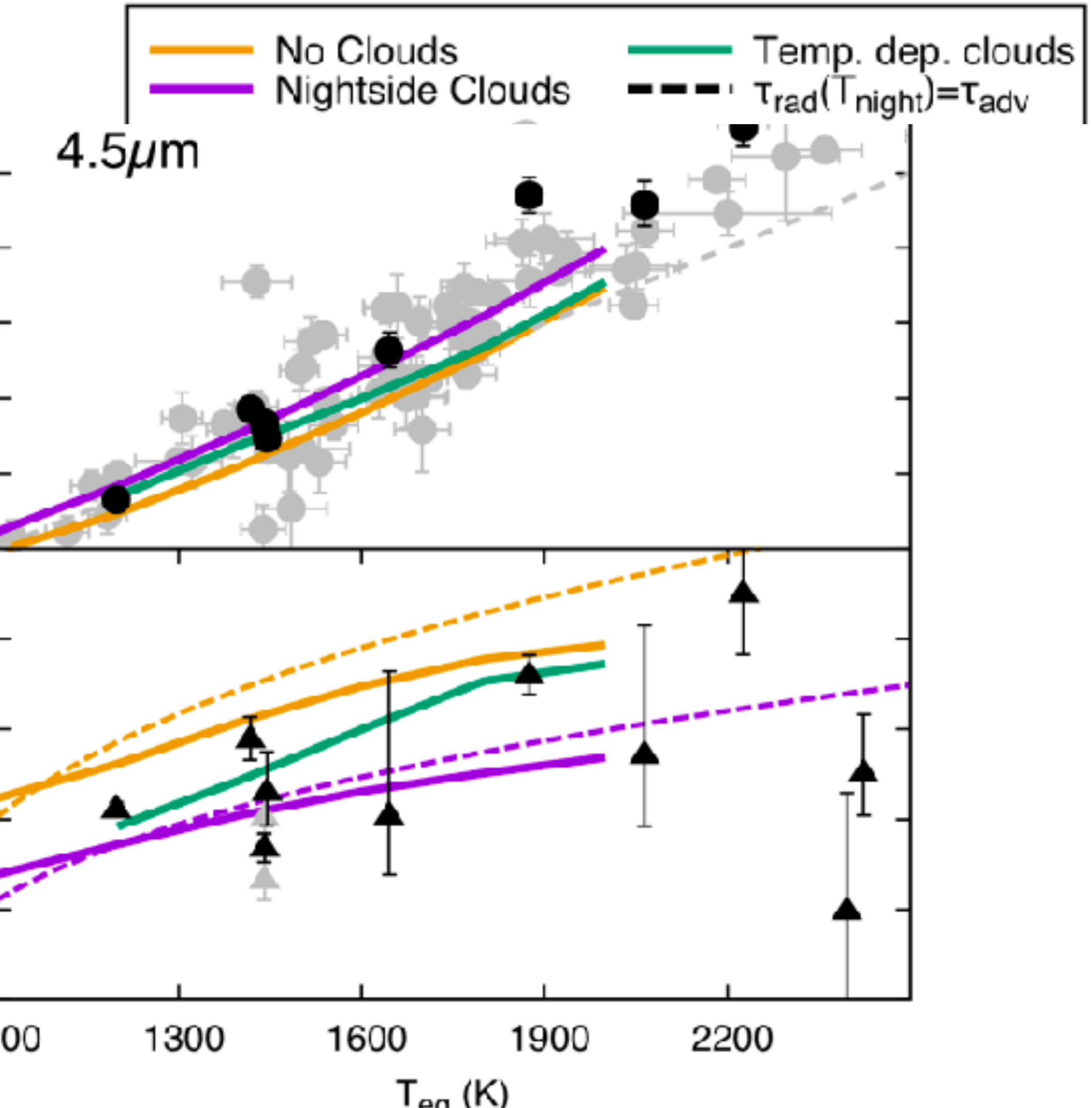

$$\tau_{\rm rad}\left(T_{\rm night}\right) \approx \tau_{\rm adv}$$

$$T_{\rm night} \approx \left(\frac{P_{\rm photo}}{g}\,\frac{c_{\rm p}}{4\sigma}\,\frac{U_{\rm jet}}{\pi R_{\rm p}}\right)^{1/3}$$

$$T_{\rm night} \propto \left(T_{\rm eq}\right)^{1/3}$$

All hot Jupiters have roughly the same nightside temperature because of the strong temperature dependance of the radiative timescale to temperature !

And clouds help….

Parmentier et al. 2020

Temperature and clouds of a Hot Jupiter with SPARC/MITgcm

G*lobal* ***C****irculation* ***M****odel* : solves the primitive equation, Euler equation adapted to atmospheres
SPARC : solves the radiative energy balance with non-grey, molecular opacities

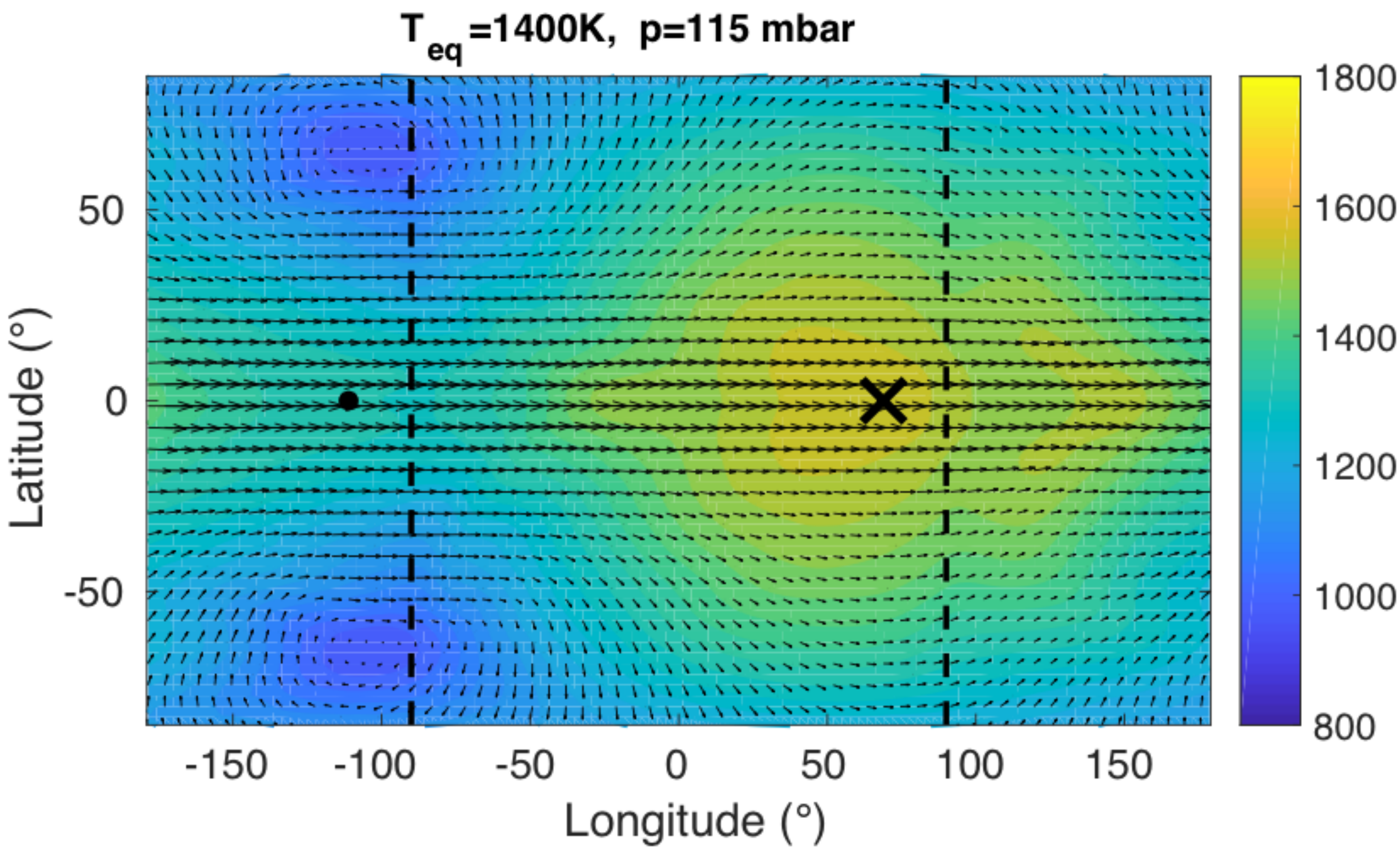

Parmentier+ in prep.

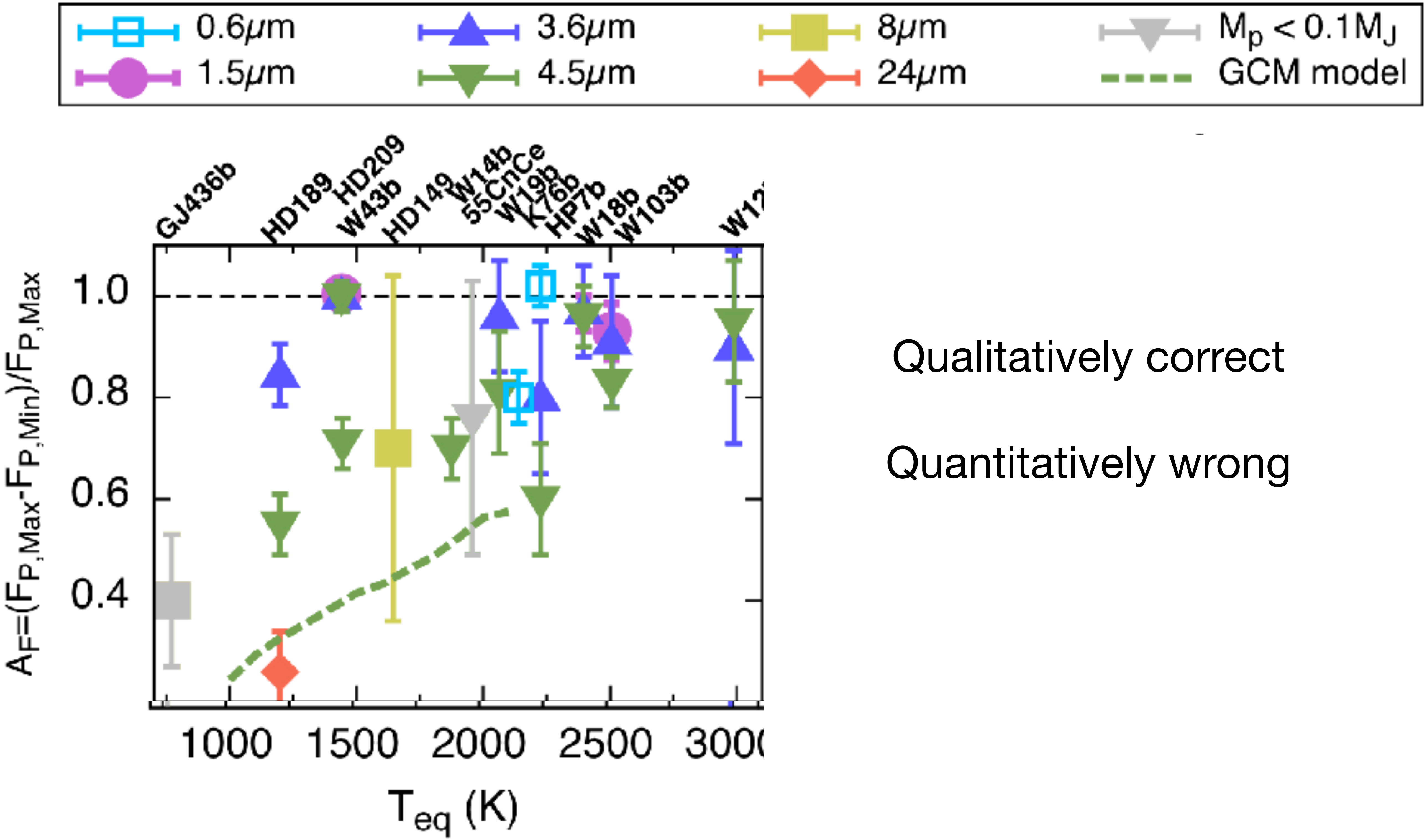

Qualitatively correct

Quantitatively wrong

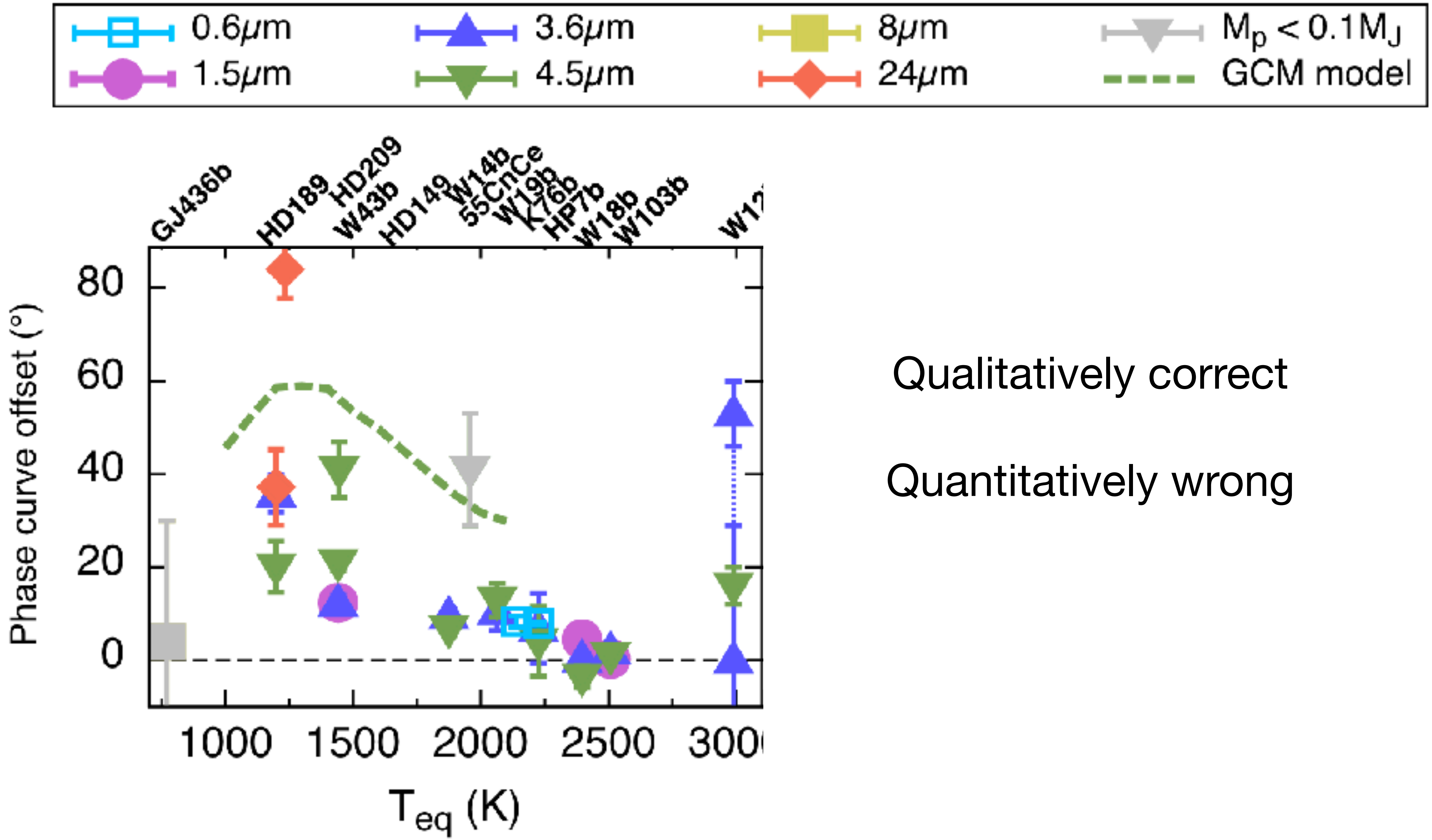

Qualitatively correct

Quantitatively wrong

Dissipation ?

Numerical drag, essential for models ?

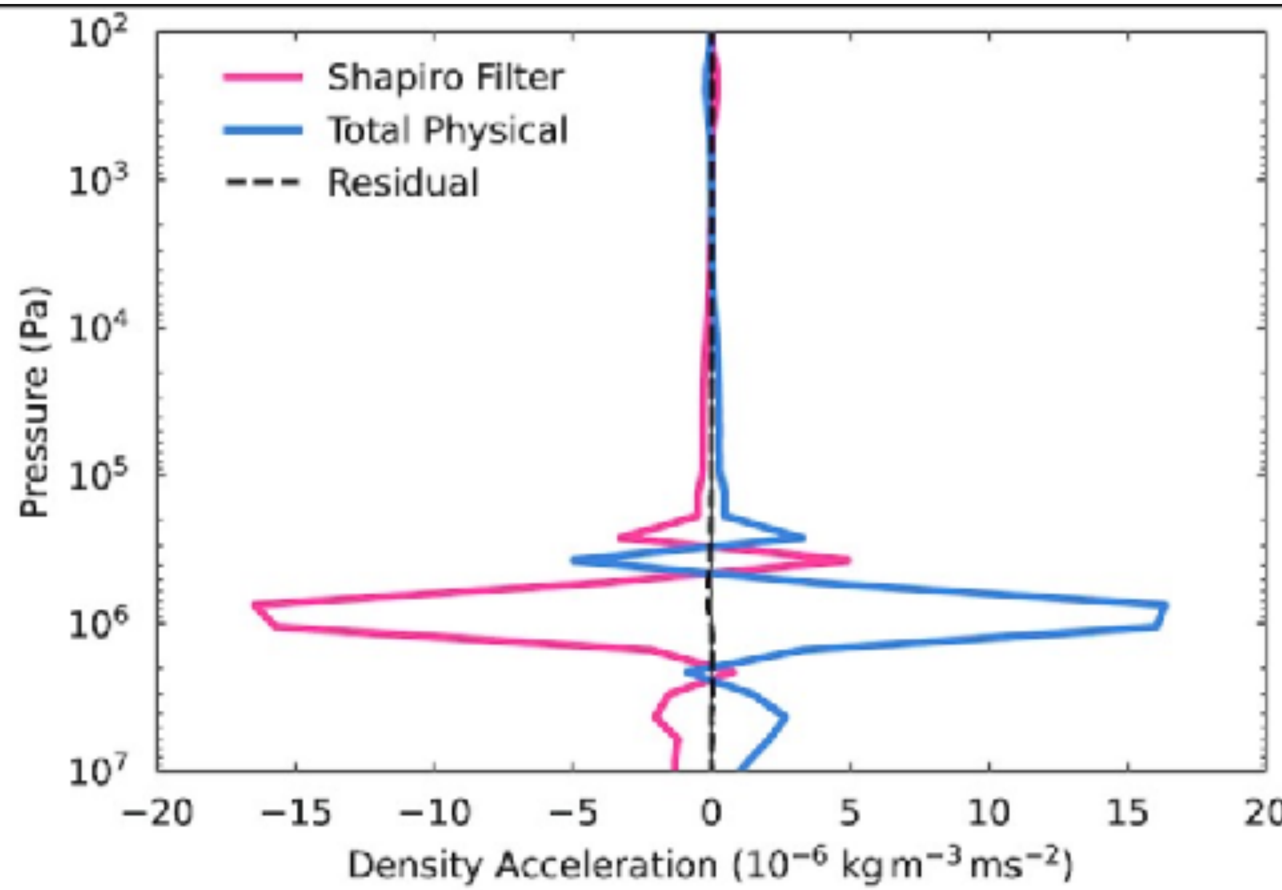

(b) MITgcm: Zonal momentum budget

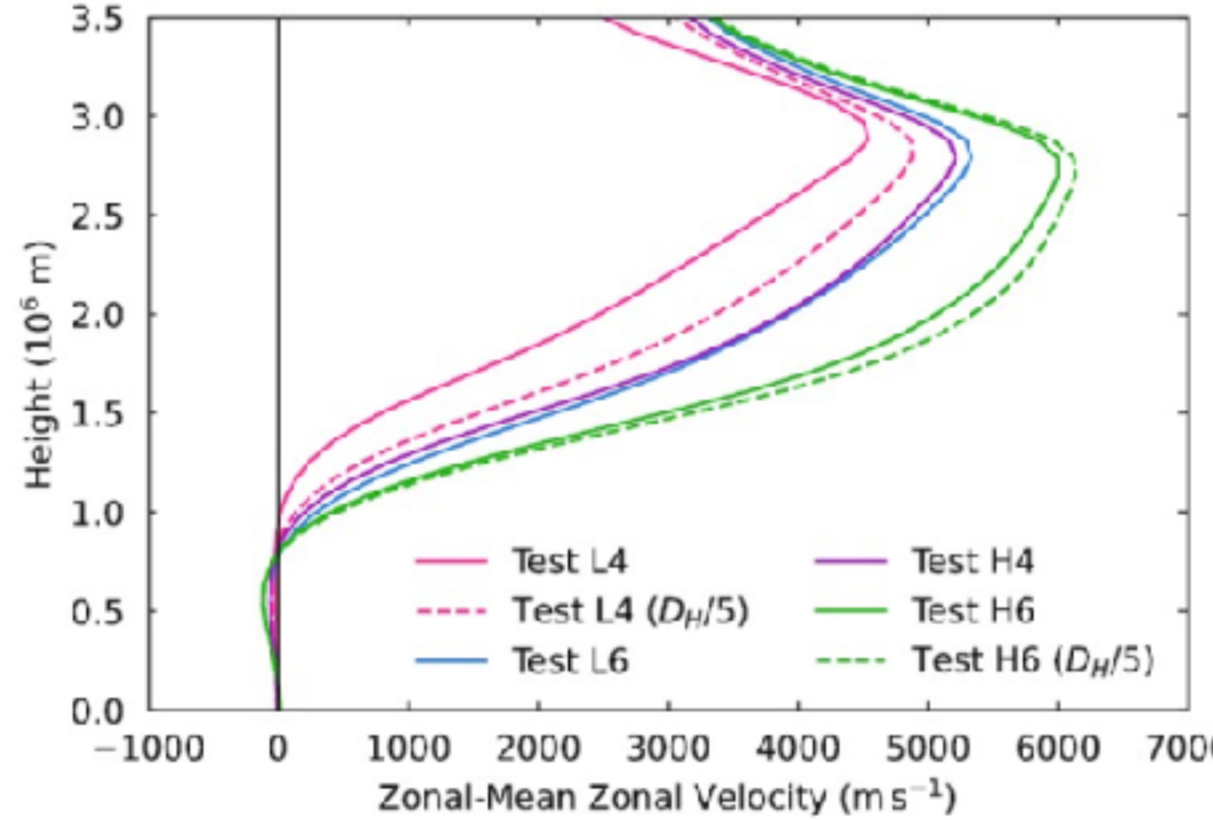

(b) Equatorial zonal-mean zonal velocity profiles

Current GCMs equilibrate the winds with the numerical drag…

And so our wind speed is very uncertain !

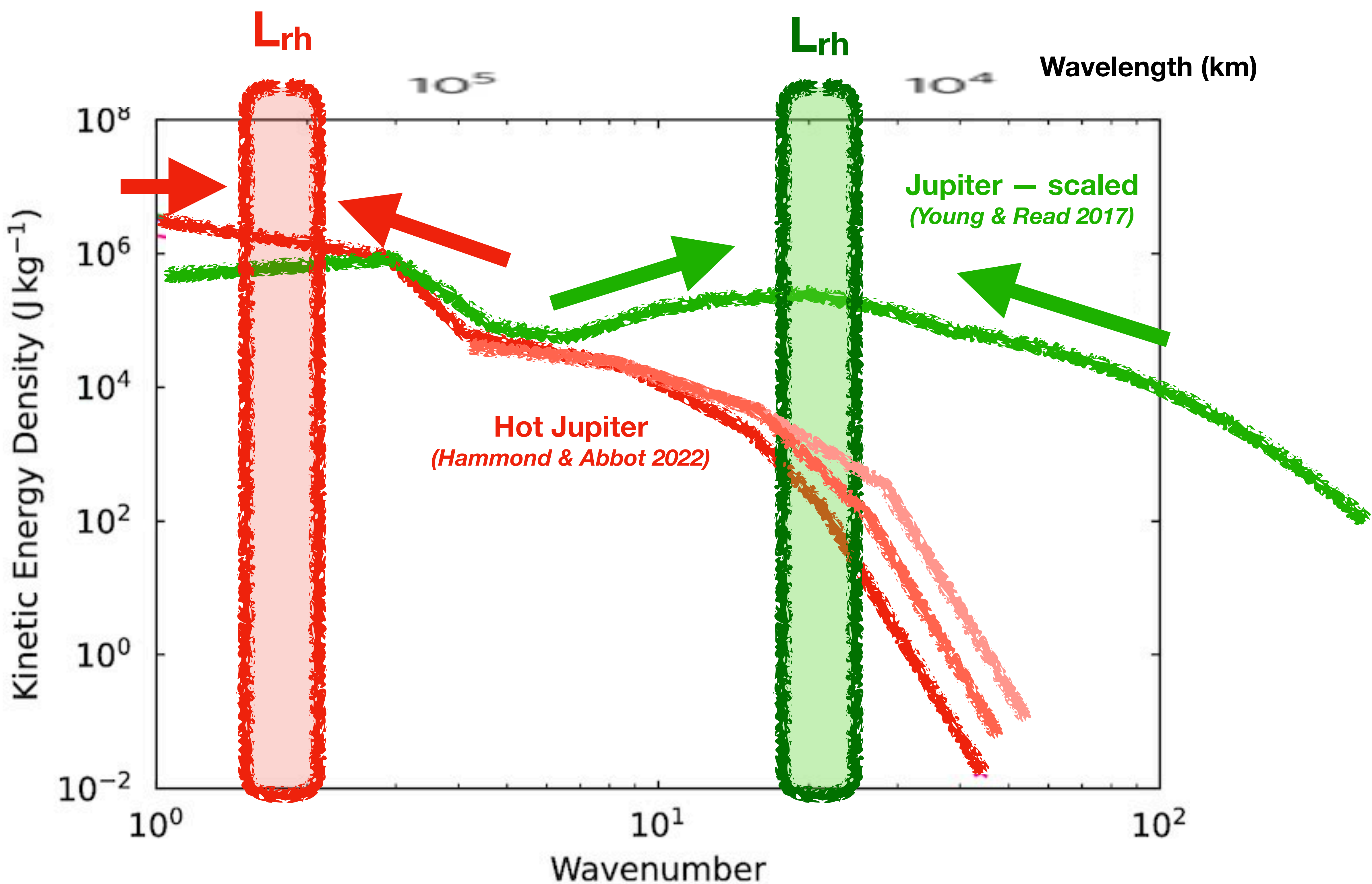

Lrh
Lrh
Wavelength (km)
10^5
10^4
Jupiter — scaled
(Young & Read 2017)
Hot Jupiter
(Hammond & Abbot 2022)
Kinetic Energy Density (J kg^−1)
10^8
10^6
10^4
10^2
10^0
10^−2
10^0
10^1
10^2
Wavenumber

When drag really goes away…

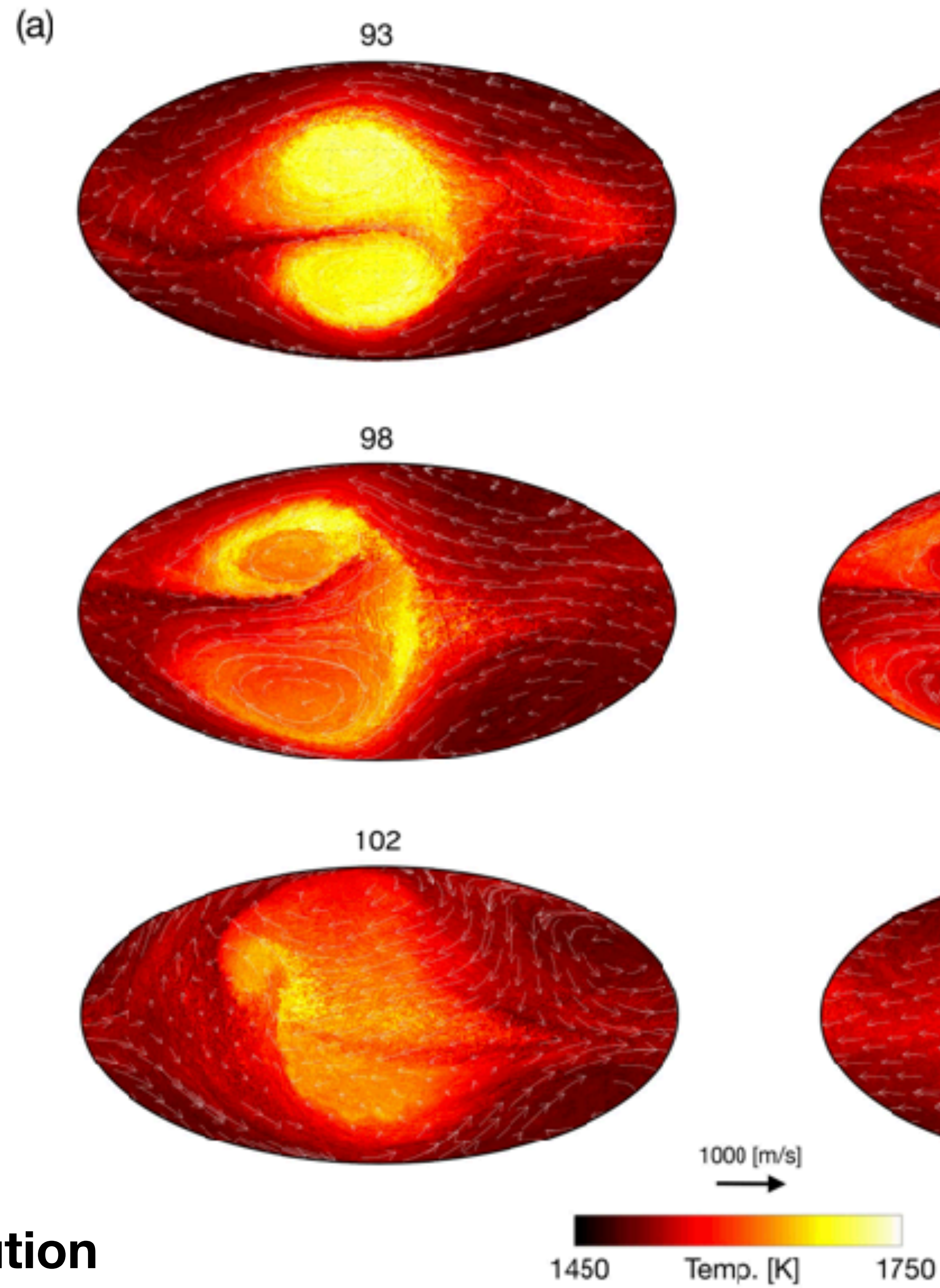

Very high spatial resolution —> Less numerical drag !

Skinner et al. 2020

When drag really goes away…

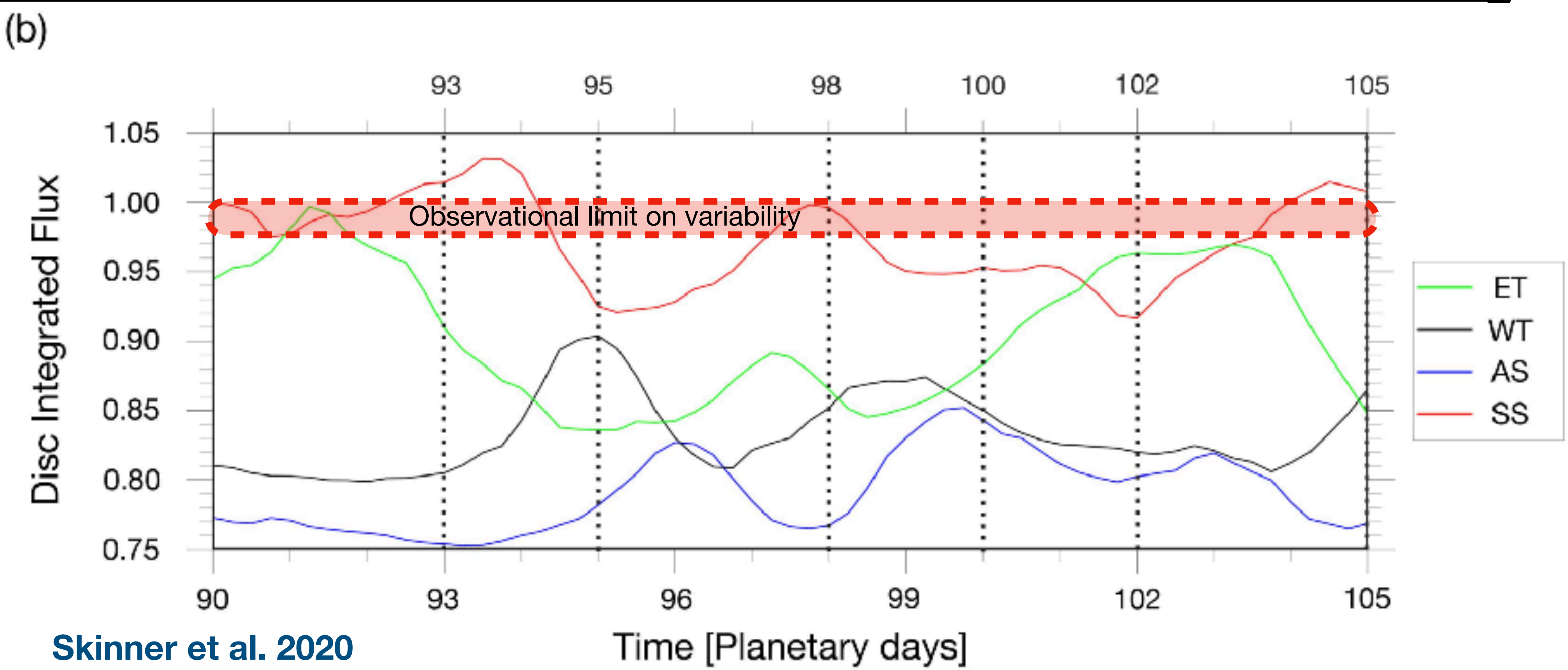

Skinner et al. 2020

Very high spatial resolution models produces variability not seen in HJ !

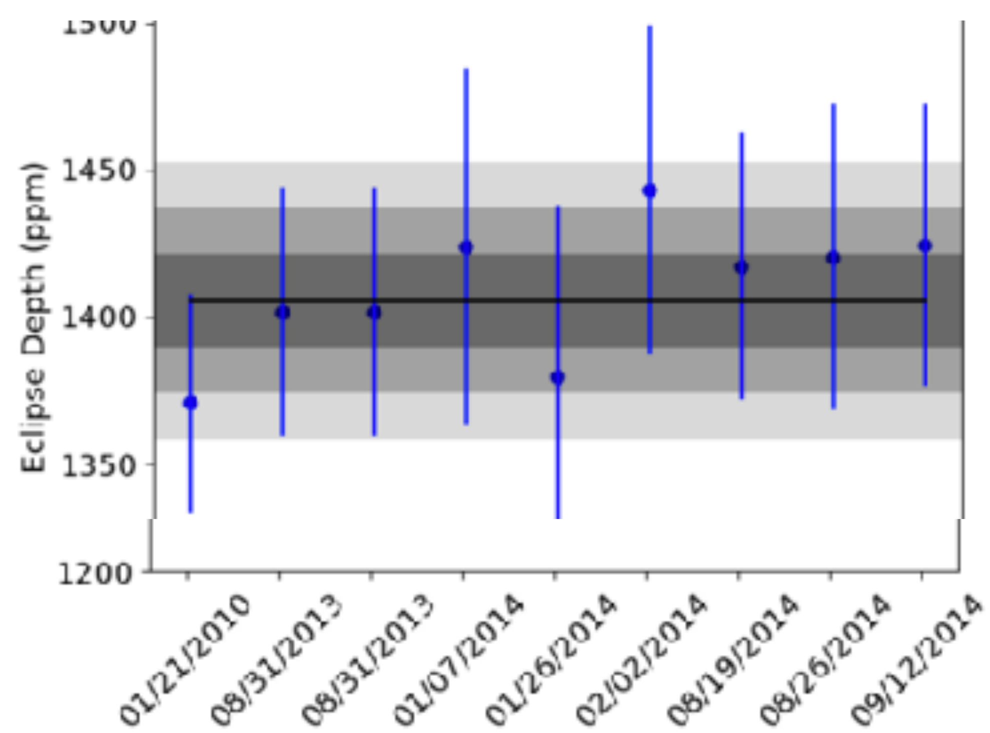

Agol et al.

Parameterizing drag

$$\mathcal{F}_{\text{drag}} = -k_v(p)\boldsymbol{v},$$

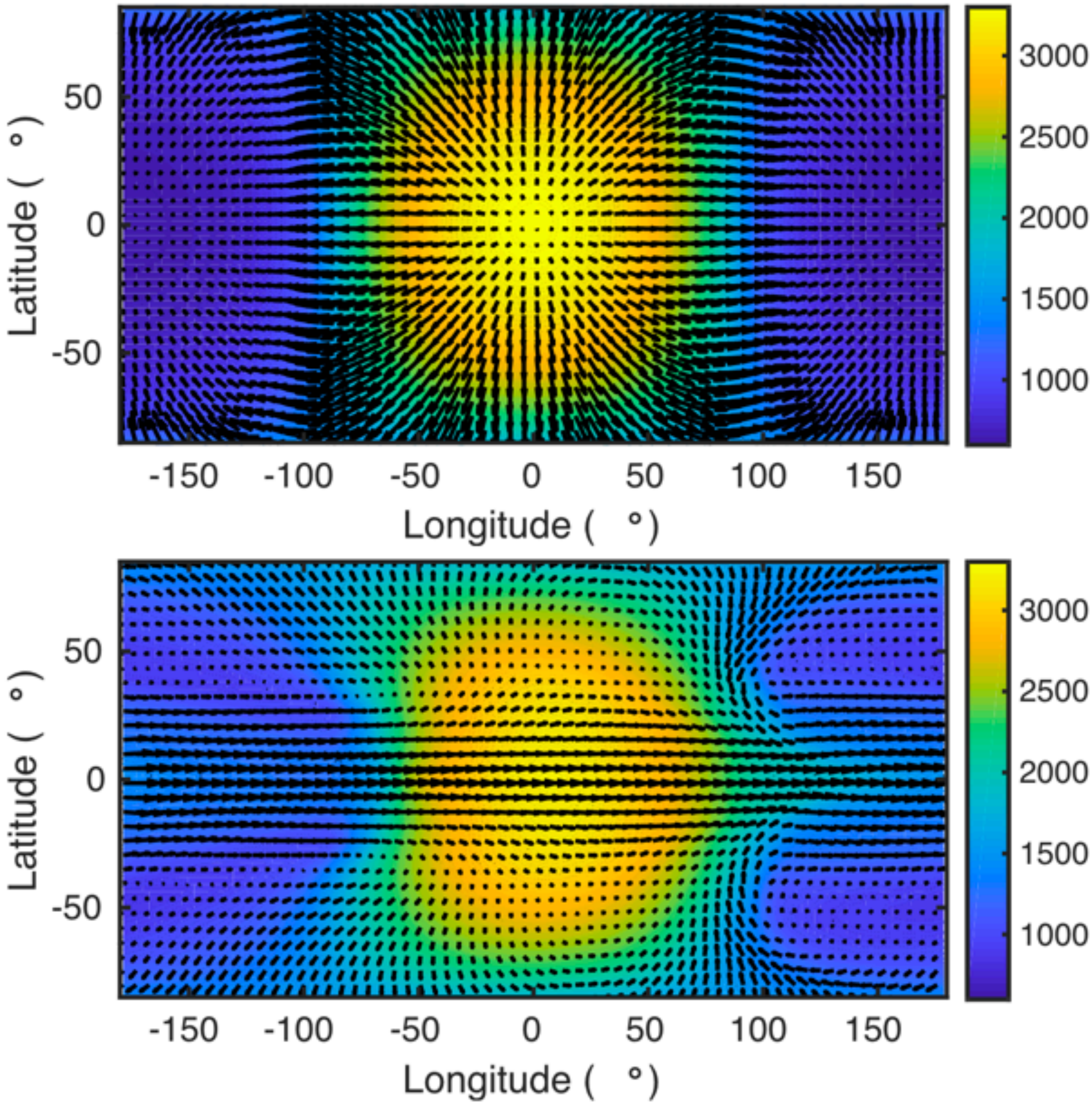

Drag equivalent to 10 GAUSS

No drag

Arcangeli et al. 2019

Drag: exemple of WASP-18b

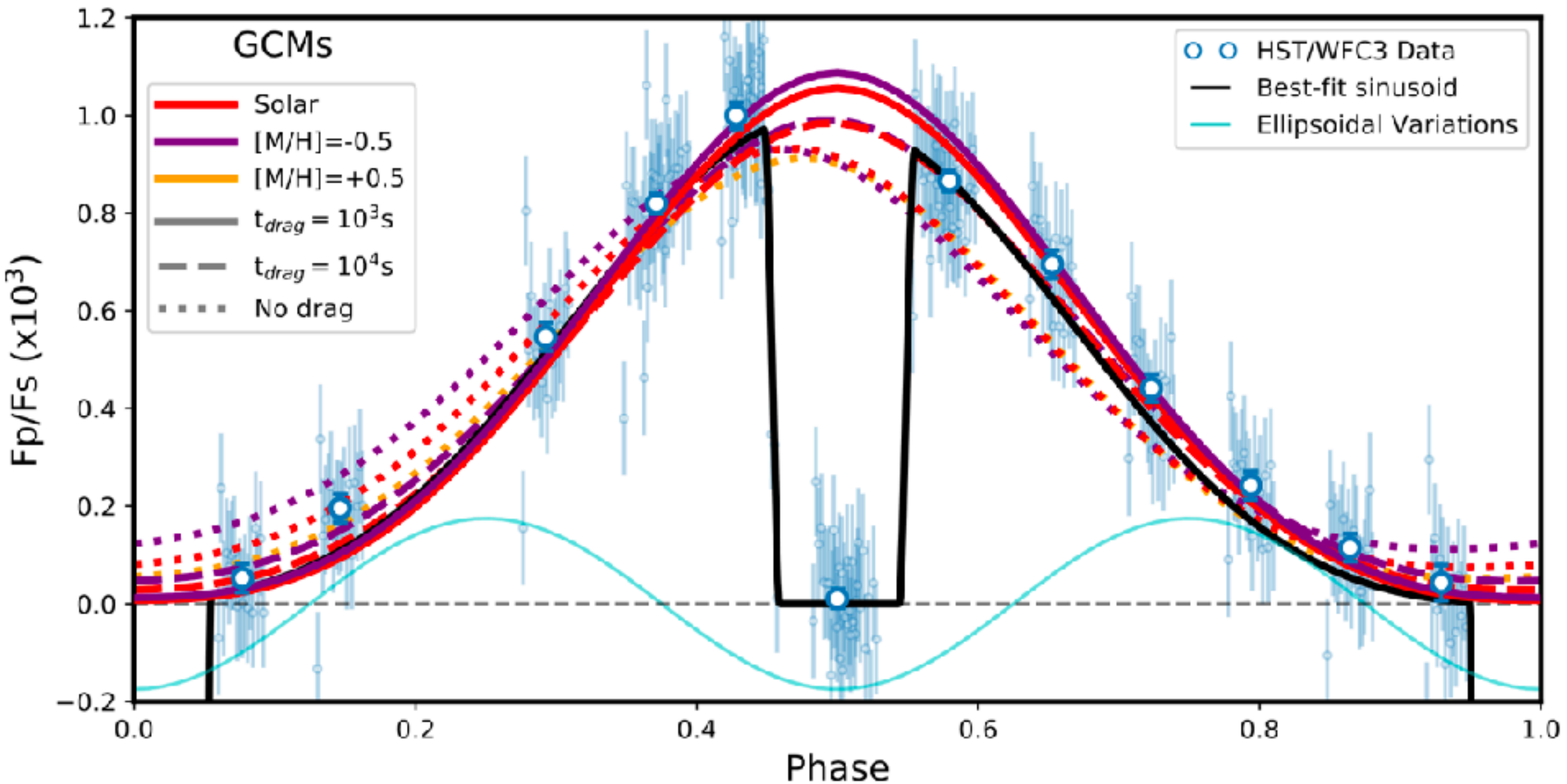

Arcangeli et al. 2019

Parameterizing drag

$$\mathcal{F}_{\text{drag}} = -k_v(p)\boldsymbol{v},$$

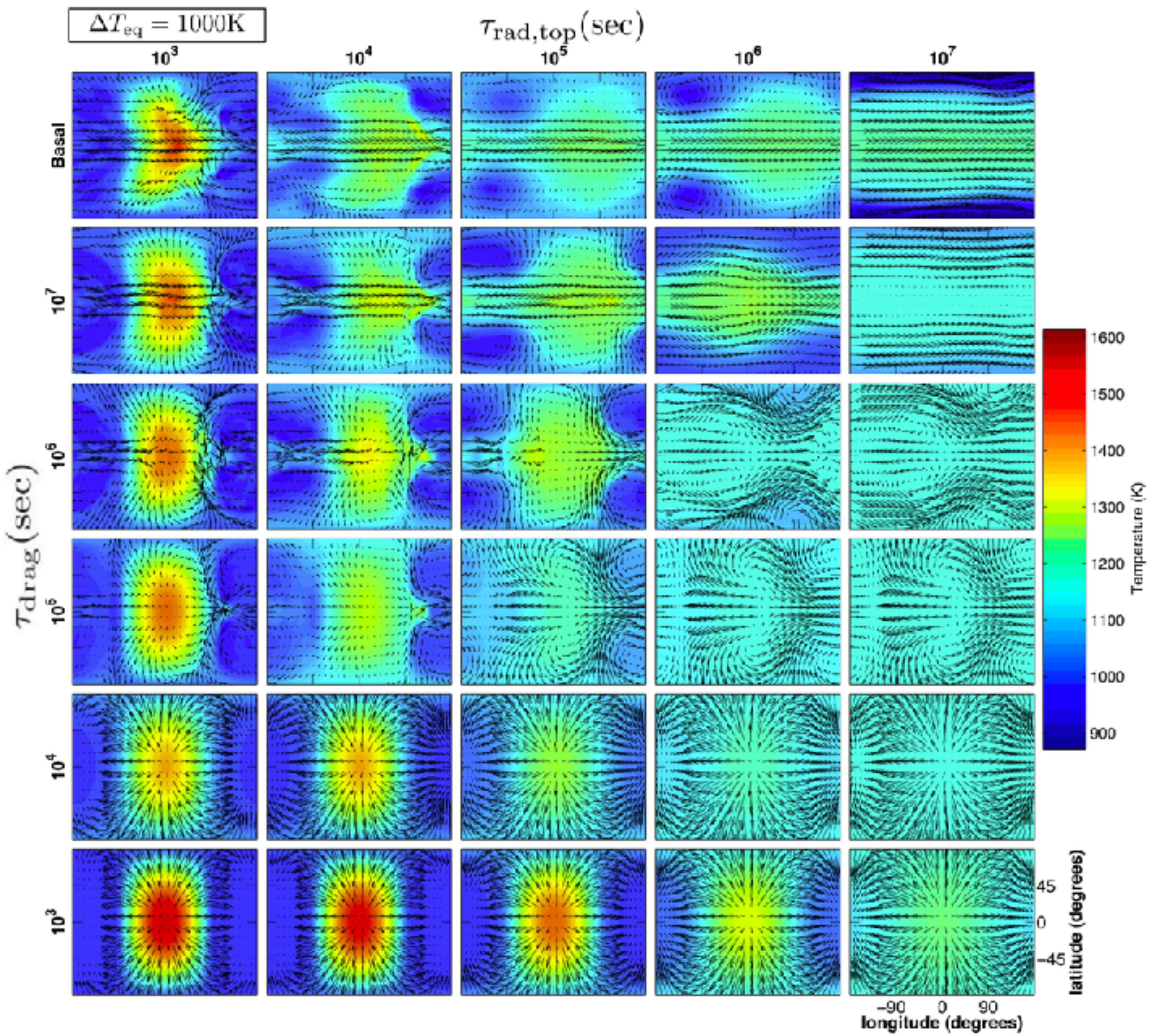

Komacek et al. 2016

Parameterizing drag

$$\mathcal{F}_{\rm drag} = -k_v(p)\boldsymbol{v},$$

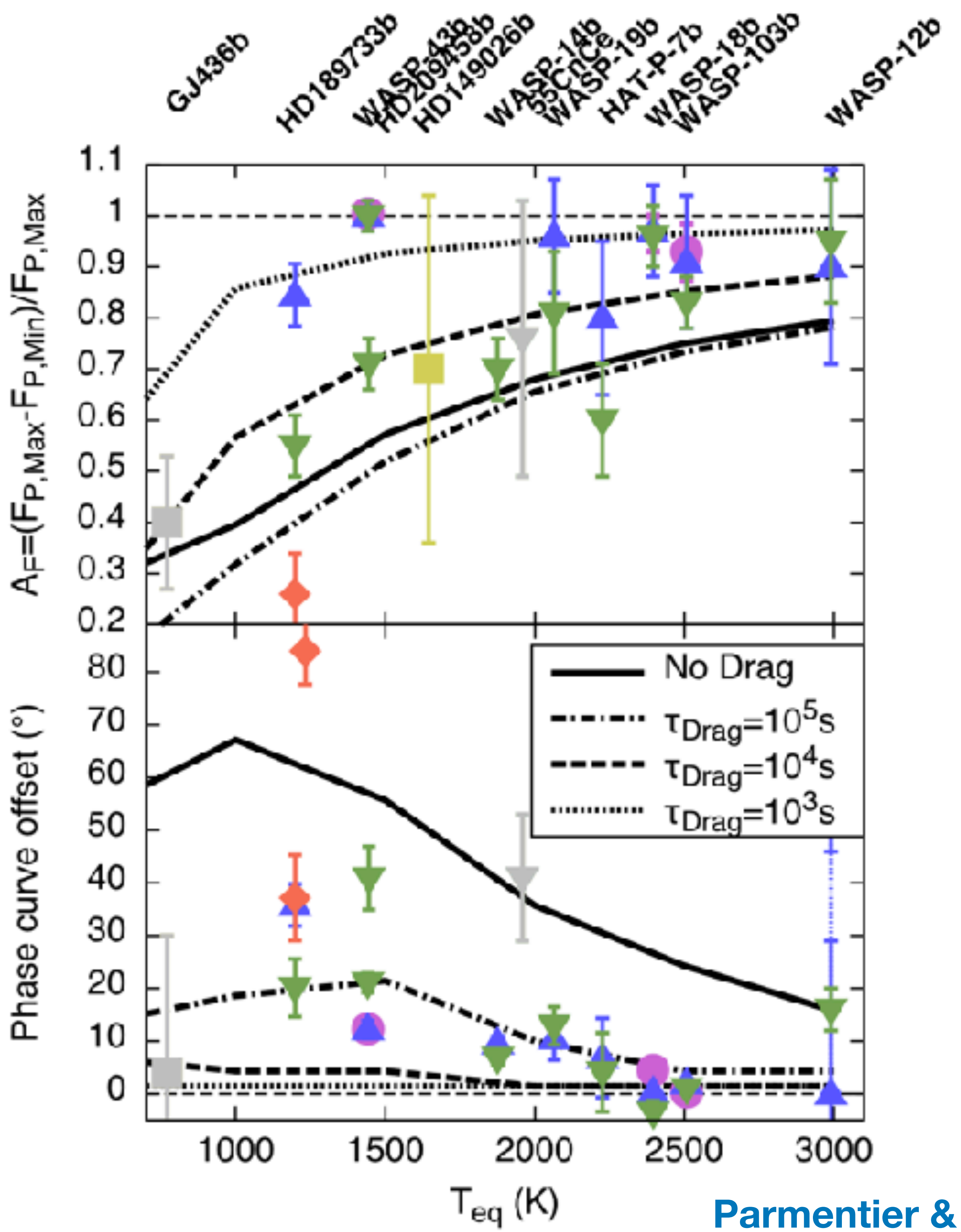

Parmentier & Crossfield 2018

Physical sources of drag

Hydrodynamical : *shear instability, Kelvin-Helmoltz instabilities, shocks, wave-jet interactions*

Magnetic : *Ohmic drag*

Shear & Kelvin Helmoltz instabilities

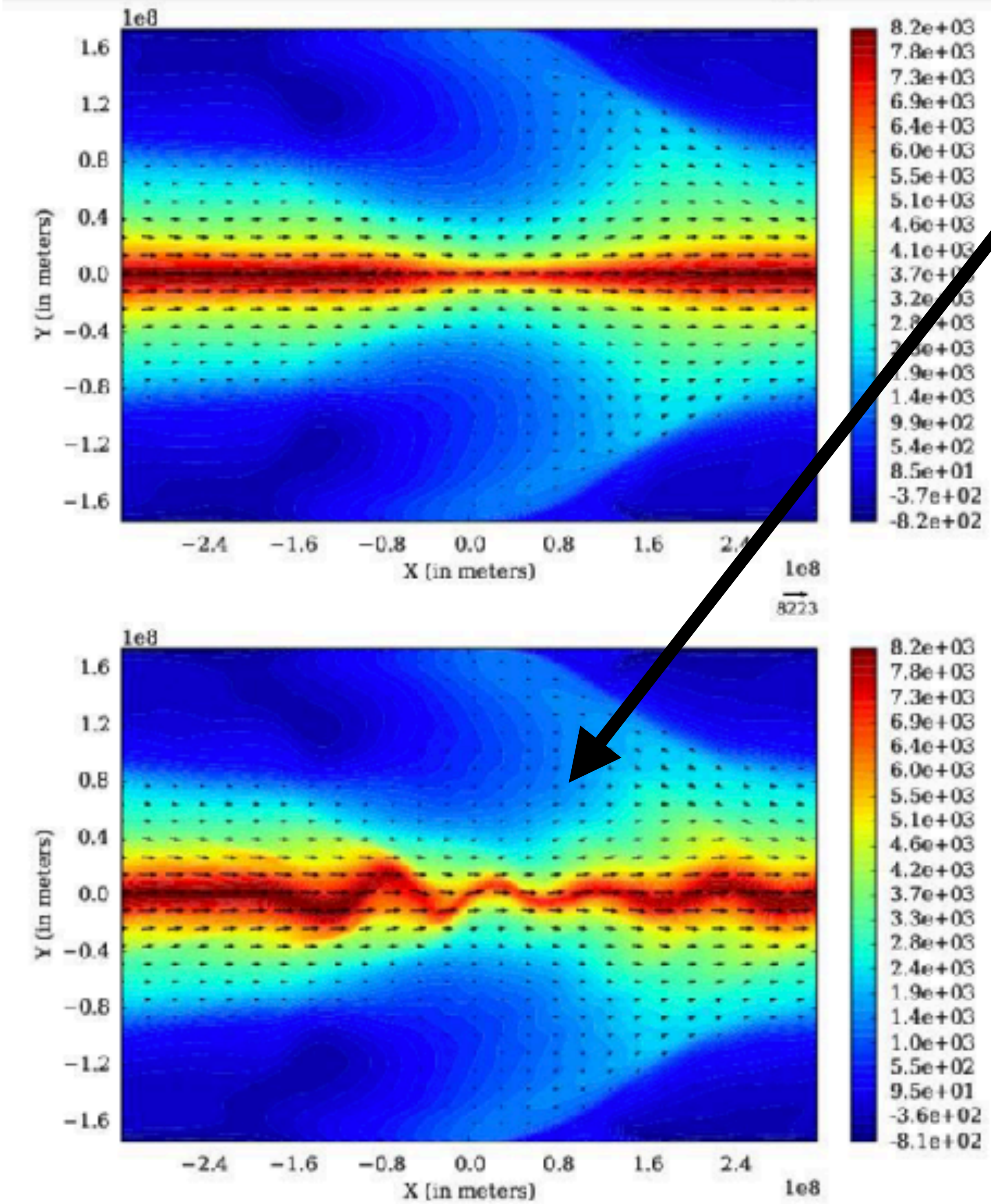

Kelvin Helmoltz instabilities

connected to…

Shear instabilities ?

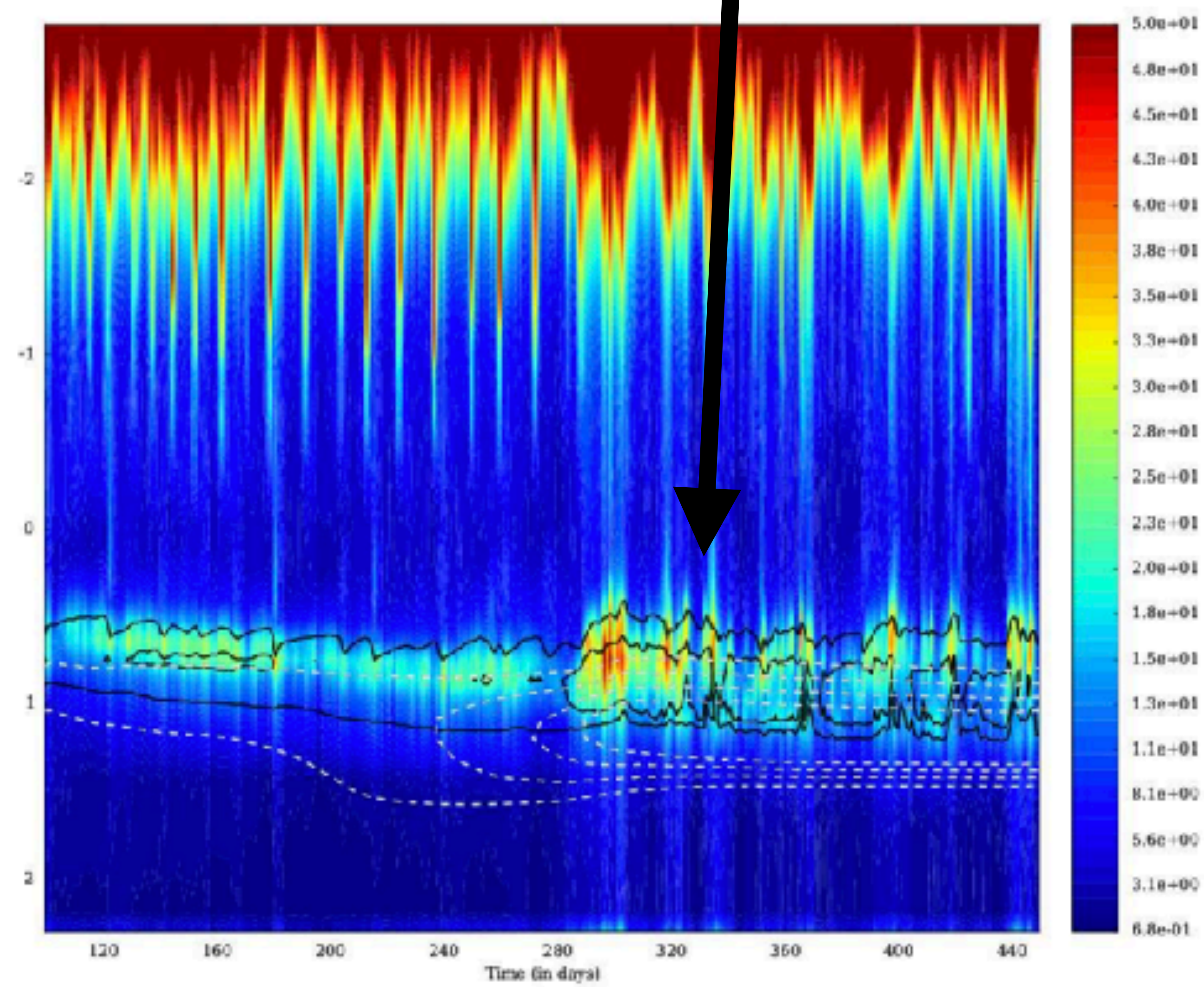

Fromang 2018

Fig. 15: Spacetime (time-pressure) diagram of the zonally averaged high frequency component of the zonal wind (see text for details) in color contours (note that the color table has been saturated at 50 m.s^{-1}). Contours of Ri (solid lines) and T (dashed lines) are overplotted. For Ri, contours are for $Ri = 0.1$ and 0.25. For the temperature, contours are for T = 1900, 2000, 2100 and 2200 K.

Shear & Kelvin Helmoltz instabilities

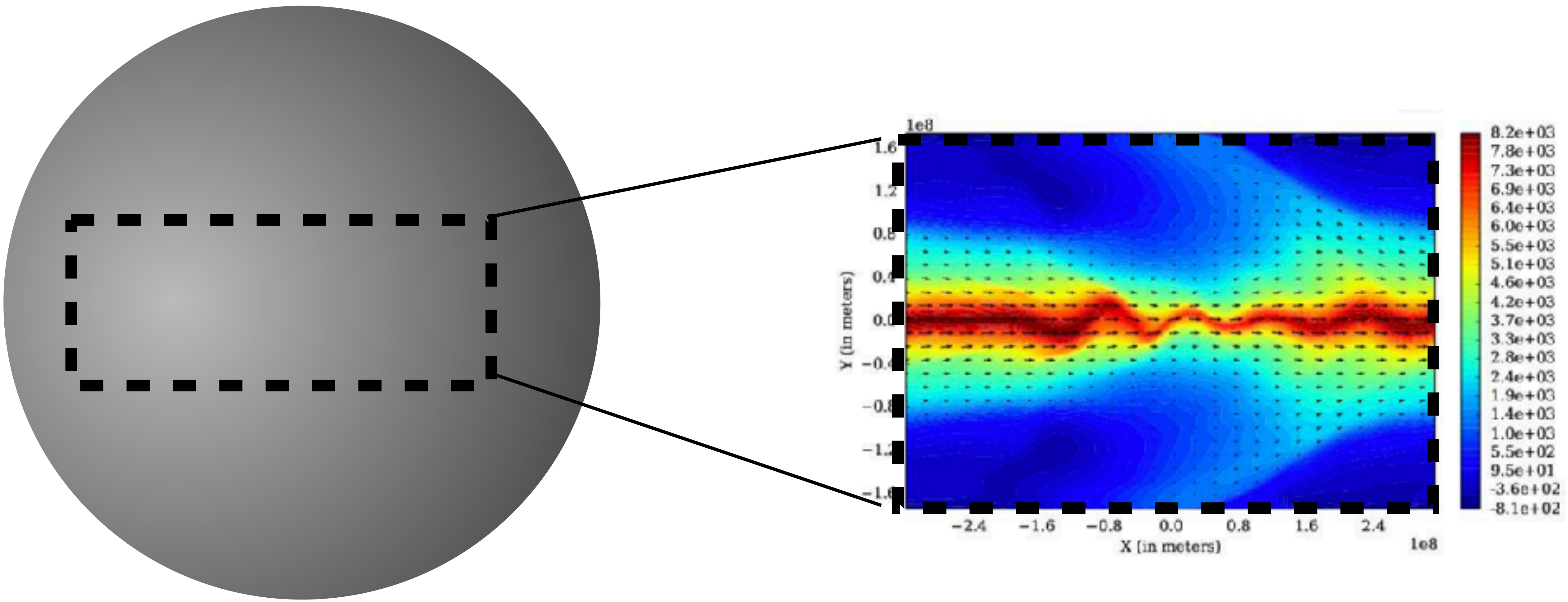

Beta plane approximation

Fromang 2018

Shear & Kelvin Helmoltz instabilities

Hot Jupiter Atmospheric Flows at High Resolution

Kristen Menou,[1,2,3]

by Fromang et al. (2016) have revealed that a barotropic (horizontal shear) instability of the equatorial jet appears at horizontal resolutions beyond those typically achieved in global models; this instability could limit wind speeds and lead to increased atmospheric variability. To address this possibility, we adapt the computationally efficient, pseudo-spectral PlaSim GCM, originally designed for Earth studies, to model Hot Jupiter atmospheric flows and validate it on the Heng et al. (2011) reference benchmark. We then present high resolution global models of HD209458b, with horizontal resolutions of T85 (128x256) and T127 (192x384). The barotropic instability phenomenology found in β-plane simulations is not reproduced in these global models, despite comparably high resolutions. Nevertheless, high resolution models do exhibit additional flow variability on long timescales (of order 100 planet days or more), which is absent from the lower resolution models. It manifests as a breakdown of north-south

incompressible approximation ?

Hot Jupiters are conductive !

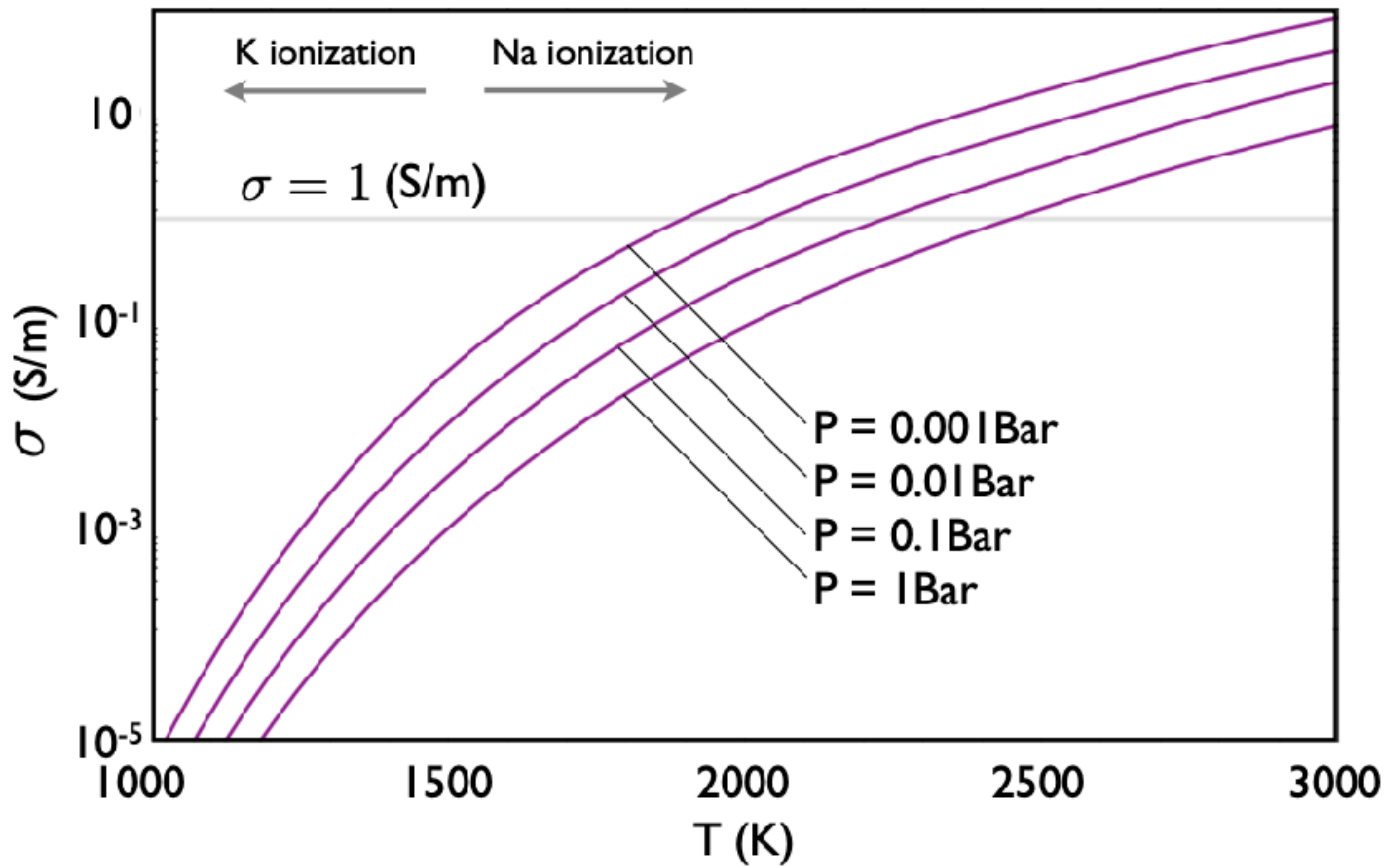

Ideal MHD

$$\nabla \cdot \bar{\rho}\mathbf{v} = 0 \quad (1$$

$$\nabla \cdot \mathbf{B} = 0 \quad (2$$

$$\rho = \left[\left(\frac{\partial \rho}{\partial T} \right)_p T + \left(\frac{\partial \rho}{\partial p} \right)_T p \right] \quad (3$$

$$\bar{\rho}\frac{\partial \mathbf{v}}{\partial t} = -\nabla \cdot (\bar{\rho}\mathbf{v}\mathbf{v}) - \nabla p - \rho \bar{g}\hat{\mathbf{r}} \quad (4$$

$$+2\bar{\rho}\mathbf{v} \times \mathbf{\Omega} + \nabla \cdot (2\bar{\rho}\bar{\nu}(e_{ij} - \frac{1}{3}(\nabla \cdot \mathbf{v})\delta_{ij}))$$

$$+\frac{1}{\mu_0}(\nabla \times \mathbf{B}) \times \mathbf{B}$$

$$\frac{\partial \mathbf{B}}{\partial t} = \nabla \times (\mathbf{v} \times \mathbf{B}) - \nabla \times (\bar{\eta}\nabla \times \mathbf{B}) \quad (5$$

$$\frac{\partial T}{\partial t} + (\vec{v} \cdot \vec{\nabla})T = \quad (6$$

$$-v_r(\frac{\partial \overline{T}}{\partial r} - (\gamma - 1)\overline{T}h_\rho) + (\gamma - 1)Th_\rho v_r$$

$$+\gamma\bar{\kappa}[\nabla^2 T + (h_\rho + h_\kappa)\frac{\partial T}{\partial r}] + \frac{T_{eq} - T}{\tau_{rad}} + \frac{\bar{\eta}}{\mu_o \bar{\rho} c_p}|\nabla \times \mathbf{B}|^2$$

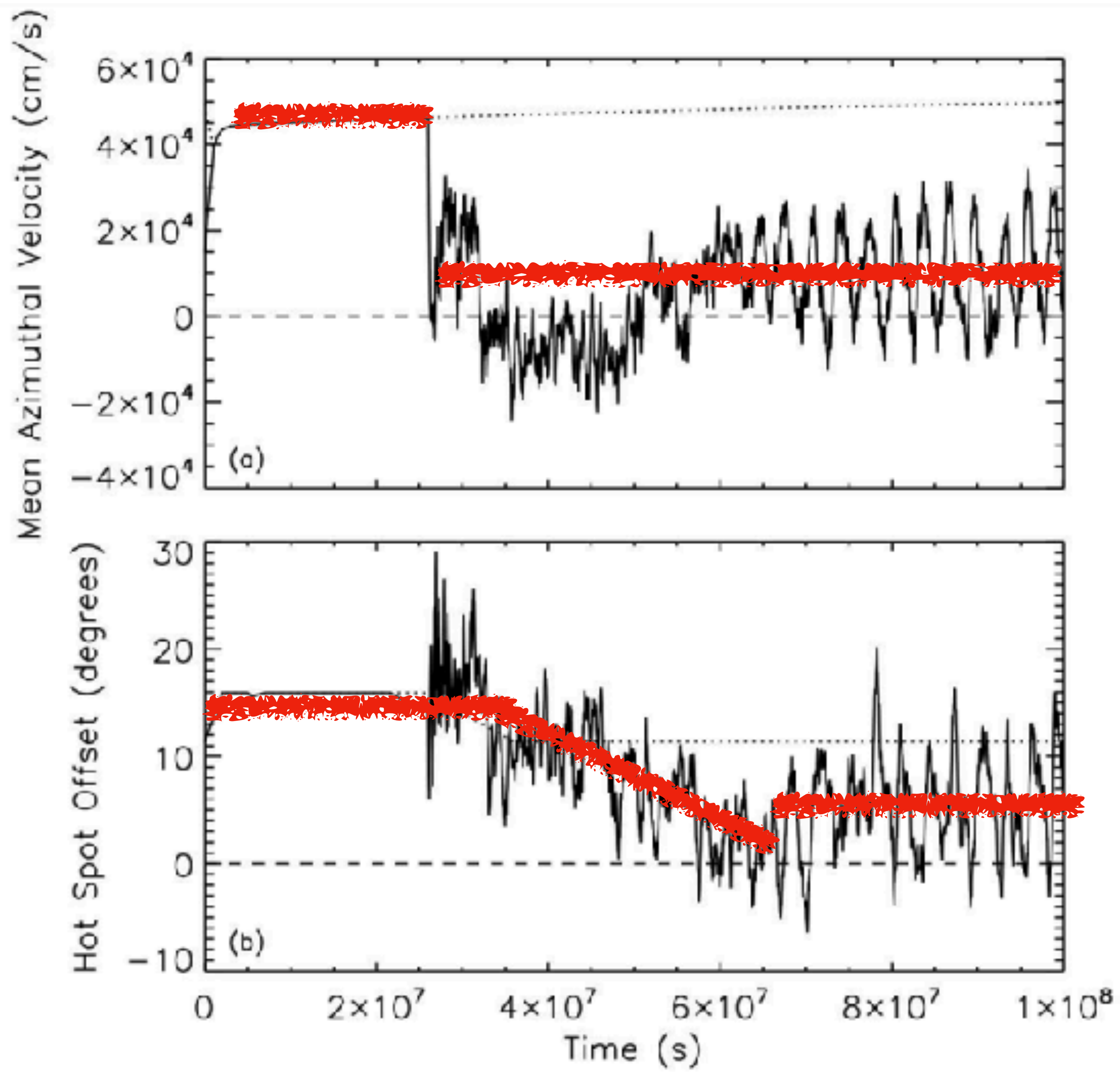

Rogers 2017

Ideal MHD : depends strongly on magnetic field strength !

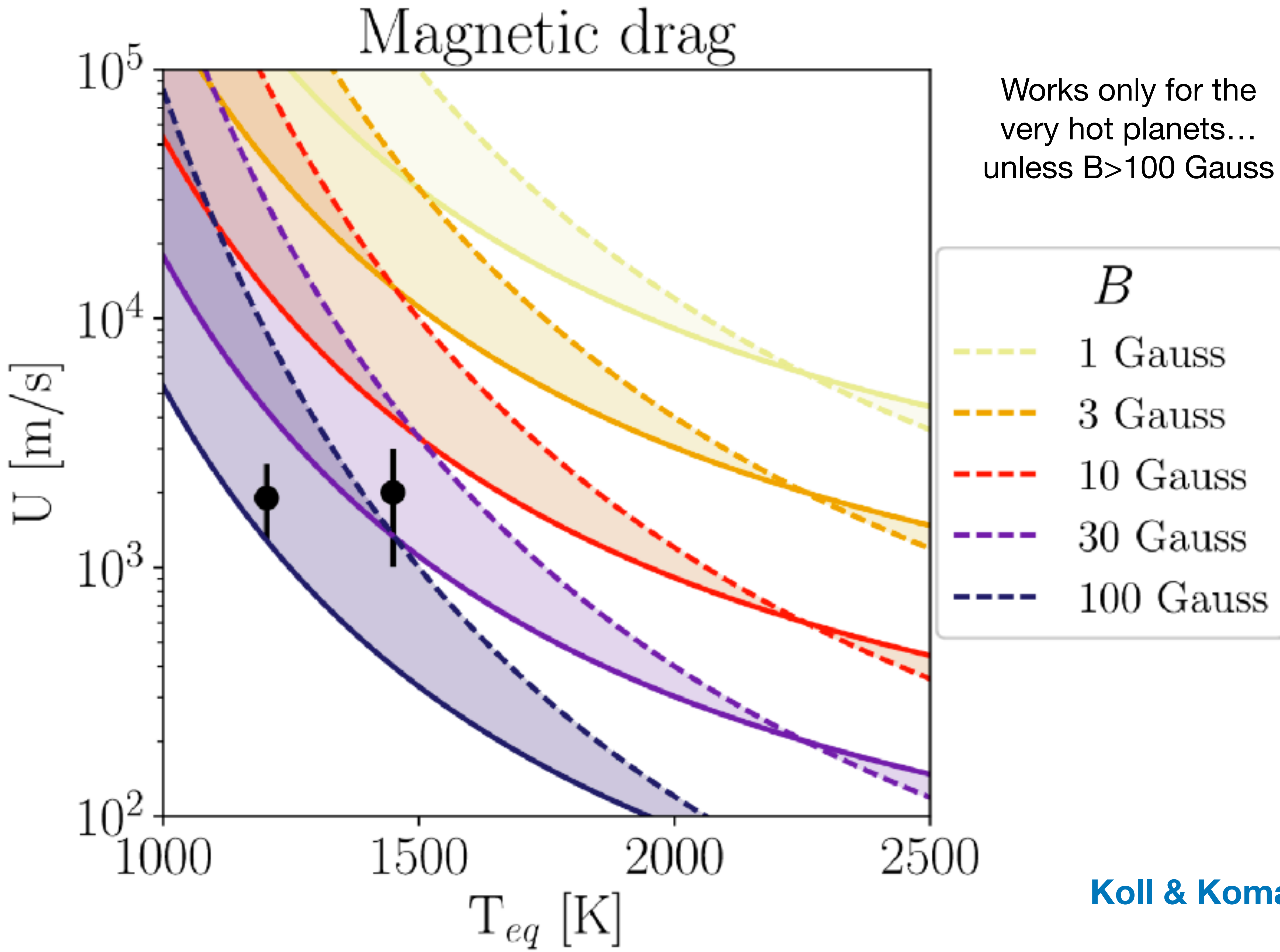

Works only for the very hot planets… unless B>100 Gauss

Koll & Komacek

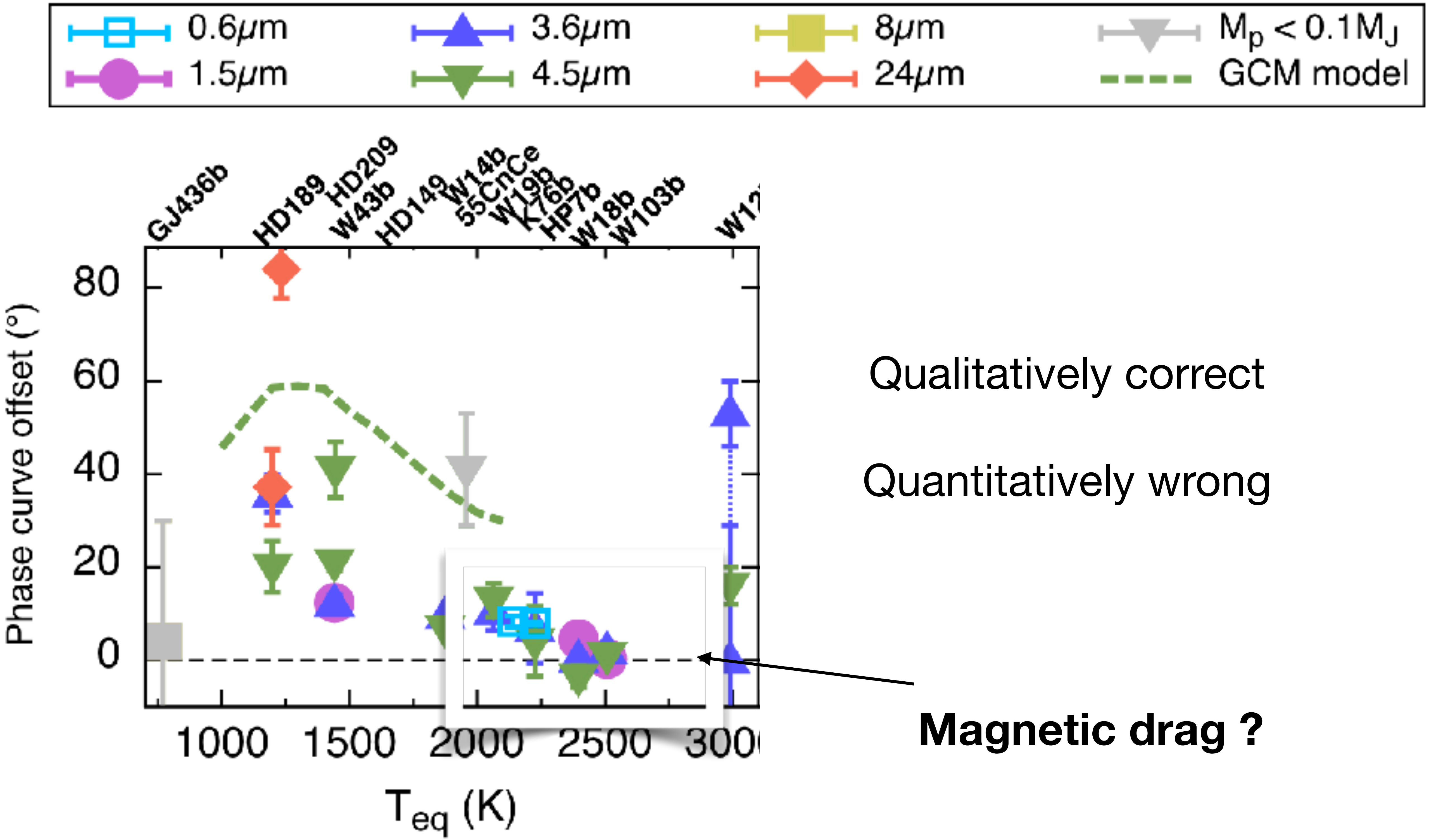

Qualitatively correct

Quantitatively wrong

Magnetic drag ?

Ideal MHD

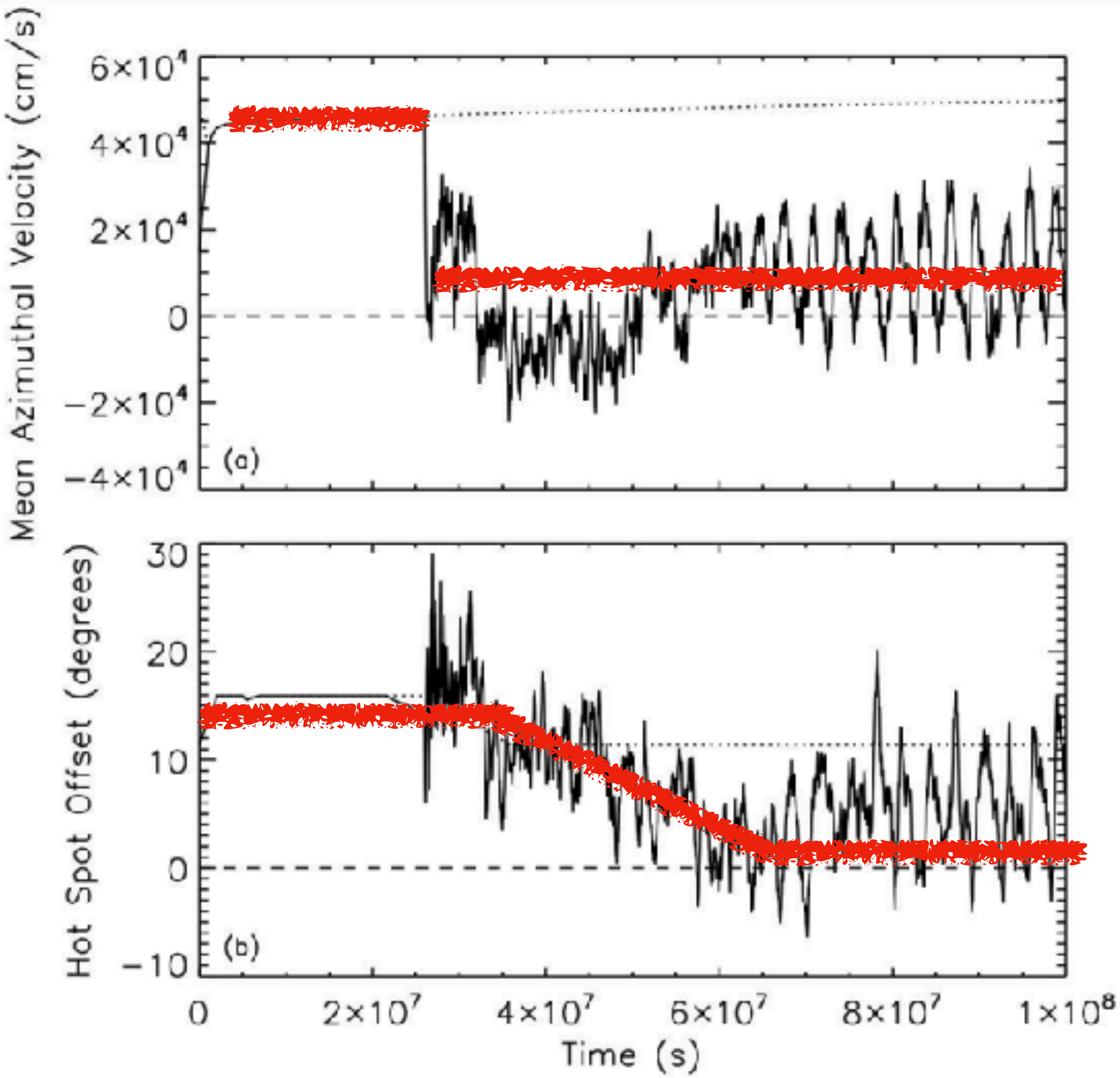

Rogers 2017

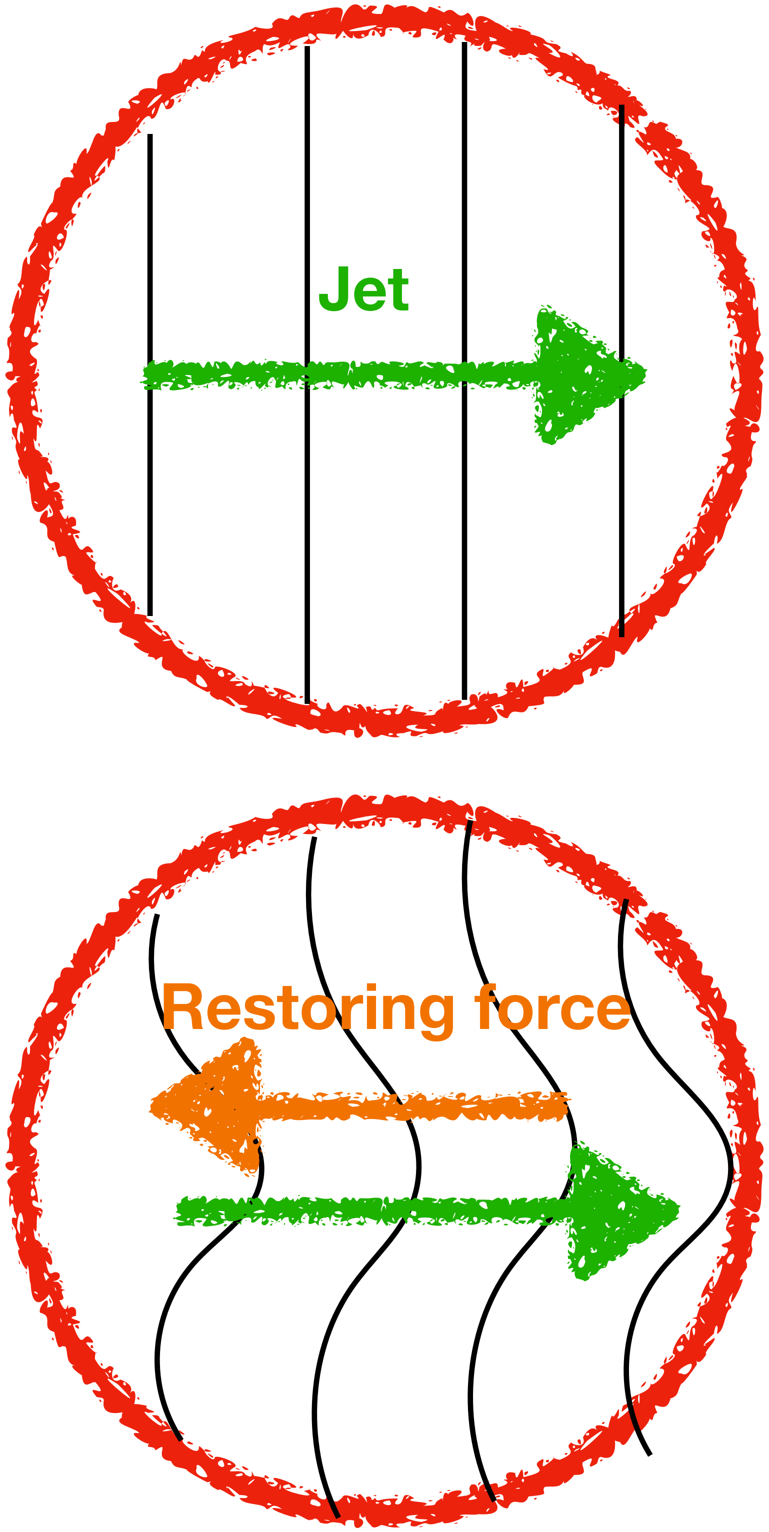

Hindle et al. 2022

Ideal MHD

Rogers et al.

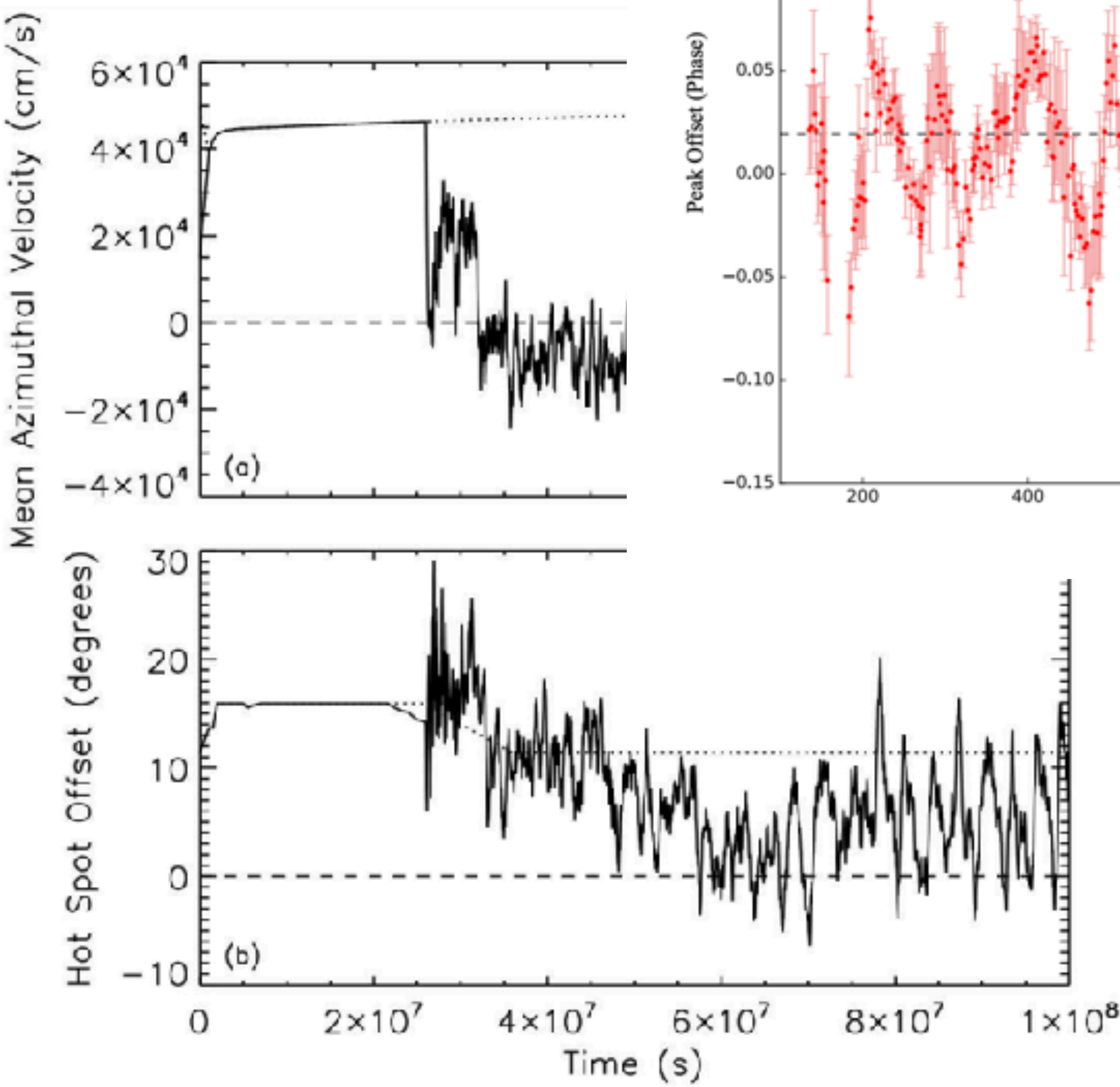

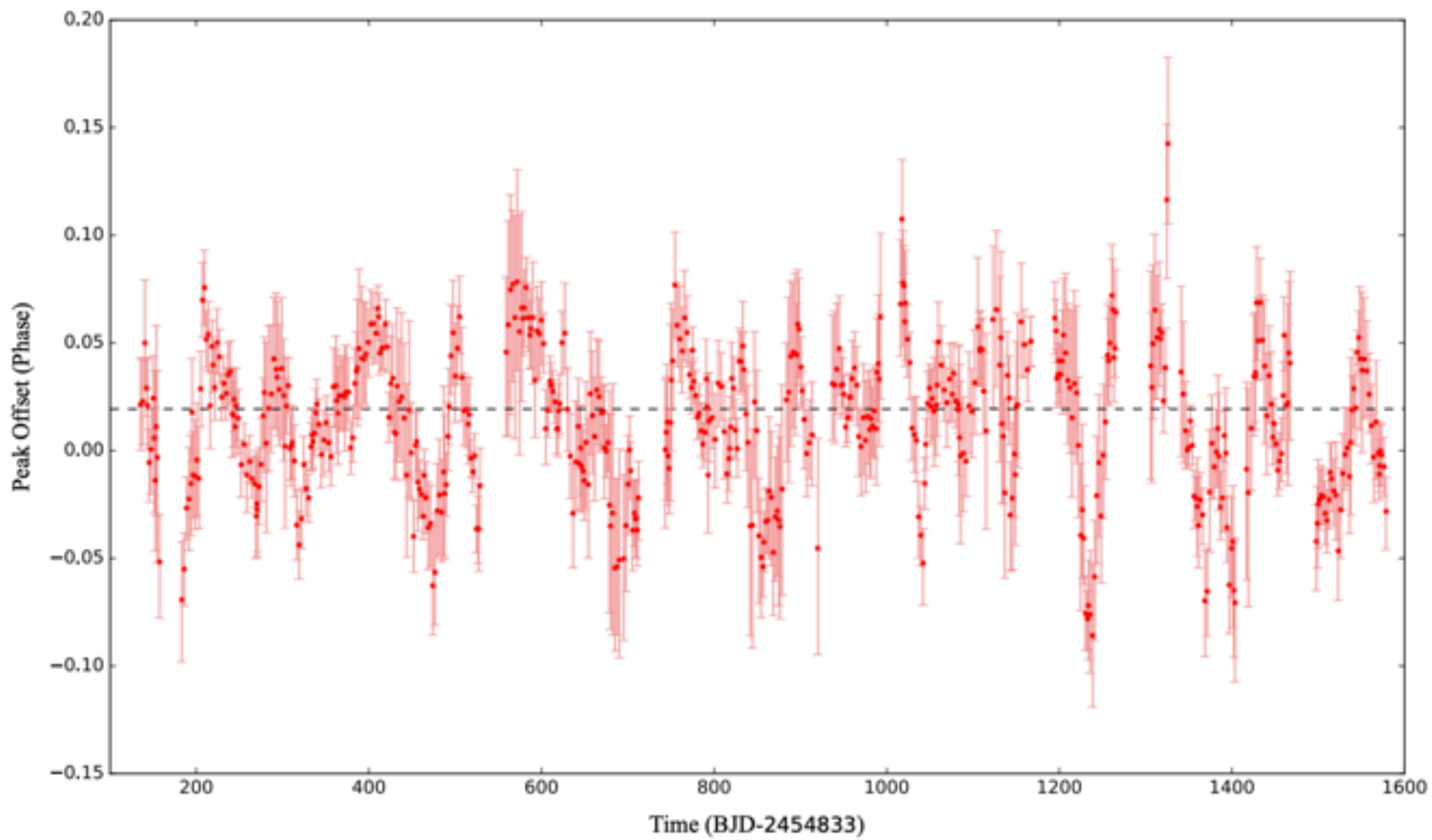

Armstrong et al.

But… only 2 planets….
Maybe instrument systematics

Clouds ?

Clouds in HST/WFC3 ?

H_2O absorption feature

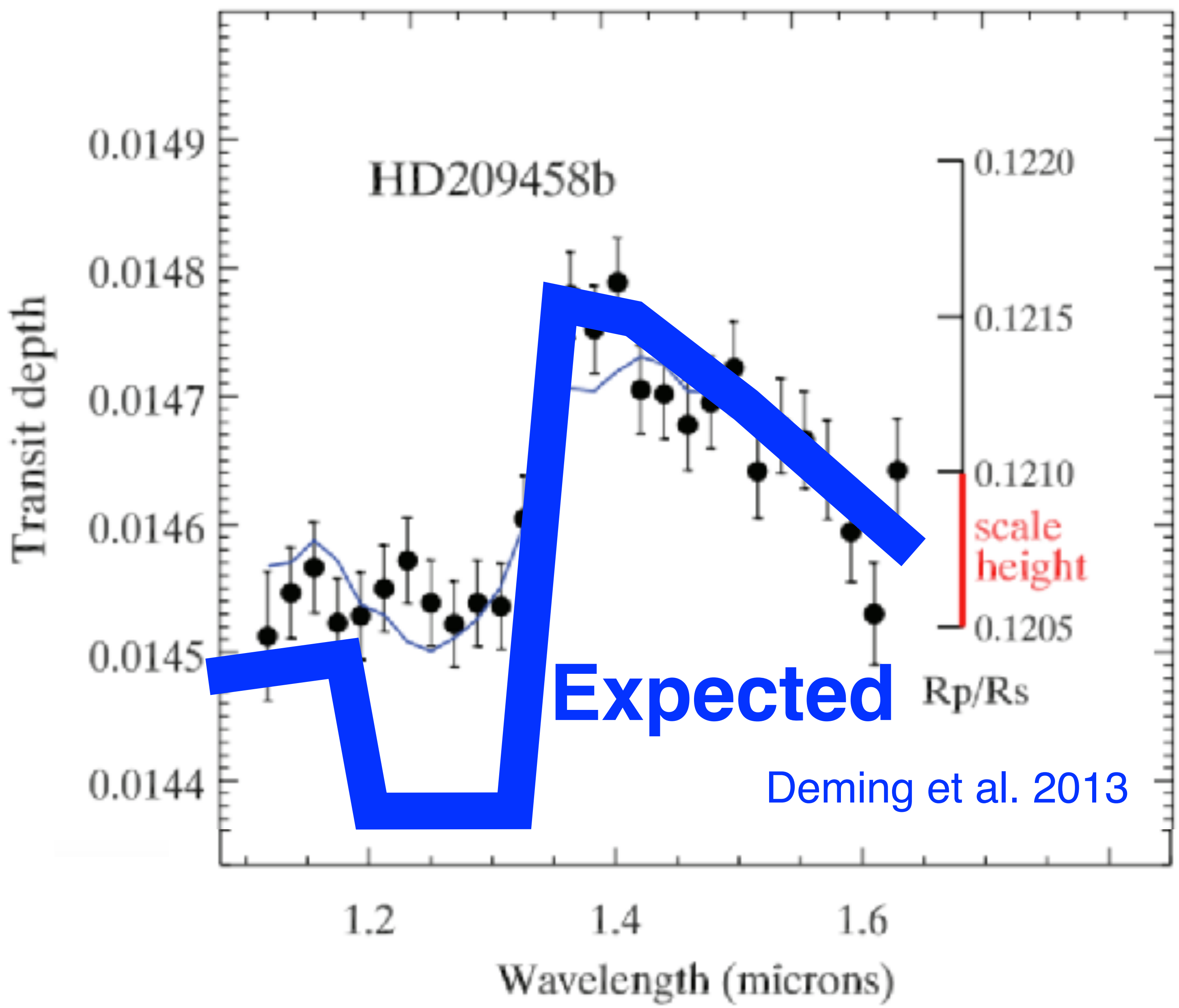

Water absorption should look like this

$$R_p(\lambda_1) - R_p(\lambda_2) = \log\left(\frac{\xi_a}{\xi_b}\frac{S_a(\lambda_1)}{S_b(\lambda_2)}\right) H$$

Abundance

Cross-section

Lecavelier Des Etangs et al. 2008, Benneke+2012, Griffith+2014, Line+2016, Heng+2017

If water only is seen then the transmission spectrum is not sensitive (to order 0) to the water abundance

Clouds in HST/WFC3 ?

WFC3 feature size in scale height

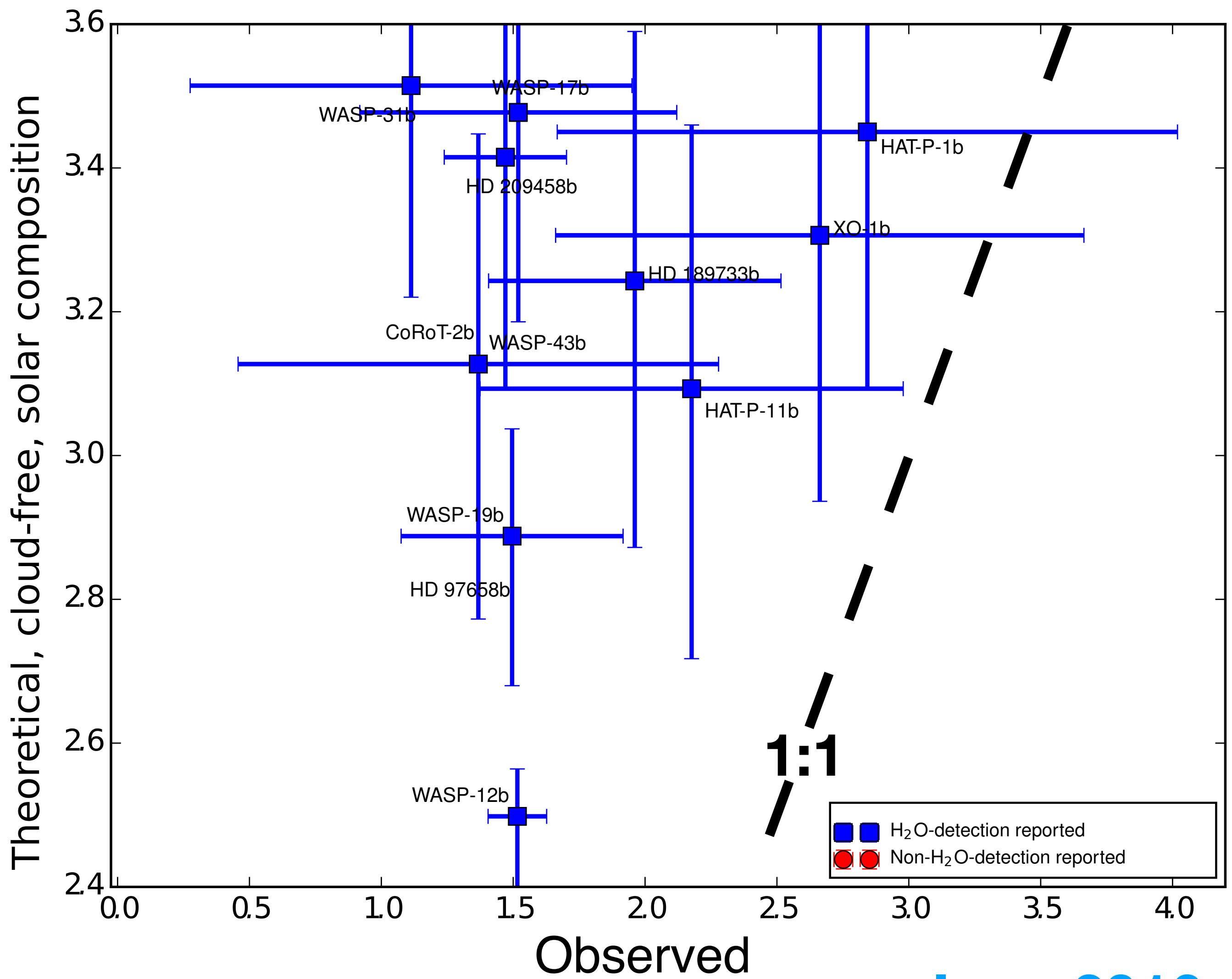

Iyer+2016

Water absorption should look like this

but it does not

$$R_\mathrm{p}(\lambda_1) - R_\mathrm{p}(\lambda_2) = \log\left(\frac{\xi_a}{\xi_b}\frac{S_\mathrm{a}(\lambda_1)}{S_\mathrm{b}(\lambda_2)}\right) H$$

Abundance

Cross-section

Lecavelier Des Etangs et al. 2008, Benneke+2012, Griffith+2014, Line+2016, Heng+2017

If water only is seen then the transmission spectrum is not sensitive (to order 0) to the water abundance

Clouds in HST/WFC3 ?

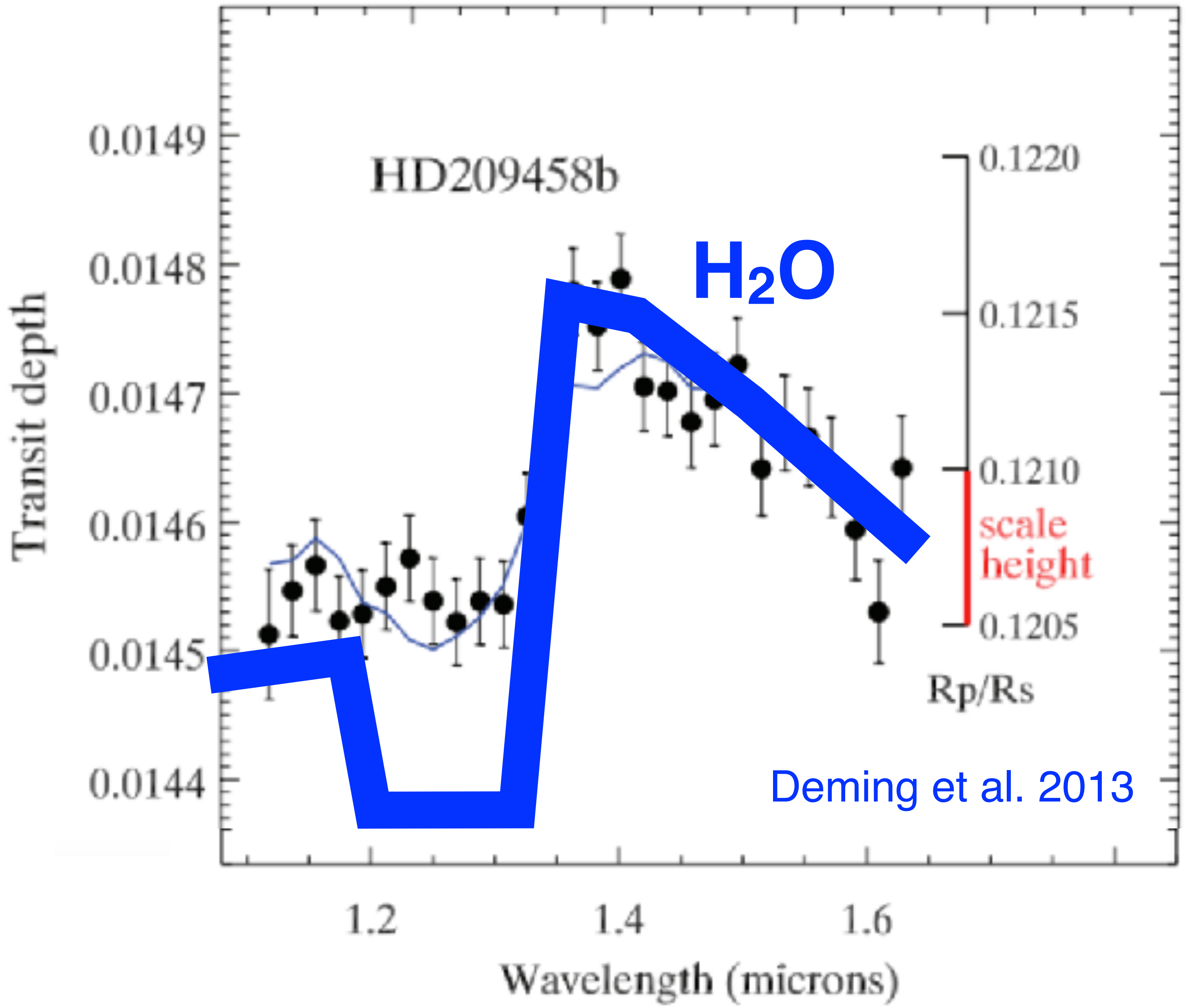

Water absorption should look like this
but it does not

$$R_p(\lambda_1) - R_p(\lambda_2) = \log\left(\frac{\xi_a}{\xi_b}\frac{S_a(\lambda_1)}{S_b(\lambda_2)}\right) H$$

Clouds in HST/WFC3 ?

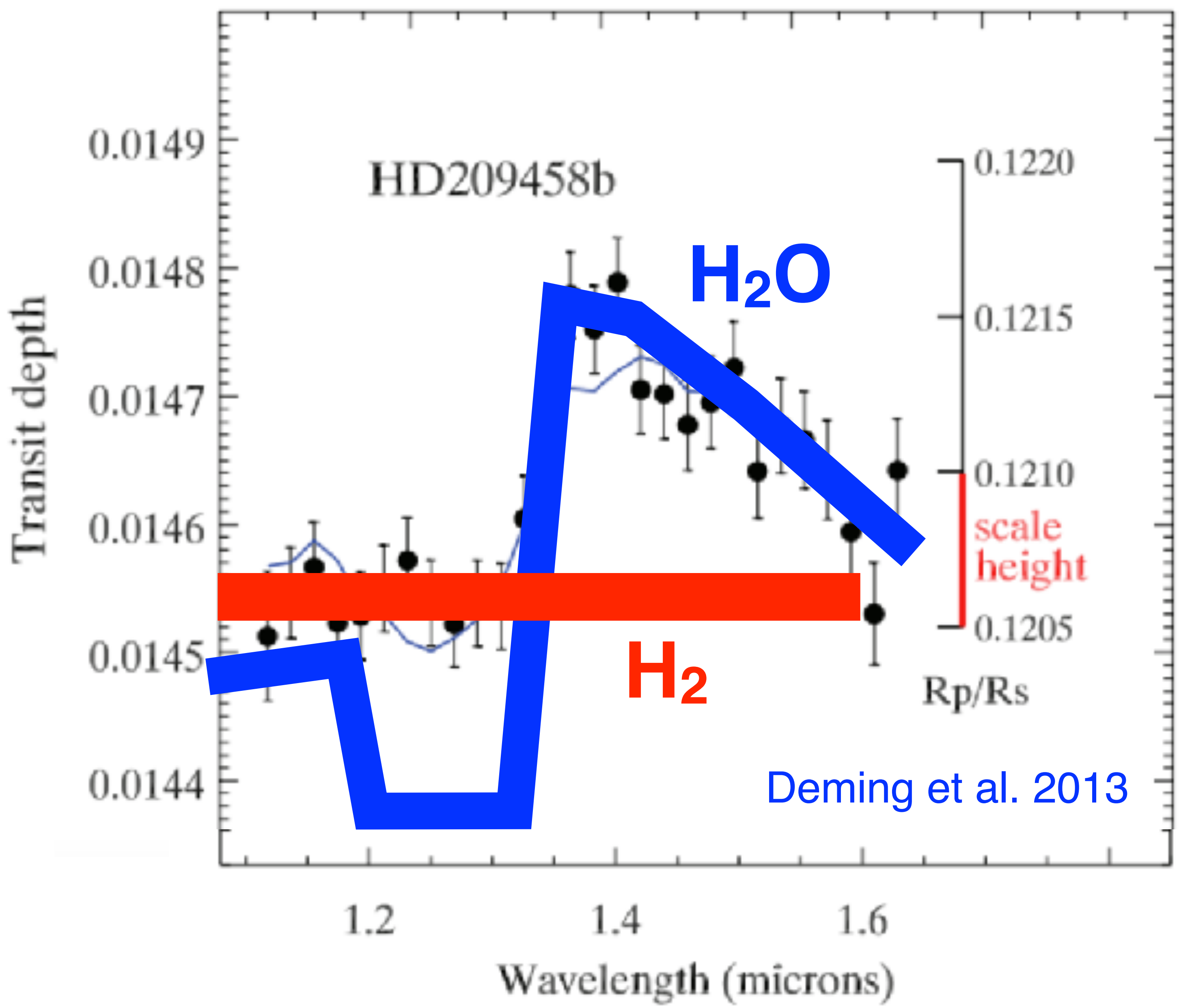

Water absorption should look like this
but it does not

→ it is obscured by H_2
small water abundance

$$R_p(\lambda_1) - R_p(\lambda_2) = \log\left(\frac{\xi_a}{\xi_b}\frac{S_a(\lambda_1)}{S_b(\lambda_2)}\right) H$$

Clouds in HST/WFC3 ?

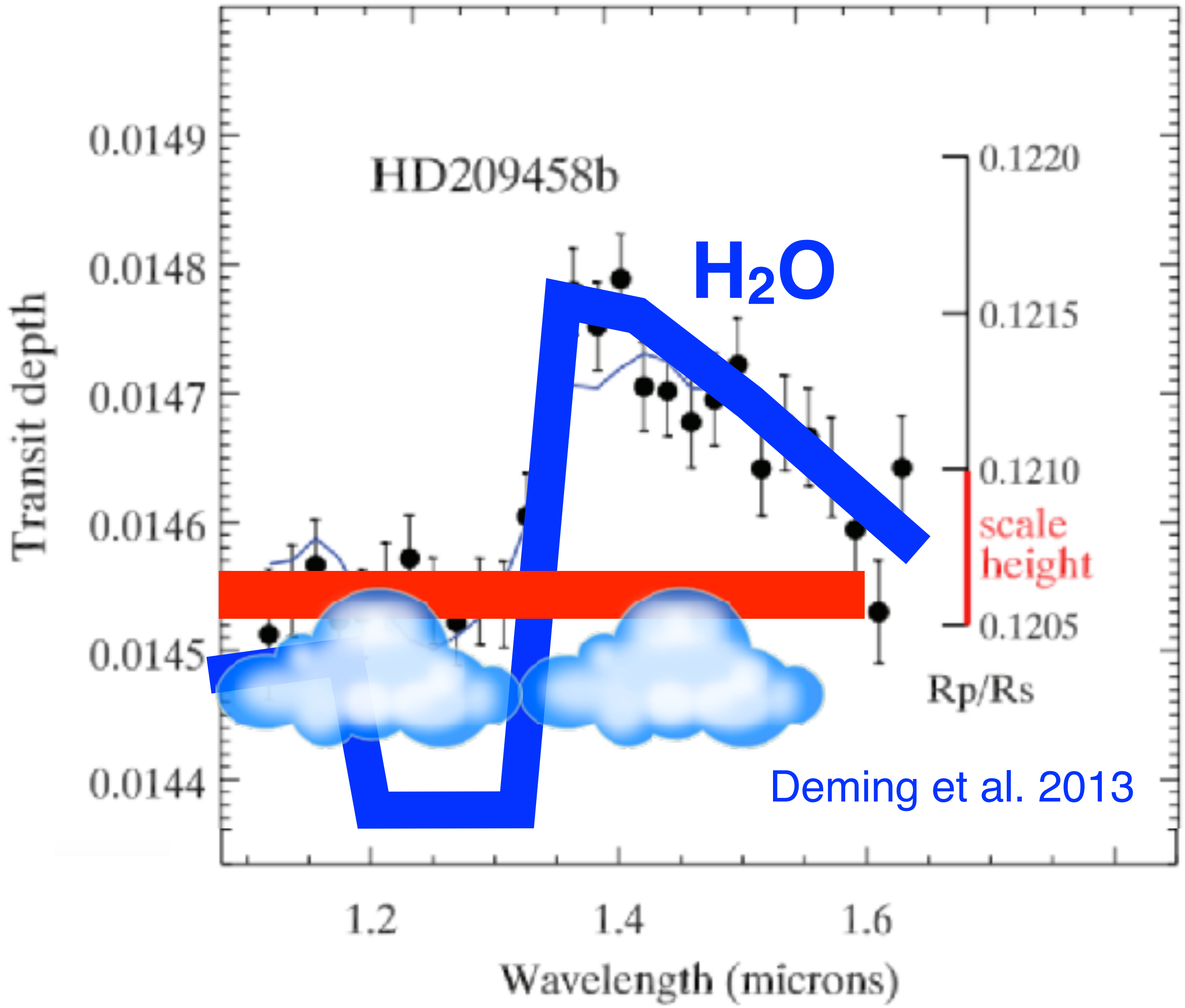

Water absorption should look like this
but it does not

→ it is obscured by H_2
small water abundance

→ it is obscured by clouds
any water abundance

$$R_\mathrm{p}(\lambda_1) - R_\mathrm{p}(\lambda_2) = \log\left(\frac{\xi_a}{\xi_b}\frac{S_\mathrm{a}(\lambda_1)}{S_\mathrm{b}(\lambda_2)}\right) H$$

Clouds in GCMs naturally form spatial patterns !

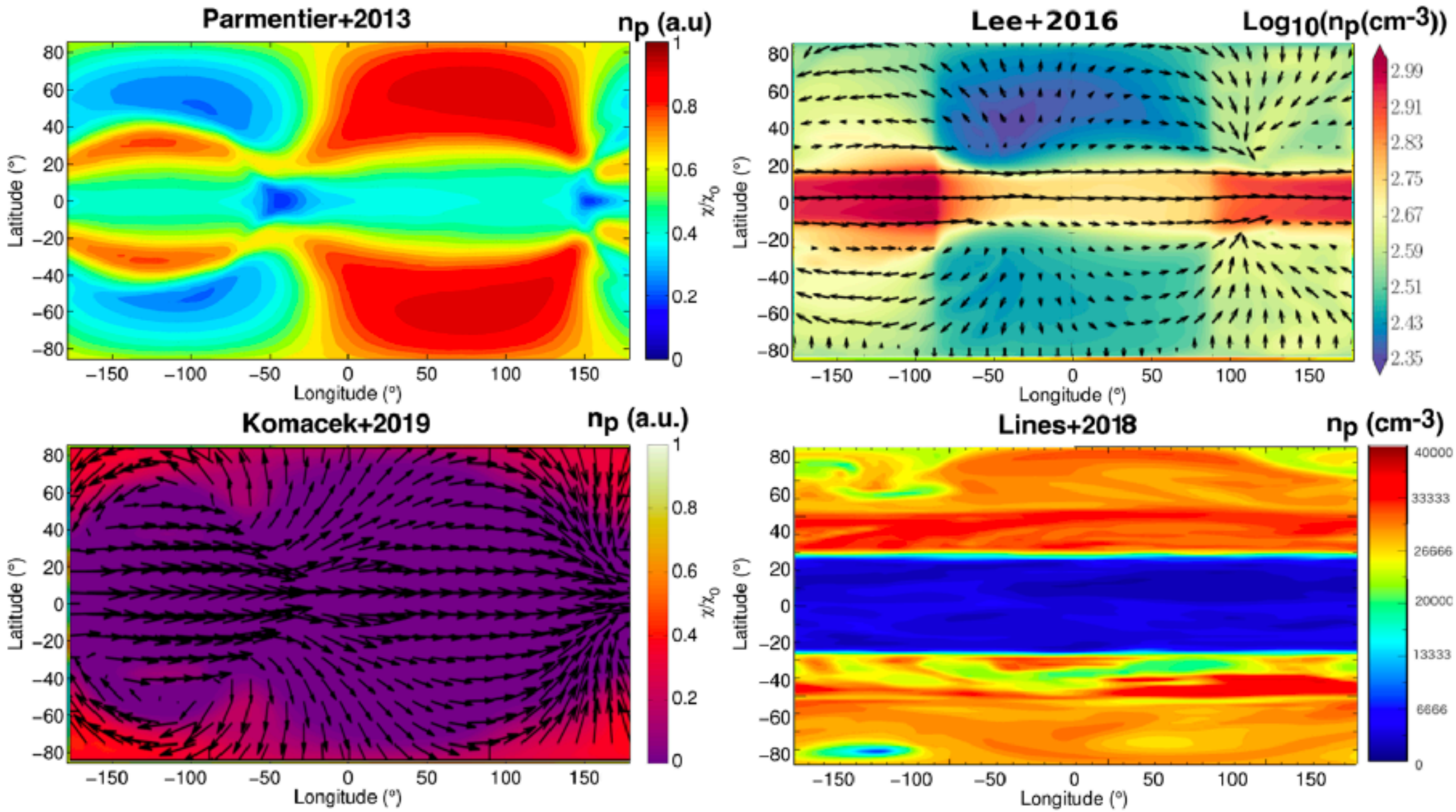

How to form partial clouds ?

— **Circulation driven partial clouds**

Probably always present,
enhanced by radiative feedback ?

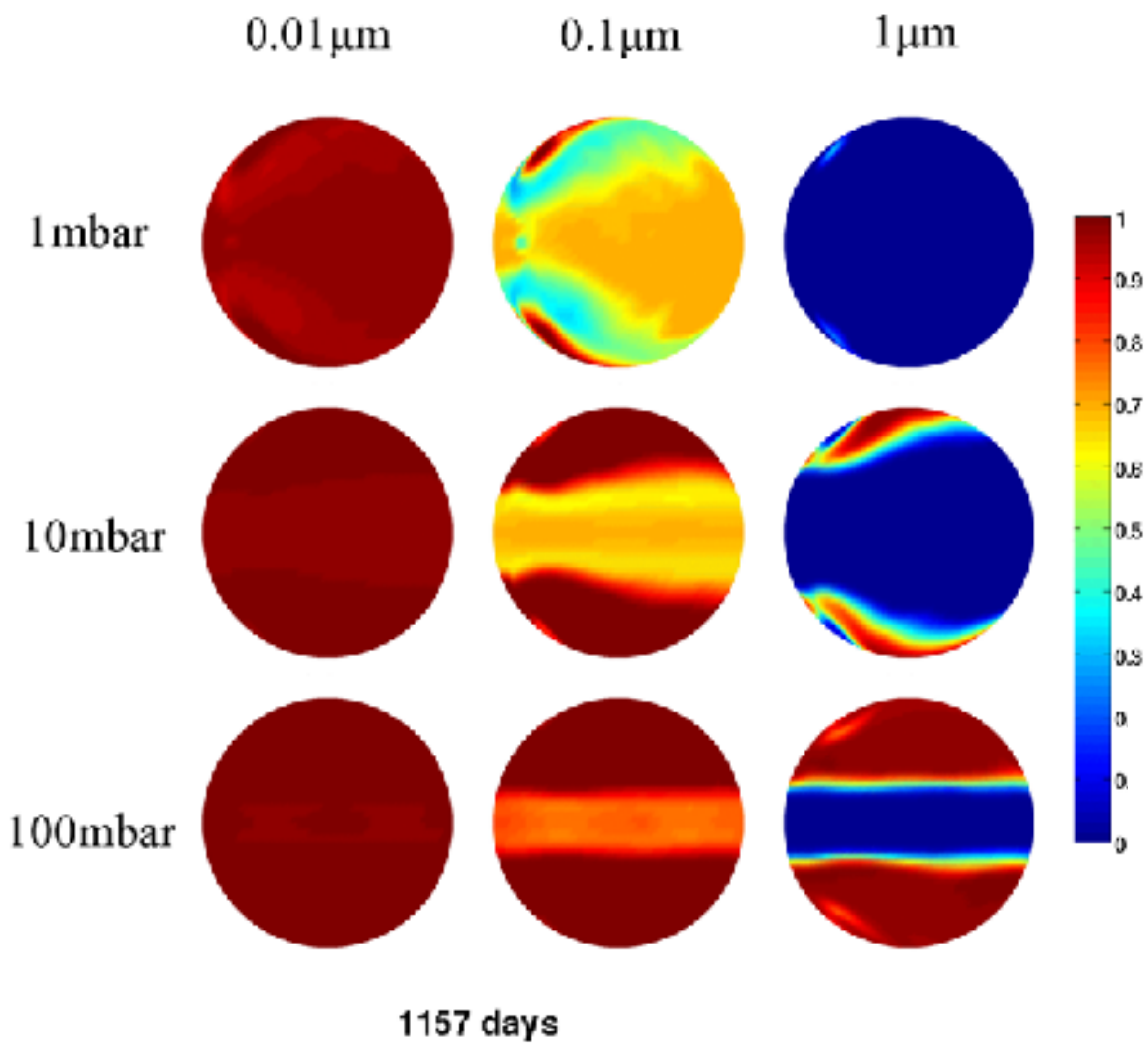

Parmentier+ 2013, passive tracers
(see also Charnay+2016)

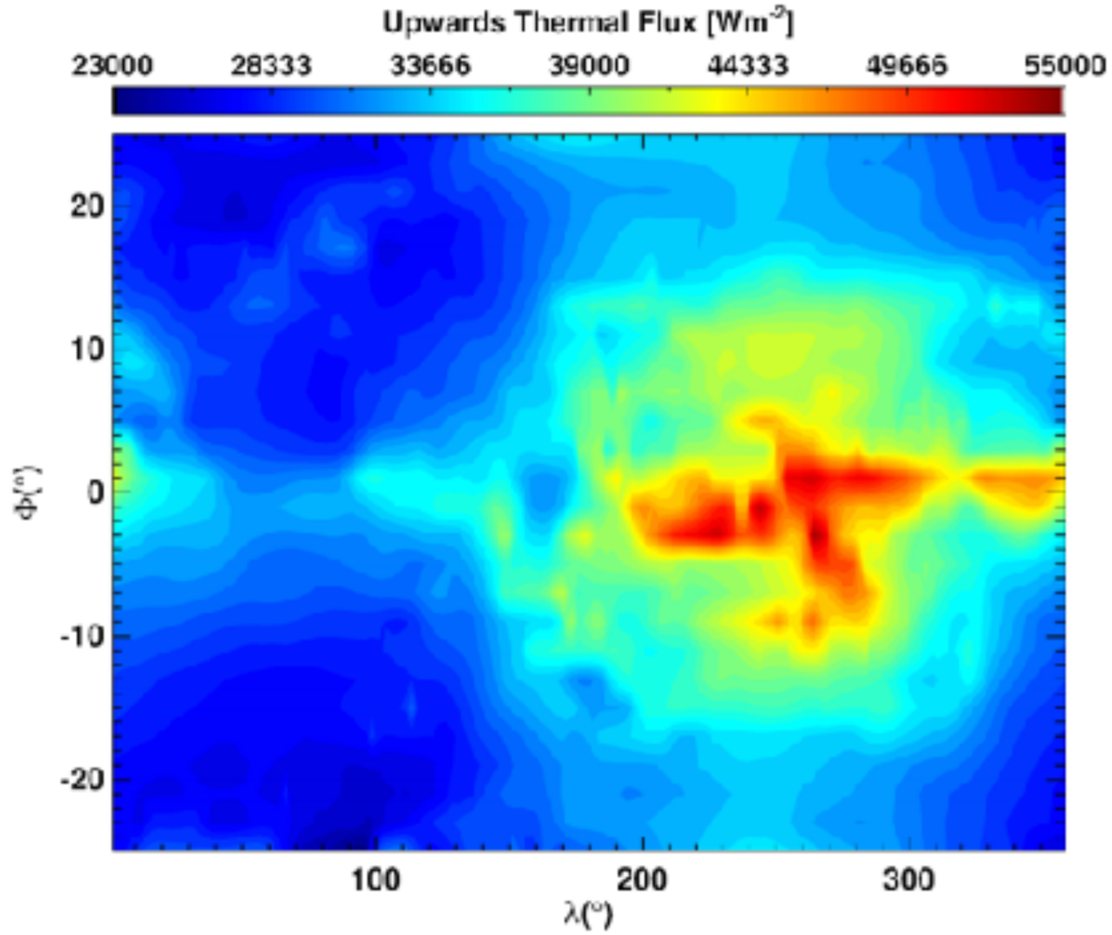

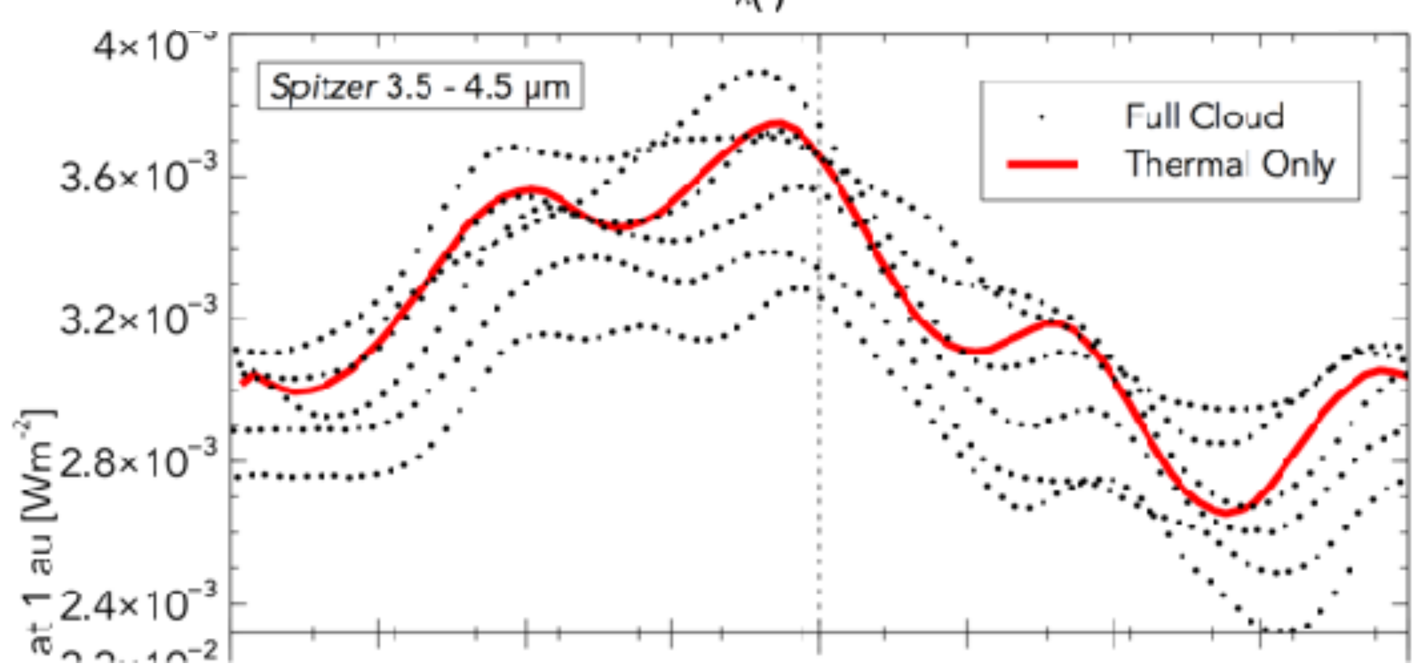

Lines+2018 radiatively active clouds

How to form partial clouds ?

— Temperature driven partial clouds

More important for hot & tidally locked

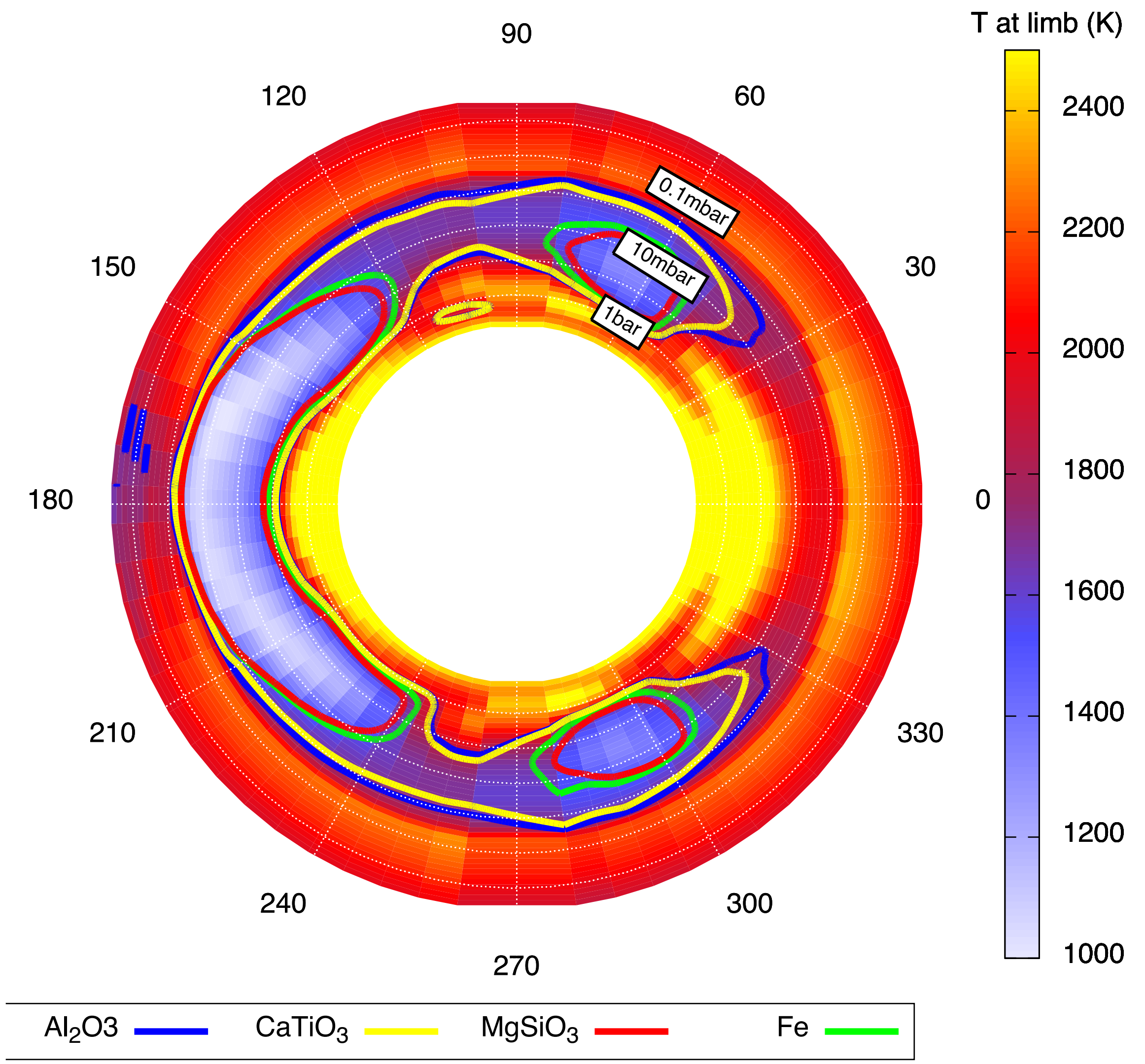

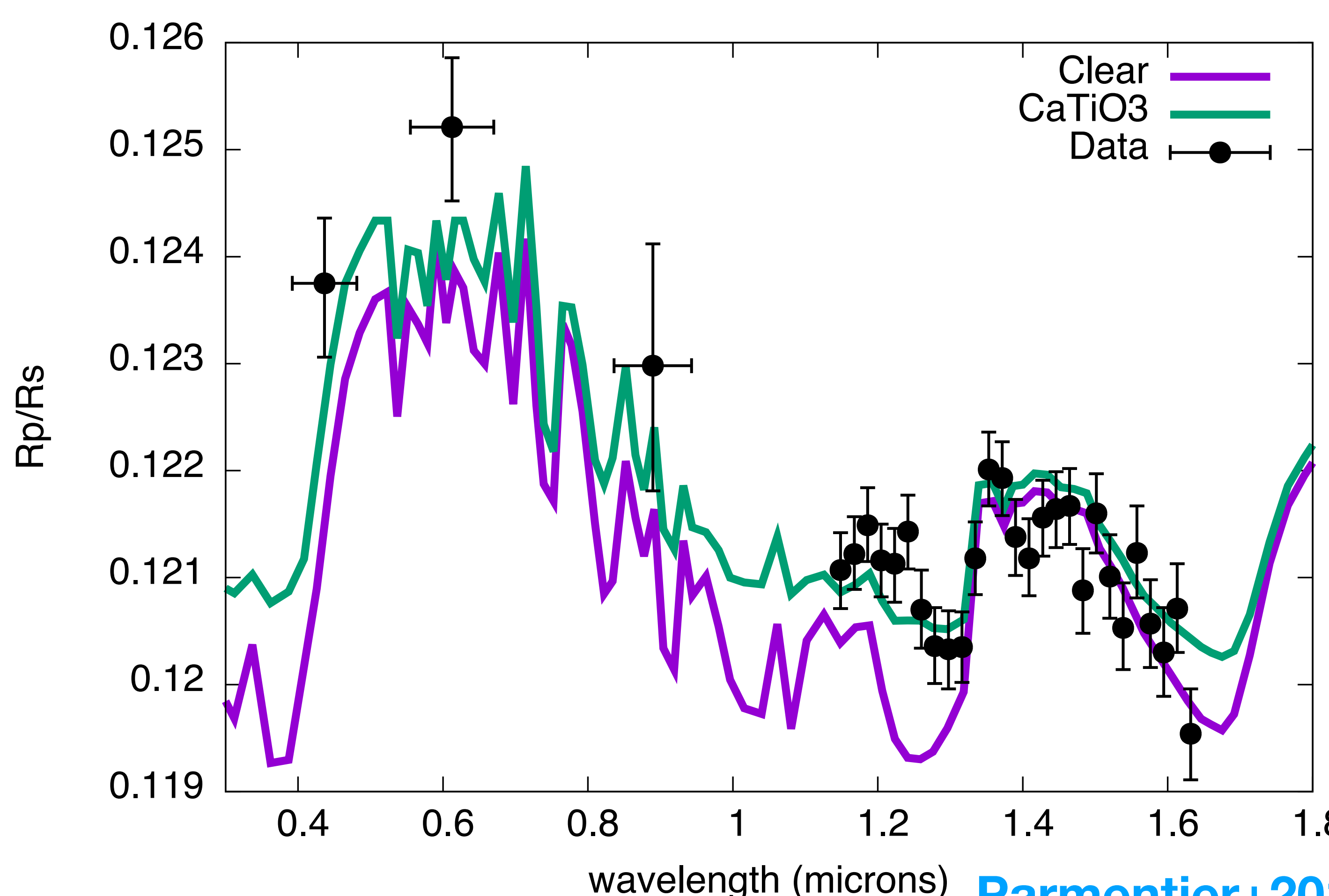

Parmentier+2018

West limb at nightside temperature **Cloudy**

East limb at dayside temperature **Cloudless**

See also: MacDonald+2016, Kempton+2018

How to form partial clouds ?

Or a combination of both

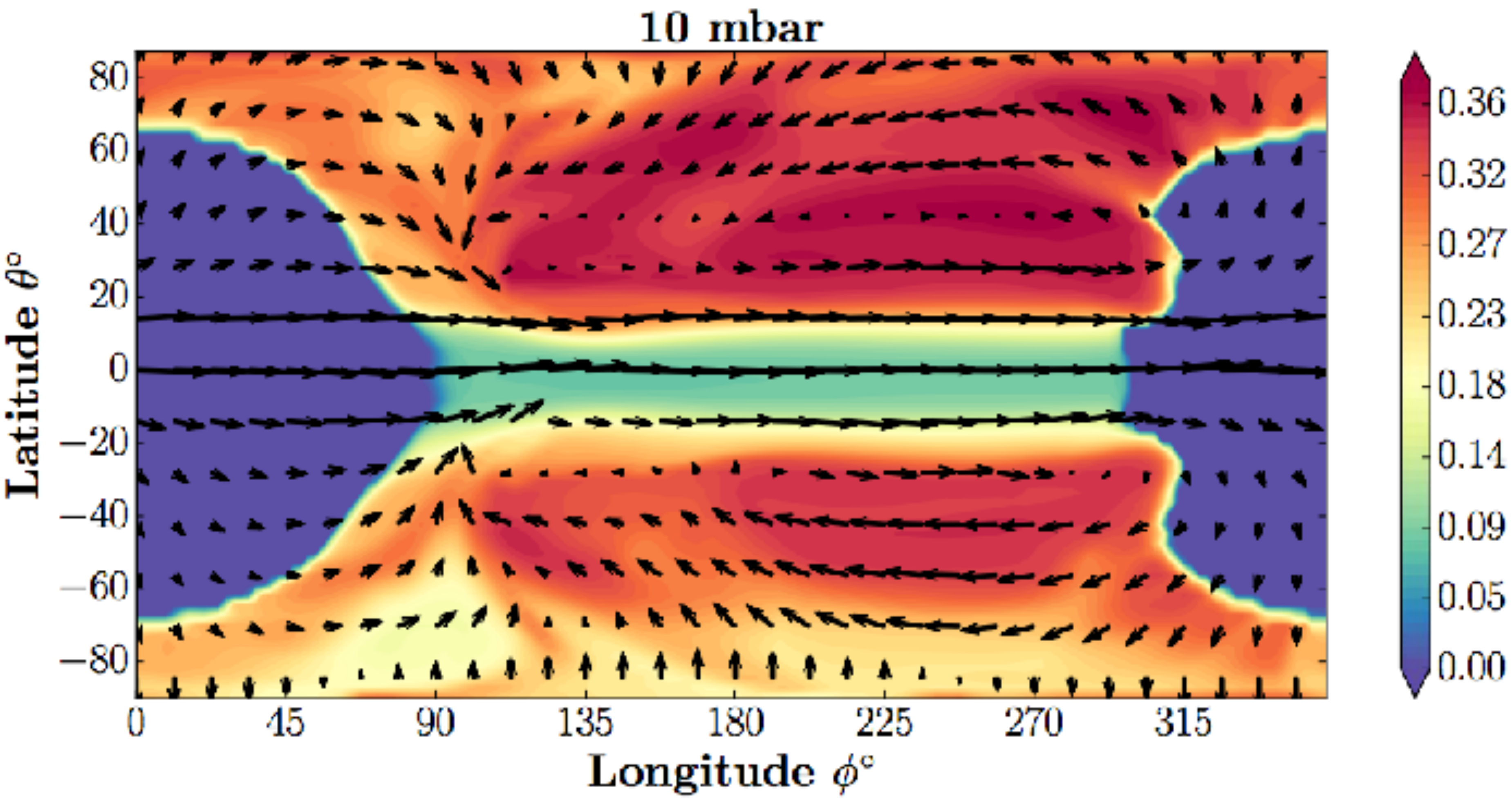

Mean particle sizes in HD189 coupled microphysics GCM
(see also Lines+2017)

Lee et al. 2016

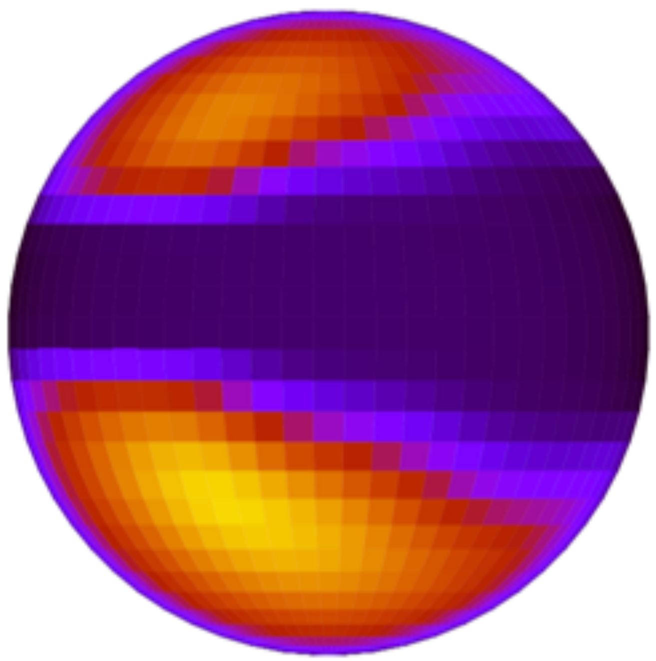

Dayside reflected light of HD189733b with MnS as passive tracers SPARC/MITgcm

Wavelength dependence of the phase curve

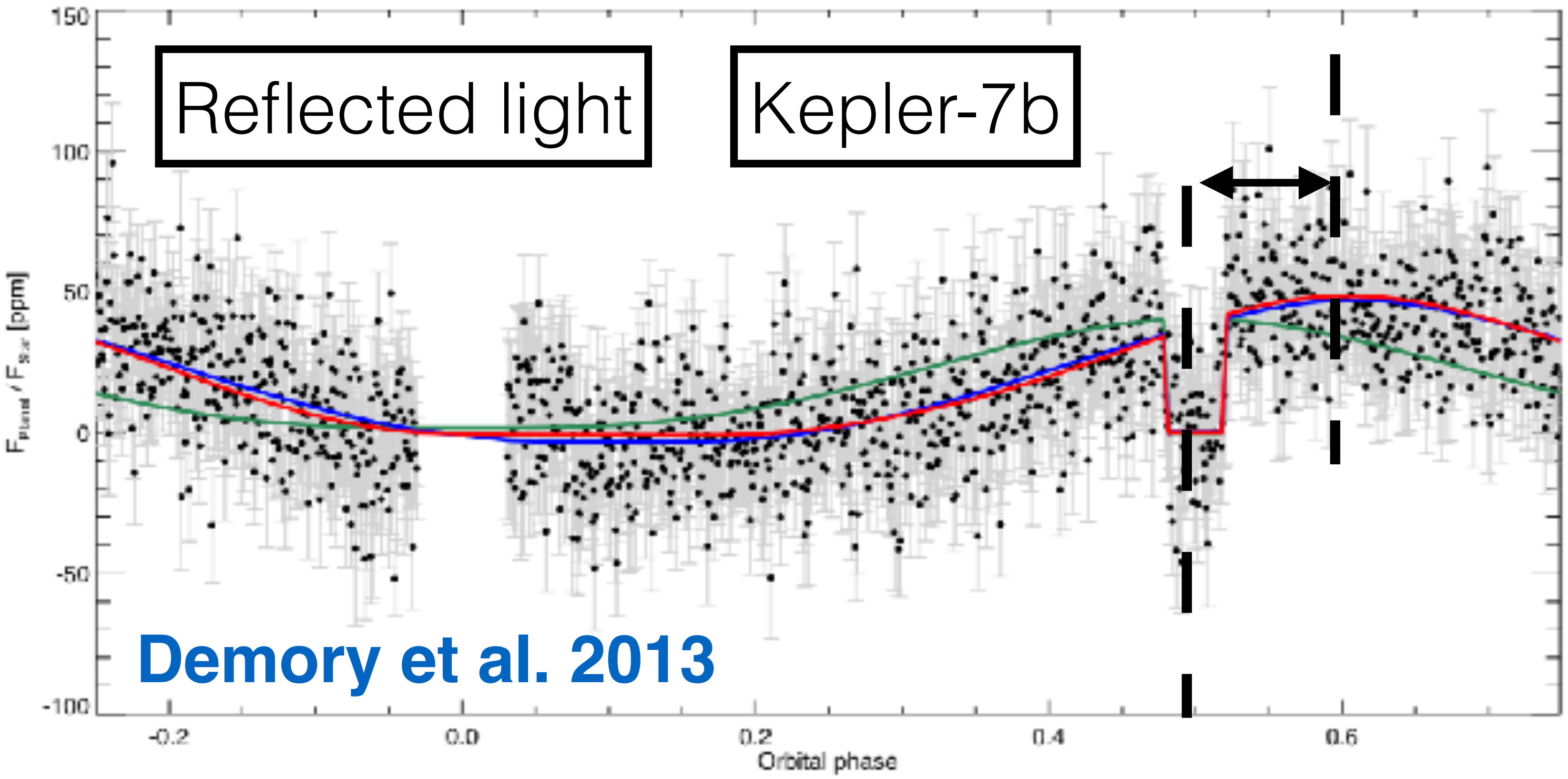

West cloudier than east

Reflected light phase curve : negative offset

Offset of the maximum

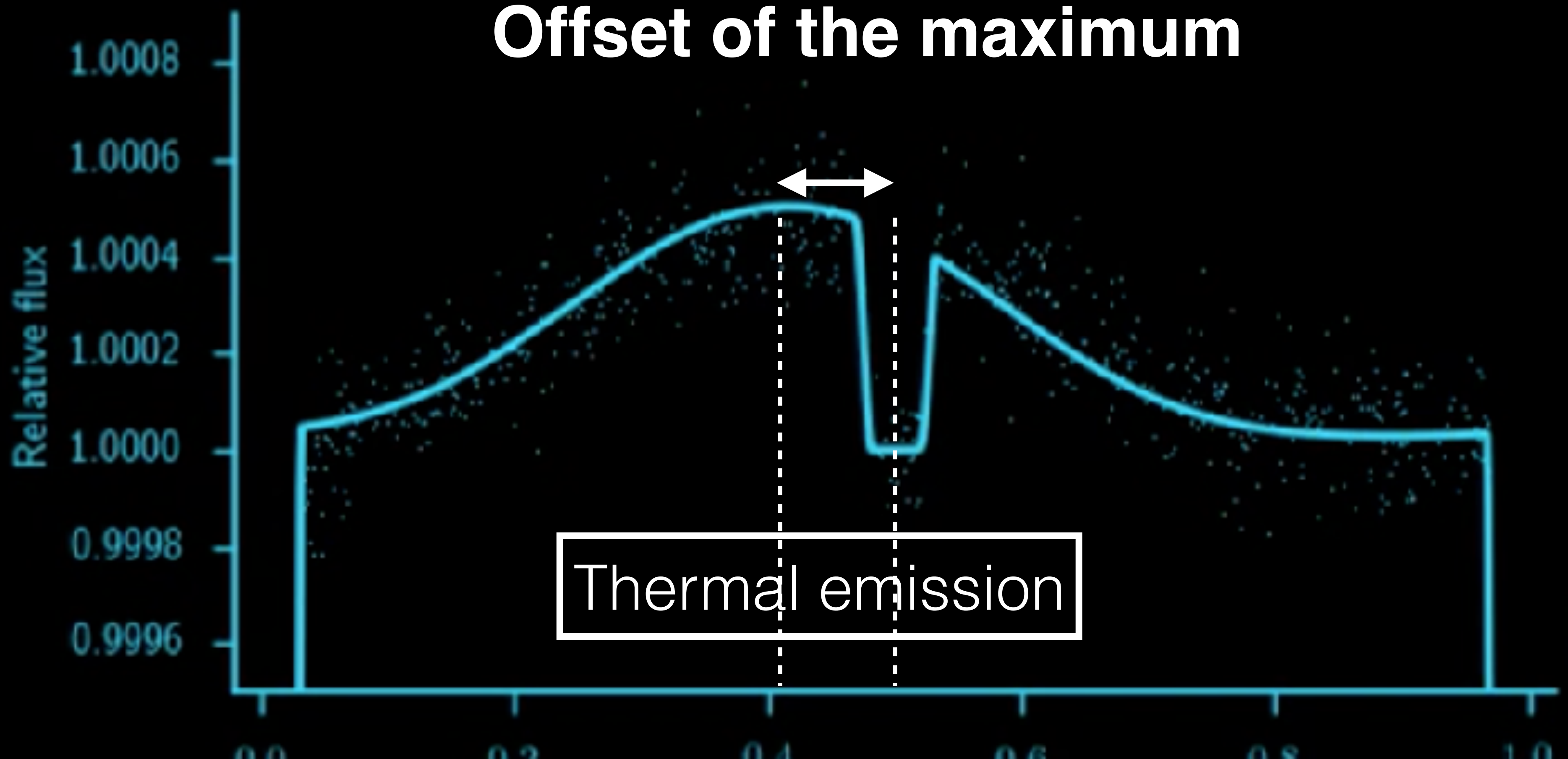

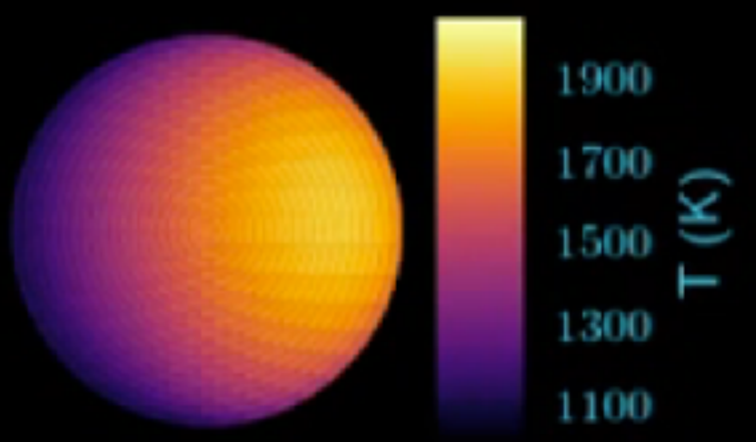

Courtesy Tom Louden

Wavelength dependence of the phase curve

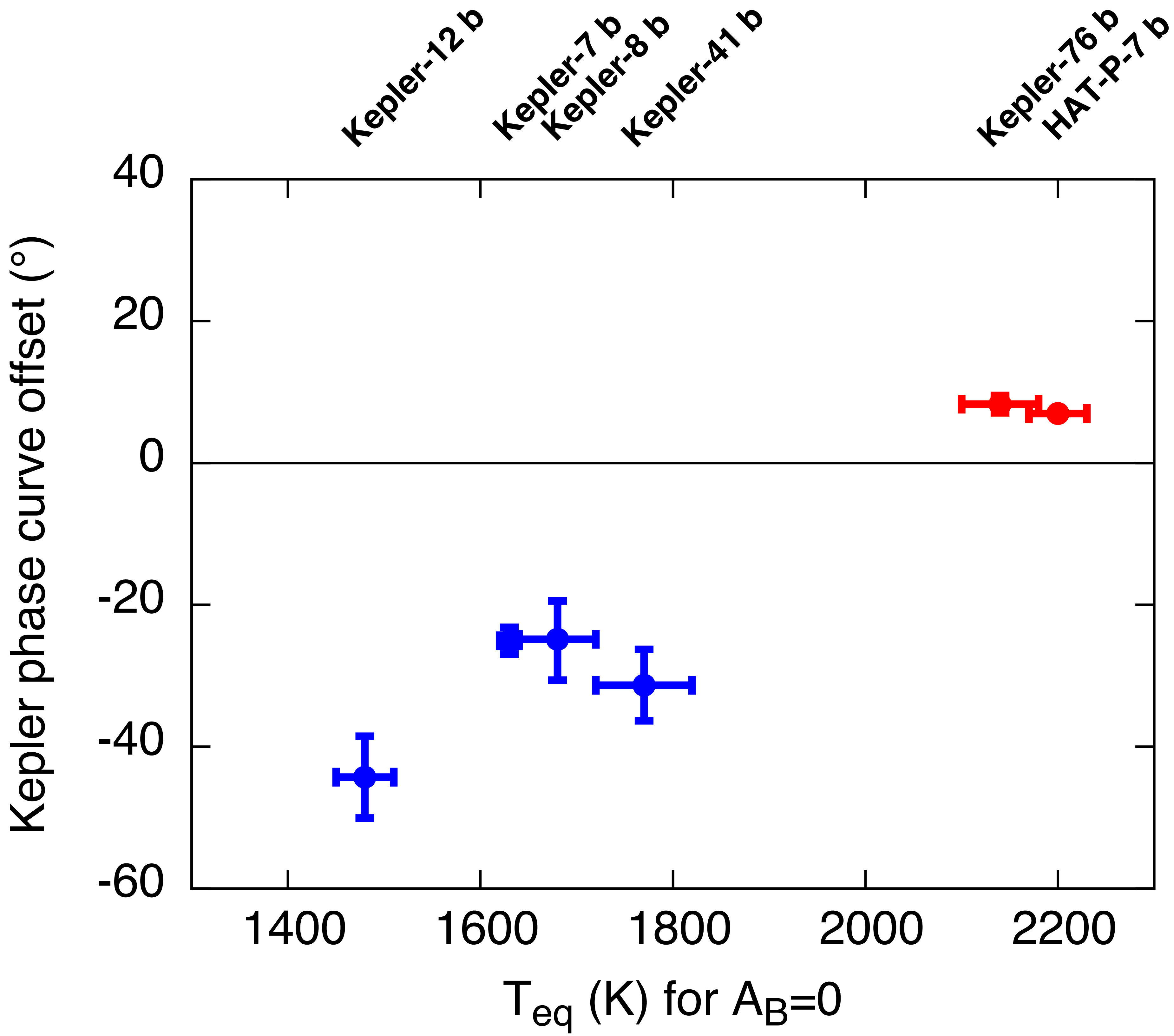

Parmentier et al. 2016

Wavelength dependence of the phase curve

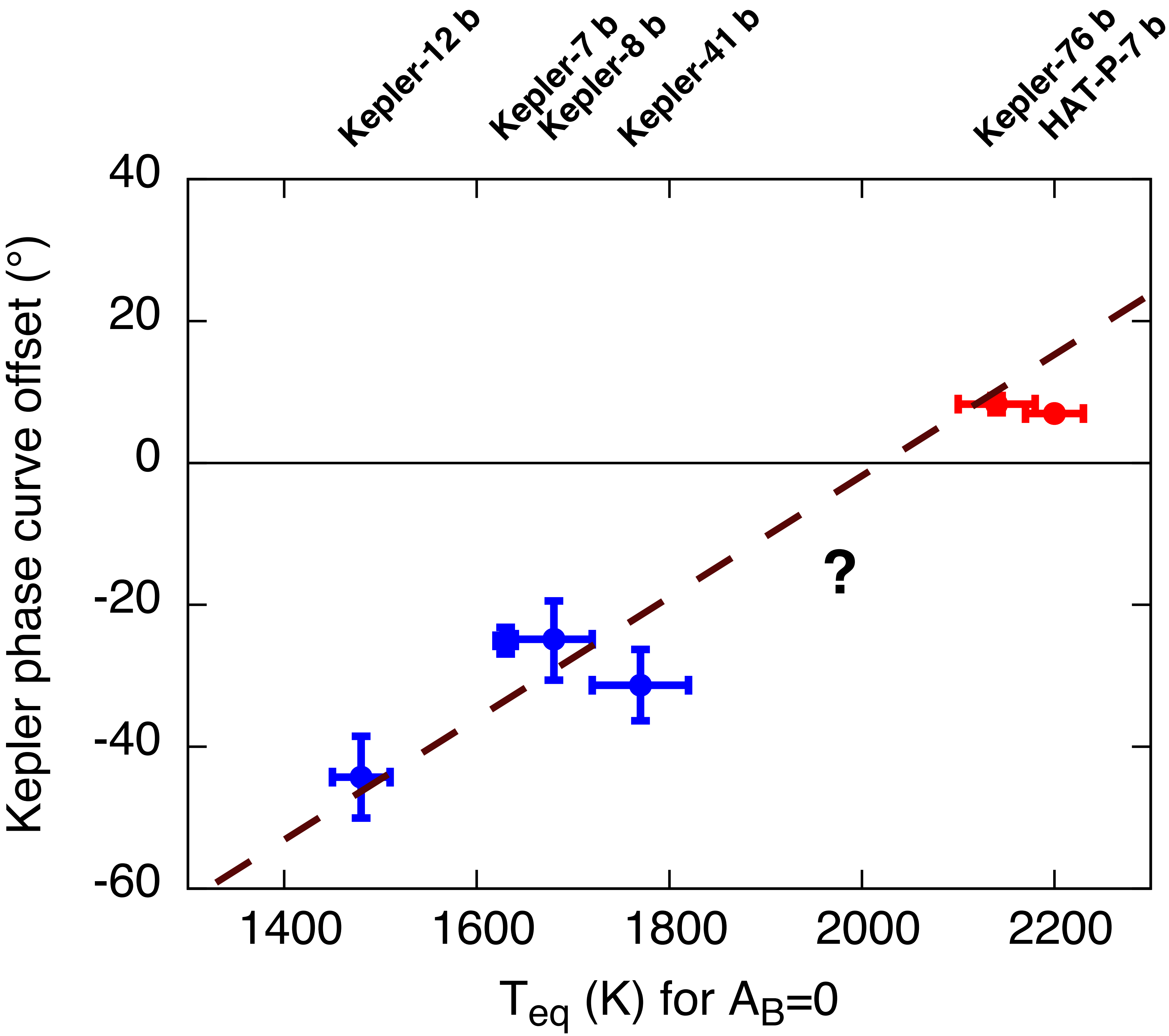

Parmentier et al. 2016

Wavelength dependence of the phase curve

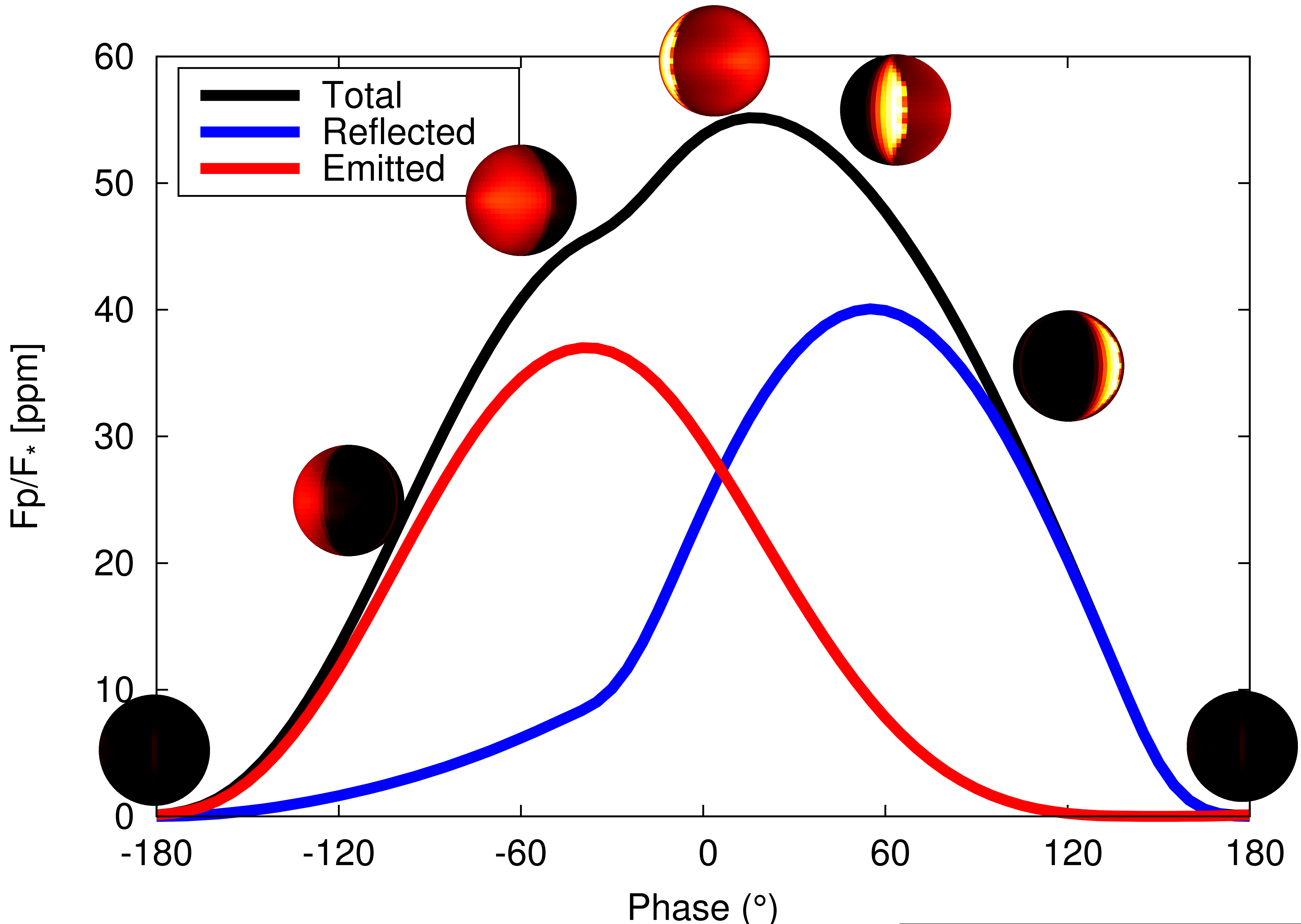

Parmentier et al. 2016

Model: Teq=1900K

Wavelength dependence of the phase curve

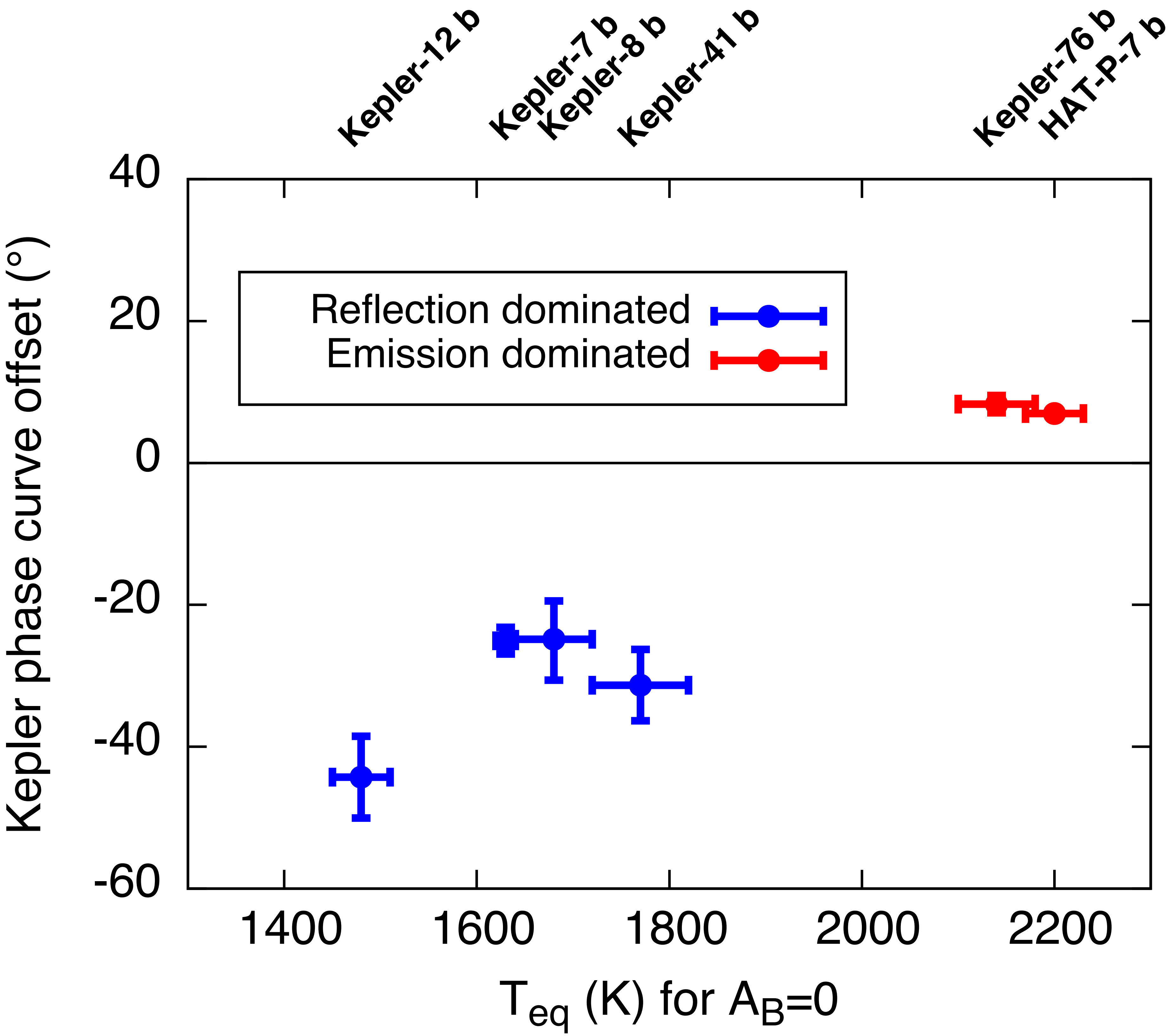

Parmentier et al. 2016

Travel to your nearest Hot Jupiter

Equilibrium temperature

Cloud chemical composition

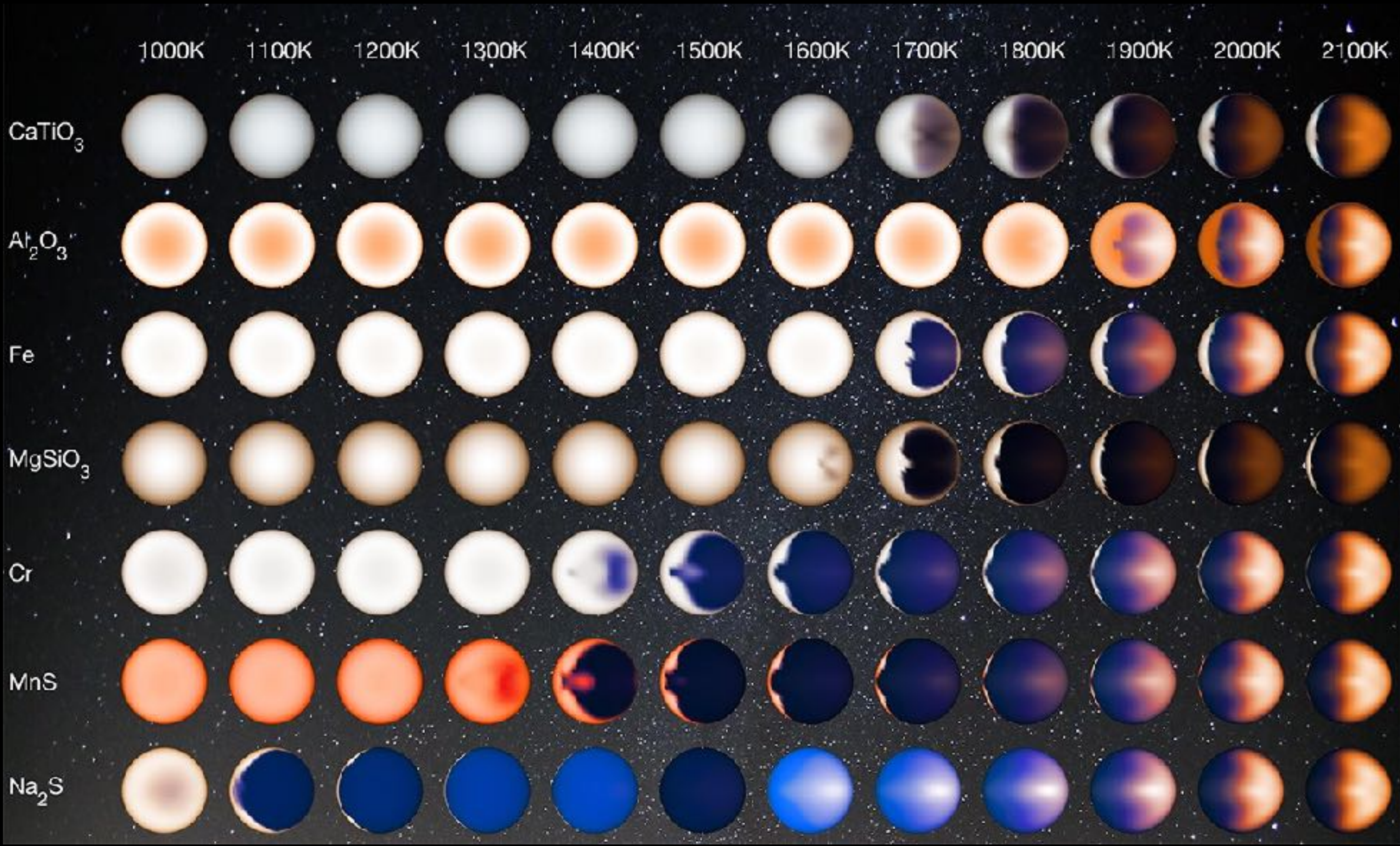

Parmentier et al. 2016

Hot Jupiter daysides as seen by a human eye

Travel to your nearest Hot Jupiter

Equilibrium temperature

Cloud chemical composition

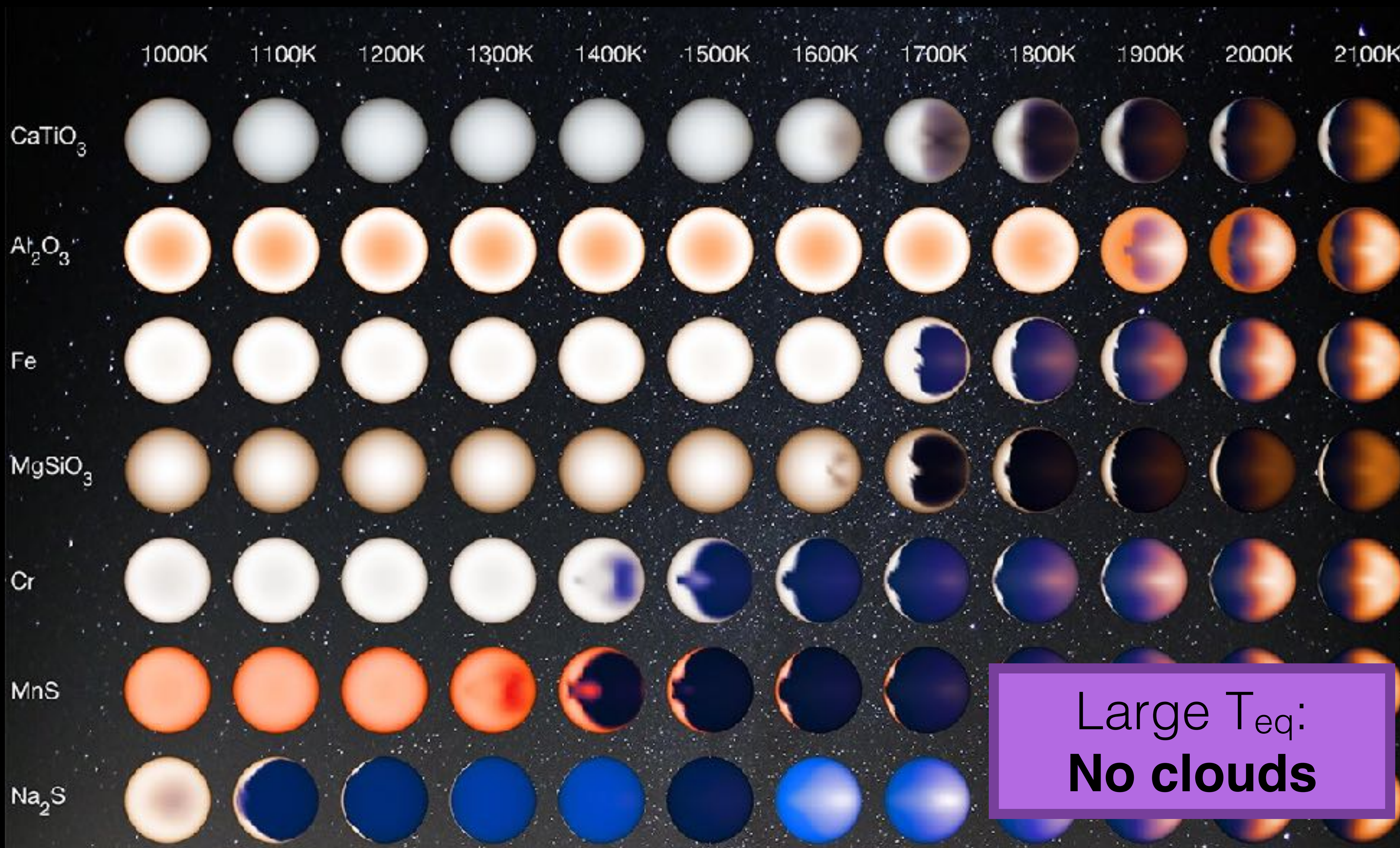

Large T_{eq}:
No clouds

Hot Jupiter daysides as seen by a human eye

Parmentier et al. 2016

Travel to your nearest Hot Jupiter

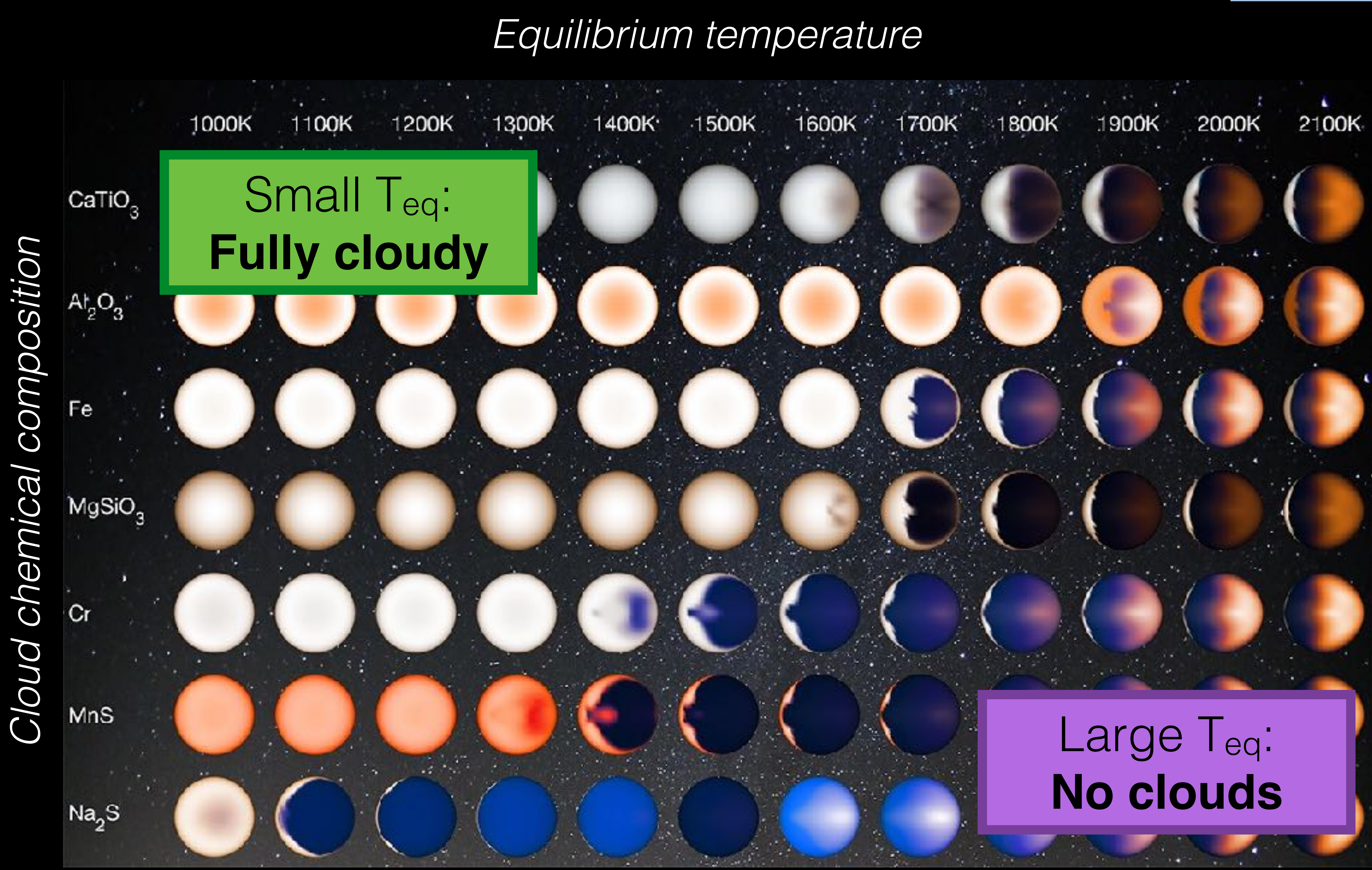

Parmentier et al. 2016

Hot Jupiter daysides as seen by a human eye

Travel to your nearest Hot Jupiter

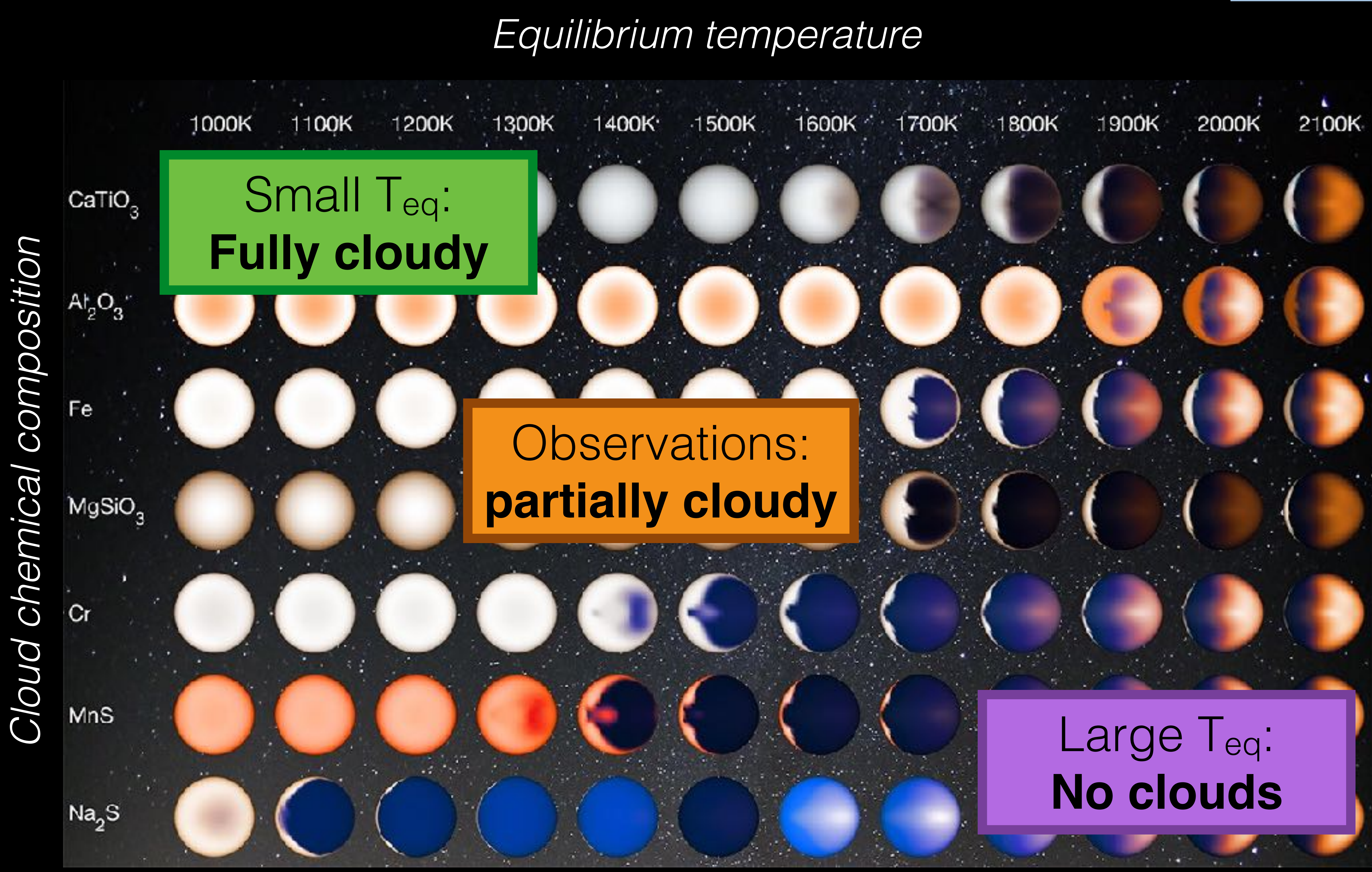

Parmentier et al. 2016

Hot Jupiter daysides as seen by a human eye

Travel to your nearest Hot Jupiter

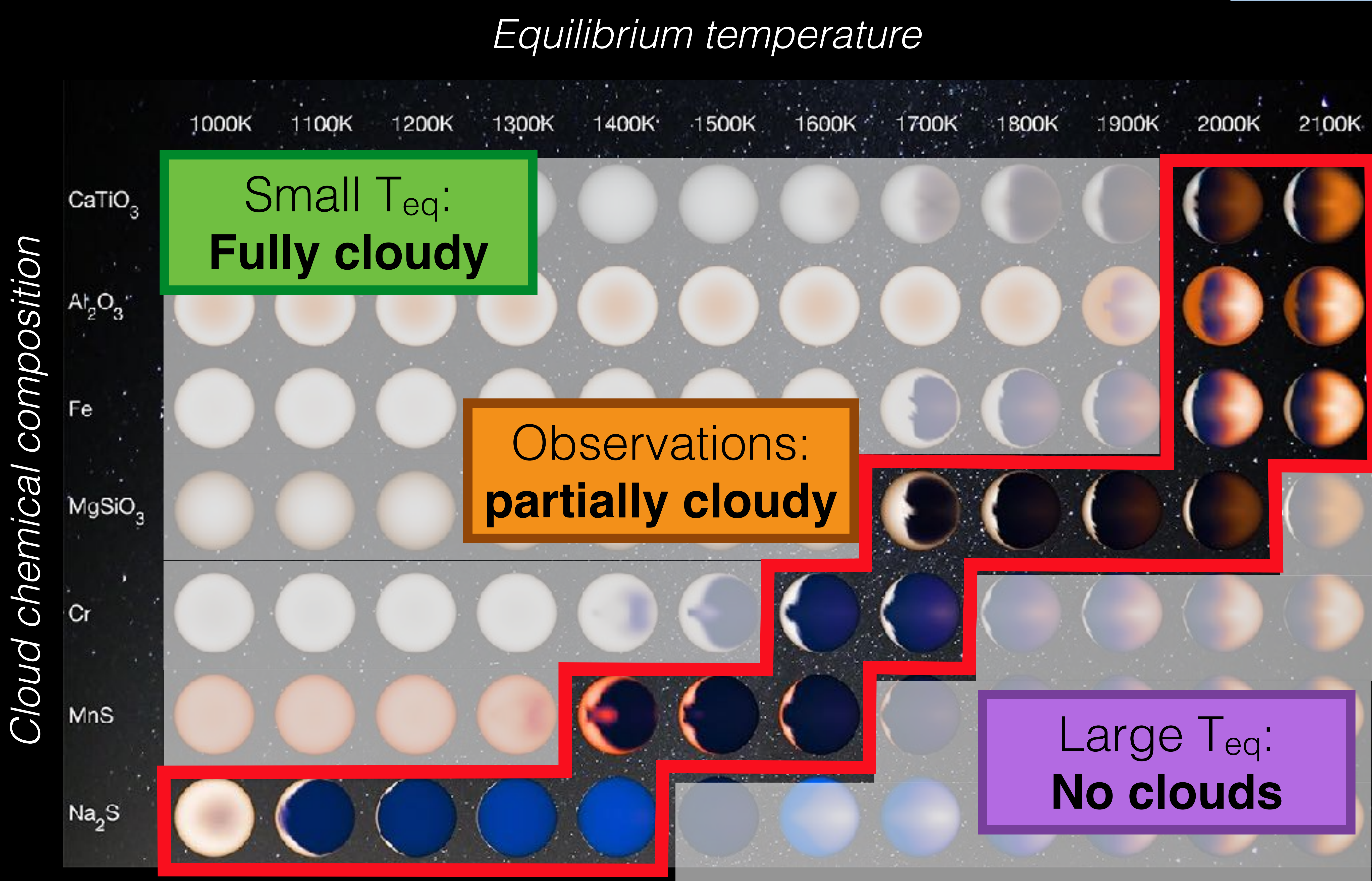

Parmentier et al. 2016

Hot Jupiter daysides as seen by a human eye

Travel to your nearest Hot Jupiter

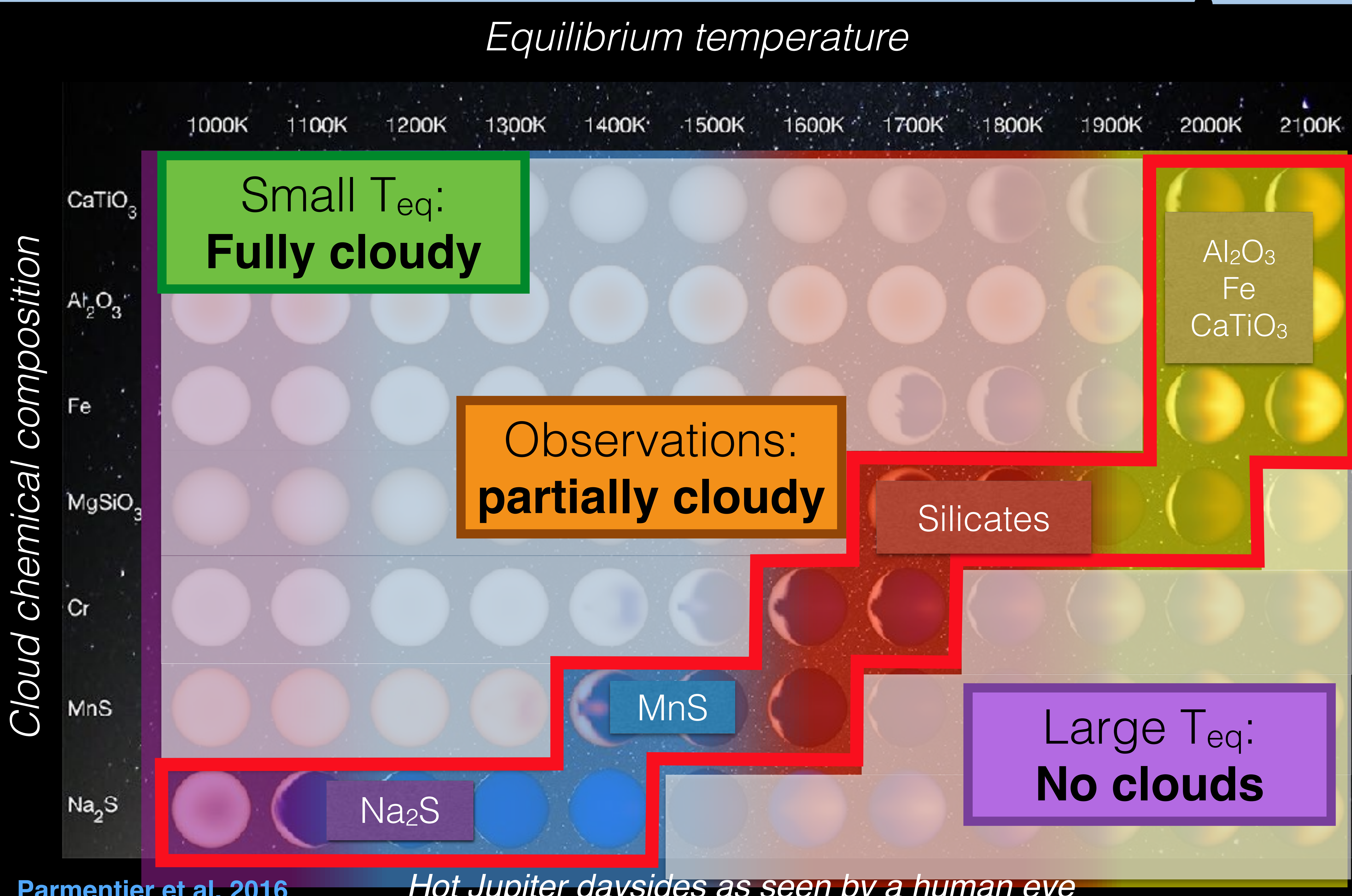

Parmentier et al. 2016

A temperature dependent cloud composition ?

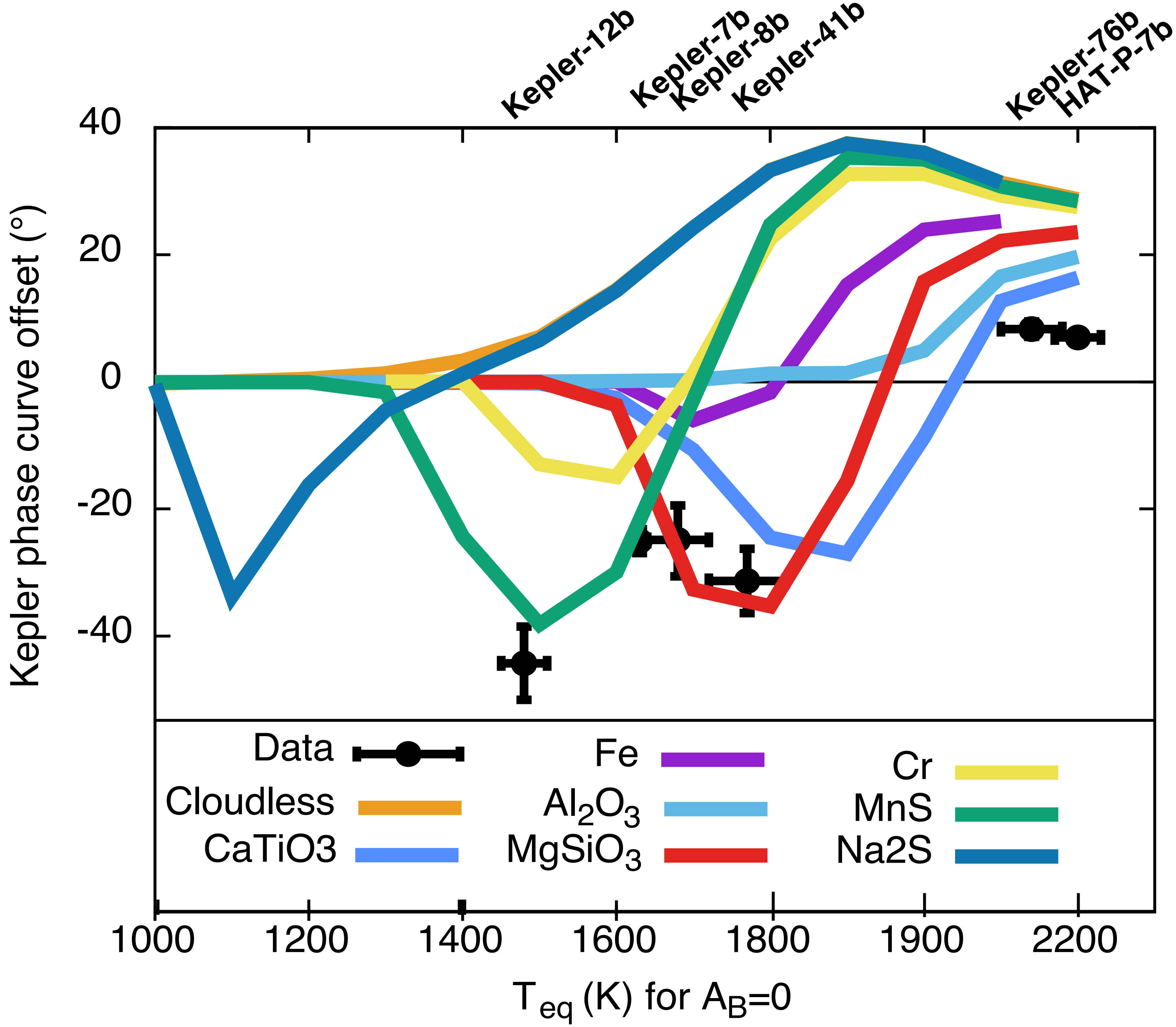

Parmentier et al. 2016

How nightside clouds affect the circulation ?

Clear atmosphere

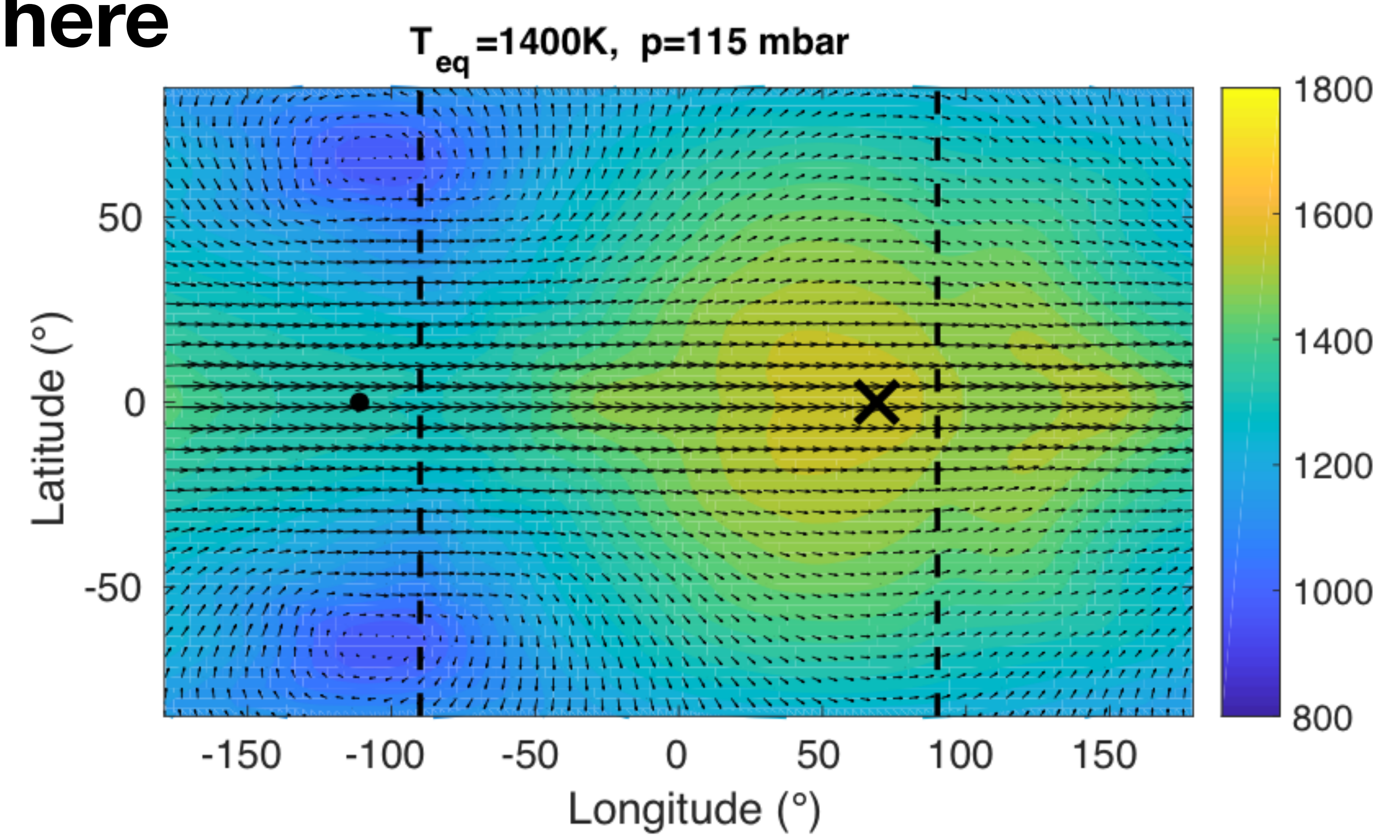

Parmentier et al. 2020

How nightside clouds affect the circulation ?

Clear atmosphere

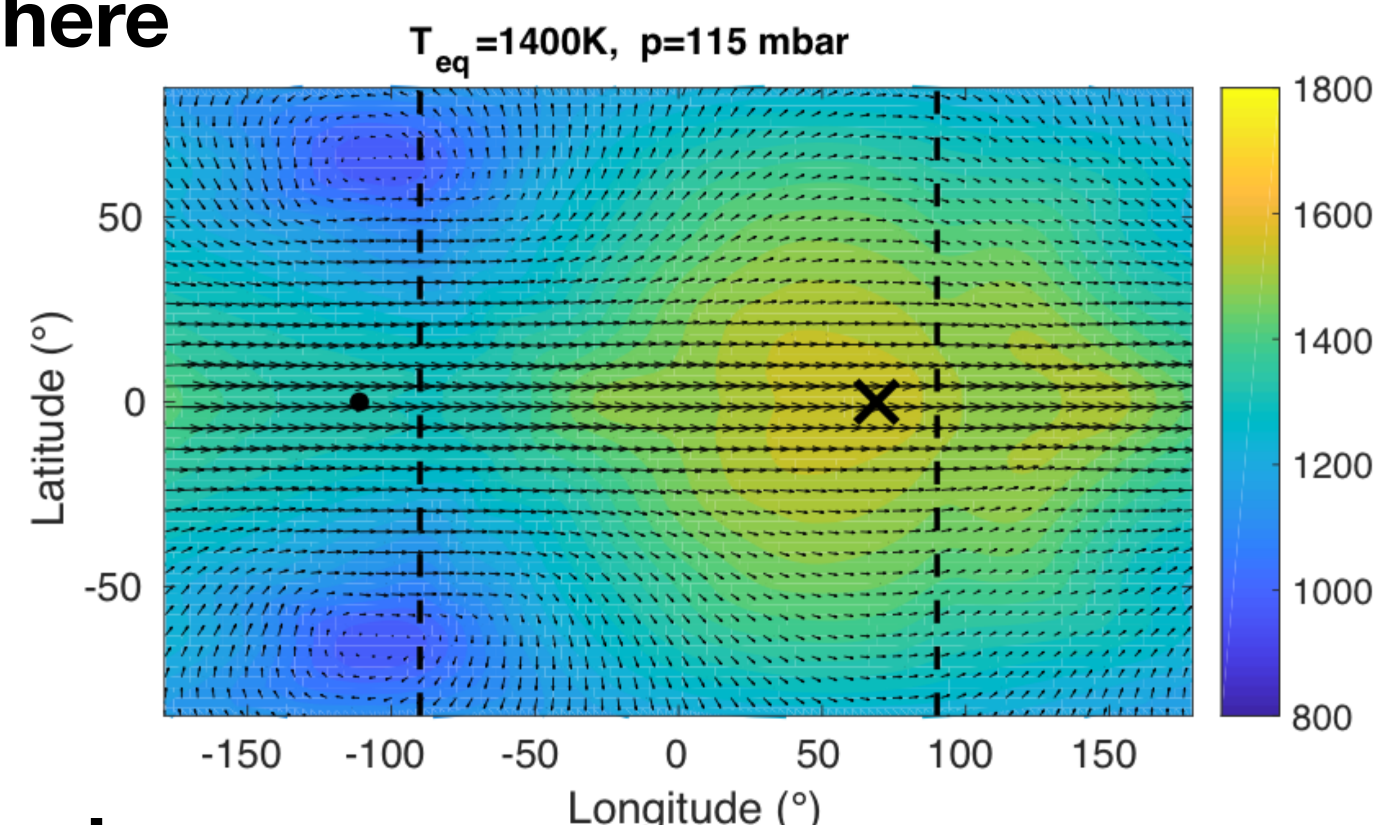

Nightside clouds

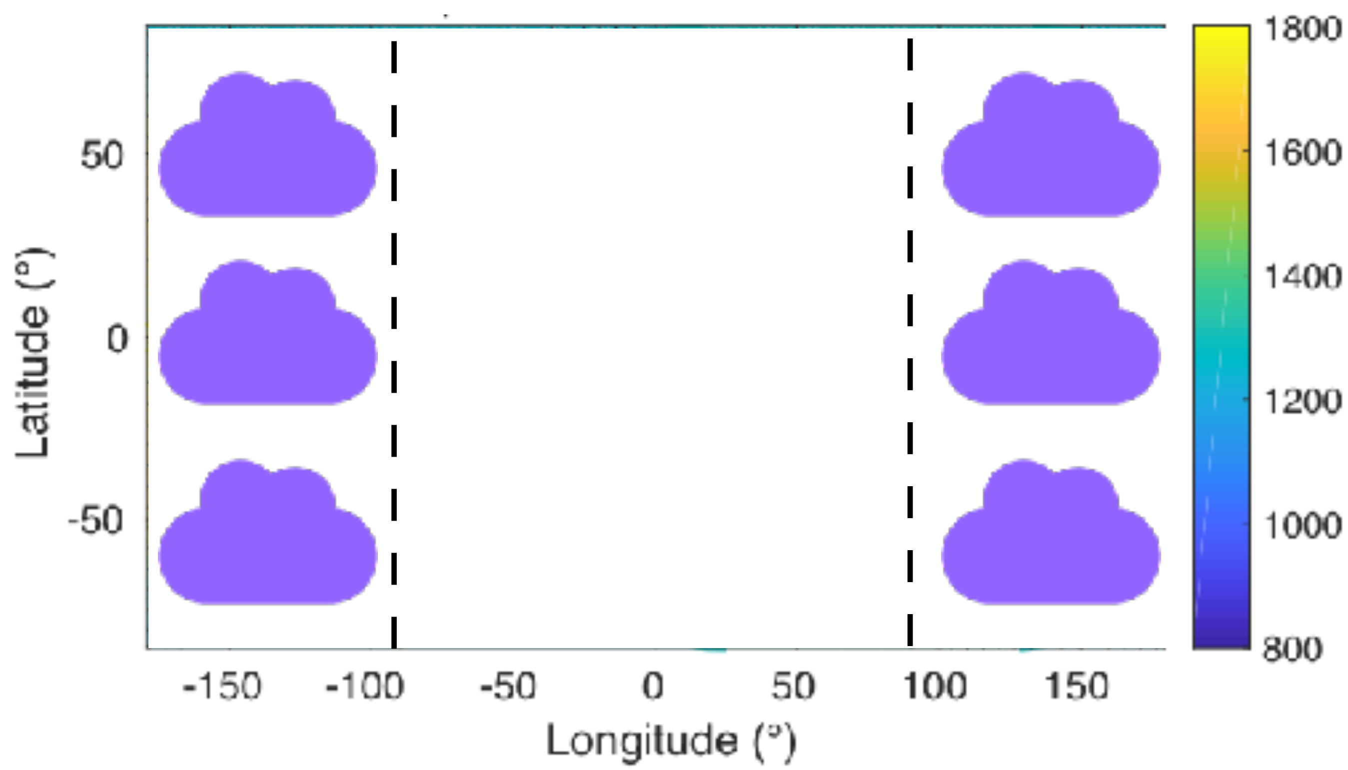

MnS optical properties & abundances

Cloud base 200mbar

Well mixed vertically

Monosize

Parmentier et al. 2020

How nightside clouds affect the circulation ?

Clear atmosphere

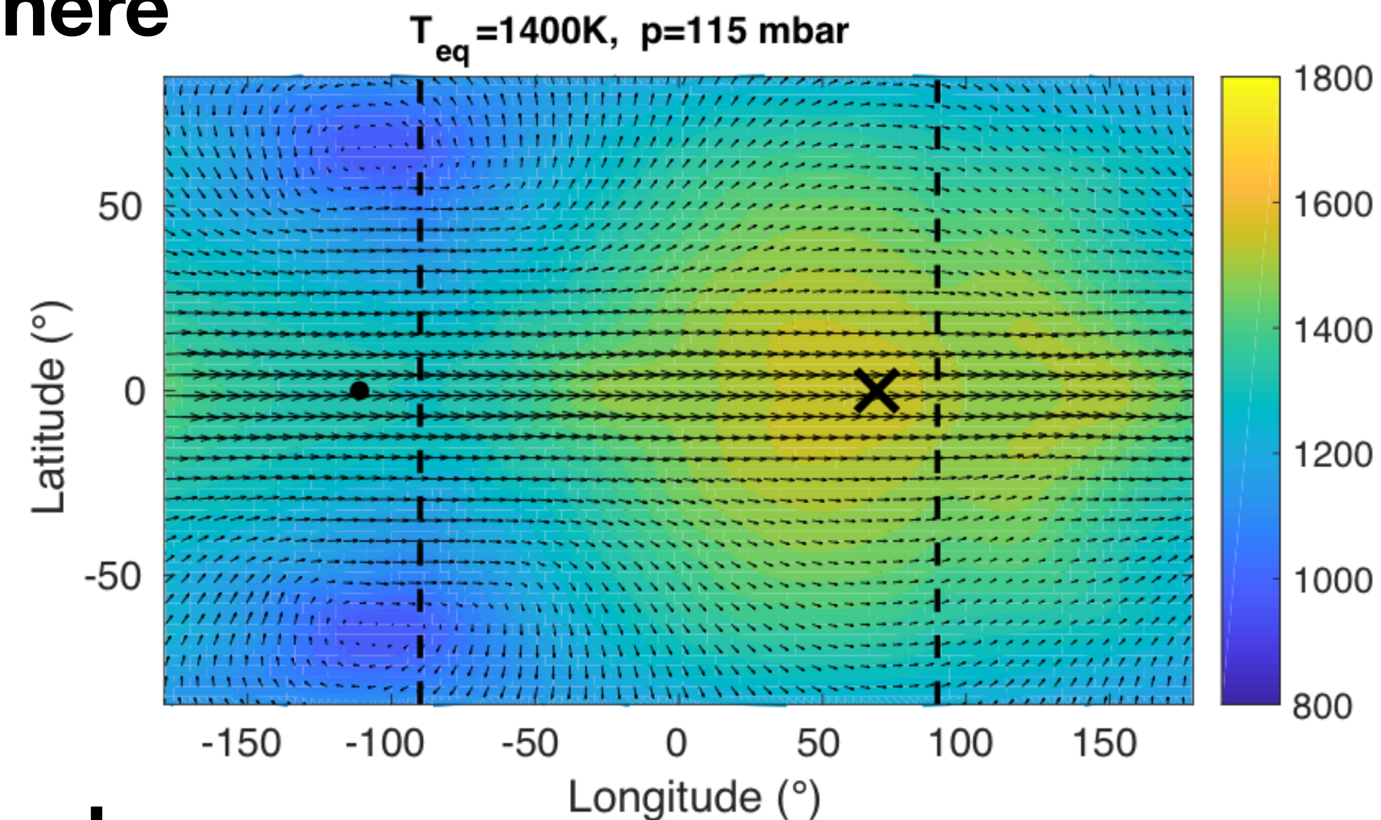

Nightside clouds

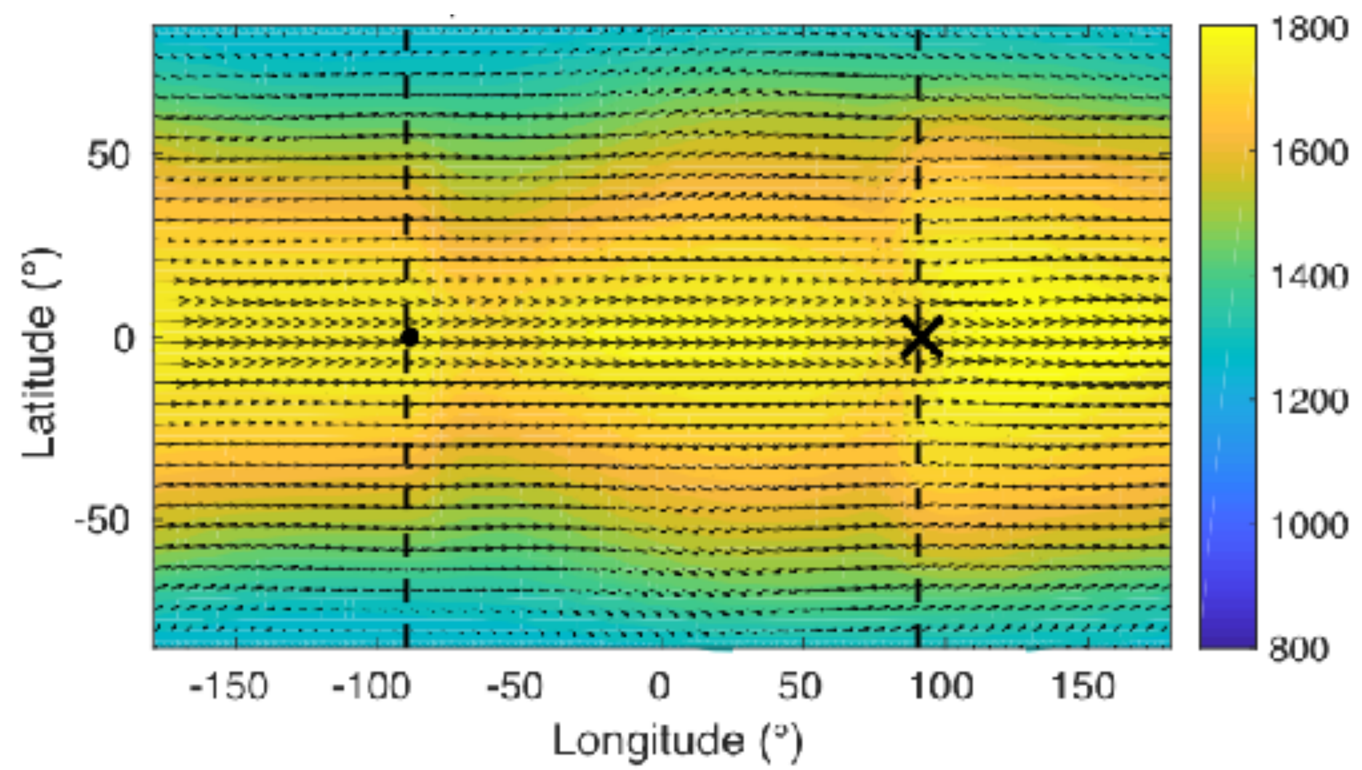

Parmentier et al. 2020

How nightside clouds affect the circulation ?

Clear atmosphere

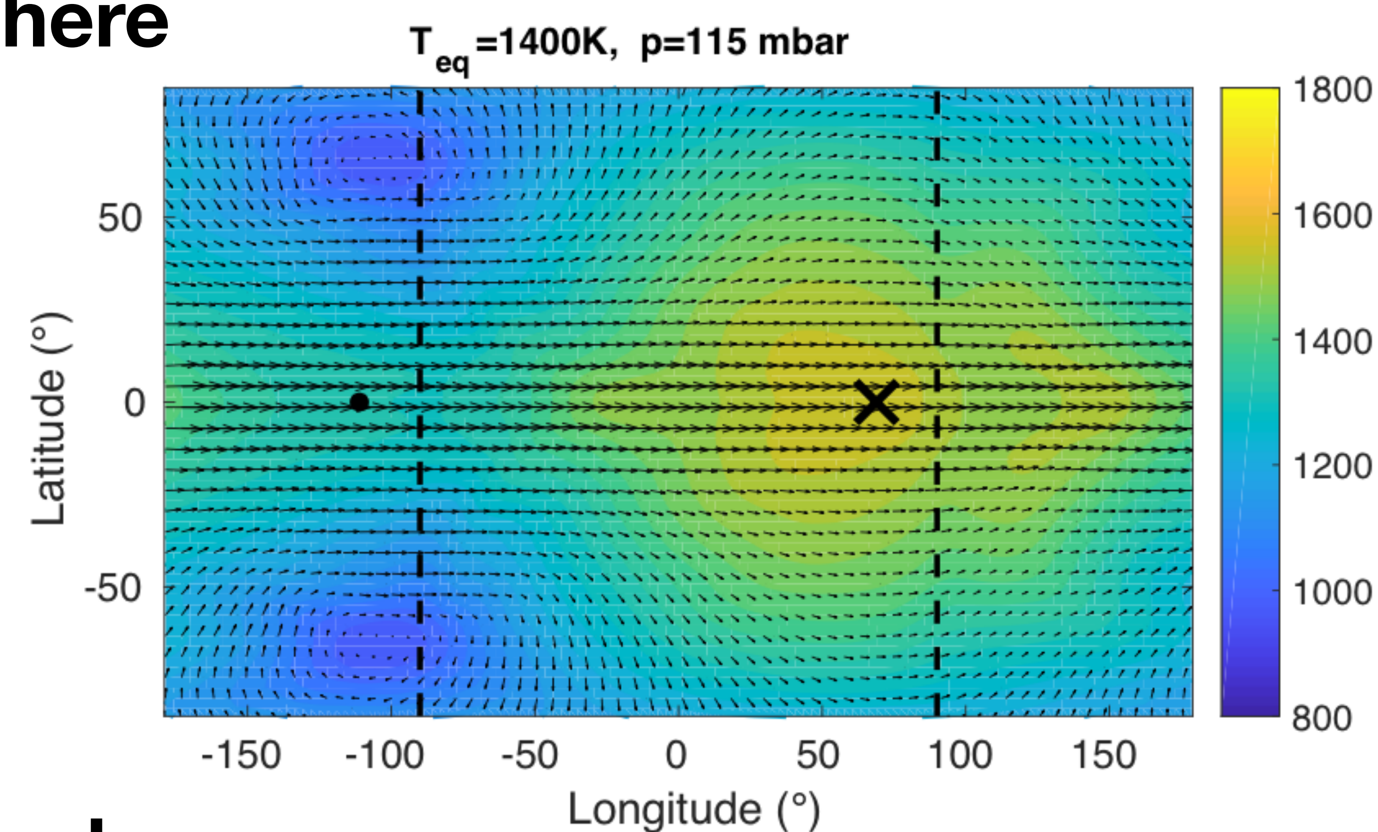

Reduce day/night temperature contrast

Nightside clouds

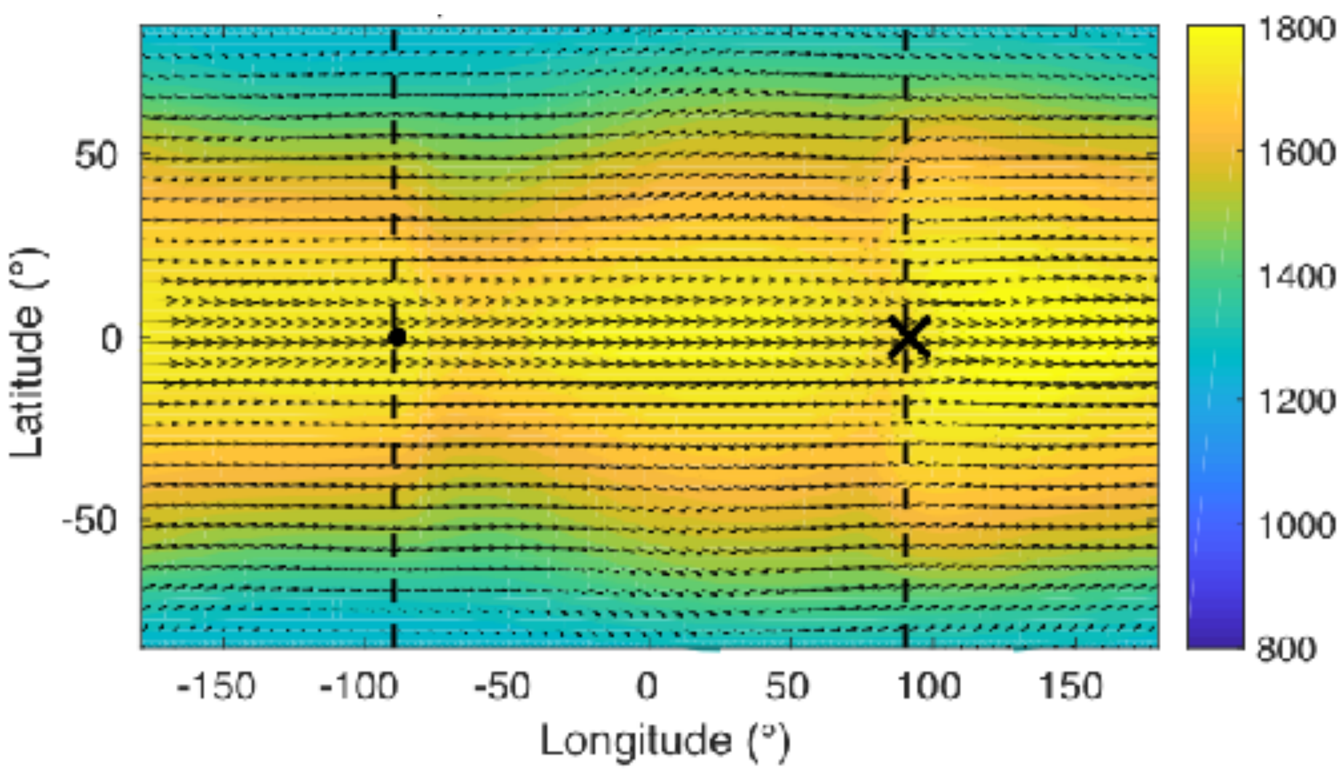

Does not affect hot spot shift

Parmentier et al. 2020

How nightside clouds affect the thermal phase curve ?

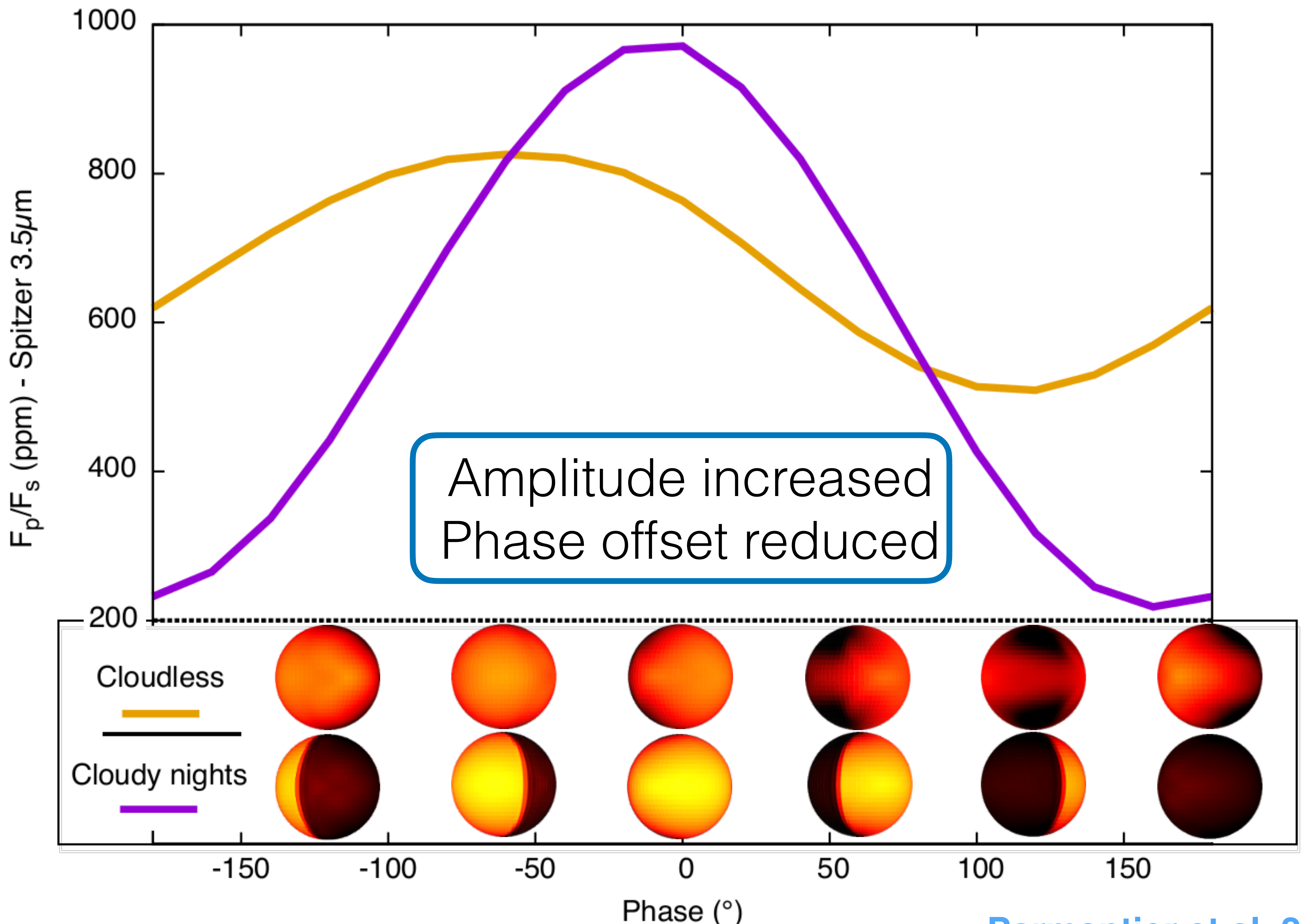

Parmentier et al. 2020

How nightside clouds affect the thermal phase curve ?

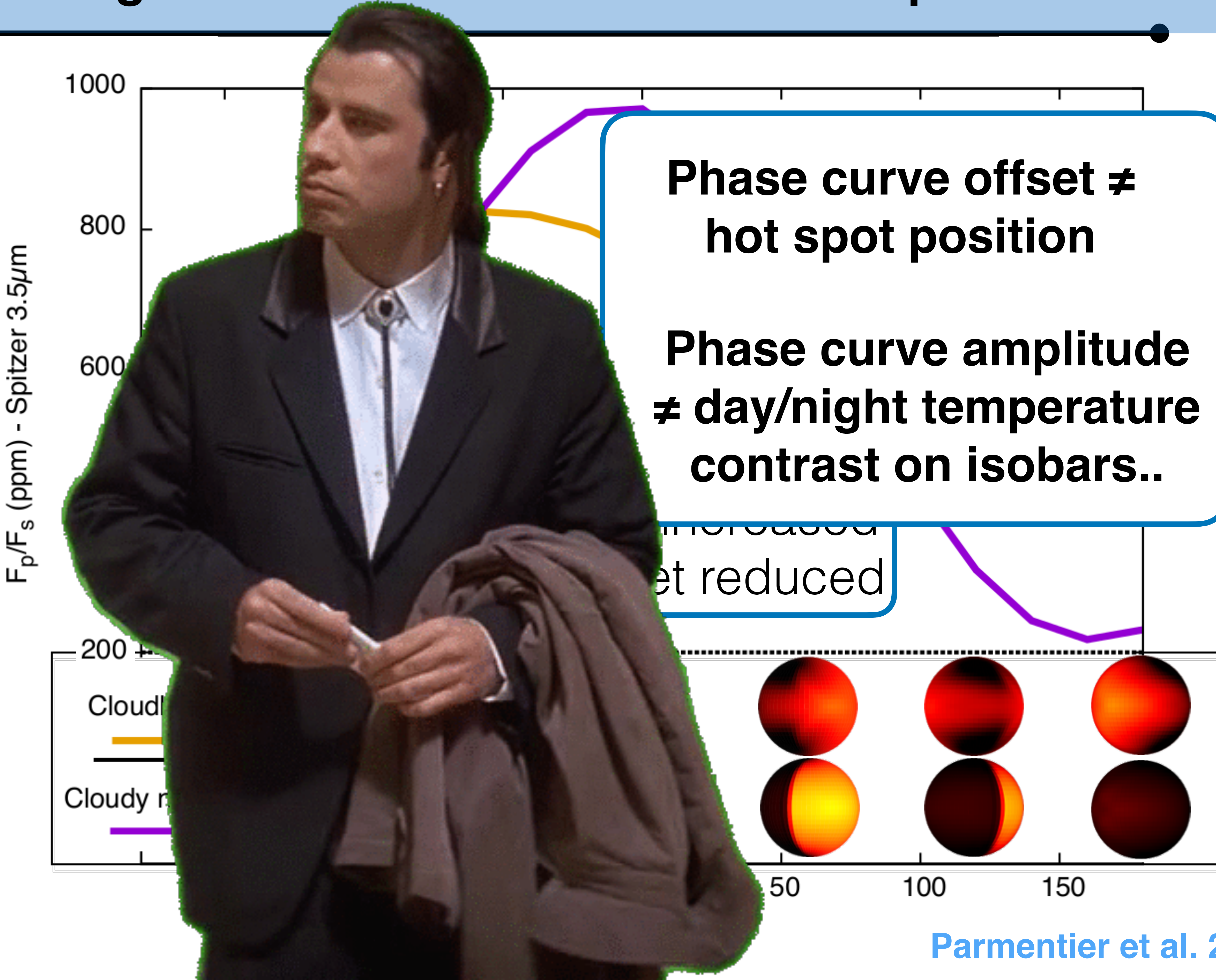

Phase curve offset ≠ hot spot position

Phase curve amplitude ≠ day/night temperature contrast on isobars..

Parmentier et al. 2020

Phase curves are not probing isobars !

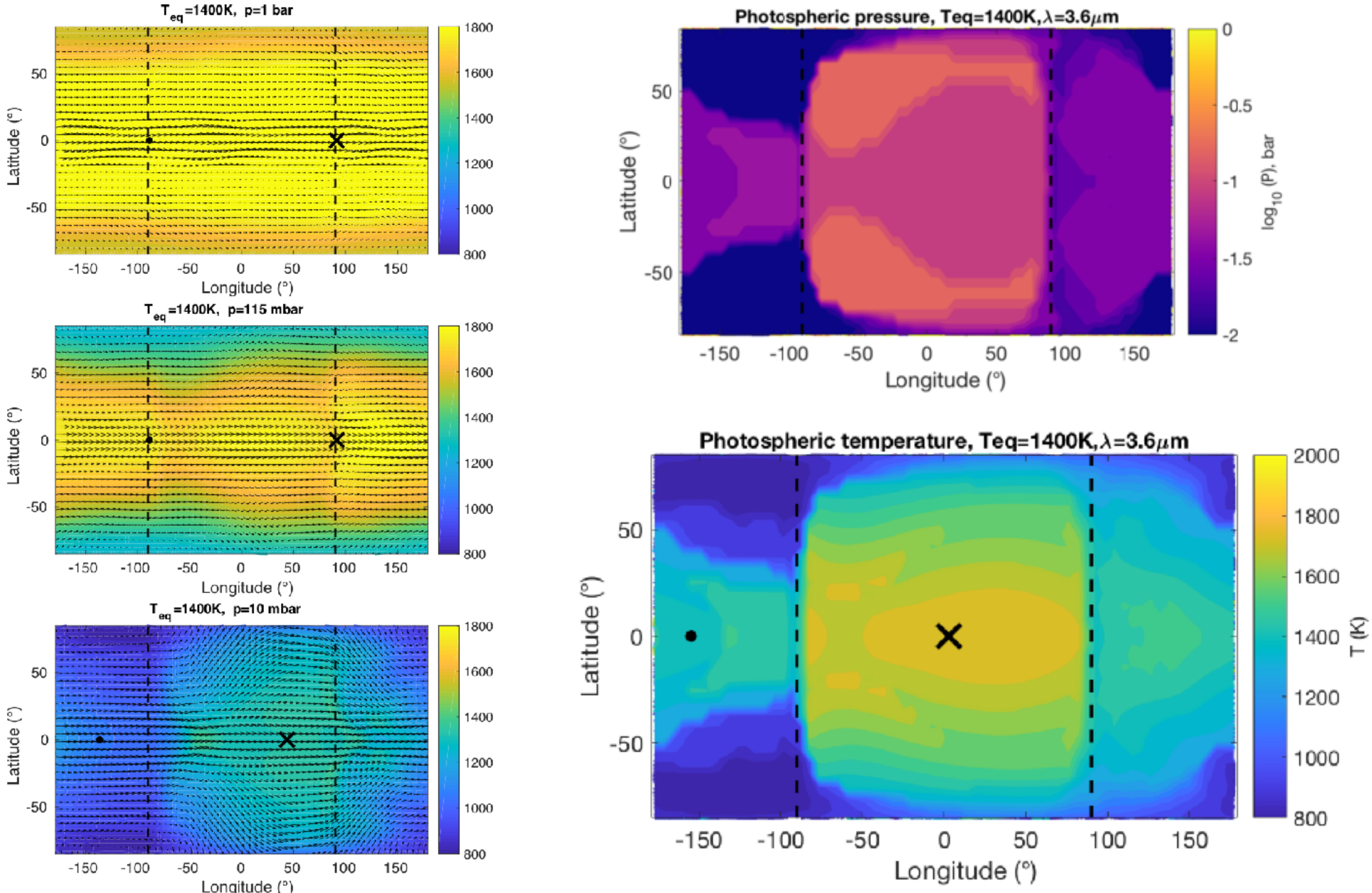

Parmentier et al. 2022

Clouds: when small changes have a big impact

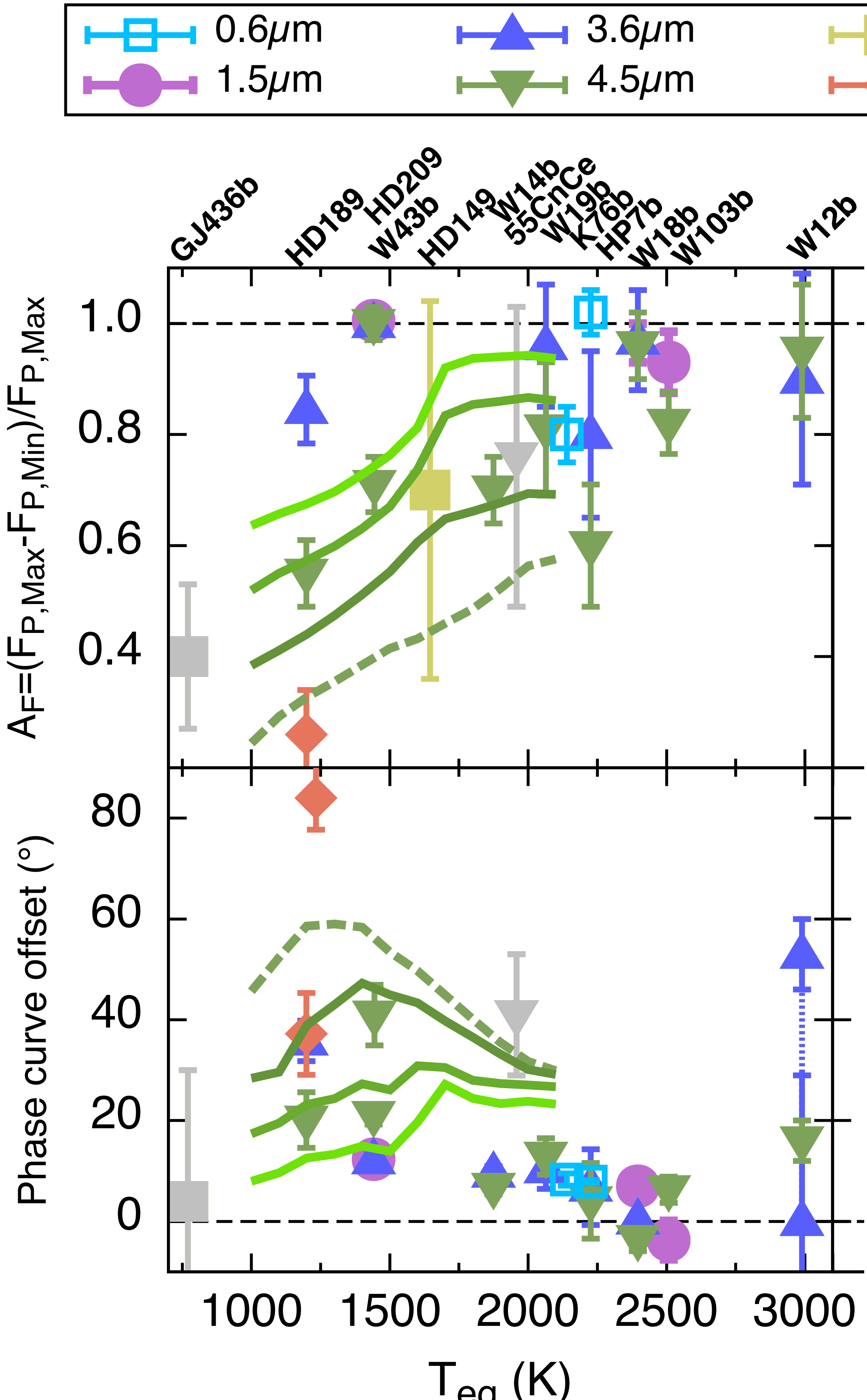

Inhomogeneous clouds allow theory and observations in **better agreement**

Hypothesis:

Cloudy nights
Clear sky days

Parmentier & Crossfield. 2017

JWST will test this before the end of the year !

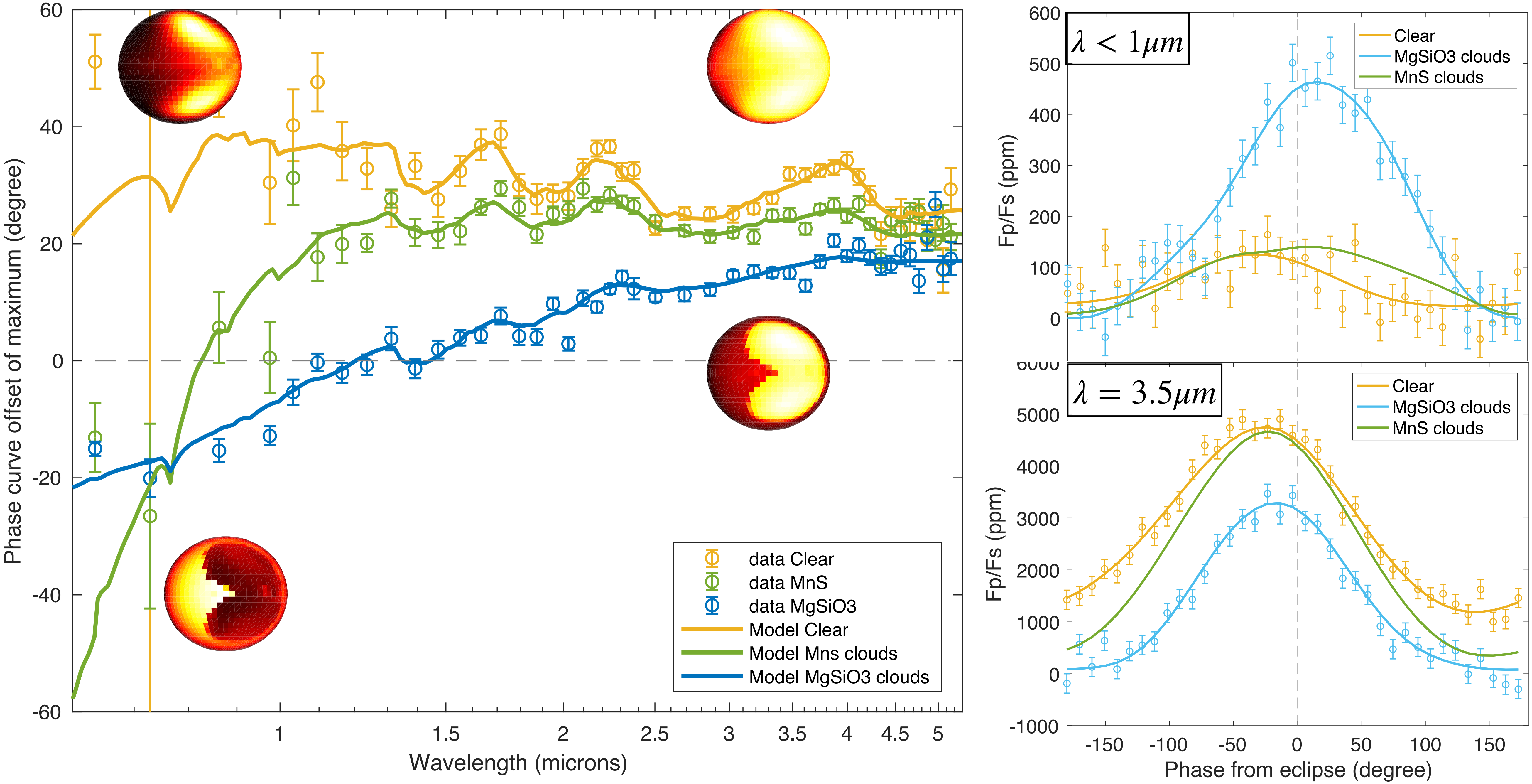

To be observed before the end go the month !

Composition ?

Molecular dissociation for hot planets

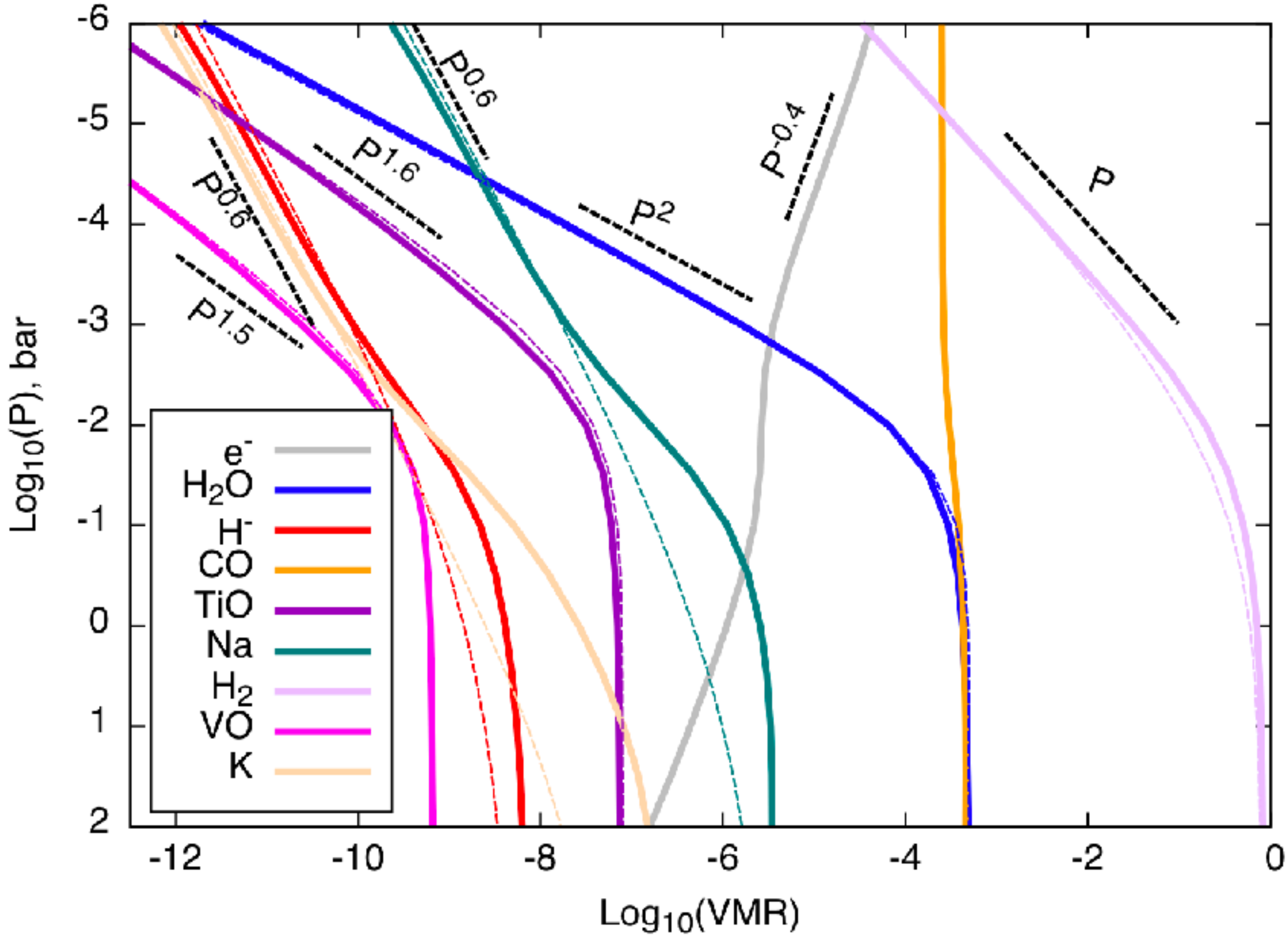

Molecular dissociation for hot planets

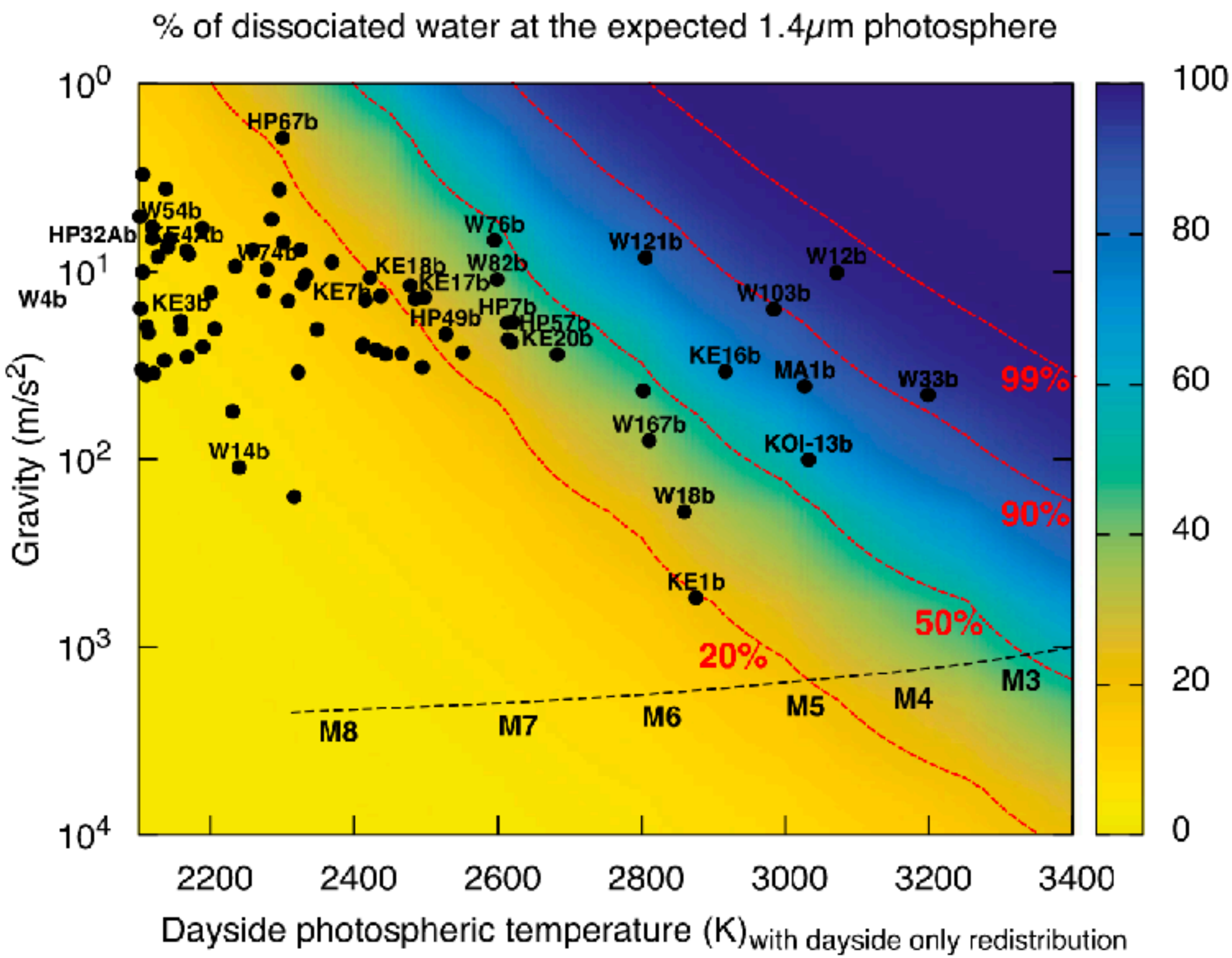

Ultra-hot Jupiters: thermal dissociation

Thermal dissociation and condensation makes 3D chemical patterns !

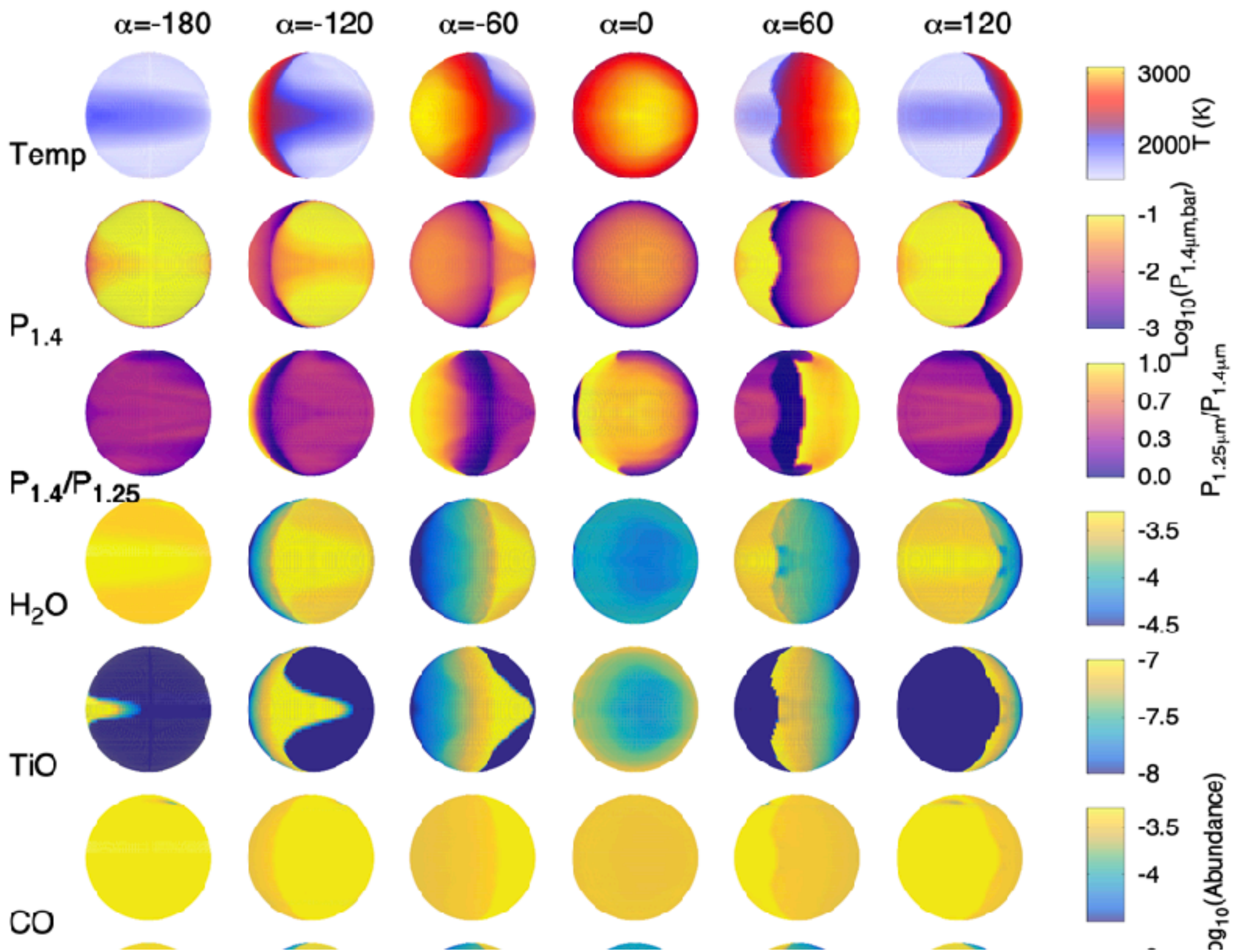

Parmentier+2018

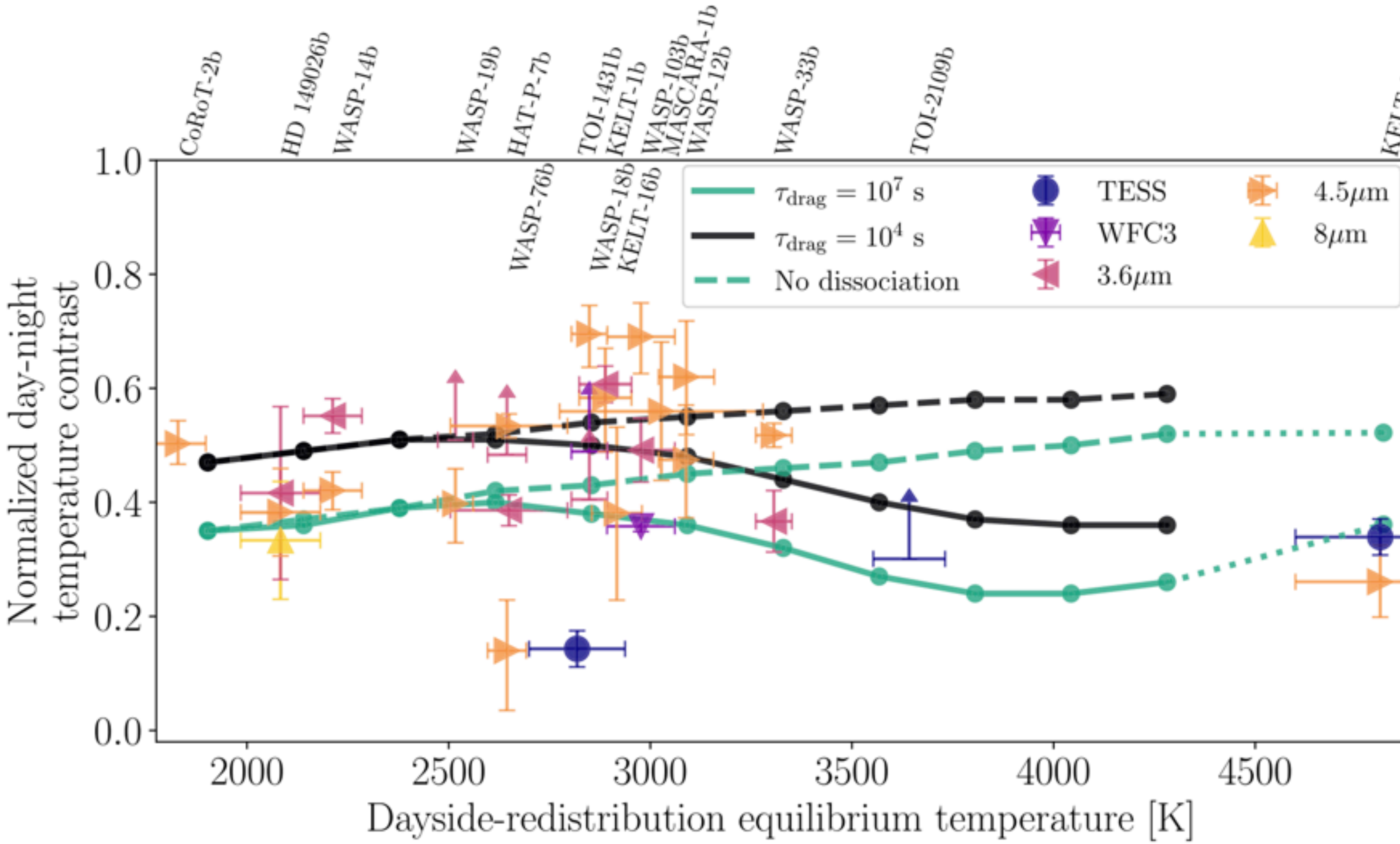

CoRoT-2b
HD 149026b
WASP-14b
WASP-19b
HAT-P-7b
TOI-1431b
KELT-1b
WASP-103b
MASCARA-1b
WASP-12b
WASP-33b
TOI-2109b
KELT-9b
WASP-76b
WASP-18b
KELT-16b
$\tau_{\rm drag} = 10^7$ s
$\tau_{\rm drag} = 10^4$ s
No dissociation
TESS
WFC3
3.6μm
4.5μm
8μm
Normalized day-night temperature contrast
Dayside-redistribution equilibrium temperature [K]

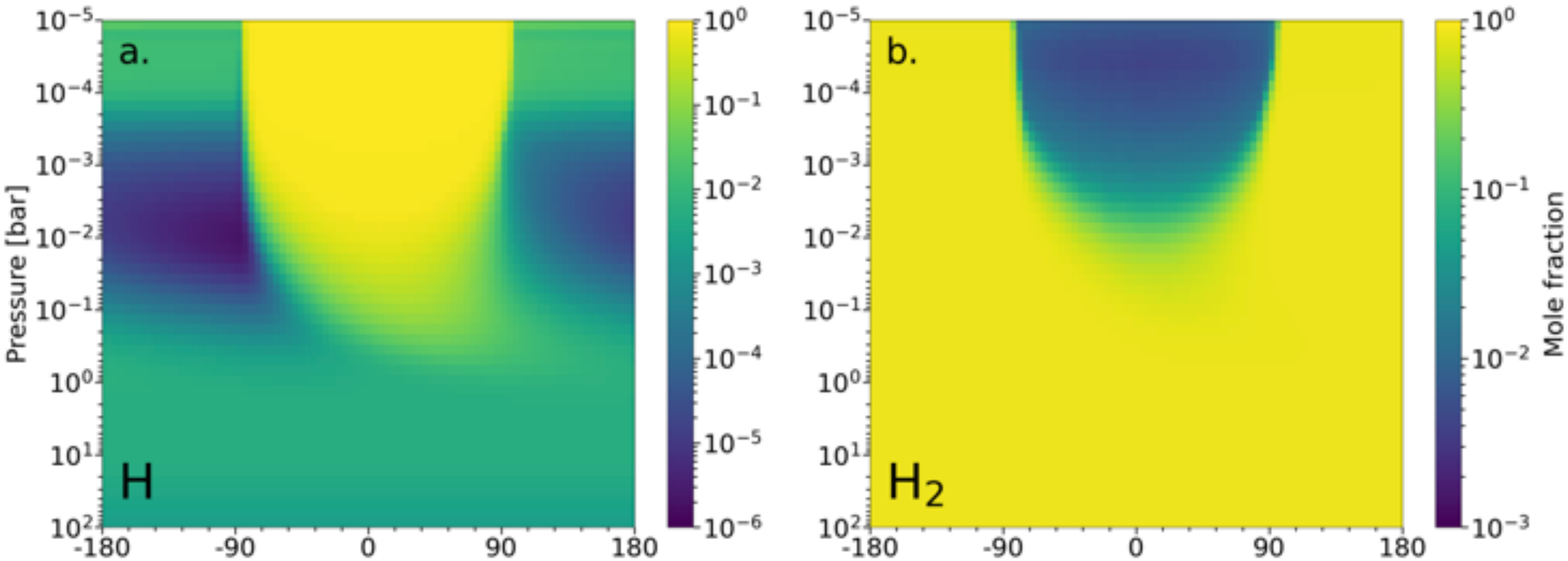

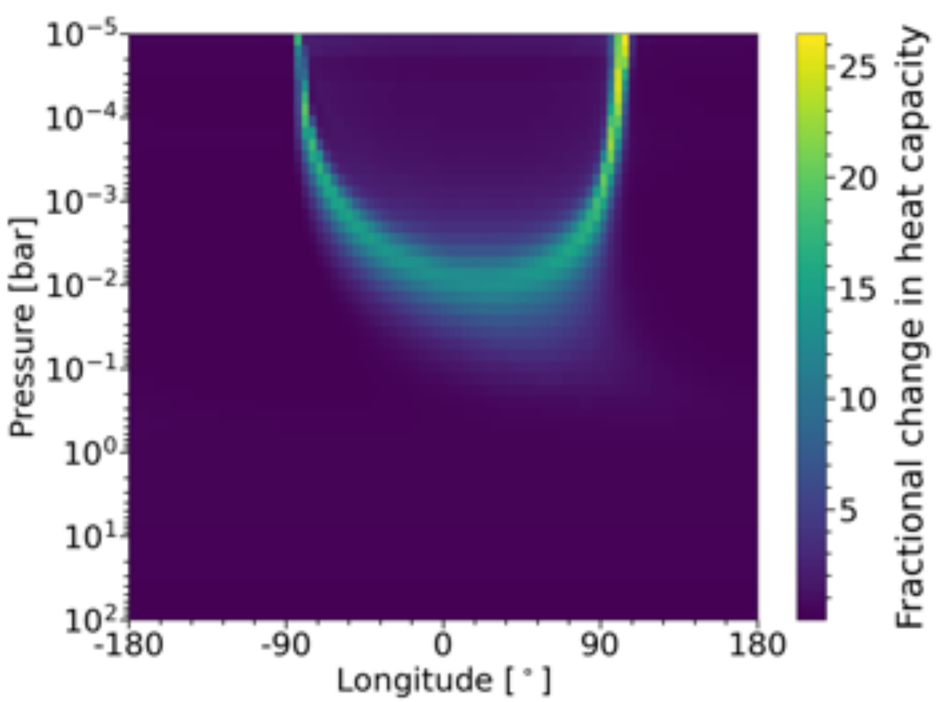

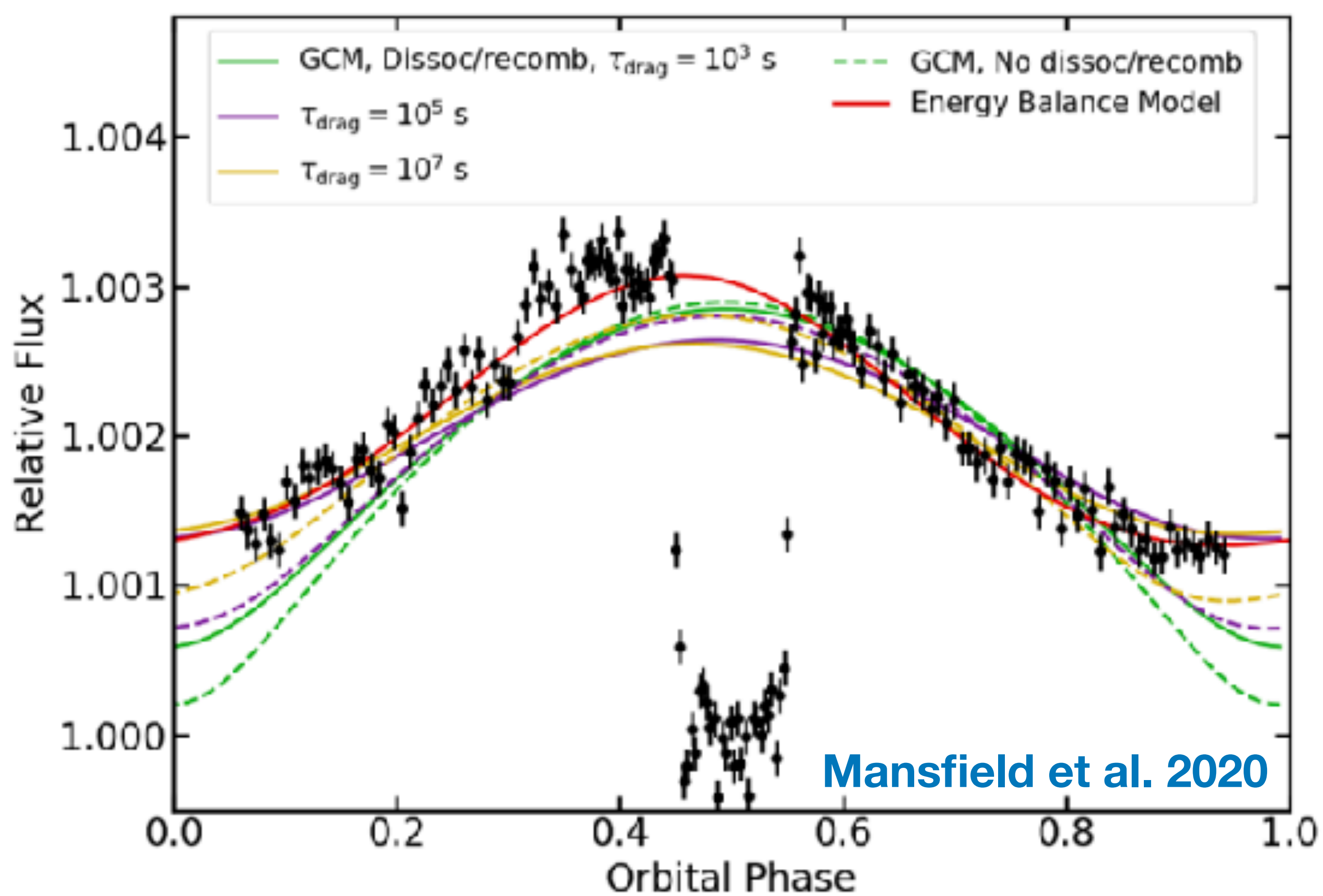

Mansfield et al. 2020

Roth et al. 2020

Modelling the high-resolution spectra of 3D exoplanets

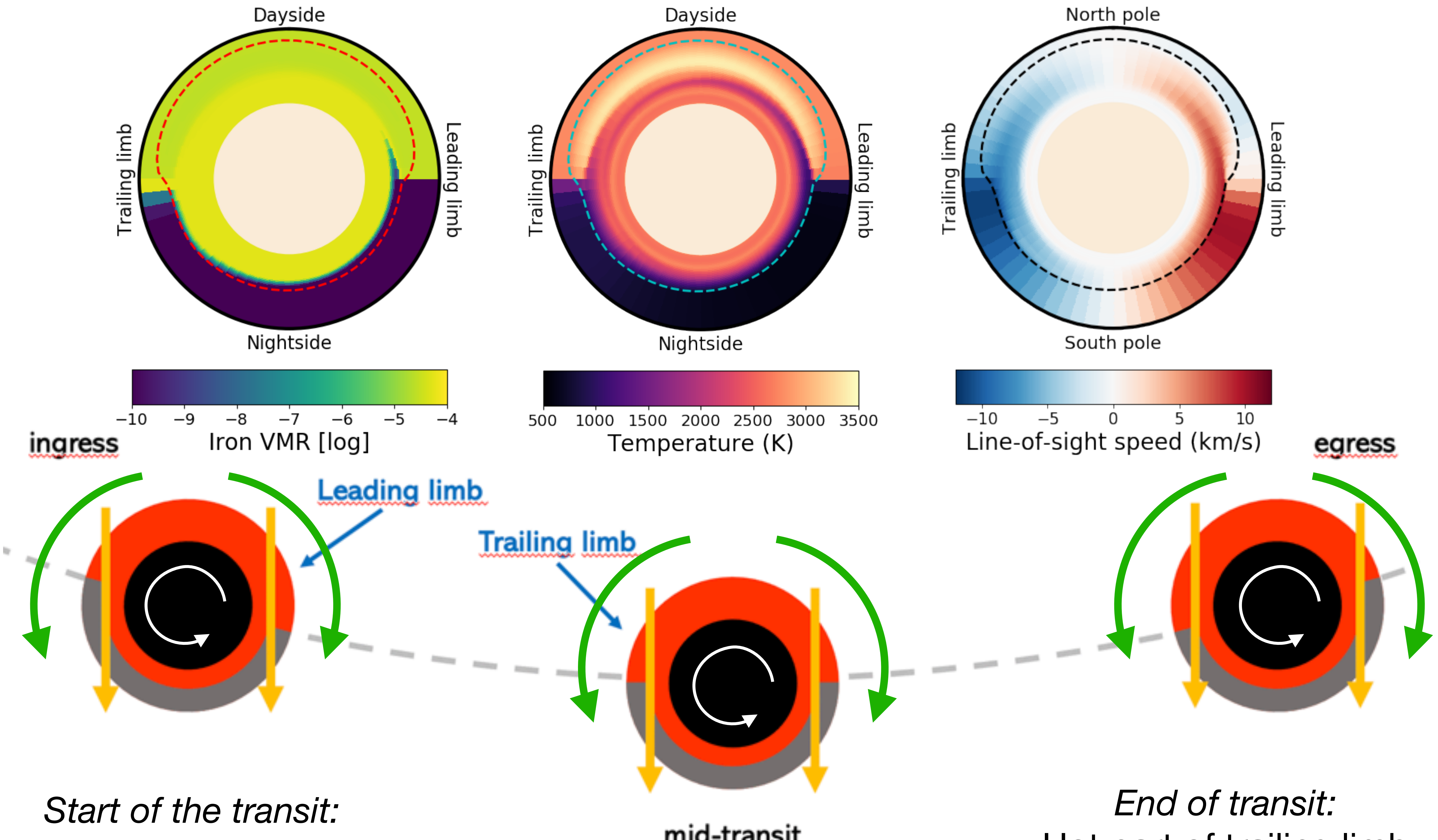

Start of the transit:
Hot part of leading limb

End of transit:
Hot part of trailing limb dominates

Wardenier et al. 2021

Measuring *local* wind speed

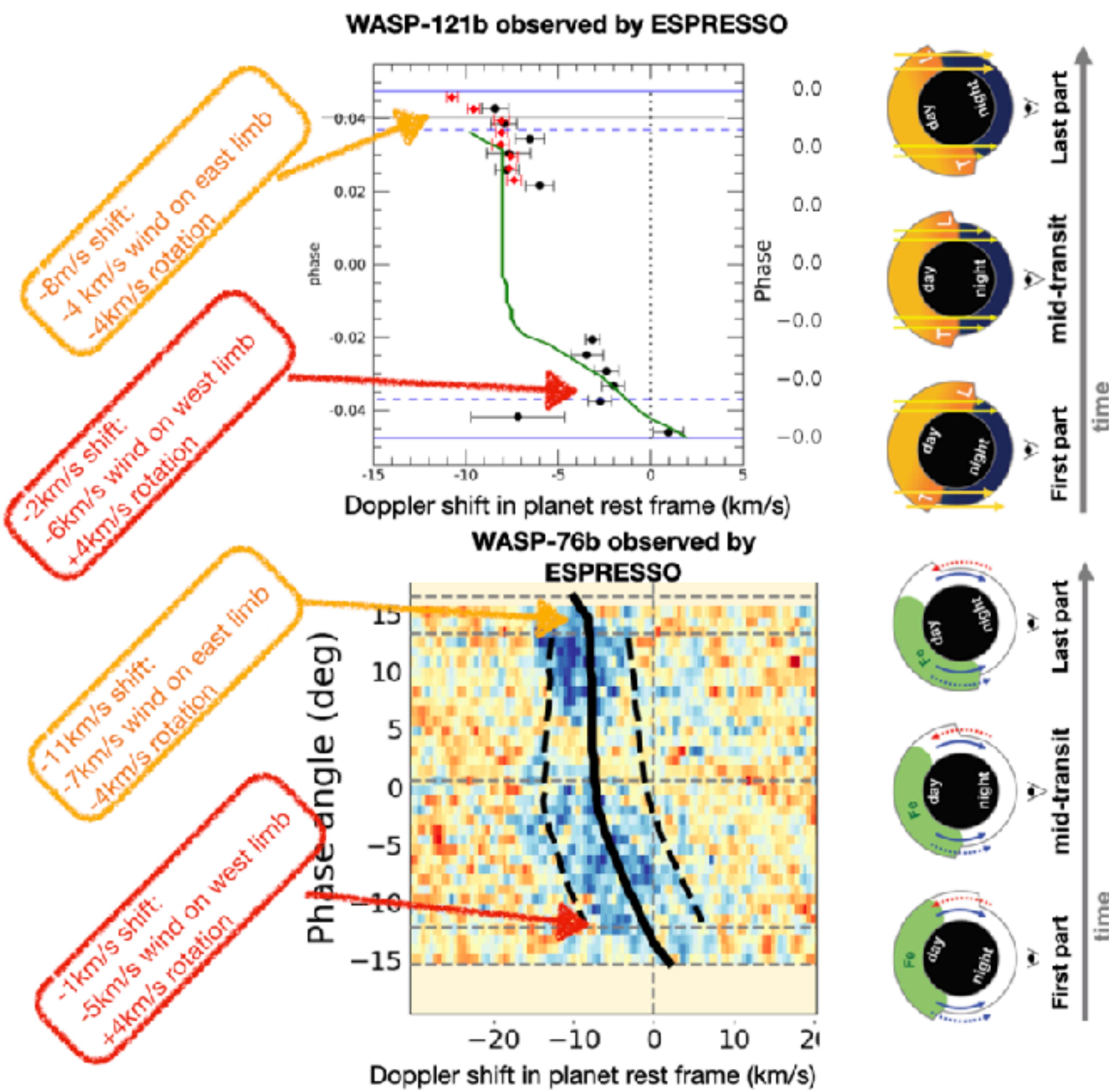

Almost local wind speed measurement is now possible !

Wardenier et al. 2021

Locally measured wind speed on WASP-76b !

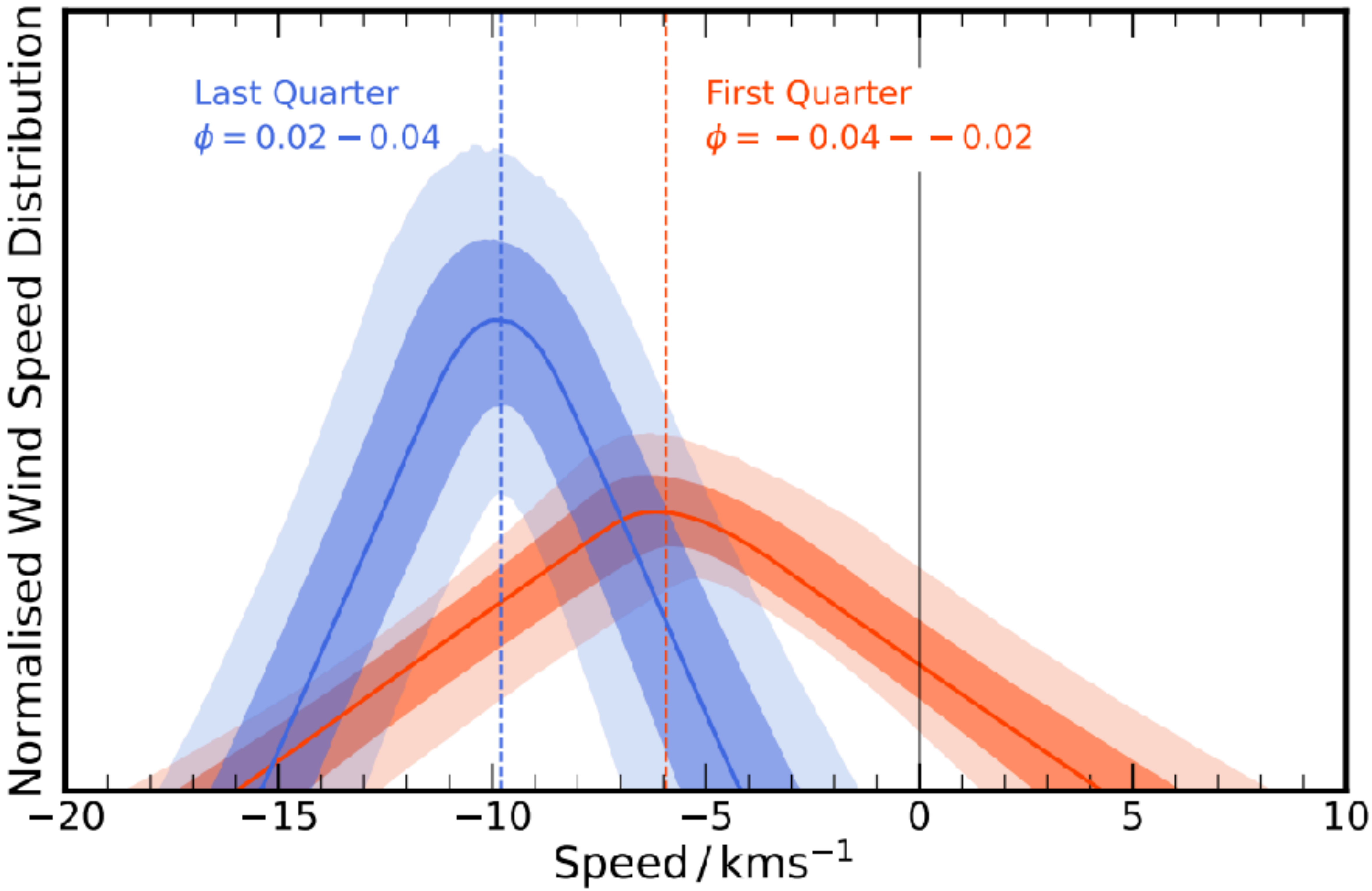

Gandhi et al. 2022

Diversity of circulation ?

A diversity of parameters

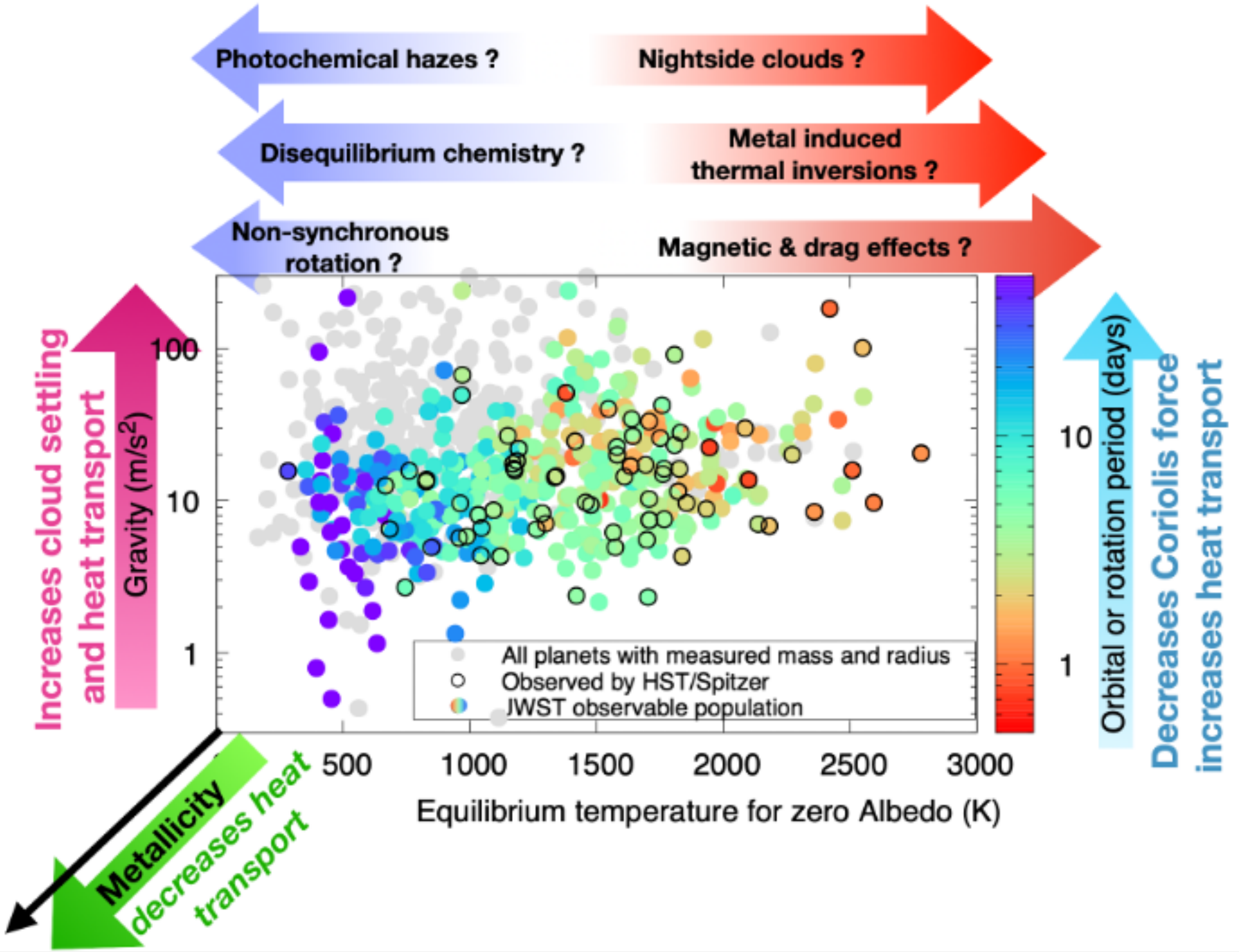

Modelling hot Jupiter's population

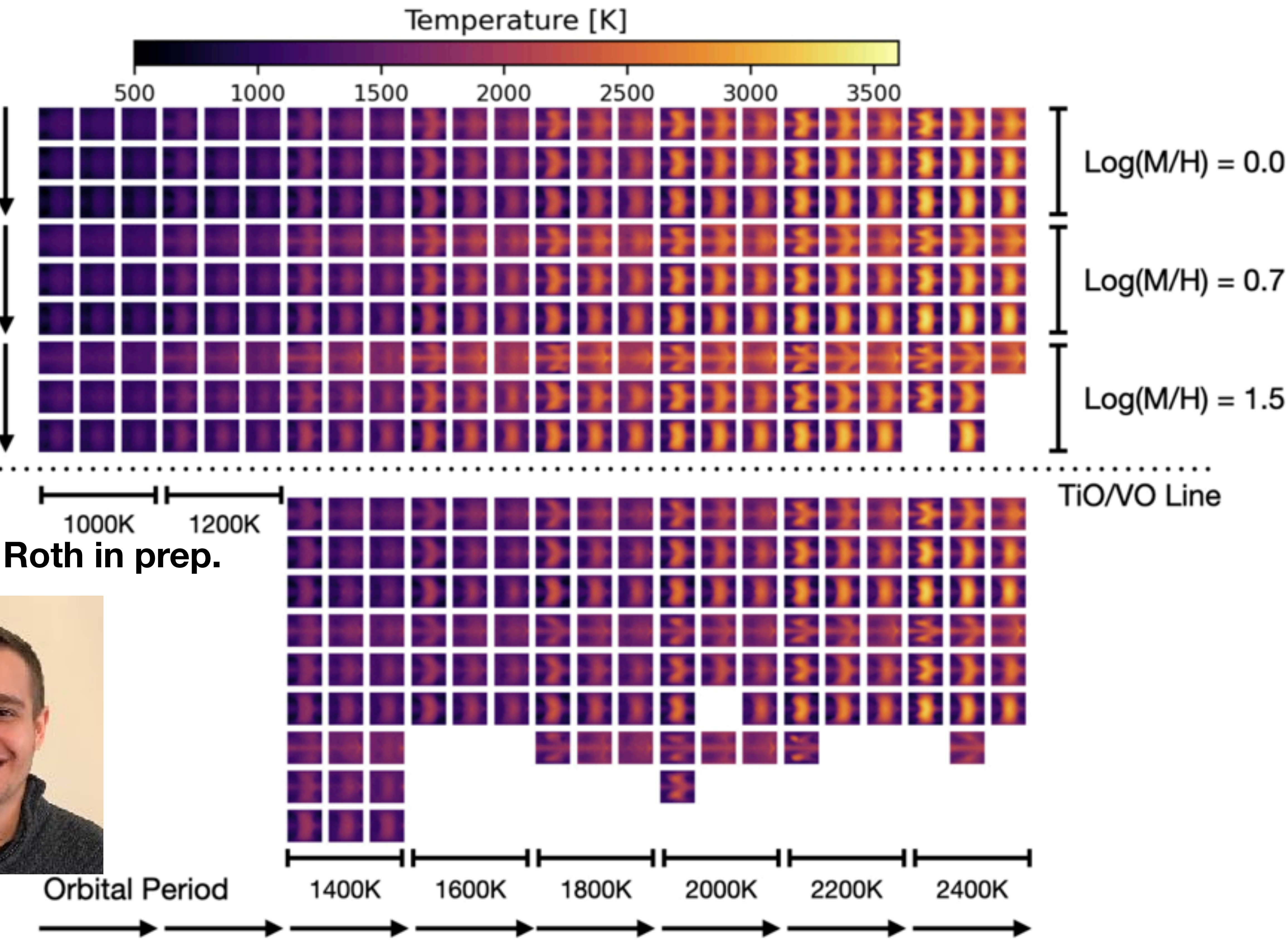

Alexander Roth in prep.

Modelling hot Jupiter's population

***G**lobal **C**irculation **M**odel* : solves the primitive equation, Euler equation adapted to atmospheres
SPARC : solves the radiative energy balance with non-grey, molecular opacities

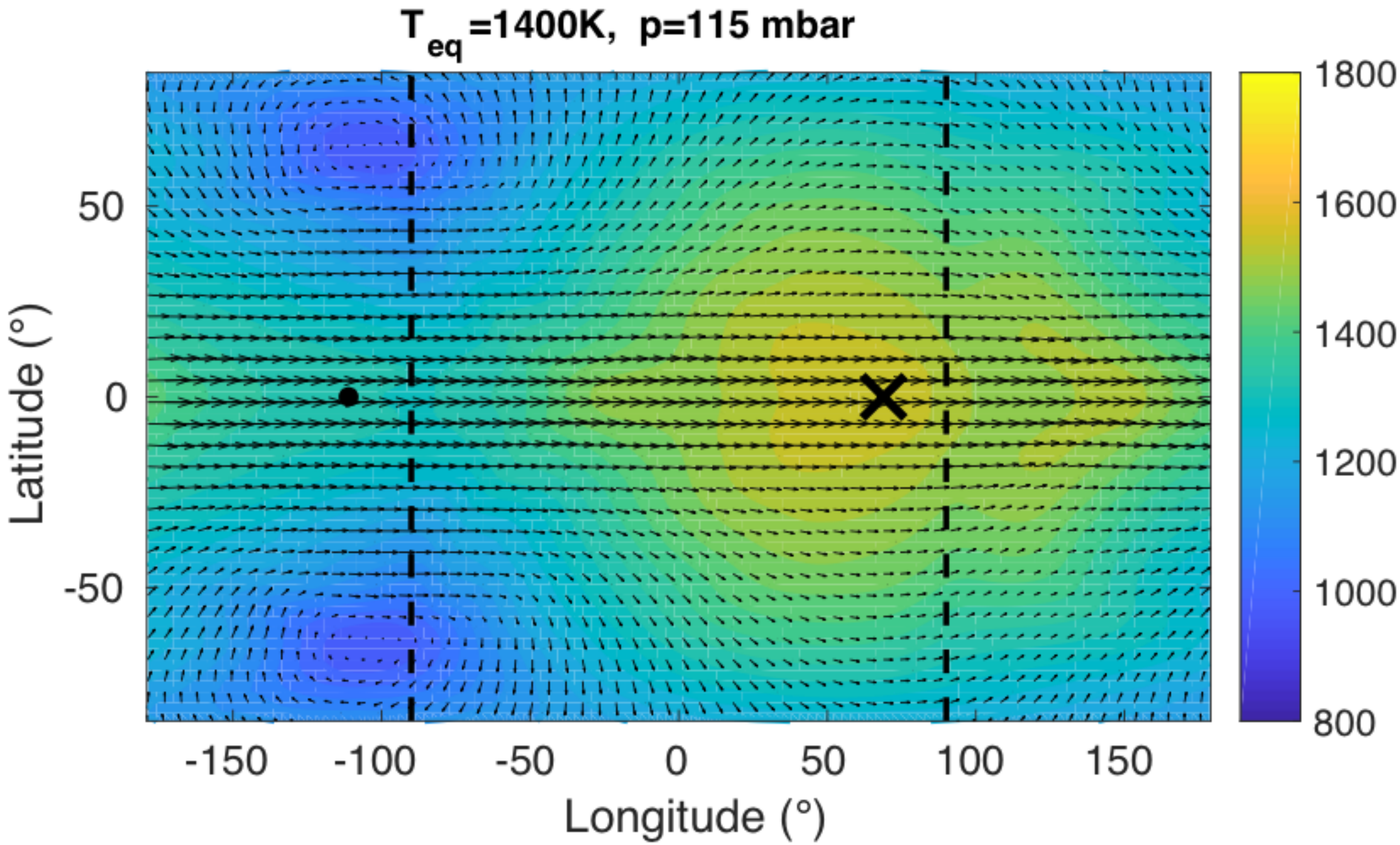

Parmentier+2020

Modelling hot Jupiter's population

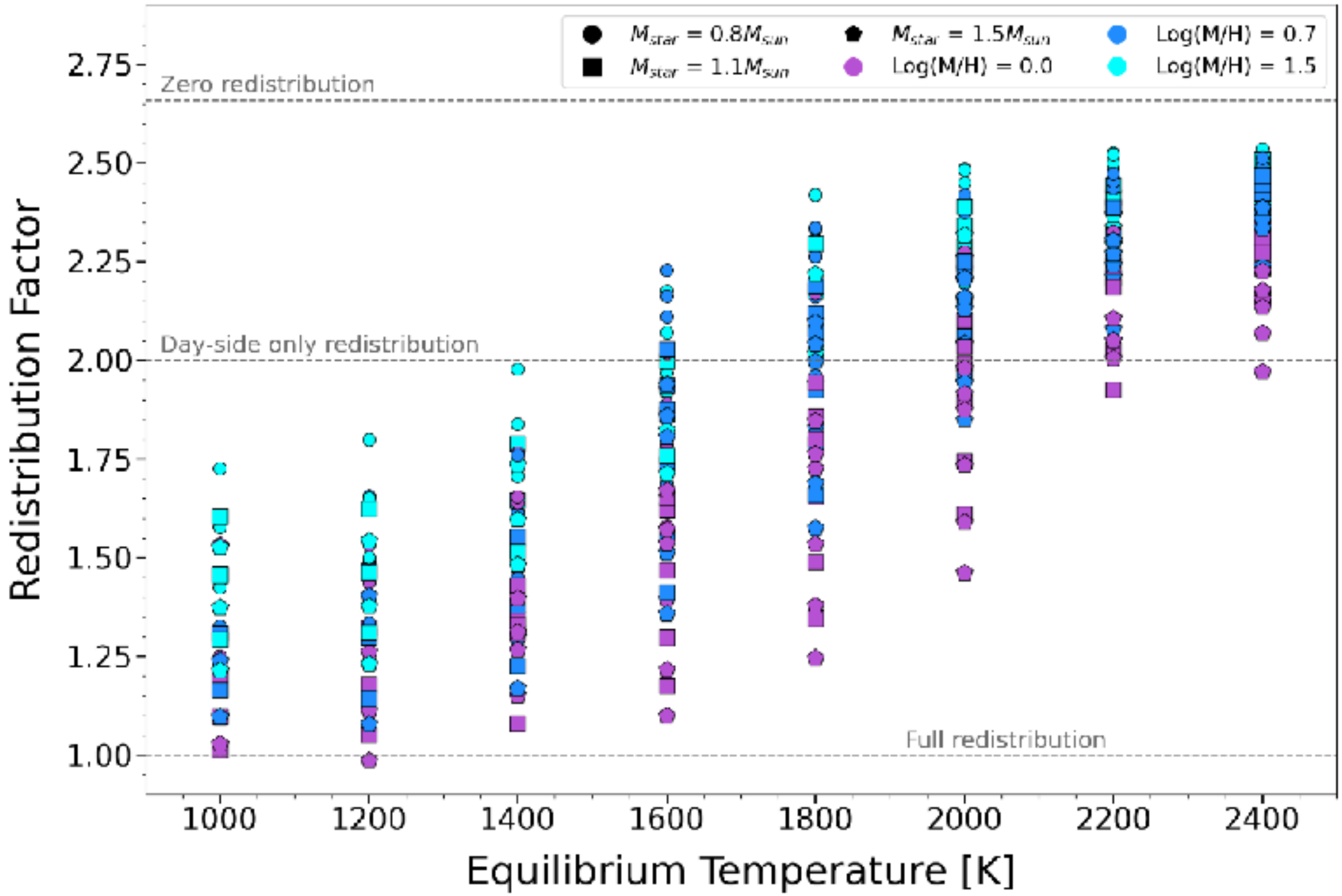

« Redistribution factor » : how hot is the dayside in terms of T^4 compared to full redistribution

Modelling hot Jupiter's population

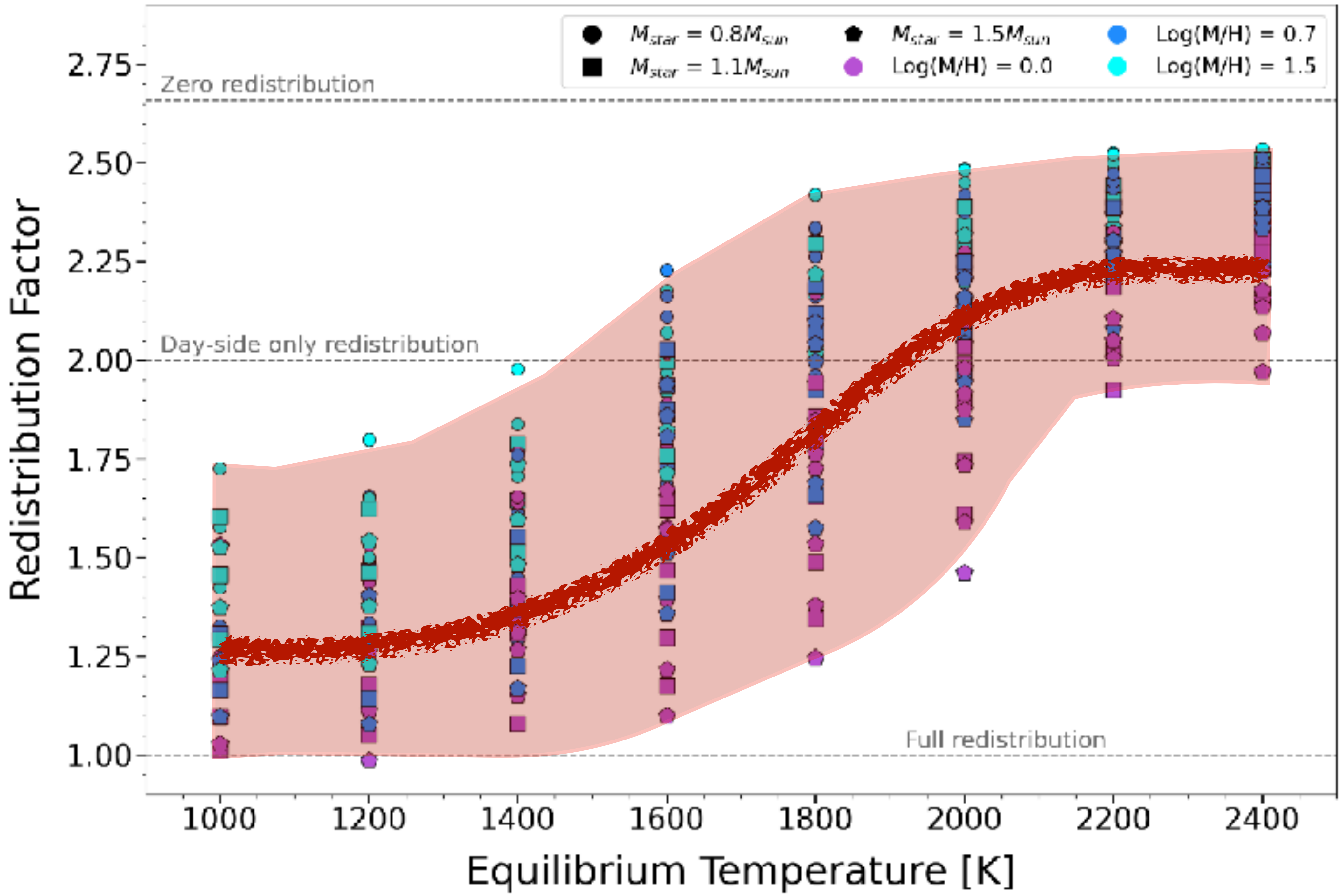

« Redistribution factor » : how hot is the dayside in terms of T^4 compared to full redistribution

Hotter planets are poorer at transporting heat
But there is an enormous variability !

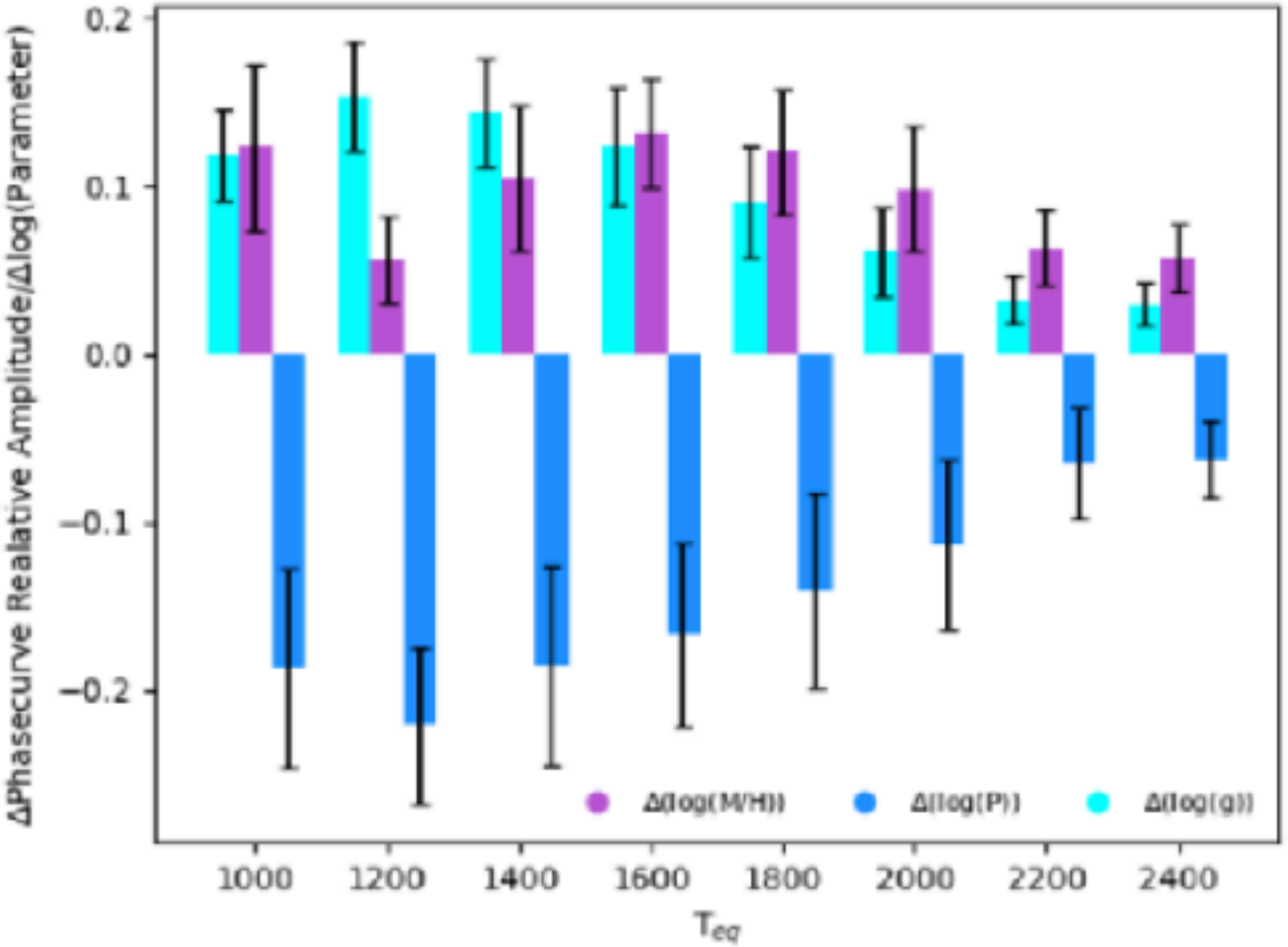

0.2
0.1
0.0
−0.1
−0.2
ΔPhasecurve Realative Amplitude/Δlog(Parameter)
1000
1200
1400
1600
1800
2000
2200
2400
T_{eq}

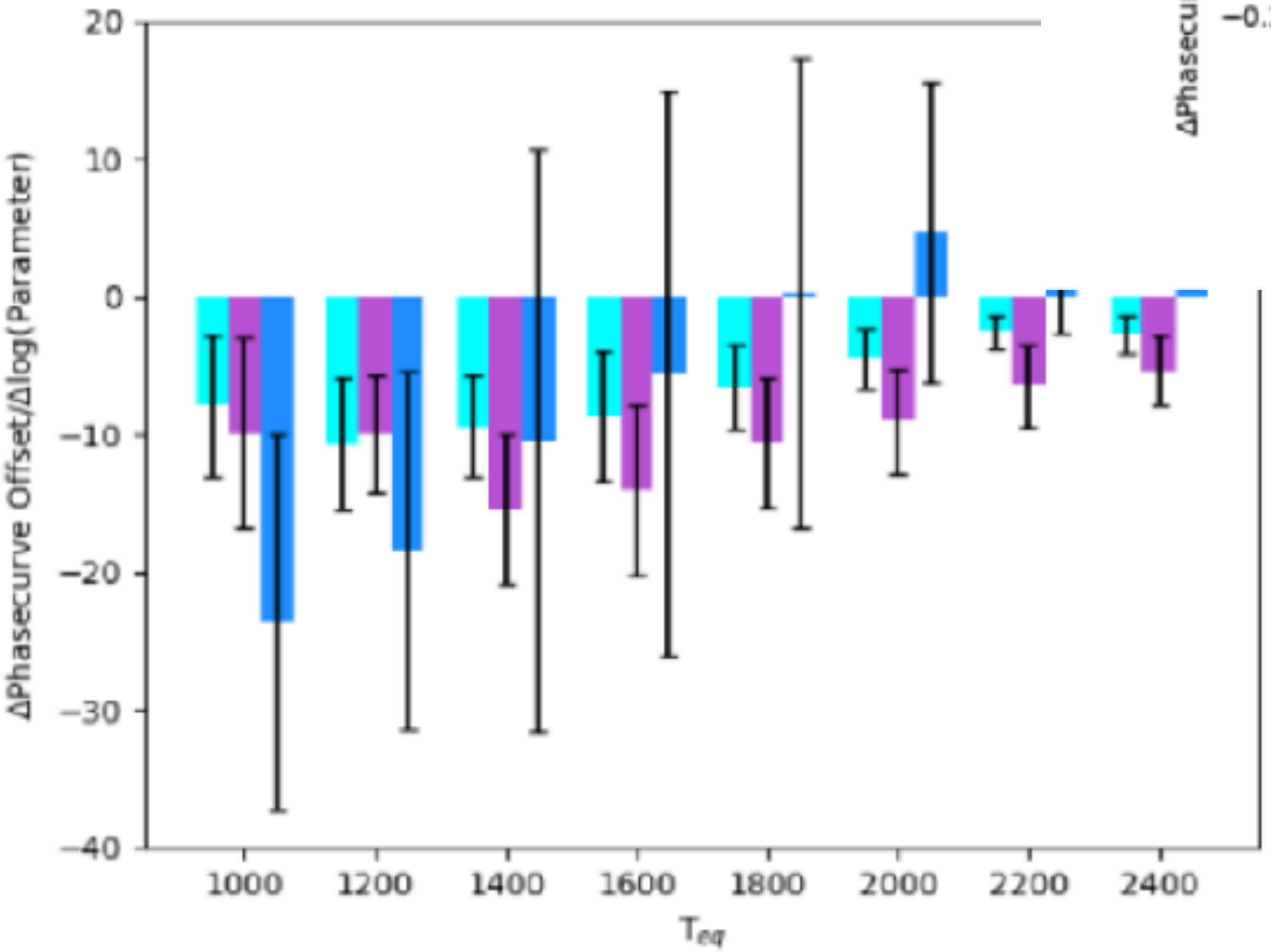

20
10
0
−10
−20
−30
−40
ΔPhasecurve Offset/Δlog(Parameter)
1000
1200
1400
1600
1800
2000
2200
2400
T_{eq}

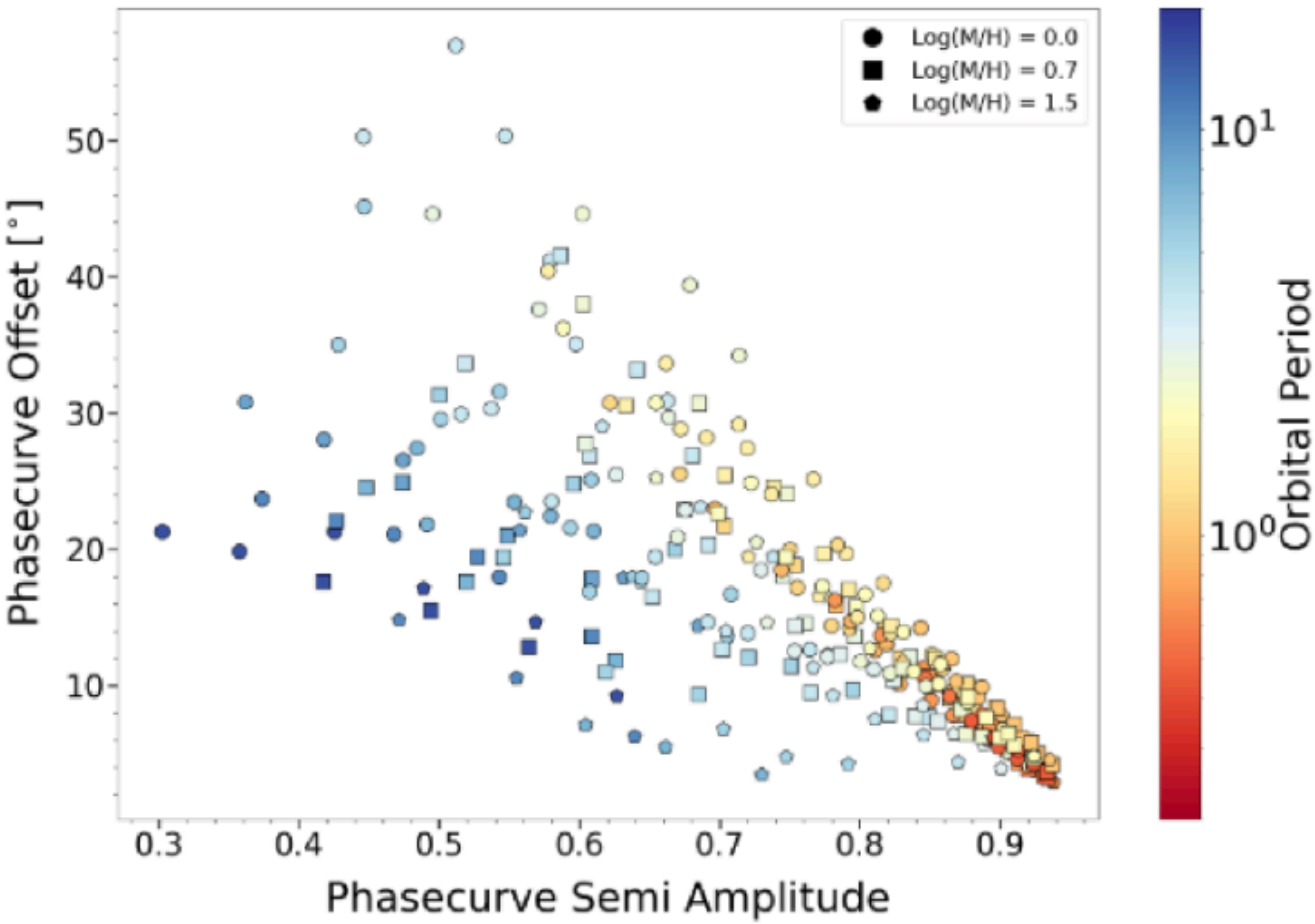
Log(M/H) = 0.0
Log(M/H) = 0.7
Log(M/H) = 1.5
Phasecurve Offset [°]
50
40
30
20
10
0.3
0.4
0.5
0.6
0.7
0.8
0.9
Phasecurve Semi Amplitude
10^1
10^0
Orbital Period

Modelling hot Jupiter's population

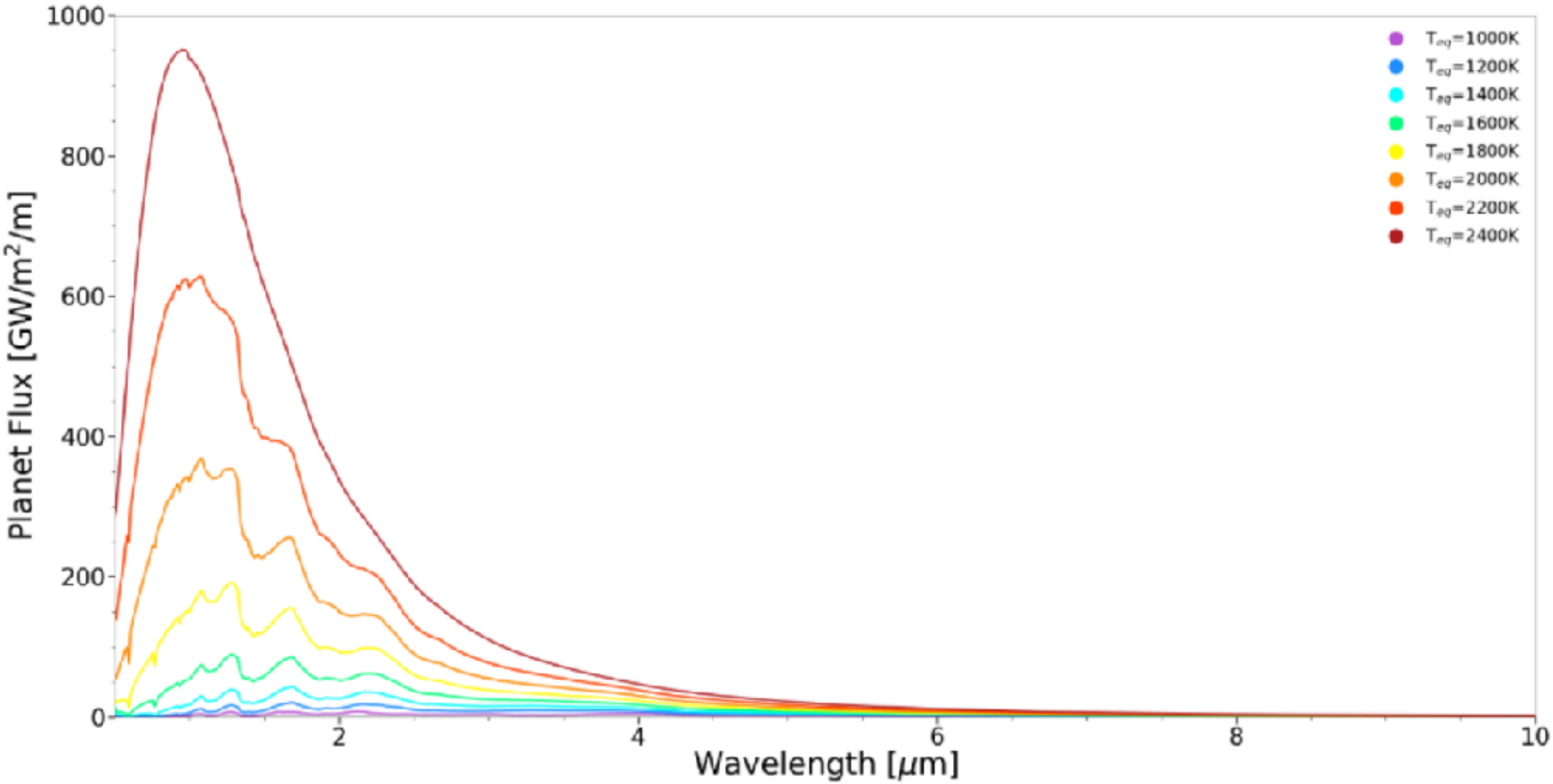

Modelling hot Jupiter's population

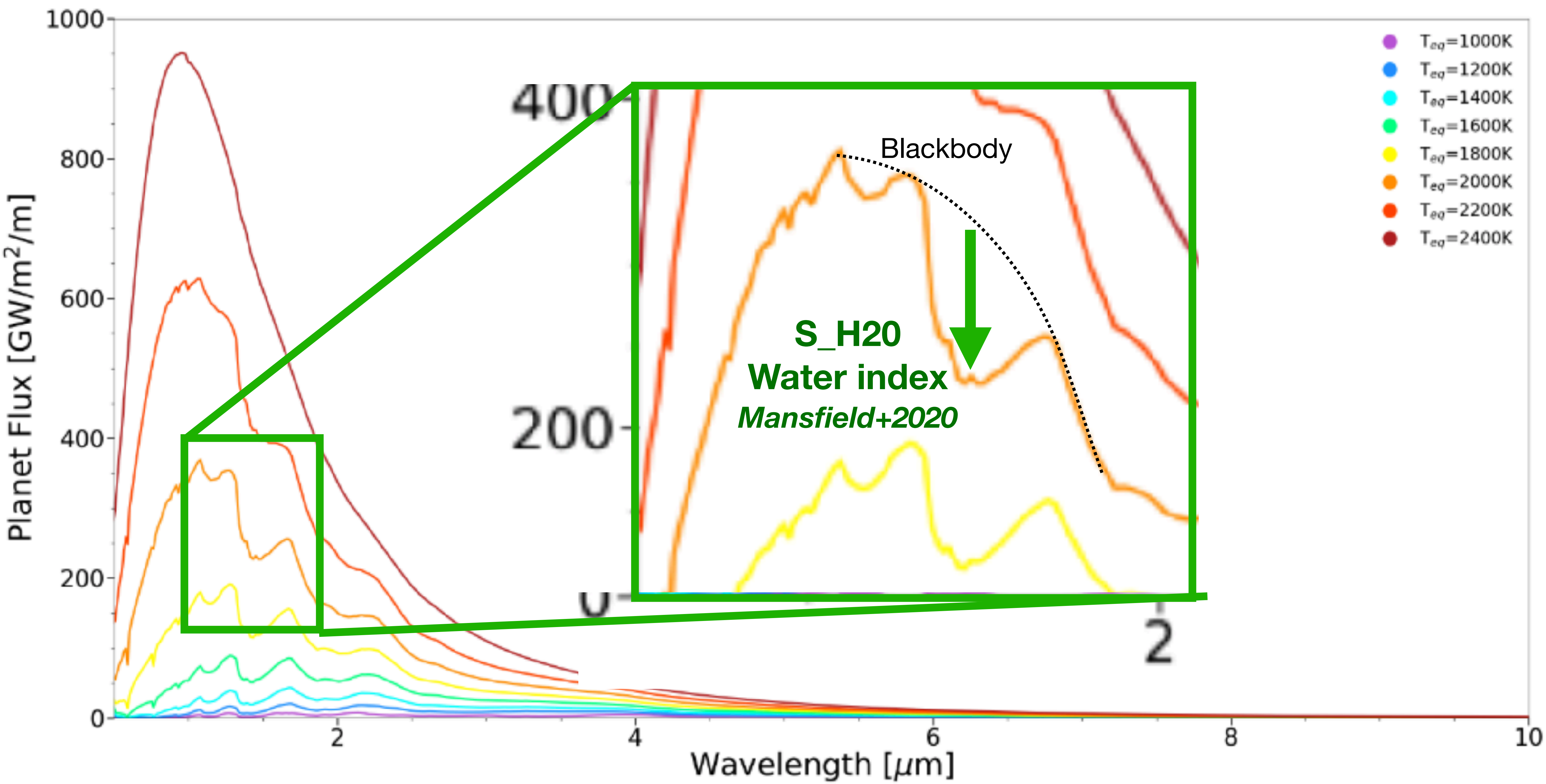

Modelling hot Jupiter's population

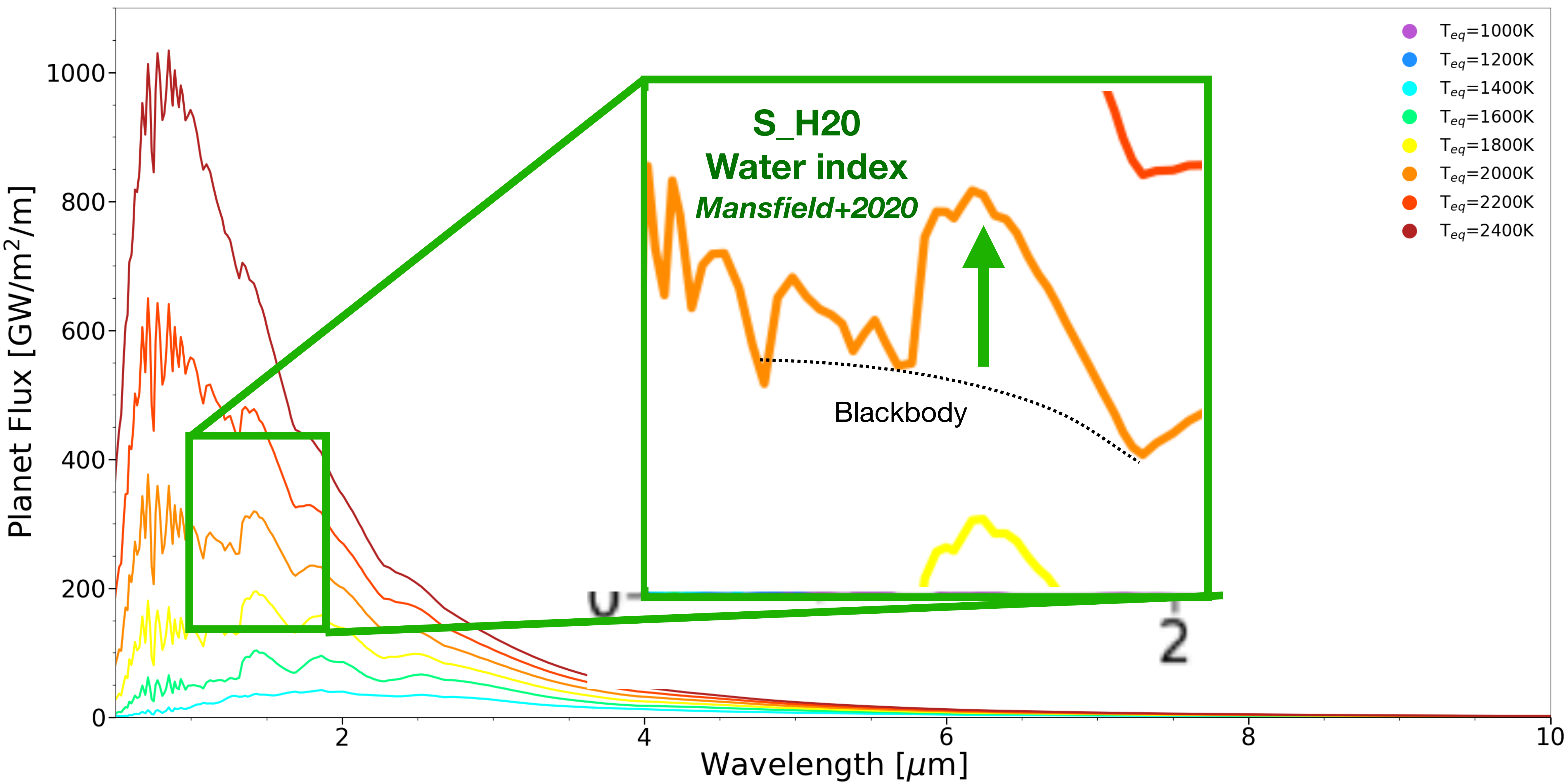

Modelling hot Jupiter's population

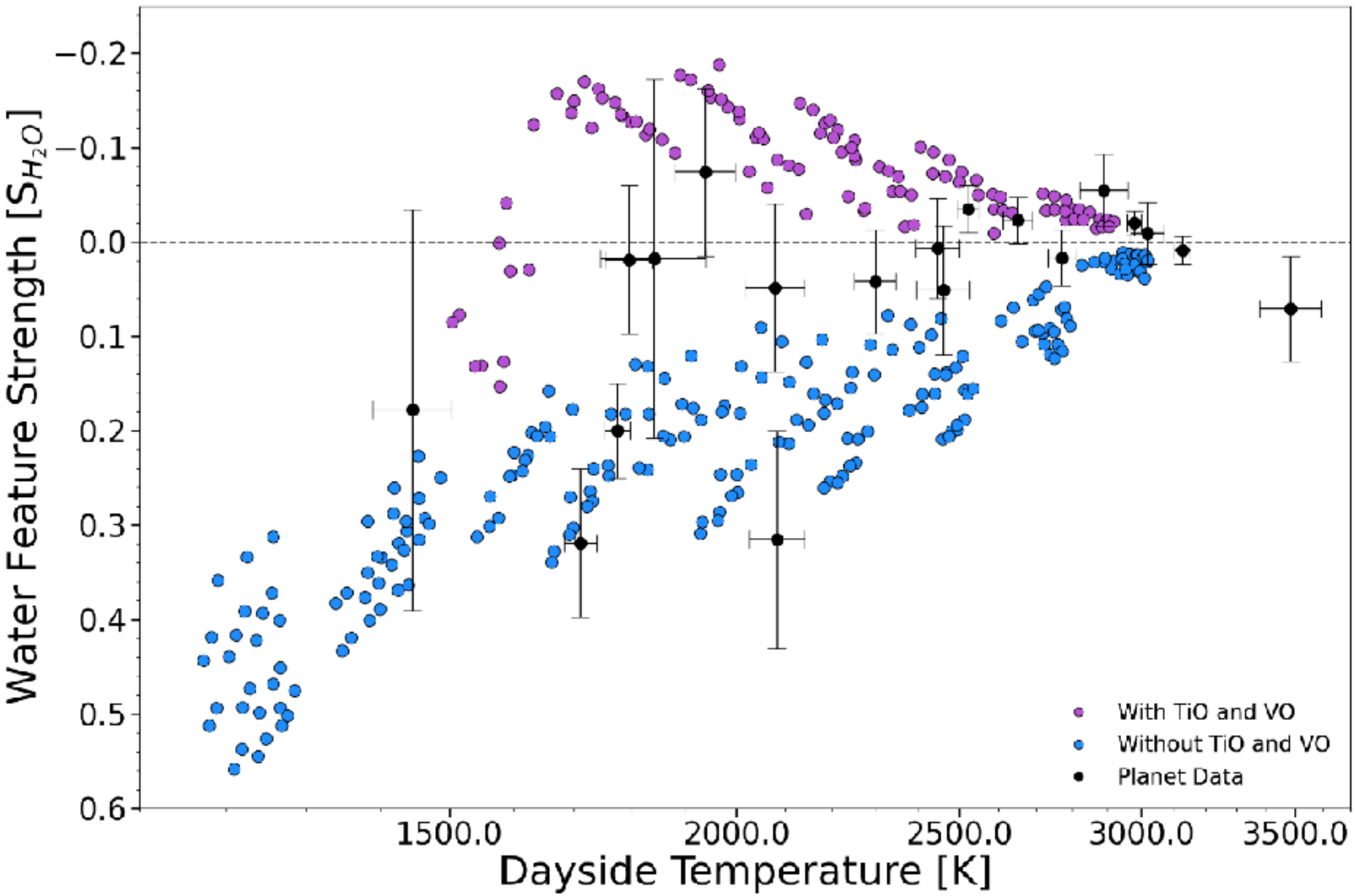

Modelling hot Jupiter's population

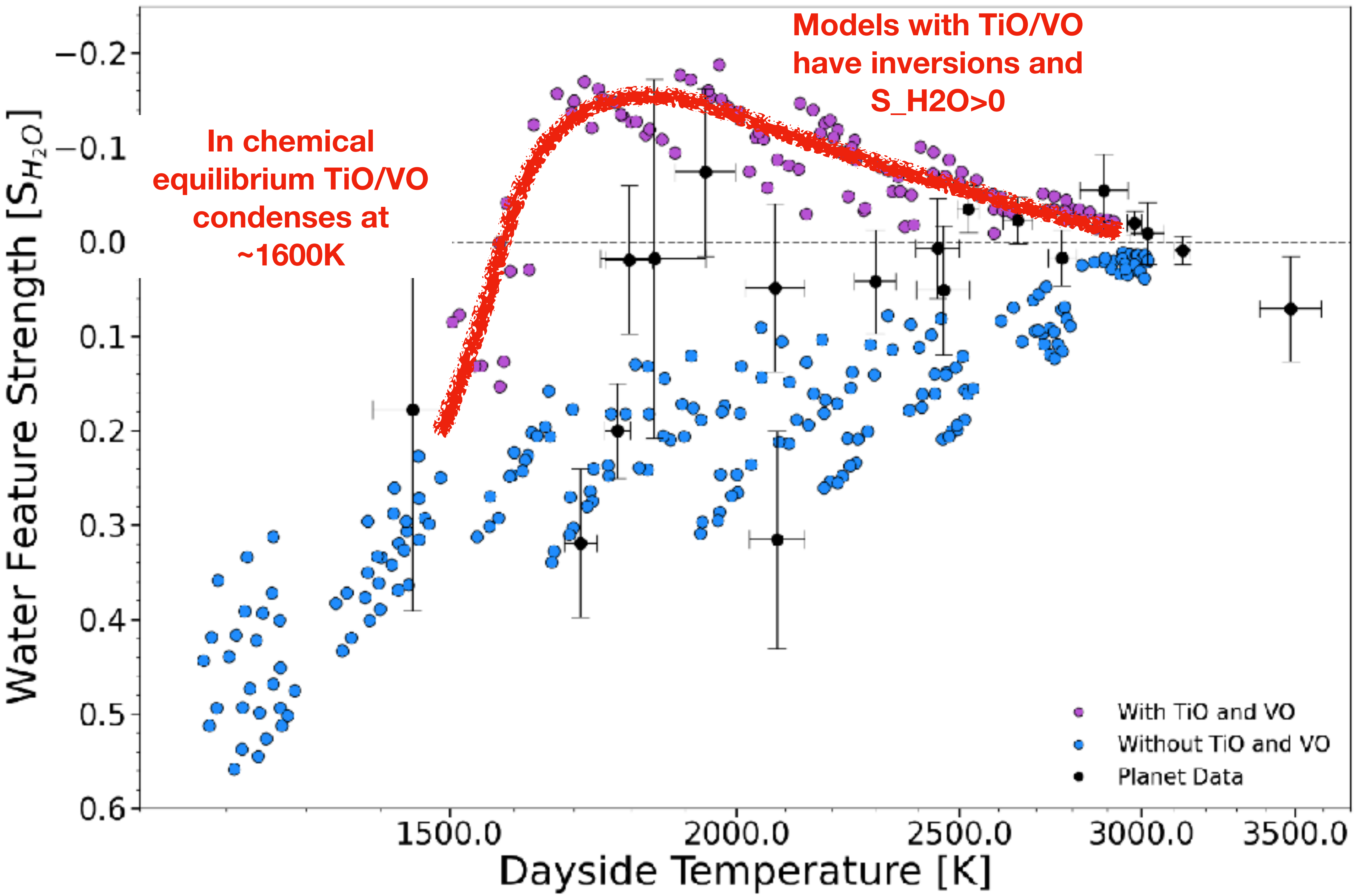

Modelling hot Jupiter's population

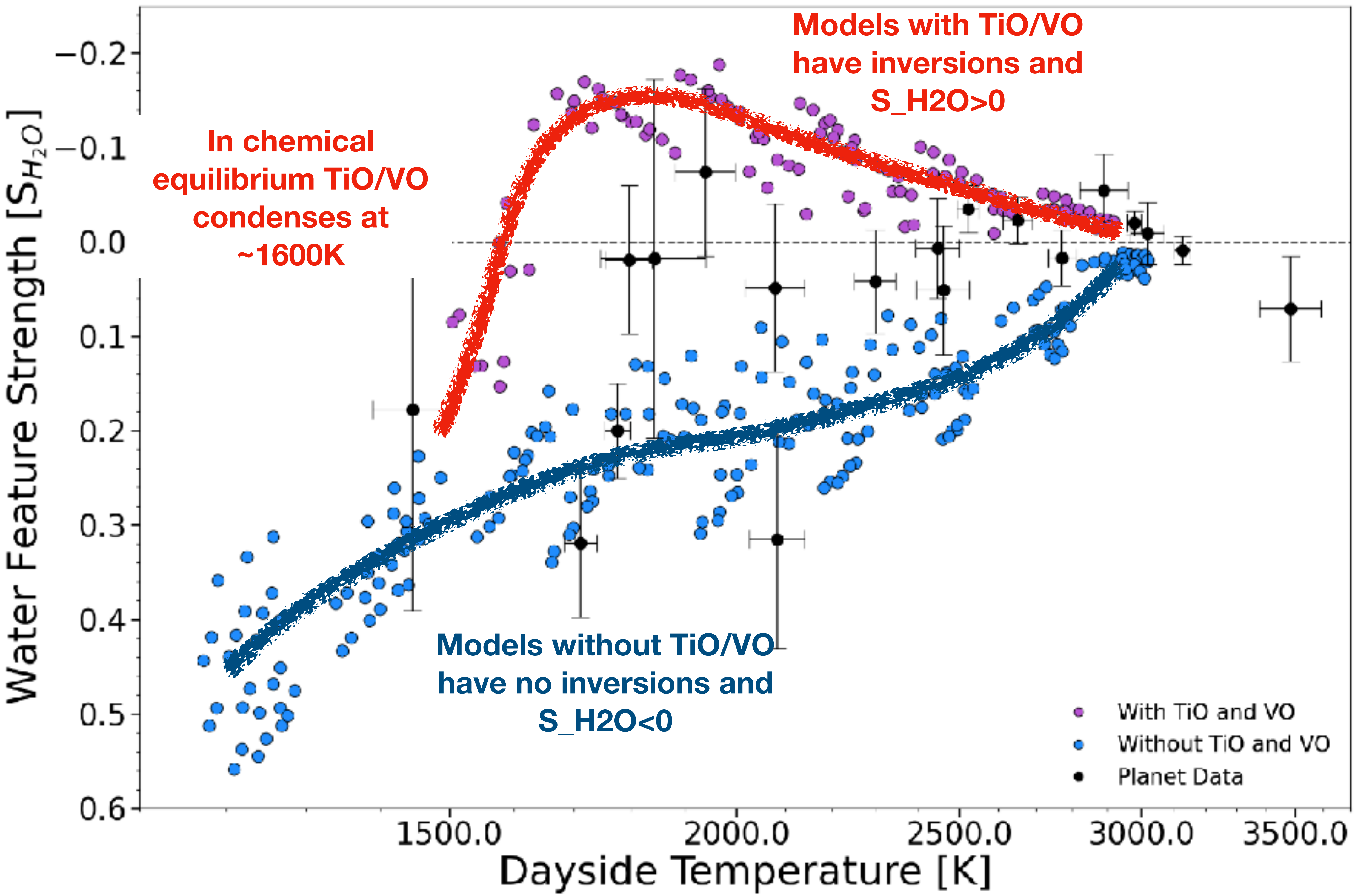

Modelling hot Jupiter's population

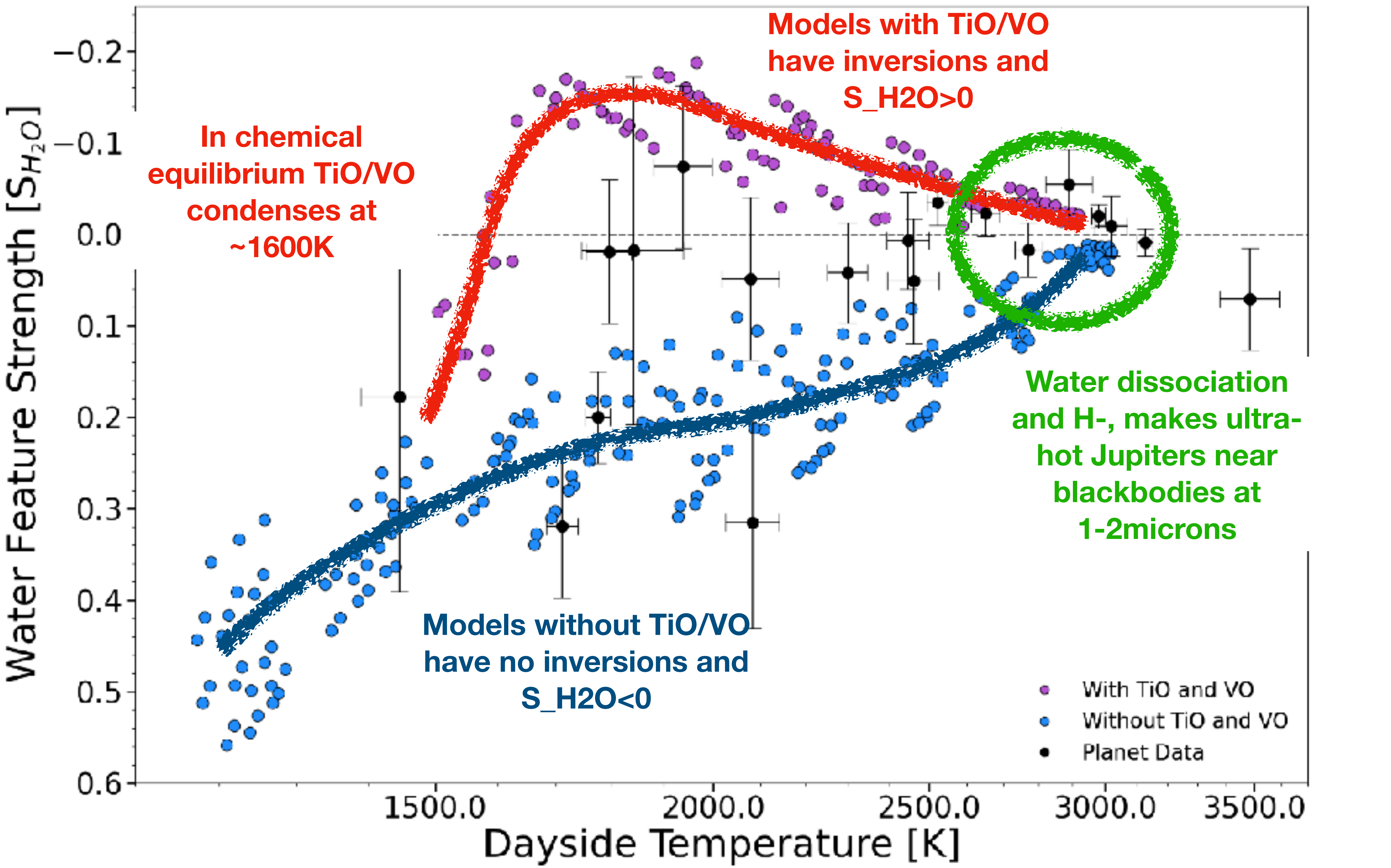

Modelling hot Jupiter's population

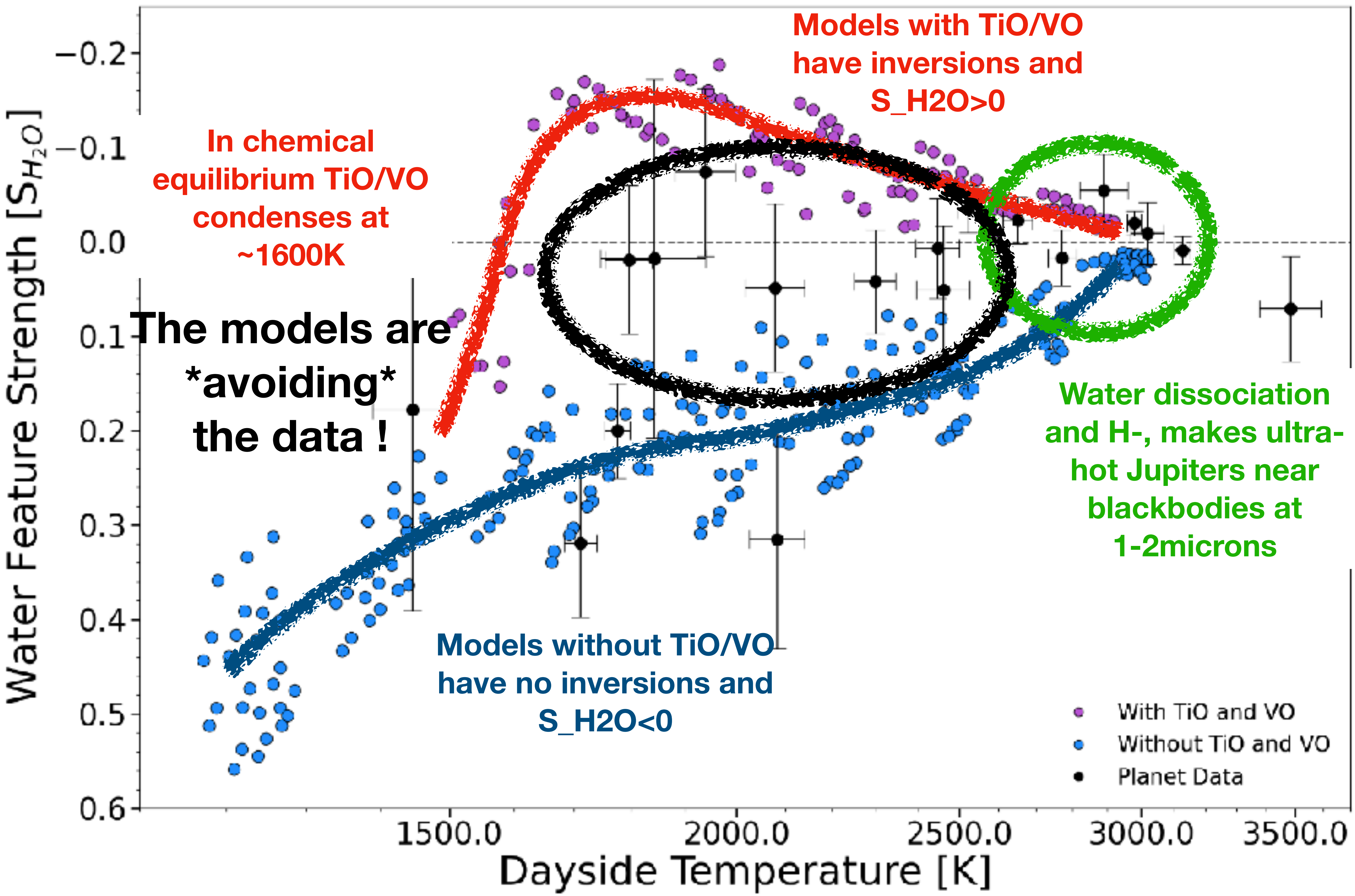

A diversity of condensates ?

		Properties		Bulk		Ices				Alkalis			Rocks										Isotope
	Planet name	Teq/ Teff (K)	M (M_{Jup})	H	He	H_2O	CO	CH_4	HCN	Na	K	Li	Fe	Fe II	Mg	Ca II	Ca	Sc II	Si	Ti II	V	Cr	^{13}CO
Transiting planets	KELT-9b	4048	2.88	H									H	H	H	H		L		H			
	WASP-33b	2781	2.1	H		L	L						H			H			L				
	WASP-189	2641	1.99										H	H	L					L	L	L	
	WASP-121b	2359	1.18	H		M				H	H	L	H	H	H	H	H	L			L	L	
	KELT-20b	2255	3.38	H		L				H			H	H	L	H			L				
	WASP-76b	2182	0.92			L				H		L	H		L	H					L	L	
	HAT-P-32b	1801	0.58	L	L	L																	
	WASP-77Ab	1741	2.29			H	L																L
	WASP-17b	1698	0.78			L				L													
	HD209458 b	1476	0.73	L	L	H	H	L	L	C				C	C		L						
	WASP-127b	1401	0.18			L				H	L	L											
	XO-2b	1327	0.566							L	L												
	HAT-P-1b	1322	0.525			L				L													
	WASP-52 b	1299	0.46	L		L				H	L												
	WASP-96b	1286	0.48			L				L													
	HD189733b	1192	1.13		H	H	H		L	H	L												
	WASP-39b	1120	0.28			L				L													
	WASP-6b	1093	0.37			L				H	H												
	WASP-69b	988	0.29		L	L				H													
	HAT-P-12b	957	0.21			L				L													
	HAT-P-18b	848	0.20		L	L																	
	HAT-P-11b	829	0.084		M	L																	
	WASP-107b	739	0.12		H	L																	
	GJ3470b	604	0.043		L	L																	
Non Transiting	Tau Bootis b	1636	5.84			C	H																
	HD179949b	1552	0.92			M	L																
	51Peg b	1260	0.46			H	L																
	HD 102195b	1053	0.46			L		L															
Directly imaged	CQ Lupi b	~2650	25			L	L																
	Beta Pictoris b	~1724	12.9			H	H																
	TYC 8998-760-1b	~1700	14			L	L																L
	HR8799c	~1100	8.1			H	H	C															
	HR8799b	~900	5.8			L	L	C															
	51 Eridani b	~760	9.1			H		H															

Confidence level:

- High observed by at least 2 instruments
- Medium: observed by one instrument multiple times
- Low: observed once by one instrument
- Controversial

Guillot+ 2022 PPVII chapter

A diversity of condensates ?

		Properties		Bulk		Ices				Alkalis			Rocks										Isotope
	Planet name	Teq/ Teff (K)	M (M_{Jup})	H	He	H_2O	CO	CH_4	HCN	Na	K	Li	Fe	Fe II	Mg	Ca II	Ca	Sc II	Si	Ti II	V	Cr	^{13}CO
Transiting planets	KELT-9b	4048	2.88	H									H	H	H	H		L		H			
	WASP-33b	2781	2.1	H		L	L						H			H			L				
	WASP-189	2641	1.99										H	H	L					L	L	L	
	WASP-121b	2359	1.18	H		M				H	H	L	H	H	H	H	H	L			L	L	
	KELT-20b	2255	3.38	H		L				H			H	H	L	H			L				
	WASP-76b	2182	0.92			L				H		L	H		L	H					L	L	
	HAT-P-32b	1801	0.58	L	L	L																	
	WASP-77Ab	1741	2.29			H	L																L
	WASP-17b	1698	0.78			L				L													
	HD209458 b	1476	0.73	L	L	H	H	L	L	C				C	C		L						
	WASP-127b	1401	0.18			L				H	L	L											
	XO-2b	1327	0.566							L	L												
	HAT-P-1b	1322	0.525			L				L													
	WASP-52 b	1299	0.46	L		L				H	L												
	WASP-96b	1286	0.48			L				L													
	HD189733b	1192	1.13		H	H	H		L	H	L												
	WASP-39b	1120	0.28			L				L													
	WASP-6b	1093	0.37			L				H	H												
	WASP-69b	988	0.29		L	L				H													
	HAT-P-12b	957	0.21			L				L													
	HAT-P-18b	848	0.20		L	L																	
	HAT-P-11b	829	0.084		M	L																	
	WASP-107b	739	0.12		H	L																	
	GJ3470b	604	0.043		L																		
Non Transiting	Tau Bootis b	1636	5.84			C	H																
	HD179949b	1552	0.92			M	L																
	51Peg b	1260	0.46			H	L																
	HD 102195b	1053	0.46			L		L															
Directly imaged	CQ Lupi b	~2650	25			L	L																
	Beta Pictoris b	~1724	12.9			H	H																
	TYC 8998-760-1b	~1700	14			L	L																L
	HR8799c	~1100	8.1			H	H	C															
	HR8799b	~900	5.8			L	L	C															
	51 Eridiani b	~760	9.1			H		H															

Confidence level:
- High observed by at least 2 instruments
- Medium: observed by one instrument multiple times
- Low: observed once by one instrument
- Controversial

Condensed corner ?

Guillot+ 2022
PPVII chapter

Condensation affects abundances

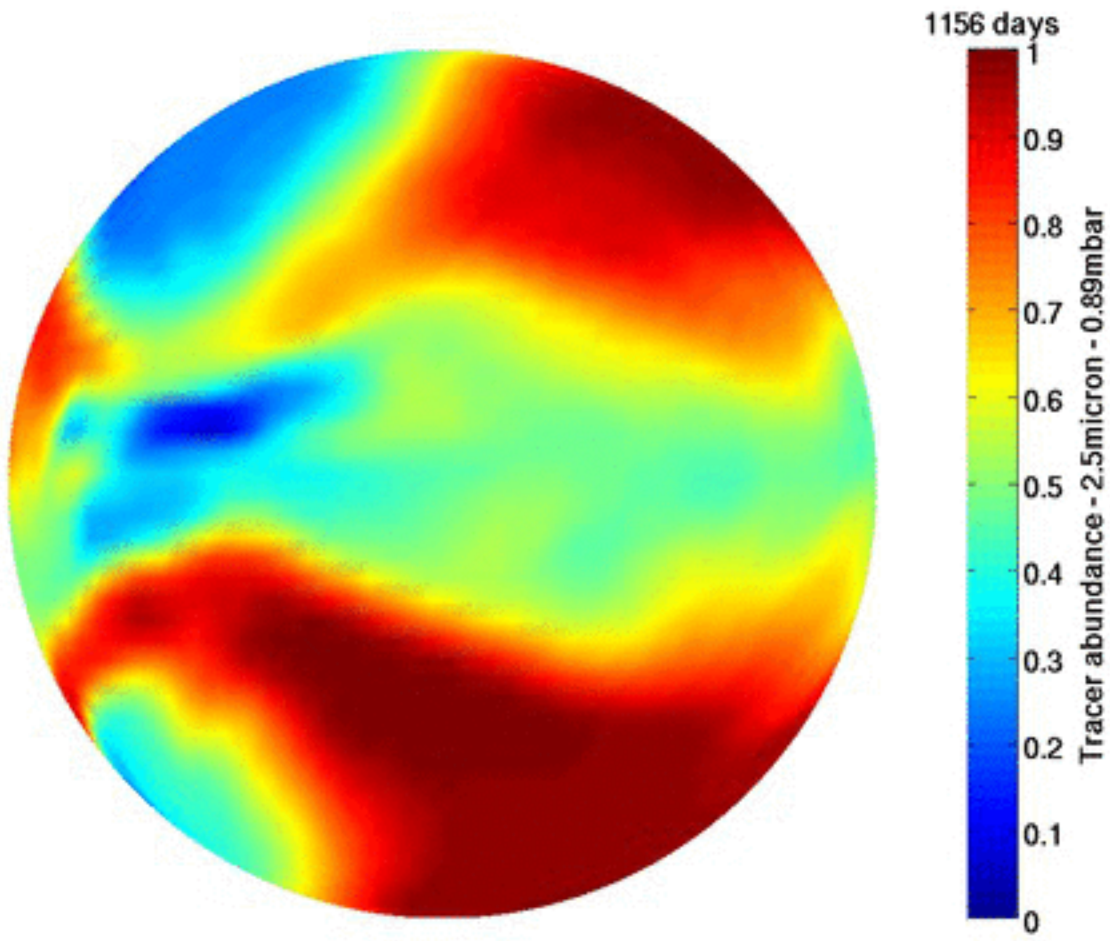

TiO abundance on the dayside of a hot Jupiter with nightside condensation

Condensation affects abundances

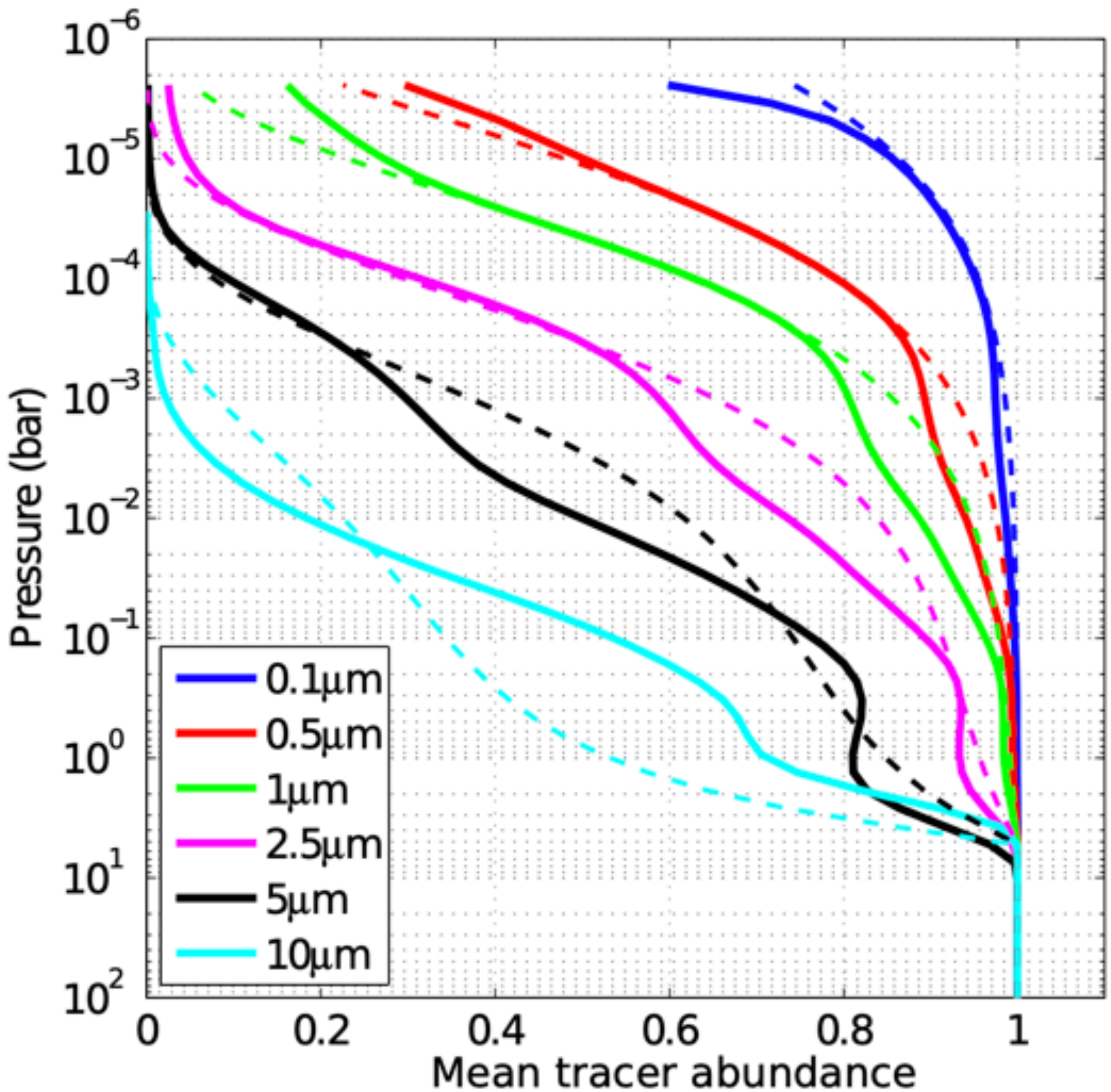

TiO abundance set by competition between

— Settling on the nightside

— Vertical mixing everywhere

If TiO is trapped in particles larger than a few microns, there won't be enough on the dayside to form a thermal inversion

TiO abundance on the planet dayside **depends on detailed microphysics on the planet nightside** !

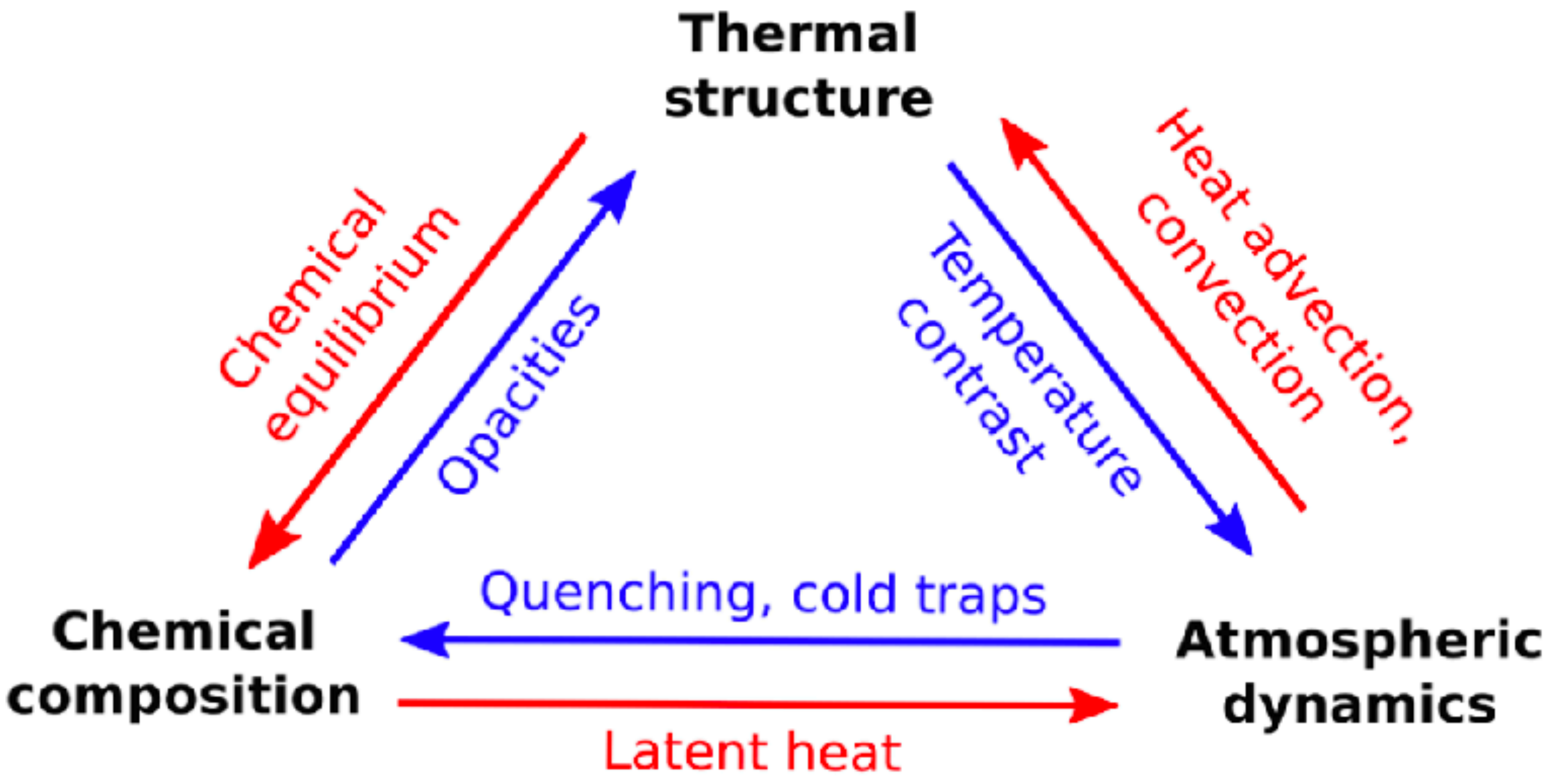

Thermal structure
Chemical equilibrium
Opacities
Temperature contrast
Heat advection, convection
Quenching, cold traps
Chemical composition
Atmospheric dynamics
Latent heat

Conclusions

— Large scale day/night heating drive pressure gradient balanced by Coriolis (period)/ drag/ advection/wave transport.

— Radiative cooling important affected by composition/clouds !

— Drag mechanisms unclear. Current models equilibrate with either numerical drag or parameterised drag

— No good estimate of actual wind speed despite observations being able to measure them directly

— Spatially varying clouds and composition can change observable. Phase curve offset to hot spot offset mapping not immediate ! *Eclipse mapping solution ?*

— Data is becoming of very good quality, models needs to up their game !